WHITE SPRUCE TREE-RINGS FROM ARCTIC TREELINE IN OLD CROW FLATS AND THE MACKENZIE DELTA, NORTHWESTERN CANADA: INDICATORS OF PAST CLIMATIC CHANGE

by

TREVOR JOHN PORTER

A thesis submitted to the Faculty of Graduate and Postdoctoral Affairs in partial fulfillment of the requirements for the degree of

Doctor of Philosophy

in

Geography

Carleton University,

Ottawa, Ontario

Library and Archives Canada

Published Heritage Branch

395 Wellington Street
Ottawa ON K1A 0N4
Canada

Bibliothèque et Archives Canada

Direction du Patrimoine de l'édition

395, rue Wellington
Ottawa ON K1A 0N4
Canada

Your file Votre référence
ISBN: 978-0-494-93701-3

Our file Notre référence
ISBN: 978-0-494-93701-3

ABSTRACT

White spruce tree-ring width and $\delta^{18}O$ in northwestern North America (NWNA) are evaluated as independent temperature-proxies, needed to improve knowledge of past climate. The paleoclimatic value of ring-width has been questioned due to a 'divergence' between ring-width and temperature at some NWNA sites. Conversely, $\delta^{18}O$-temperature signals can be complicated by atmospheric circulation variability. The main objectives of this thesis are to improve understandings of these complications and conduct quantitative paleoclimate reconstructions if warranted.

Ring-width series networks were developed in Old Crow Flats and the Mackenzie Delta, and existing series across NWNA were compiled, to study divergence. Divergence was widespread during the 20th century which implicates a large-scale forcing, potentially drought stress. But not all trees were affected suggesting local-scale ecological factors moderate a tree's susceptibility to divergence. Growth patterns of affected and unaffected trees were coherent before the 20th century and reflect temperature fluctuations over most of the past millennium, suggesting divergence is unique to the 20th century. White spruce ring-widths contain valuable climate information but divergent signals must be accounted for. A Mackenzie Delta chronology was developed by excluding divergent signals and used to reconstruct June-July minimum temperatures since AD 1245. The reconstruction is verified by local climate and proxy-temperature data, and suggests the late-20th century was the warmest period on record.

Temperature signals in a Mackenzie Delta tree-ring $\delta^{18}O$ record were also tested using 20th century climate data, a period of significant atmospheric circulation variability.

The $\delta^{18}O$-temperature response was time-stable during this period suggesting $\delta^{18}O$ in this area is not strongly impacted by circulation, a finding supported by isotope-enabled GCM simulations. The $\delta^{18}O$ record was used to reconstruct April-July minimum temperatures since AD 1780, which found a relatively warm late-20^{th} century, providing independent verification for the ring-width-based reconstruction.

Lastly, this thesis makes one methodological contribution. The *status quo* method used in many laboratories to estimate the precision of tree-ring stable isotope ratios does not account for sample-processing uncertainties. A method was developed to address this issue, by exposing quality assurance standards to the same processing steps that sample tree-rings undergo, and demonstrated for the Mackenzie Delta $\delta^{18}O$ data.

CO-AUTHORSHIP

Chapters 3-6 are manuscripts co-authored by myself and others. The contributions of each co-author are outlined as follows:

Chapter 3 – Porter TJ and Pisaric MFJ (2011) Temperature-growth divergence in white spruce forests of Old Crow Flats, Yukon Territory, and adjacent regions of northwestern North America. *Global Change Biology* 11: 3418-3430.

As the lead investigator, I was the architect of this study. I oversaw all aspects of sample collection, data compilation/analysis, and wrote the manuscript. Michael Pisaric contributed to the study design, secured funding, assisted in the field, and gave comments on multiple drafts of the manuscript before it was submitted to *Global Change Biology* on January 19, 2011. The manuscript was accepted for publication on July 9, 2011.

Chapter 4 – Porter TJ, Pisaric MFJ, Kokelj SV and deMontigny P (unpublished manuscript) A reconstruction of June-July temperatures since AD 1245 from white spruce tree-rings in the Mackenzie Delta region, northwestern Canada.

As the lead investigator, I was the architect of this study. I oversaw all aspects of sample collection, data compilation/analysis, and wrote the manuscript. Michael Pisaric contributed to the study design, secured funding, assisted in the field, and gave comments on multiple drafts of the manuscript. Steve Kokelj provided funding and comments on the manuscript. Peter deMontigny provided field and laboratory support.

Chapter 5 – Porter TJ and Middlestead P (2012) On estimating the precision of stable isotope ratios in processed tree-rings. *Dendrochronologia*, 30: 239-242.

As the lead investigator, I was the architect of this study. I oversaw all aspects of sample collection, data compilation/analysis, and wrote the manuscript. Paul Middlestead contributed to the study design, supplied the analytical resources, and provided comments that helped to improve the manuscript before it was submitted to *Dendrochronologia* on November 10, 2011. The manuscript was accepted for publication on February 13, 2012.

Chapter 6 – Porter TJ, Pisaric MFJ, Field R, Kokelj SV, Edwards TWD, deMontigny P, Healey R and LeGrande A (unpublished manuscript) April-July minimum temperatures since AD 1780 reconstructed from stable oxygen isotope ratios in white spruce tree-rings from the Mackenzie Delta, northwestern Canada.

As the lead investigator, I was the architect of this study. I oversaw all aspects of sample collection, data compilation/analysis, and wrote the manuscript. Michael Pisaric contributed to the study design, secured funding, assisted in the field, and gave comments on the manuscript. Steve Kokelj provided funding. Tom Edwards provided comments on the manuscript. Peter deMontigny provided field and laboratory support. Richard Healey and Allegra LeGrande provided simulated meteoric $\delta^{18}O$ data used in the study. Robert Field assisted with spatial correlation analysis and provided comments on the manuscript.

ACKNOWLEDGEMENTS

In part, this dissertation represents the last several years of my life. It amazes me how so much time can be compressed here. I have grown a lot from this experience, and there are many people to thank for making this all possible.

To my wife, Benjapon (Jeab) Porter, I would not be where I am today without you. You are my inspiration and, as you know, you are the reason I began this journey at the undergrad level almost ten years ago. Your love and support has allowed me to follow my dreams and I cannot thank you enough for that. I love you more than anything *teerak ja*, and I want you to know that it is my highest priority in life to be there for you as you have for me.

Family has been central to my success and sanity, and there are many people to thank: Ernest & Katherine Rutledge, Lyle & Dianne Gillespie, Stanley & Eileen Porter, Doug & Nancy Porter, the Hanson's, the Gray's, the Hewitt's, the Pommerville's, and the Ritchie's. Thanks for your love and support. Special thanks to my parents John Porter & Laurie Rutledge, siblings Joshua Porter and Rebecca Osorio, and brother-in-law Dennis Osorio. Mom and dad, thanks for everything, the many early-morning hockey practices, the life lessons, and supporting me as I travelled the globe to find my path. I would not be half the man I am today without your love and support. Bro and sis, I am so privileged to have you in my life. We have a friendship I have depended on for so much over the years, and no matter what, I know you always have my back. You guys mean the world to me! Finally, Dennis, thank you for taking good care of my sister (one less thing I have had to worry about), and for making me an uncle! I can't wait to meet my little nephew *in utero*!

To Michael Pisaric, my advisor, mentor, and friend, there are so many reasons to thank you. Where do I begin? Next to my wife and closest family, you have had one of the biggest and most positive impacts on the course of my life. During my undergrad, you saw potential in me that even I didn't recognise. In my second year, you took me under your wing as a research assistant in your lab, and this was the catalyst for my continued interest in northern environmental change research. Your supervision and support in these early years gave me the confidence I needed to reach lofty goals and take the next step to the M.Sc. program, and your confidence in me was critical in my decision to fast-track to the Ph.D. program. I have learned so much from you about how to conduct high-quality research, be successful in academia, and the importance of a balance between family and professional life. And here I am about to take another major step, westward, and I want to thank you for preparing me for the road ahead.

Thanks are due to so many others: my committee Elyn Humphreys and Ian Clark for your guidance; Tom Edwards for your friendship and so many great tree-ring isotope debates; Greg King for your help in the field, your friendship, and a Dempster Highway trip I will never forget; *mahsi cho* to everyone in Old Crow for your hospitality during the International Polar Year; *mahsi cho* to David Maxwell for our great adventures in Old Crow Flats; *mahsi cho* to Erika Tizya-Tramm for your help in the field; Pete deMontigny for excellence in research assistantship; Andrew Burn for field assistance; DGES support staff – Hazel Anderson, Natalie Pressburger, Elsie Clement, Judy Eddy, Judy Donaldson, Quang Ngo, and David Bertram for all that you do to support us graduate students; Paul Middlestead, Wendi Abdi, Michelle Chartrand, Patricia Wickham, and Gilles St-Jean for showing me the ropes at the G.G. Hatch Stable Isotope Lab; my CUPL lab mates for our

great years together; Jonny Vandewint for all your home reno advice and attending my wedding on the other side of the planet; John Seay and Tim Ensom for so many fierce squash matches and follow-up pints; Tom Melvin and Ed Cook for helpful conversations on signal-free standardisation and other tree-ring-related matters; and a general thanks to many colleagues from Carleton and elsewhere I met along the way – you have all made a difference!

Financial and logistical support for this research is from a variety of sources: the Natural Sciences and Engineering Research Council of Canada; Aboriginal Affairs and Northern Development Canada; Government of Canada International Polar Year grant; Polar Continental Shelf Program; and Carleton University – Department of Geography and Environmental Studies and Faculty of Graduate and Postdoctoral Affairs.

TABLE OF CONTENTS

ACRONYMS

20CR – 20th Century Reanalysis

AD – *Anno Domini*

AL – Aleutian Low

AMJJ – April-July

CE – Coefficient of Efficiency

DFRC – Divergence Free Regional Chronology

DW – Durbin-Watson

ENSO – El Niño-Southern Oscillation

EPS – Expressed Population Signal

IPCC – Intergovernmental Panel on Climate Change

IRMS – Isotope Ratio Mass Spectrometer

IsoGCM – Isotope-Enabled General Circulation Model

IT – Identical Treatment

ITRDB – International Tree-Ring Databank

GC – Gas Chromatography

GCM – General Circulation Model

GISS – Goddard Institute for Space Studies

MDEC – Mackenzie Delta East Channel

NDJF – November-February

MDRC – Mackenzie Delta Regional Chronology

NASA – National Aeronautics and Space Administration

NCAR – National Center for Atmospheric Research

NCEP – National Centers for Environmental Prediction

NH – Northern Hemisphere

NOAA – National Oceanic and Atmospheric Administration

NPI – North Pacific Index

NWNA – Northwestern North America

NWT – Northwest Territories, Canada

PRCol – Mt. Logan Prospector Russell Col

QA – Quality Assurance

R – Pearson's Product Moment Correlation Coefficient

R^2 – Coefficient of Determination

RCS – Regional Curve Standardisation

RE – Reduction of Error

SE – Standard Error of the Estimate

SID – Stable Isotope Dendrochronology

SFS – Signal Free Standardisation

SOL – Surficial Organic Layer

TC-EA – Thermal Conversion Elemental Analyzer

UV-B – Ultraviolet Radiation, B Spectrum

VPDB – Vienna Pee Dee Belemnite

VSMOW – Vienna Standard Mean Ocean Water

YT – Yukon Territory, Canada

LIST OF TABLES

LIST OF FIGURES

Figure 2.8. Adapted from D'Arrigo et al. (2005). A comparison of observed (red) and predicted (blue) Dec-May North Pacific Index. Predicted NPI is a tree-ring-based reconstruction from 18 ring-width chronologies along coastal NWNA. The reconstruction demonstrates that NPI variability over the 20th century has been comparable to the range of variability since AD 1600.

Figure 3.1. (a) White spruce sites sampled in Old Crow Flats (site codes indicated, see Table 3.1). Major lakes and channels are shaded grey. (b) Climate stations at Fairbanks (FAI), Fort Yukon (FTY), Inuvik (INU), Aklavik (AKL), and Fort McPherson (FTM). (c) Large-scale context of Old Crow Flats. Boreal treeline was delineated in (b) and (c) from the Circumpolar Arctic Vegetation Map dataset (Walker et al. 2005). The shaded relief in panels (b) and (c) is based on the GTOPO30 digital elevation model (U.S. Geological Survey; http://www1.gsi.go.jp/geowww/globalmap-gsi/gtopo30/gtopo30.html) and differentiates between low (light grey) and high (dark grey) elevations.

Figure 3.2. Monthly normals (1971-2000) for minimum, mean, and maximum temperatures (lines), and total precipitation (bars) at Old Crow, Yukon Territory (http://www.climate.weatheroffice.ec.gc.ca).

Figure 3.3. (a/b) Group 1/Group 2 site chronologies (grey lines); all site chronologies are defined by ≥ 4 series (≥ 2 trees). The mean Group 1/Group 2 chronologies (black lines) were calculated using a robust bi-weight mean for all years defined by 2 or more site chronologies. Sample depth curves are indicated above each plot. (c) A comparison of the mean Group 1 (1555-2007) and Group 2 (1620-2007) chronologies. The running 51-year correlation (above plot) indicates coherence between the chronologies (dashed line is $p \leq 0.05$ level). (d) High-pass filtered (40-year cubic smoothing spline, 50% frequency cut-off; Cook and Peters 1981) comparison of the mean Group 1 and Group 2 chronologies; the high-pass series were smoothed with a 3-year cubic-smoothing spline for ease of comparison.

Figure 3.4. Comparisons between mean Group 1/Group 2 (black lines) and previous-year July maximum/growth-year June minimum temperatures (grey lines); correlations are significant at $p \leq 0.001$.

Figure 3.5. Locations of all NWNA site chronologies compared to the mean Group 1/Group 2 chronologies (site numbers indicated, refer to Table 3.3). The shaded relief is based on the GTOPO30 global digital elevation model (U.S. Geological Survey; http://www1.gsi.go.jp/geowww/globalmap-gsi/gtopo30/gtopo30.html) and differentiates between low (light grey) and high (dark grey) elevations.

Figure 3.6. (a/b) NWNA 1/NWNA 2 site chronologies (Table 3.4; including the mean Group 1/Group 2 chronologies) (grey lines); all site chronologies are defined by a

minimum of 4 series from at least two different trees. The mean NWNA 1/NWNA 2 chronologies (black lines) were calculated using a robust bi-weight mean for all years defined by a minimum of two site chronologies. Sample depth curves are indicated above each plot. (c) A comparison of the mean NWNA 1 and NWNA 2 chronologies. The running 51-year correlation (above plot) indicates coherence between the chronologies (dashed line is $p \leq 0.05$ level). (d) High-pass filtered (40-year cubic smoothing spline, 50% frequency cut-off; Cook and Peters 1981) comparison of the mean NWNA 1 and NWNA 2 chronologies; the high-pass series were smoothed with a 3-year cubic-smoothing spline for ease of comparison.

Figure 3.7. Comparison between the mean NWNA 1 (dotted)/NWNA 2 (grey) chronologies and NWNA-scale June/July instrumental temperature anomalies (solid black line). Temperature anomalies were calculated from the CRUTEM3v dataset (Brohan et al., 2006).

Figure 3.8. (a) Northern Hemisphere (NH) temperature reconstructions by Jones et al. (1998), Briffa (2000), Esper et al. (2002), D'Arrigo et al. (2006), Wahl and Ammann (2007), Wilson et al. (2007) (grey lines); mean reconstruction (black line). The reconstructions were expressed as z-scores relative to the common period of overlap (1750-1980). (b) Comparison of the mean NH temperature reconstruction (thick black line; smoothed with 15-year cubic smoothing spline, Cook and Peters 1981) against the mean NWNA 1 (dotted)/NWNA 2 (grey line) chronologies. The mean NWNA chronologies are defined by a minimum of 2 site chronologies.

Figure 4.1. White spruce study sites in the Mackenzie Delta region are marked by white dotted circles; site numbers correspond to Table 4.1; water bodies are shaded grey; boreal treeline is delineated from the Circumpolar Arctic Vegetation Map (Walker et al., 2005). White spruce sites from other studies (inset map) are marked by grey dotted circles; site networks from the same study are bounded together.

Figure 4.2. Comparisons between each of the 29 site chronologies (black lines; calculated for all years defined ≥ 6 trees) and regional mean chronologies (grey lines; the mean of all other trees from the remaining 28 sites). Upland sites are denoted by an '*'; all other sites are delta plain sites. Inter-series correlations are in brackets; all correlations are significant at $p \leq 0.001$.

Figure 4.3. (a) The Mackenzie Delta Regional Chronology (AD 1245-2007; dark grey line); the MDRC is shown for years with an Expressed Population Signal (EPS) ≥ 0.7; EPS ≥ 0.85 is indicated; the 5-95 (light grey) and 25-75 (medium grey) percentile ranges for all tree indices are indicated; the number of trees defining the MDRC (black line). (b) Comparison of the MDRC (grey) and reconstructed mean June-July temperatures (black) by Szeicz and MacDonald (1995; see Appendix C, SI-Note 4.3). (c) Comparison of the

MDRC (grey) and a composite of 6 hemispheric-scale temperature reconstructions (black; see Appendix C, SI-Note 4.4). (d) Comparison of first-differenced June-July temperatures (black) and the mean of all first-differenced tree indices (grey). Note that the time axes differ between plots (a), (b-c) and (d).

Figure 4.4. (a-c) Regional averages of Group 1 (blue), Group 2 (red), and Snag (black) ring-width indices; regional averages are shown for all years with an EPS ≥ 0.7 (EPS $\geq$ 0.85 is indicated); the 5-95 (light grey) and 25-75 (medium grey) percentile ranges are given. (d) Comparison of the Group 1, Group 2, and Snag regional chronologies. (e) Interannual standard deviations (grey) of all ring-width indices; a 41-year cubic smoothing spline (green) is used to highlight the low-frequency trend. (f) Divergence-Free Regional Chronology.

Figure 4.5. Mackenzie Delta regional June-July minimum temperature reconstruction (dark grey; 2×SE interval light grey) versus: (a) instrumental (observed) June-July minimum temperatures; (b) Szeicz and MacDonald (1995) ring-width-based June-July mean temperature reconstruction; (c) Porter et al. (2009) tree-ring $\delta^{18}O$ record, March-July minimum temperature proxy; (d) Porter and Pisaric (2011) OCF-Group-2 ring-width chronology, June minimum temperature proxy; (e) D'Arrigo et al. (2009) Coppermine River ring-width chronology, June-July temperature proxy; (f) 6-study composite hemispheric-scale reconstructed temperatures; (g) Kaufman et al. (2009) circum-Arctic temperature reconstruction. (h) The Mackenzie Delta regional June-July minimum temperature reconstruction from this study. Correlations represent the period of overlap between the Mackenzie Delta reconstruction and the comparison series; all correlations are significant at $p \leq 0.001$. Refer to SI-Note 5 (Appendix C) for details on each comparison series, some of which are modified from their original published form. Note that time axes differ between plots (a), (b-d), and (e-h).

Figure 6.1. Map of study sites (triangles) and climate stations (solid dots) of interest. The shaded relief is based on the GTOPO30 digital elevation model (U.S. Geological Survey; http://www1.gsi.go.jp/geowww/globalmap-gsi/gtopo30/gtopo30.html) and differentiates between low (light grey) and high (dark grey) elevations.

Figure 6.2. Timber site $\delta^{18}O$ tree-ring data: individual series (grey); median of Porter et al. (2009) data (blue) and new data from this study (red); the master Timber chronology (black); interpolated $\delta^{18}O$ values for the years 1972 and 1976 (black dots); inter-correlation between Porter et al. (2009) and new data during the period of overlap (1850-1870) is highly significant ($p \leq 0.001$). Expressed Population Signal (EPS) and sample depth (no. trees) are indicated; a 31-year cubic smoothing spline with a 50% frequency cut-off (Cook and Peters, 1981) is used to illustrate general EPS trends.

Figure 6.3. A correlation analysis between NPI and simulated meteoric $\delta^{18}O$ (influence of temperature on $\delta^{18}O$ removed) for fall-winter (NDJF; top) and spring-summer (AMJJ; bottom) months. Results from Runs 1 (left) and 2 (right) are compared. Points 1, 2, and 3 are Timber, PRCol, and Jellybean Lake, respectively.

Figure 6.4. A correlation analysis between NPI and precipitation amount for fall-winter (NDJF; top) and spring-summer (AMJJ; bottom) months. Results from Runs 1 (left) and 2 (right) are compared. Points 1, 2, and 3 are Timber, PRCol, and Jellybean Lake, respectively. These correlation patterns were also assessed using the longer NCEP/NCAR Reanalysis (1948-2009; Kalnay et al., 1996) and ERA-40 Reanalysis (1958-2002; Uppala et al., 2005) datasets, and are provided in Appendix D (SI-Fig. 6.2).

Figure 6.5. (a) Comparison between observed (colour) and predicted (black) April-July minimum temperatures since AD 1871; the observed temperature data are a composite of local temperature (Appendix D, SI-Fig. 6.1) and 20CR (Appendix D, SI-Fig. 6.3) data; the shaded confidence interval represents two standard errors of the prediction (± 2.48°C). (b) Comparison of the $\delta^{18}O$- temperature reconstruction (this study) and ring-width-inferred June-July temperatures for the Mackenzie Delta region (Porter et al., 2012). All correlations are significant at $p \leq 0.001$.

SI-Figure 3.1. Standardized ring-width indices (grey lines) and mean site chronologies (black lines) for each site in Old Crow Flats based on signal-free standardisation (Melvin and Briffa, 2008) using data-adaptive 'negative exponential' or 'negative-to-zero slope linear' curve fits (Fritts et al., 1969). Sample depth (red lines) indicates the number of series defining the mean chronology. The mean chronologies were calculated with a robust bi-weight mean (Cook, 1985); more details on each chronology are provided in Table 3.1.

SI-Figure 3.2. A comparison of each mean site chronology produced using 'signal-free' (black lines) and non-signal-free (red lines) methods. Inter-series differences can be considered the result of 'trend distortion' (Melvin and Briffa, 2008). Due to differences in non-age-related growth (i.e., forced by climate, disturbance, etc.) between sites, trend distortion effects are more pronounced in some chronologies (e.g., JC1, OC9, OC54, SC1, and TH1) than in others (e.g., DP26, OC50, OC52, TM1, and TM2).

SI-Figure 3.3. Magnified comparison of the mean Group 1 and Group 2 chronologies during (a) 1600-1800 and (b) 1800-2000. Smoothed chronologies were calculated using a 15-year cubic smoothing spline with a 50% frequency cut-off (Cook and Peters, 1981).

SI-Figure 3.4. Old Crow Flats sites: Group 1 (negative temperature response), Group 2 (positive temperature response), and Mixed (mixed negative/positive temperature response).

SI-Figure 4.1. An overhead view of a 'white spruce/crowberry-lichen' forest site (Pearce et al., 1988) which is representative of most of the delta plain sites sampled in this study. These sites are easy to spot from overhead due to their sparse canopies and abundance of reflective lichen.

SI-Figure 4.2. A representative view of 'CDU2'. This site is characterised by an open-canopy, thick understory of mosses and lichens, and an irregular, rocky terrain. These site characteristics are also shared by 'CDU' and 'CDU1' (see Szeicz and MacDonald, 1996, for photographs of CDU).

SI-Figure 4.3. Tree-averaged ring-width indices (light grey) and mean site chronologies (dark grey) for all 29 sites; the number of trees defining each year of the mean site chronologies is indicated (black).

SI-Figure 4.4. Climate stations included in the regional temperature and precipitation composites. Periods of station operation are indicated (n.b., data are not available for all years of operation). 'Fort McPherson*' represents two non-overlapping station records: 'Fort McPherson' (1892-1977) and 'Fort McPherson A' (1981-2007). 'Fort Good Hope*' is a merged record representing 'Fort Good Hope 2' (1897-1966) and 'Fort Good Hope A' (1944-2007).

SI-Figure 4.5. Comparison of monthly minimum temperatures from Tuktoyaktuk, Inuvik, Aklavik, Fort McPherson, Norman Wells, and Fort Good Hope (red lines); regional means (black lines). 'rbar' is the mean inter-series correlation (all are significant at $p \leq 0.001$). 'trend' is the slope of the regional mean from AD 1910-2007, a period defined by two or more stations in most cases. See SI-Note 4.2 for more details.

SI-Figure 4.6. Comparison of monthly mean temperatures from Tuktoyaktuk, Inuvik, Aklavik, Fort McPherson, Norman Wells, and Fort Good Hope (red lines); regional means (black lines). 'rbar' is the mean inter-series correlation (all are significant at $p \leq 0.001$). 'trend' is the slope of the regional mean from AD 1910-2007, a period defined by two or more stations in most cases. See SI-Note 4.2 for more details.

SI-Figure 4.7. Comparison of monthly maximum temperatures from Tuktoyaktuk, Inuvik, Aklavik, Fort McPherson, Norman Wells, and Fort Good Hope (red lines); regional means (black lines). 'rbar' is the mean inter-series correlation (all are significant at $p \leq 0.001$). 'trend' is the slope of the regional mean from AD 1910-2007, a period defined by two or more stations in most cases. See SI-Note 4.2 for more details.

SI-Figure 4.8. Comparison of total monthly precipitation from Inuvik, Aklavik, and Fort McPherson (red lines); regional means (black line). 'rbar' is the mean inter-series

correlation (*$p \leq 0.05$). 'trend' is the slope of the regional mean from AD 1932-2007, a period defined by two or more stations in most cases. See SI-Note 4.2 for more details.

SI-Figure 6.1. Comparison of monthly minimum temperatures from Tuktoyaktuk, Inuvik, Aklavik, Fort McPherson, Norman Wells, and Fort Good Hope (red lines); regional means (black lines). 'rbar' is the mean inter-series correlation (all are significant at $p \leq 0.001$). 'trend' is the slope of the regional mean from AD 1910-2007, a period defined by two or more stations in most cases.

SI-Figure 6.2. A correlation analysis between NPI and precipitation amount for fall-winter (NDJF; top) and spring-summer (AMJJ; bottom) months. Both the NCEP/NCAR Reanalysis (Kalnay et al., 1996; left) and ERA-40 Reanalysis (Uppala et al., 2005; right) datasets were used. The correlation maps were plotted using the KNMI Climate Explorer (http://climexp.knmi.nl); correlations significant at $p < 0.05$ are in bold colour, non-significant correlations are in light colour. Points 1, 2, and 3 are Timber, PRCol, and Jellybean Lake, respectively.

SI-Figure 6.3. Comparison April-July minimum temperatures for the Mackenzie Delta region (red) and 20CR (20^{th} Century V2 Reanalysis; Compo et al., 2011) April-July mean temperatures for the area 60-70°N, 130-140°W; the mean and variance of the 20CR data were adjusted to the local temperature data by linear scaling; the inter-correlation is 0.69 ($p \leq 0.001$).

CHAPTER ONE

INTRODUCTION

1.1 RATIONALE FOR THE STUDY

Over the last hundred years of instrumental data (1912-2011) surface air/ocean temperatures have warmed by 1.37°C in the Arctic (64-90°N) in comparison to 0.73°C globally and 0.76°C for the Northern Hemisphere (Hansen et al., 2010; NASA-GISS, 2012), highlighting the climatic sensitivity of high-latitude regions due to feedbacks that amplify global trends (Serreze et al., 2009; Bintanja et al., 2011). This recent warming has caused directional changes to many environmental variables that are central to cold-adapted biological systems and traditional life in the north (ACIA, 2005; Hinzman et al., 2005; Smol et al., 2005), and the possibility these trajectories will continue well into the future has raised valid concerns over the ability of northern systems to cope with future changes (Anisimov et al., 2007). Moreover, continued Arctic changes are soon expected to have significant impacts on global energy balance and synoptic climate regimes due to changing Arctic Ocean and tundra albedo, reduced Atlantic deep-water formation/global thermohaline circulation due to a fresher Arctic Ocean, and the potential release of large carbon pools, as CO_2 or CH_4, currently frozen in boreal-tundra soil and marine sediments (Clark et al., 2002; Serreze et al., 2009; Shakhova et al., 2010; Mack et al., 2011; Schuur and Abbott, 2011). The timing and magnitude of these changes remain uncertain but have created the impetus for improved knowledge of the Arctic climate system and how it will evolve in the future. The general theme of advancing knowledge of Arctic climate frames this doctoral research.

Knowledge of the Arctic climate system is derived mainly from observations of the past. Recent Arctic climate changes have been characterised by a sparse network of instrumental records, of which most are shorter than 100 years (Lawrimore et al., 2011). This network is suitable for characterising recent, broad-scale changes, but insufficient for evaluating the long-term, regional-scale context for these changes. Longer records are needed to evaluate the natural, pre-industrial range of climate variability and whether or not recent climate is anomalous with respect to natural variability. Such a perspective is key to assessing the role of natural versus anthropogenic forcings (Overpeck et al., 1997; Mann et al., 1998; Briffa, 2000), but at present a well-constrained assessment for high-latitude regions is hindered by the paucity and brevity of instrumental climate data. In the absence of these data, proxy-based datasets (e.g., tree-rings, ice-cores, etc.) appear to be well positioned to address these critical knowledge gaps.

Paleoclimatologists use a wide variety of proxy archives to study past climate, all having their own strengths and limitations (see Bradley, 1999; Jansen et al., 2007). The focus of this research is Arctic treeline tree-ring chronologies, one of the most important proxies for temperature reconstructions over the past millennium (Briffa, 2000; D'Arrigo et al., 2006). Key strengths of tree-ring chronologies are that they provide absolute dating control, they can be developed for most parts of the world wherever trees grow, several climatically-sensitive tree-ring variables can be measured (e.g., ring-width, density, and stable isotopes), and they are annually-resolved making them comparable to instrumental climate data (Hughes, 2011). Because trees from the same region tend to share a common growth pattern driven by regional climate, multiple tree-ring series across a region can be cross-dated, averaged into composite chronologies to enhance the shared signal, and used

to reconstruct the climate variable that is most limiting to tree growth. Similarly, shared growth patterns allow tree-ring series from deadwood of unknown age to be cross-dated against living tree-ring series whose dates of ring formation are well known and used to extend climate reconstructions back in time by hundreds or, in some cases, thousands of years. In this way, tree-ring chronologies can be used to provide a long-term context for recent climate change (Briffa et al., 1992; Jones et al., 1998; Büntgen et al., 2005; Wilson et al., 2007).

Another important application of tree-ring-based climate reconstructions is to provide initialisation and validation datasets for General Circulation Models (GCMs) (Jansen et al., 2007). Such datasets have allowed climate modellers to evaluate the skill of GCMs over a wide range of prehistoric climate conditions (driven by known changes in solar, volcanic, other aerosol, and trace gas forcings; Crowley, 2000) that far exceed the range of climate variability observed during the relatively short instrumental era (Jones et al., 1998; Trenberth and Otto-Bliesner, 2006). Such experiments are crucial for examining the contribution of various forcings to climate and establishing confidence in future projections, many which are also well outside the range of instrumental period conditions (Meehl et al., 2007). At present, GCMs do not perform well in high-latitude regions (Christensen et al., 2007) and there is a major lack of long-term validation data for these regions needed to diagnose the source of discrepancies between modelled and observed climate (Serreze and Barry, 2005). Again, dendroclimatic records may be well positioned to provide these critical data.

Most tree-ring studies employ ring-width measurements due to the often strong sensitivity of this variable to climate and the fact it is relatively inexpensive to measure in

comparison to other tree-ring variables (e.g., stable isotope ratios). The most climatically-sensitive ring-width chronologies are often found at the margins of a species' ecological range where rates of growth and treeline position are strongly limited by climate (Fritts, 1976). Tree-ring growth rates in marginal environments are more restricted compared to less marginal environments which increases tree longevity, making these environments ideal for the development of long, climatically-sensitive ring-width chronologies (Briffa, 2000). Arctic treeline is one particular marginal environment where growing seasons are brief and cool, and warm-season temperatures are a primary limitation to growth (Jacoby and D'Arrigo, 1989; Briffa et al., 2002).

Major efforts to develop a circumpolar Eurasian-North American tree-ring-width network for climate reconstruction purposes began in the 1980s and '90s (Cropper and Fritts, 1981; Jacoby and Cook, 1981; Jacoby and D'Arrigo, 1989; Schweingruber and Briffa, 1996), and this work made possible many large-scale temperature reconstructions for the past millennium (e.g., Jones et al., 1998; Briffa, 2000; Esper et al., 2002; D'Arrigo et al., 2006; Wahl and Ammann, 2007; Wilson et al., 2007). The scientific merit of this network cannot be overstated as it has been and continues to be an important resource for paleoclimate studies (Jansen et al., 2007). However, many of the original chronologies in this network end 2-3 decades before present, and there is a pressing need for new, up-to-date chronologies from Arctic treeline. Further, there are spatial gaps in the network that must be filled, especially in parts of northwestern North America (NWNA), to provide a more detailed account of regional climate dynamics and to better represent these areas in large-scale climate reconstructions.

For this research, new tree-ring records are developed for two areas of NWNA where little to no tree-ring research has been done before. These areas are Old Crow Flats, Yukon Territory, and the Mackenzie Delta, Northwest Territories. Standard dendroclimatology methods (Fritts, 1976; Speer, 2010) are used to develop new, multi-century white spruce (*Picea glauca* [Moench] Voss) ring-width chronologies for 23 sites in Old Crow Flats, and 19 sites in the Mackenzie Delta. Ten pre-existing chronologies from the Mackenzie Delta (Szeicz and MacDonald, 1996; Bégin et al., 2000; Pisaric et al., 2007) are used to supplement the new chronologies. These networks are two of the densest regional-scale networks ever compiled in NWNA, and this approach provides the opportunity to better isolate regionally-coherent growth patterns linked to climate while attenuating site-specific noise (Hughes, 2011). These data are used to develop long tree-ring chronologies for the study regions and infer warm-season (June-July) temperatures over much of the past millennium.

In addition to ring-width, tree-ring stable oxygen isotope ratios ($\delta^{18}O$) from one Mackenzie Delta site are used to reconstruct spring-weighted (April-July) temperatures over the last two centuries. The added benefit to using $\delta^{18}O$ is in its ability to reconstruct a slightly different seasonal window of temperature compared to ring-width (April-July vs. June-July), thus providing a broader perspective on past climate. Further, over long time-scales, both proxies provide mutual, independent verification which is particularly meaningful as the physical processes leading to preservation of temperature signals in both proxies are mutually-exclusive. Porter et al. (2009) were the first to investigate the potential of tree-ring $\delta^{18}O$ in the Mackenzie Delta and found it is a good first-order-proxy for spring-summer minimum temperatures. This research builds upon Porter et al.'s study

by extending their chronology back in time, conducting a revised temperature-$\delta^{18}O$ analysis using a new regional climate record to validate the proposed temperature response, and reconstructing spring-summer weighted temperatures back to AD 1780.

For both proxies, much attention is given to the robustness of their temperature signals. Before a proxy-based climate reconstruction is carried out, the time-stability of the proxy-climate relation must be assessed over the modern instrumental period (Cook and Kairiukstis, 1990). If the relation is time-stable, this provides some confidence it may also have been time-stable in the past. And finally, if it is reasonable to assume the same proxy-climate relation applied in the past (i.e., assumption of uniformitarianism), linear regression techniques are then used to translate tree-ring data to inferred climate based on the modern proxy-climate relation. However, in NWNA there are potential complications for both ring-width and $\delta^{18}O$ with respect to the long-term stability of their temperature response, and these are a major focus of this research.

For ring-width, the boreal forest Divergence Problem (hereafter 'divergence'; D'Arrigo et al., 2008) is a chief concern and is observed at sites bracketing the tree-ring networks examined here (Jacoby and D'Arrigo, 1995; D'Arrigo et al., 2004; Wilmking et al., 2004; Driscoll et al., 2005; Pisaric et al., 2007; Earles, 2008). Divergence can be described as an unstable temperature-growth response that has affected some ring-width chronologies in NWNA since around the mid-20th century. The cause(s) of divergence is not yet clear, partly due to a lack of tree-ring data needed to characterise the phenomenon and diagnose its cause(s) (D'Arrigo et al., 2008). As its cause(s) is not well understood, the likelihood it has or has not occurred in the past remains a key uncertainty with major implications for ring-width-based temperature reconstructions (Jansen et al., 2007).

Based on a limited dataset, Cook et al. (2004) found that divergence is likely unique to the late-20th century and that the temperature-growth response of high-latitude forests was time-stable over the last 1100 years. However, further studies are needed to support this finding and improve understandings of divergence. This thesis contributes in both regards, providing novel insights into the origin of divergence and implications for tree-ring-based temperature reconstructions in NWNA.

For $\delta^{18}O$, variability in atmospheric circulation is a concern. At middle- to high-latitude sites, temperature shares a strong relation with the $\delta^{18}O$ of meteoric water due to its influence on condensation leading to preferential rainout of isotopically-heavy water (Dansgaard, 1964; Rozanski et al., 1992), and this 'temperature effect' is the reason many tree-ring $\delta^{18}O$ records worldwide are so strongly associated with temperature (Barbour et al., 2001; Rebetez et al., 2003; Porter et al., 2009; Seftigen et al., 2011). For some areas, however, the stability of the meteoric $\delta^{18}O$-temperature relation is sensitive to variability in atmospheric circulation (Sodemann et al., 2008b; Birks and Edwards, 2009; Field et al., 2010; Sturm et al., 2010), which may complicate the interpretation of tree-ring $\delta^{18}O$ as a first-order temperature proxy. Of importance to the Mackenzie Delta is the Aleutian Low (AL) which determines atmospheric circulation patterns over NWNA (Burns, 1973; Wahl et al., 1987; Mock et al., 1998; Dyke, 2000; Serreze and Barry, 2005). However, it is not known how sensitive the Mackenzie Delta tree-ring $\delta^{18}O$-temperature response is to AL variability. This doctoral research provides new insights that address this uncertainty.

Finally, this thesis makes one methodological contribution to the field of stable isotope dendrochronology (SID). As SID is still a relatively young field, improvements to

analytical methods are ongoing (McCarroll and Loader, 2004; Robertson et al., 2008). There are several sources of analytical uncertainty that can influence stable isotope ratio (δ) measurements, and the added variance due to this uncertainty can be significant with respect to inter-ring δ variability. As such, it is common practice in virtually all SID studies to report the 2σ precision estimate associated with δ measurements. However, it is shown here that the *status quo* method used in isotope laboratories to estimate δ precision does not reflect uncertainties associated with sample processing, where wholewood tree-rings are converted to α-cellulose or cellulose-intermediates using a chemical extraction procedure prior to isotope analysis (e.g., Leavitt and Danzer, 1993; Brendel et al., 2000). It is conceivable that uncertainties in sample processing, e.g., inadvertent and unrealised operator error, could lead to significant error in δ measurements and, therefore, they must be accounted for in the precision estimate. The proposed method addresses this issue, and provides a system for assessing inter-batch reproducibility.

1.2 RESEARCH OBJECTIVES AND STATEMENTS OF ORIGINALITY

The key research objectives and original aspects of this research are as follows: Objective 1 – Develop ring-width networks from white spruce forests in the Old Crow Flats and Mackenzie Delta regions, identify regionally-coherent growth patterns, and explore their climate response. There are several novelties to this objective. For one, this is the first study to examine white spruce growth in Old Crow Flats and the central and western portions of the Mackenzie Delta. Secondly, this research compiles two of the densest regional-scale tree-ring networks ever examined in NWNA allowing regionally-

important patterns to be isolated, which has not been possible in many previous NWNA studies based on individual site chronologies.

Objective 2 – Determine the presence, severity, spatiotemporal extent, and likely cause(s) of divergence in NWNA. Divergence has been poorly understood for nearly two decades, partly due to a lack of current tree-ring datasets. To date, only a small number of studies recognising divergence have been conducted across NWNA, mostly from interior Alaska (Jacoby and D'Arrigo, 1995; Lloyd and Fastie, 2002; D'Arrigo et al., 2004; Wilmking et al., 2004; Driscoll et al., 2005; Wilmking and Juday, 2005; Pisaric et al., 2007). This thesis makes a substantial data contribution in two areas of NWNA that were previously understudied. This greatly expanded dataset provides an opportunity to characterise the spatiotemporal extent of divergence in the two regions, identify ubiquities at the NWNA-scale, and yield novel insights on the cause(s) of divergence and implications for ring-width-based climate reconstructions in NWNA.

Objective 3 – Reconstruct past warm-season temperatures from ring-width chronologies. This objective is achievable only if it can be demonstrated that the proxy-climate relation is time-stable, and this will be determined in Objective 2. The long-term, high-resolution climate histories of the study areas are not well known, and this is a limitation to current understandings of regional climate dynamics in NWNA. Completing this objective would provide these critical data which are lacking.

Objective 4 – Propose a method for estimating the precision of tree-ring δ measurements that accounts for uncertainties associated with sample processing. The *status quo* method currently used by many stable isotope laboratories worldwide does not account for processing uncertainties, and there are no published recommendations on how these uncertainties can be accounted for. Completing this objective represents the first attempt to resolve this issue, and is expected to yield a method that all stable isotope laboratories specialising in tree-ring analysis could readily adopt.

Objective 5 – Evaluate the stability of the Mackenzie Delta tree-ring $\delta^{18}O$-temperature relation over periods of variable AL strength. Several lines of inquiry are followed. First, the tree-ring $\delta^{18}O$-temperature relation is evaluated using local temperature records from AD 1892-2003, a period that experienced a large range of AL variability (Trenberth and Hurrell, 1994) that is thought to be representative of the range of AL variability since AD 1600 (D'Arrigo et al., 2005). If the temperature-$\delta^{18}O$ relation is robust over this period, it would imply that the $\delta^{18}O$ record is insensitive to circulation effects. Secondly, Porter et al.'s (2009) tree-ring $\delta^{18}O$ record (AD 1850-2003) will be extended back to AD 1780 to look for signs of a putative AL regime shift thought to have occurred at ca. AD 1840 according to two $\delta^{18}O$ records from southwestern Yukon (Fisher et al., 2004; Anderson et al., 2005). A marked $\delta^{18}O$ depletion was found in both records, which cannot be explained by a classic temperature effect since temperatures in the region have likely increased since AD 1840 (Szeicz and MacDonald, 1995; Davi et al., 2003; D'Arrigo et al., 2006; Viau et al., 2012), and so the depletion was interpreted as evidence of a major AL regime shift. If consistent evidence is found in the Mackenzie Delta tree-ring $\delta^{18}O$

record, it would imply that it may not be a simple first-order temperature proxy. Lastly, the expected response of meteoric $\delta^{18}O$ in the study region to changes in AL strength is assessed using the NASA-GISS ModelE isotope-enabled general circulation model (Schmidt et al., 2005, 2006). All lines of inquiry will provide new insights on the robustness of Mackenzie Delta tree-ring $\delta^{18}O$ as a first-order temperature proxy.

Objective 6 – Reconstruct spring-summer temperatures from the tree-ring $\delta^{18}O$ record if the temperature-$\delta^{18}O$ relation is robust. Satisfying this objective would provide a long-term context for evaluating recent climate change in the study region. Furthermore, it would be the first tree-ring based reconstruction in NWNA that is equally weighted by spring and summer temperatures. This seasonal window is unique compared to what most high-latitude ring-width-based temperature reconstructions are sensitive to (Jones et al., 2009) and, therefore, a spring-summer weighted temperature reconstruction will provide a broader understanding of past climate.

1.3 DISSERTATION STRUCTURE

The dissertation is organised into a series of four primary research manuscripts (Chapters 3-6), all of which concern the analysis of tree-rings in paleoclimatic research. Chapter 2 provides a broad literature review in support of the four primary manuscripts. Chapter 3 addresses Objectives 1 and 2, and focuses mainly on Old Crow Flats. Chapter 4 focuses on the Mackenzie Delta region, but builds on insight gained in Chapter 3 and addresses Objectives 1-3. Chapter 5 addresses Objective 4, and uses the extended tree-ring $\delta^{18}O$ data to demonstrate the proposed method. Chapter 6 addresses Objectives 5 and

6. Finally, Chapter 7 provides a summary of the novel aspects of this research and future considerations.

CHAPTER TWO

LITERATURE REVIEW

2.1 OVERVIEW

The primary focus of this research is the use of tree-ring width and $\delta^{18}O$ from white spruce forests near Arctic treeline as temperature proxies. High-latitude ring-width chronologies have long been used to reconstruct warm-season temperatures (Briffa et al., 1988, 1992; Jacoby and D'Arrigo, 1989; Overpeck et al., 1997; D'Arrigo et al., 2006). In contrast, tree-ring $\delta^{18}O$ has not been widely used for temperature reconstruction purposes, but its paleoclimatic 'potential' is well established (Gray and Thompson, 1976; Libby et al., 1976; Burk and Stuiver, 1981; Barbour et al., 2001; Porter et al., 2009). This chapter reviews literature supporting the use of tree-ring width and $\delta^{18}O$ as temperature proxies in high-latitude regions.

Developing a dendroclimatic reconstruction involves many steps that must be carried out with the utmost care to avoid non-climatic biases. The generic steps involve site selection, sample collection, cross-dating, tree-ring variable measurement (e.g., ring-width or $\delta^{18}O$), detrending age-related growth trends, integrating individual series into a master chronology, identifying the optimal climate response, testing the robustness of the climate response, and calibrating a regression model to translate the chronology into a climate reconstruction (Fritts, 1976; Cook and Kairiukstis, 1990). Of particular interest to this thesis is the robustness of temperature signals in tree-ring width and $\delta^{18}O$ as they are affected by divergence and atmospheric circulation variability, respectively. These two factors are reviewed here.

2.2 TEMPERATURE SIGNALS IN HIGH-LATITUDE TREE GROWTH

2.2.1 Empirical evidence and physical basis for the temperature-growth relation

According to Schulman (1944), Douglass (1919) was one of the first to explore high-latitude tree-ring growth patterns in Europe. Douglass began his work in northern Scandinavia in 1912-1913, and shortly thereafter Fennoscandian scientists became more involved, albeit to address botanical-related questions. Most of this research focussed on Scots pine (*Pinus sylvestris* L.), the dominant species of the region. By the 1940s, many ring-width chronologies across the region had been developed and it was known that the interannual growth patterns of these northern trees were mostly sensitive to June-July temperatures (Schulman, 1944). According to Briffa et al. (1988), tree-ring research in Fennoscandia gained momentum in the 1950s and '60s, and as more chronologies from the region amassed it also became clear that temperature-growth sensitivity was strongest at treeline (altitudinal and latitudinal) while trees further from treeline were less sensitive. Geographical patterns of the temperature-growth response over the instrumental period remained the focus of dendroclimatic studies in northwestern Europe for several decades before focus turned toward the development of multi-centennial chronologies for climate reconstruction purposes (Fig. 2.1; Briffa et al., 1988, 1990). In more recent years, multi-millennial-length chronologies in this region have been developed using sub-fossil wood recovered from peat and lake sediments, and used to infer summer temperatures over the last 7400 years (Grudd et al., 2002; Linderholm and Gunnarson, 2005).

According to Gostev et al. (1996), dendroclimatic research in the former Soviet Union was slower to develop, but some work in the 1970s and '80s concerning Dahurian larch (*Larix gmelini*) helped to demonstrate that ring-width chronologies across the taiga

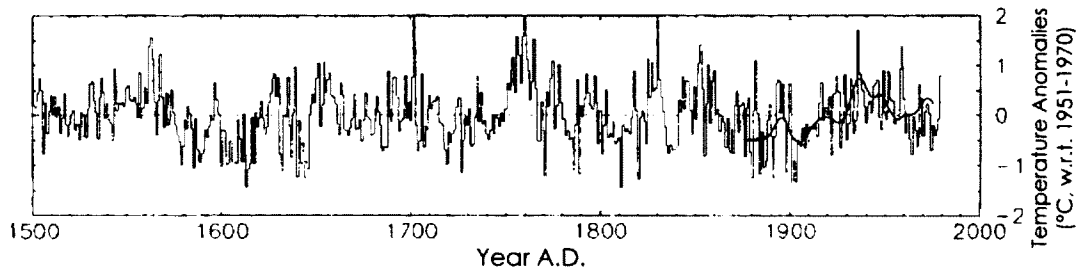

Figure 2.1. Adapted from Briffa et al. (1990). Comparison between April-August mean instrumental temperatures (red; AD 1876-1975) and reconstructed temperatures based on a ring-width chronology from northern Fennoscandia. Instrumental temperatures were smoothed with a 10-year low-pass filter. Unsmoothed temperatures explain 26% of annual ring-width variability.

treeline were highly sensitive to summer temperature (Fig. 2.2). Dendroclimatic research in northern Russia remains sparse today, but some multi-century- and millennial-length chronologies have been developed for this area and used to reconstruct past temperatures (Graybill and Shiyatov, 1992; Earle et al., 1994; Briffa, 2000; Jacoby et al., 2000).

High-latitude tree-ring research in North America began later than in Europe. In Alaska, Giddings (1938, 1954) was the first to study the growth patterns of white spruce, a dominant species across the North American boreal treeline (Hare and Ritchie, 1972). Giddings' research in Alaska spanned nearly two decades, although focussed mostly on the archaeological utility of tree-ring dating. However, he discovered early on that trees nearest to treeline were most sensitive to June-July temperatures (Giddings, 1943), as was found in Europe (Schulman, 1944). Oswalt (1949, 1960) carried on Giddings' work and helped to amass an extensive Alaskan chronology network that would later prove useful in showing the paleoclimatic value of white spruce in NWNA (Cropper and Fritts, 1981). Dendroclimatic research in Alaska and northern Canada gained momentum in the 1980s (Garfinkel and Brubaker, 1980; Cropper and Fritts, 1981; Jacoby and Cook, 1981; Jacoby and Ulan, 1982; Jacoby et al., 1982, 1985), and by then it was apparent that high-latitude white spruce growth was a valuable metric for reconstructing past summer temperatures. The longest temperature reconstructions are from NWNA, and are mostly restricted to the last millennium (Bégin et al., 2000; Esper et al., 2002; D'Arrigo et al., 2006).

Consistent evidence for the temperature-sensitivity of high-latitude tree growth is demonstrated by biogeographical studies linking the northern position of the boreal/taiga treeline to summer isotherms or other climatic boundaries. According to Bryson (1966), one of the first attempts to link the North American boreal treeline position and summer

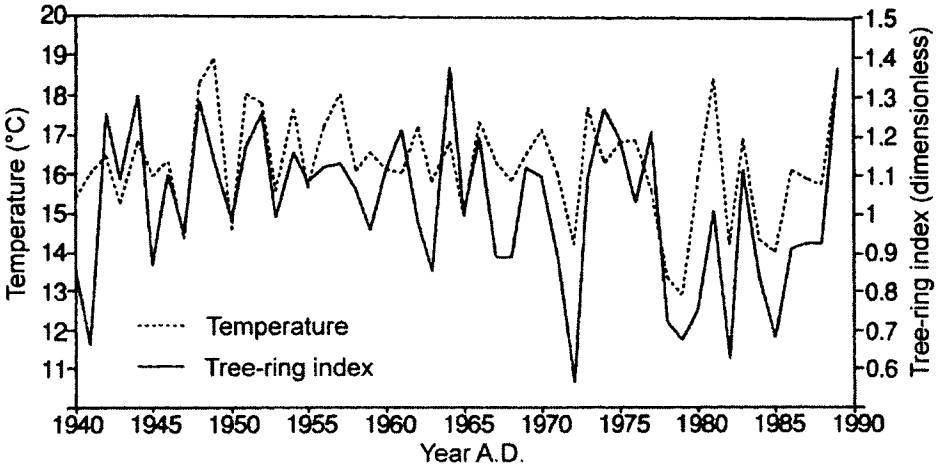

Figure 2.2. Adapted from Earle et al. (1994). Comparison between summer (June-August) average daily maximum temperatures for the instrumental period (AD 1940-1989) and a tree-ring width chronology for the Upper Kolyma Region, Northeastern Russia. The inter-series correlation for the entire period is 0.699.

temperatures was by Hare (1950, 1951), although Hare described his own results as 'hit-and-miss affairs with no rational basis'. Fifteen years on, using an improved high-latitude meteorological network augmented by the Distant Early Warning Line, Bryson (1966) conducted a much more thorough analysis and observed a clear correspondence between the boreal treeline and the summertime position of the Arctic front, implying that the cool Arctic air to the north was a limitation to boreal treeline advance. Although it is important to note that position of treeline may be somewhat responsible for the climatic boundaries due to its impact on the surface energy balance (Bryson, 1966; Foley et al., 1994). Krebs and Barry (1970), inspired by Bryson, conducted a similar analysis for the Eurasian taiga treeline and they too found a clear correspondence between the taiga treeline position and summertime Arctic front. Roughly three decades later, with an even more improved high-latitude meteorological network, MacDonald et al. (2000a) found that the North American treeline is well constrained by the 10-12.5°C mean July isotherms. Lastly, circum-Arctic palynological and macrofossil datasets provide good evidence that boreal/taiga treeline has been closely linked to summer warmth since the Last Glacial Maximum (Ritchie and Hare, 1971; Ritchie, 1977; Anderson and Brubaker, 1994; Cwynar and Spear, 1995; MacDonald et al., 2000b; Pisaric et al., 2000; Kaufman, 2004).

The positive association between high-latitude tree growth and temperature is thought to be a complex integration of many biophysical and environmental processes. For example, warmer temperatures may cause earlier snowmelt and ground-thaw, leading to a longer period for cambial activity and xylogenesis (Gregory and Wilson, 1968; Fritts, 1976; Tranquillini, 1979; Vaganov et al., 1999; Rossi et al., 2008). During late-summer, as cell expansion slows and trees prepare for winter (paced by the photoperiod – Rossi et

al., 2006), photosynthesis may persist longer during warmer years, even after cambial shut down, leading to a greater surplus of stored carbohydrates to augment growth during the following year (Mooney and Billings, 1960; Kozlowski, 1992); such is thought to be the physical basis for the high autocorrelation often observed in high-latitude ring-width series (Fritts, 1976; Cropper and Fritts, 1981). Conversely, cool years may reduce growth season length, primary growth and carbohydrate storage, and it is conceivable that frost events are more frequent in cold periods which could inhibit bud maturation and damage other tissues/organs important to productivity (Jacoby and D'Arrigo, 1989). Other causal mechanisms might include the influence of temperature on soil nutrient cycling (Jacoby and D'Arrigo, 1989) or on the carbon allocation ratio (Körner, 1998). Some proportion of the temperature-growth association could be the result of increased sunlight augmenting photosynthetic rate, as summer daytime temperatures correlate with cloud conditions and sunlight penetration, or perhaps the direct influence of temperature on photosynthetic rate (Kozlowski and Pallardy, 1997).

There are likely many other growth-limiting processes at the ecosystem- to cellular-scale that are directly or indirectly limited by temperature. However, due to the co-variability between temperature and many biophysical/environmental variables in natural systems, it is neither practical nor realistic to identify a single cause for the strong temperature-growth response. Rather, the idea that temperature integrates many primary growth-limiting factors is the conceptual basis for interpreting tree-ring growth records as proxies for past temperature.

2.2.2 Implications of temperature-growth divergence

Since the 1990s, high-latitude tree-ring chronologies have been one of the most important sources of annually-resolved temperature proxy data for the past millennium (Bradley and Jones, 1993; Overpeck et al., 1997; Mann et al., 1998; Esper et al., 2002; Jansen et al., 2007; Jones et al., 2009). However, the ability to use high-latitude tree-ring chronologies as a robust temperature proxy has been questioned in more recent years due to the poorly-understood divergence between temperature and tree growth (ring-width and -density) at some, not all, boreal sites.

D'Arrigo et al. (2008, pg. 290) describe divergence as "the tendency for tree growth at some previously temperature-limited northern sites to demonstrate a weakening in the mean temperature response in recent decades, with the divergence being expressed as a loss in climatic sensitivity and/or a divergence in trend". In most examples, divergence emerges in the middle- to late-20th century. A commonly cited example is from a white spruce elevational treeline site in central Yukon, Twisted Tree Heartrot Hill, where the mean ring-width chronology closely tracked summer temperatures for the first two thirds of the 20th century, but responded negatively to warming during the last third (since AD 1965), also the warmest part of the 20th century (Fig. 2.3). This basic form of divergence is found at several other high-latitude and -elevation treeline sites in NWNA (Jacoby and D'Arrigo, 1995; Wilmking et al., 2004; Driscoll et al., 2005; Wilmking and Juday, 2005; Pisaric et al., 2007; Earles, 2008; Andreu-Hayles et al., 2011; Porter and Pisaric, 2011) and Eurasia (Briffa et al., 1998b, 2004; Jacoby et al., 2000; Büntgen et al., 2006). Similar divergence is found at mid-latitude sites (Fig. 2.4; Briffa et al., 1998a, 2004), although many of these sites may not be expected to have a stable temperature-

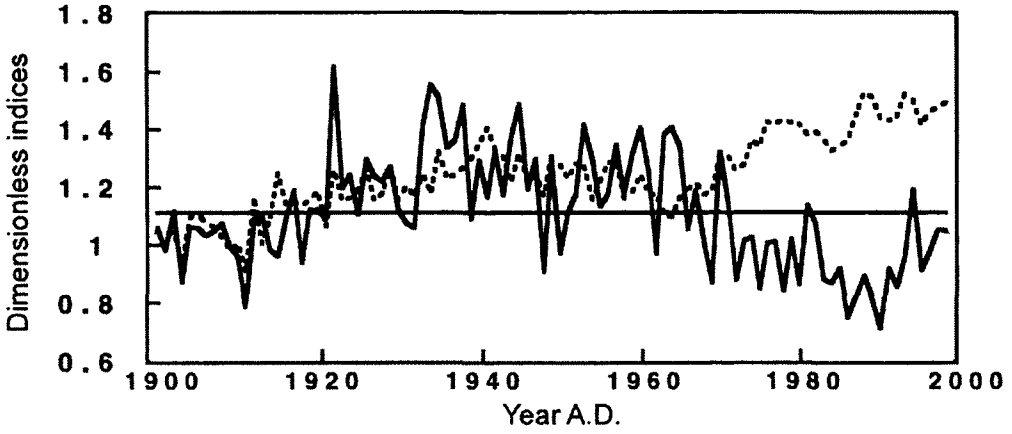

Figure 2.3. Adapted from D'Arrigo et al. (2004). Comparison between actual (solid line) and predicted (dashed line) ring-width for white spruce trees at the 'Twisted Tree-Heartrot Hill' site in central Yukon Territory. Modelled ring-width is based on April-August temperatures (first-order autocorrelation built in). The comparison demonstrates that actual growth at this site has systematically under-estimated temperatures (modelled growth) since ca. AD 1965.

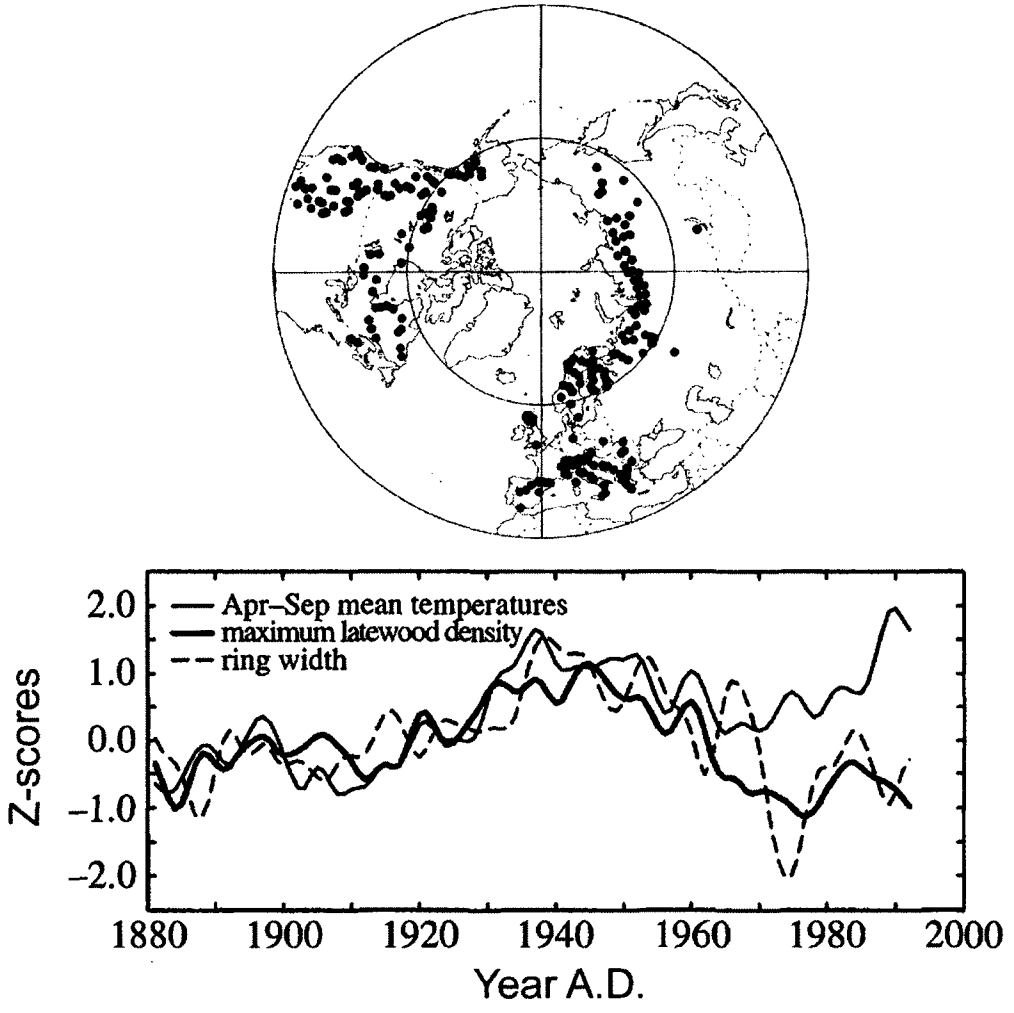

Figure 2.4. Adapted from Briffa et al. (1998). (top) Map of temperature-sensitive ring-density chronologies (dots) from the Northern Hemisphere. (bottom) Comparison between hemispheric averaged instrumental temperatures and tree-ring (width and density) inferred April-September temperatures. Inferred temperatures are based on a composite of chronologies shown in the map. All series were smoothed with a 20-year cubic smoothing spline to illustrate the common trends. As in Fig. 2.3, this comparison demonstrates a decoupling between temperature and tree-rings since ca. AD 1965.

growth relation as not all are from temperature-limited treeline boundaries (D'Arrigo et al., 2008).

Considering only the most temperature-limited high-latitude and -elevation sites, it has been demonstrated that southern and northern temperature-sensitive chronologies from the Northern Hemisphere infer the same pattern of temperature variability over the last 1100 years, except during the late 20th century when northern chronologies diverge (Cook et al., 2004). This evidence suggests that divergence is a northern phenomenon and restricted to the late-20th century. Unfortunately, this idea cannot be verified directly using instrumental temperature records since instrumental records are largely restricted to the last century (Lawrimore et al., 2011). But the long-term coherence of the northern and southern chronologies separated by hundreds to thousands of kilometres shows that they responded to the same climate variable over the last millennium, and temperature may be the only variable so coherent over such distances and timescales (Jones et al., 2009). Thus, it appears likely that divergence is restricted to the 20th century. If this is true, it would follow that the pre-divergence portion of affected chronologies may represent a robust temperature response and, thus, could be used to reconstruct past temperatures (Jacoby et al., 2000; D'Arrigo et al., 2006).

Because northern tree-ring chronologies are a major source of climate proxy data for the past millennium (Jansen et al., 2007), a physical understanding of divergence is needed to further evaluate the reliability of these chronologies to infer past climate. As it is for most understandings of natural phenomena, the process by which divergence occurs might only be fully understood after its form has been adequately characterized across space and time. Currently, there are many spatiotemporal gaps in the high-latitude tree-

ring network, especially in NWNA, that preclude knowledge of divergence (D'Arrigo et al., 2008). Updating of existing chronologies and development of new chronologies in areas where tree-ring research has been largely absent is needed to better characterise the phenomenon in NWNA (D'Arrigo et al., 2008). This thesis contributes in this regard by developing 23 new chronologies in Old Crow Flats and 19 chronologies in the Mackenzie Delta, and revisiting existing chronologies from these and neighbouring regions to better understand the spatiotemporal extent of divergence.

The observation that divergence is widespread and restricted to the 20th century suggests it was caused by a large-scale forcing unique to the 20th century. One possible cause is enhanced UV-B radiation (Briffa et al., 2004). Clorofluorocarbons released into the environment during the mid- to late-20th century have reduced stratospheric ozone over the Arctic, which has allowed more UV-B radiation to reach ground level. Increased UV-B radiation is detrimental to photosynthetic plant tissues in trees and has potentially reduced growth, especially in high-latitude regions where ozone loss has been significant. Another sunlight-related hypothesis is 'global dimming' (D'Arrigo et al. 2008). Aerosols of all particle sizes have increased in the troposphere in recent decades due to industrial activity, which effectively blocks some visible light from reaching the ground. A reduced supply of photosynthetically active radiation could account for reduced tree growth, but global dimming is not specific to higher-latitudes and does not explain why northern trees are more susceptible to divergence than southern trees.

Another possible reason for divergence is snow cover changes (Vaganov et al., 1999). Winter snowfall has increased in some parts of Siberia over the 20th century, and this has led to a delayed snow-free season and initial cambial activity. Vaganov et al.

(1999) argue that there is a period of 'maximal growth sensitivity to temperature', and that the delayed start of the growing season means that less of the period of active growth occurs during the period of maximal temperature-growth sensitivity. While this appears to be a valid reason for reduced growth in some parts of Siberia, it does not hold for most Arctic regions which has experienced reduced snowfall, increased rain, warmer temperatures, and earlier/longer growing seasons (ACIA, 2005; Serreze and Barry, 2005).

The relatively warm late-20th century has also been blamed for divergence. It has been suggested that late-20th century temperatures have crossed an optimal temperature threshold, where further warmth has negatively impacted primary productivity (D'Arrigo et al., 2004; Wilmking et al., 2004). The concept of optimal temperature thresholds has been known for some time from experimental studies on plants, where productivity is often expressed as an inverse parabola function of temperature (Kozlowski and Pallardy, 1997). Therefore, for a lower range of temperatures, temperature should have a positive impact on productivity, but after a point (varies by species) temperatures have a negative impact on growth. D'Arrigo et al. (2004) and Wilmking et al. (2004) estimate this point to be 11-12°C for July-August mean temperatures for white spruce in central Yukon and interior Alaska, respectively.

The most commonly proposed reason for divergence, or negative temperature-growth relations in general, is moisture stress (Jacoby and D'Arrigo, 1995; Barber et al., 2000; Lloyd and Fastie, 2002; Wilmking and Juday, 2005; McGuire et al., 2010). Based on a circumpolar (>55°N) network of ring-width chronologies, Lloyd and Bunn (2007) found that negative temperature-growth responses are more common at warm, dry sites where moisture is more limited, and positive temperature-growth responses are common

at cool, wet sites. Across interior Alaska, divergence is increasingly more common to the east, corresponding with a negative precipitation gradient (Wilmking and Juday, 2005); i.e., stands with less precipitation are more likely to exhibit divergence. Similarly, stands with a high tree density have less water per capita and are more susceptible to divergence than lower-density stands (Wilmking and Juday, 2005). Given the evaporative demands of a warmer climate, it is also likely that late-20th century warming (ACIA, 2005; Serreze and Barry, 2005) has exacerbated moisture stress in northern regions (Barber et al., 2000, 2004). Circum-Arctic temperatures reconstructed from ice- and lake-core proxies suggest that the 20th century has been the warmest period in more than two millennia (Kaufman et al., 2009), implying that 20th century evaporative demands may be unprecedented, which may explain why divergence is restricted to the 20th century.

Lastly, it is also possible that some cases of divergence have been artificially detected. Esper and Frank (2009) identified methodological 'pitfalls' that could account for divergence. One potential pitfall is the 'standardisation' process used to remove age-related trends from raw tree-ring series. Traditionally, standardisation involves fitting raw series with expected growth curves (as a function of age) and removing these curves to yield an index that can be related to climate. 'Data-adaptive' curves are often used (Fritts et al., 1969; Cook, 1985), usually negative exponential or negative to zero sloping lines, determined by the least-squares solution. However, data-adaptive fits do not differentiate between very low-frequency climate and age trends and, therefore, some low-frequency climate signals are unavoidably lost during standardisation. The lowest frequency signals that can be resolved by traditional data-adaptive methods is 1/n years (n = series length), and for a mean site chronology the frequency is related to the mean series length (Cook et

al., 1995). Because temperature records are not detrended while tree-ring data are, there is some potential for a misfit between temperature and tree-ring series.

One possible solution to the loss of low-frequency signals in tree-ring series is Regional Curve Standardisation (RCS; Briffa et al., 1992; Esper et al., 2003). The RCS method assumes all trees have the same underlying age trend masked by climate and environmental signals, and noise at a variety of frequencies due to geographic, genetic, or ecological dispositions. If the age-related trend is known, it can be removed from each tree to produce standardised series that are averaged into a mean chronology to elucidate the climate signal. RCS attempts to characterise the common age trend by estimating the mean growth curve of all trees aligned by cambial age, known as the 'regional curve'. Several criteria should be met to properly define the regional curve: pith offset data are available for samples which did not contain the first year of growth; a large number of trees are included; sample trees began growing under a wide range of climatic conditions, from several hundreds of years ago to present; and trees from these various time/climate intervals are equally represented in the regional curve. In theory, RCS should facilitate the preservation of low-frequency climate signals. However, many published datasets do not satisfy the RCS criteria, which is perhaps one reason RCS has not been widely used in the literature compared to more traditional data-adaptive methods. RCS is not used in this thesis as the datasets of interest do not conform well to the RCS criteria. Use of RCS without meeting these criteria can lead to a flawed regional curve, which could distort the mean chronology and lead to inaccurate climate-growth analysis results.

Another drawback to traditional data-adaptive curve fits is the potential for 'trend distortion' in the modern portion of mean chronologies. Ideally, the estimated age-related

curve should reflect growth that would occur under an unvarying climate. However, since data-adaptive curves are unable to separate very low-frequency age and climate signals, the estimated age trend will be distorted by the climate signal (termed 'trend distortion') and removal of the curve fits will result in distorted standardised series with some loss of the climate signal. Trend distortion is most severe at the series ends since data-adaptive curves are so heavily weighted towards the series ends. In the case of mean chronologies where the modern ends of many living tree-ring series terminate on the same year and are averaged, trend distortion will be especially significant (Melvin and Briffa, 2008). Such a distortion in the modern portion of mean chronologies could account for a misfit between tree-ring and climate data.

Trend distortion has been addressed by Melvin and Briffa (2008) who developed a method known as Signal-Free Standardisation (SFS). SFS is an iterative procedure that attempts to isolate and remove the common climate signal shared by a group of tree-ring series, resulting in signal-free measurements that are used to more accurately define the age-related growth trend of each series. The main steps are as follows: (1) each raw series is detrended using standard data-adaptive curves and a mean chronology is calculated; the mean chronology is then considered the best estimate of the common climate signal; (2) each raw series is divided by the mean chronology to produce 'signal-free' measurements (i.e., common climate signal removed); (3) data-adaptive curves are fitted to the signal-free measurements to better estimate the true age-related trend, and the detrending curves are applied to the raw series to produce standardised indices; and (4) the indices are used to calculate a revised mean chronology which is considered the new best estimate of the common climate signal (Melvin and Briffa, 2008). This procedure is repeated from Step

(2) until one of the following conditions are met: the number of iterations is equal to 1 + number of trees/20; or, if smoothly-varying detrending curves are used (e.g., spline fit; Cook and Peters, 1981), the difference in mean value between consecutive iterations of the mean chronology (high-pass filtered) is less than 0.0005 (Melvin and Briffa, 2008). SFS is used in this thesis to guard against trend distortion. It is important to note that the lowest climate signal frequencies that can be recovered using SFS are limited to 1/n and, thus, there is still some potential for offsets between temperature and tree growth indices at lower frequencies.

Other methodological pitfalls may include the use of tree-ring chronologies that are not strongly limited by temperature (e.g., trees from non-marginal environments) or ones that are prone to natural disturbance events such as insect outbreaks or fire, which might lead to growth suppressions or releases in the surviving trees that are unrelated to climate. All of the sites examined in this thesis are near Arctic treeline where temperature is generally considered a major growth limiting factor. Spruce bud worm (*Choristoneura spp.*) or bark beetle (*Dendroctonus spp.*) outbreaks are destructive to *Picea* forests in more southern parts of the boreal forest (McCullough et al., 1998), but are not known to occur in Old Crow Flats and the Mackenzie Delta regions due to the harsh winters. Fire is common throughout the boreal forest (Johnson, 1992). Low intensity fires tend to occur in sparse canopy *Pinus* forests and generally do not cause stand mortality, and may result in growth suppressions or releases in the surviving trees (Lageard et al., 2000). However, high intensity crown fires (Johnson, 1992) are more common in northern *Picea* forests due to the dense crown foliage and are generally stand-replacing events (i.e., no surviving trees). As such, *Picea* tree-ring chronologies are typically free of fire-related suppressions

and releases since they do not survive the fire. Wild fire is common in NWNA (Johnstone et al., 2010), but many sites in the study region have not burned for centuries (Szeicz and MacDonald, 1996; Bégin et al., 2000; Pisaric et al., 2007), as is evident by the presence of the many multi-centennial-length tree-ring chronologies presented herein.

2.3 TEMPERATURE SIGNALS IN HIGH-LATITUDE TREE-RING $\delta^{18}O$

2.3.1 Empirical evidence and physical basis for the temperature-$\delta^{18}O$ relation

Tree-ring $\delta^{18}O$ research has a much younger history compared to traditional ring-width-based dendroclimatic research. Libby and Pandolfi (1974) were the first to measure tree-ring $\delta^{18}O$, from German oak trees (*Quercus spp.*), and demonstrate its potential as a temperature proxy. However, their discovery of the temperature signal in tree-ring $\delta^{18}O$ was not serendipitous, but rather was inspired by earlier paleotemperature studies of $\delta^{18}O$ in Greenland ice (Dansgaard et al., 1969), and understandings of $\delta^{18}O$ in the hydrologic cycle that had emerged over the prior two decades. By the 1950s and '60s, major efforts were underway to characterise and better understand the global spatiotemporal variability of stable water isotopes in natural waters. Notable findings from these efforts were that sea water $\delta^{18}O$ is largely uniform (Epstein and Mayeda, 1953; Craig and Gordon, 1965), evaporated water $\delta^{18}O$ is depleted relative to sea water, and precipitated (meteoric) water $\delta^{18}O$ is correlated with air temperature over much of the planet (Dansgaard, 1953, 1954, 1964).

The mechanism for the meteoric $\delta^{18}O$-temperature relation can be conceptualised starting with a moist air parcel evaporated from the ocean. If evaporation proceeds slowly such that the moist air reaches its saturation point (i.e., evaporation rate = condensation rate) before it is swept inland, the vapour will be in isotopic equilibrium with the surface

water. At equilibrium, vapour $\delta^{18}O$ will be depleted by 9‰ relative to the surface water due to vapour pressure differences between $H_2{}^{16}O$ and $H_2{}^{18}O$ (i.e., $H_2{}^{16}O$ being 9% more volatile than $H_2{}^{18}O$; Dansgaard, 1964). Subsequently, atmospheric circulation guides the moist air to higher elevations and latitudes where lower temperatures cause the vapour to condense which leads to preferential rainout of $H_2{}^{18}O$ due to its lower vapour pressure.

Because temperature plays a central role in water isotope distillation, meteoric $\delta^{18}O$ tends to co-vary seasonally and annually with mean air temperatures, especially at mid- to high-latitude sites (Fig. 2.5 and 2.6) (Dansgaard, 1964; Rozanski et al., 1993). However, at tropical sites, evaporation-condensation kinetics are complex and result in a negative correlation between precipitation amount and $\delta^{18}O$, the so-called 'amount effect' (Dansgaard, 1964). The $\delta^{18}O$-temperature relation at higher-latitude sites has been well-known and exploited by paleoclimatologists for decades, perhaps the best examples being the use of the Greenland and Antarctica ice-core $\delta^{18}O$ records to infer temperatures over the last several hundred millennia (Dansgaard et al., 1969; Johnsen et al., 2001; Augustin et al., 2004). The paleoclimate value of these ice-core records cannot be overstated (Jones et al., 2009), but they are spatially limited to Greenland, Antarctica, and some high-alpine areas. For more continental areas where ice-cores are not available, tree-ring $\delta^{18}O$ could be used to reconstruct past temperatures at much finer spatiotemporal scales.

The basic model of $\delta^{18}O$ in tree-rings ($\delta^{18}O_{tr}$) is $\delta^{18}O_{tr} = \delta^{18}O_s + f \cdot \Delta^{18}O_e + \varepsilon_{wc}$ (Dongmann et al., 1974; DeNiro and Epstein, 1981; Sternberg et al., 1986; Farquhar and Lloyd, 1993; Saurer et al., 1997a; Roden et al., 2000; Barbour et al., 2005), where $\delta^{18}O_s$ is the $\delta^{18}O$ of soil water, $\Delta^{18}O_e$ is the evaporative enrichment of leaf water above $\delta^{18}O_s$ due to transpiring leaves, ε_{wc} (ca. +27‰) is a biochemical fractionation constant that accounts

for isotopic exchange between carbonyl oxygen of cellulose precursors (e.g., sucrose) and cellular water, and f is the bulk 'dampening factor' representing processes that nullify the $\Delta^{18}O_e$ signal in $\delta^{18}O_{tr}$ (e.g., mixing of leaf water with unaltered trunk water in cells where cellulose formation occurs and re-equilibration by ε_{wc}). In systems where $\delta^{18}O_s$ variability greatly exceeds $\Delta^{18}O_e$ variability or where dampening factors are substantial (i.e., $f << 1$), $\delta^{18}O_{tr}$ will largely reflect $\delta^{18}O_s$ variability; this scenario is often observed for natural sites (Edwards and Fritz, 1986; Robertson et al., 2001; Saurer et al., 2012). If, in such systems, $\delta^{18}O_s$ is strongly related to meteoric $\delta^{18}O$ (i.e., negligible groundwater) and meteoric $\delta^{18}O$ is strongly associated with temperature, $\delta^{18}O_{tr}$ may be a suitable temperature proxy.

Since Libby and Pandolfi's (1974) founding study, many tree-ring $\delta^{18}O$ studies have demonstrated strong associations with seasonally-averaged temperatures for a wide variety of species at mid- to high-latitude sites (Gray and Thompson, 1976; Libby et al., 1976; Burk and Stuiver, 1981; Saurer et al., 1997b; Barbour et al., 2001; Rebetez et al., 2003; Treydte et al., 2007; Porter et al., 2009; Seftigen et al., 2011), reflecting the use of $\delta^{18}O_s$ that has been isotopically-labelled by air temperature as described above. However, despite the numerous examples of the 'potential' to use tree-ring $\delta^{18}O$ as a temperature proxy, there are few examples worldwide where tree-ring $\delta^{18}O$ has been explicitly used to reconstruct temperatures. Rather, almost all tree-rings $\delta^{18}O$ studies to date have focussed on exploring climate-growth relations over the instrumental period, which was a point of criticism by Gagen et al. (2011) who advocated for tree-ring isotope case studies to move beyond demonstrations of 'potential' and focus on developing longer chronologies for paleoenvironmental reconstruction purposes.

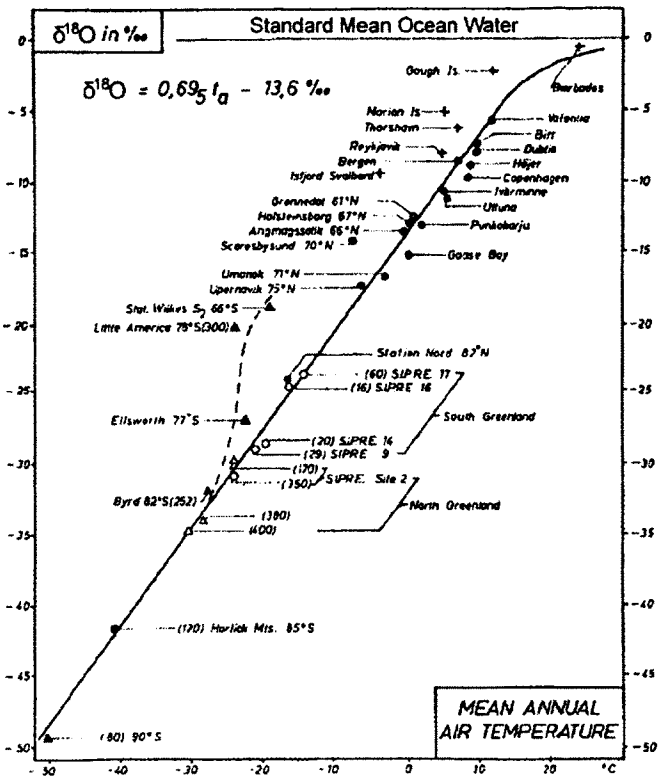

Figure 2.5. Adapted from Dansgaard (1964). Comparison between mean annual temperatures and annual meteoric $\delta^{18}O$ from mid- to high-latitude stations (Barbados being an exception).

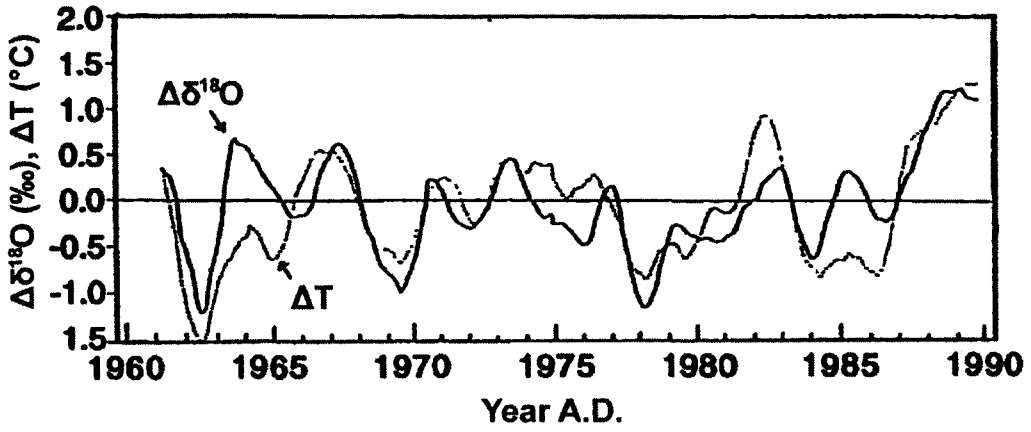

Figure 2.6. Adapted from Rozanski et al. (1992). A time-series comparison between mean annual temperatures and meteoric $\delta^{18}O$ for a composite network of 47 European sites; the inter-series $r^2 = 0.42$.

One of the few known tree-ring $\delta^{18}O$-based temperature reconstructions is for a high-Arctic site on Ellesmere Island, Beaver Pond, where several chronologies (20-250 years in length) from extinct fossil larch trees (*Larix spp.*) from the early-Pliocene (ca. 4-5 Ma) were used to provide valuable insights on interannual temperature variability and mean climate of that period (Ballantyne et al., 2006, 2010; Csank et al., 2011). The only known 'modern' tree-ring $\delta^{18}O$-based temperature reconstructions was by Edwards et al. (2008) who developed a multi-species (*Picea engelmannii*; *Pinus albicaulis*), millennial-length $\delta^{18}O$ chronology for the eastern Rocky Mountains; however, they did not use their $\delta^{18}O$ chronology as a first-order temperature proxy, but rather it was used in combination with a paired $\delta^{13}C$ chronology in an attempt to resolve the separate effects of temperature and relative humidity in both records (Edwards et al., 2000). Surprisingly, tree-ring $\delta^{18}O$ records have not yet been used as a first-order temperature proxy for the late-Holocene, even though current knowledge of meteoric and tree-ring $\delta^{18}O$ suggest this is possible.

2.3.2 Implications of atmospheric circulation variability

Given the strong relation between temperature and tree-ring $\delta^{18}O$ at many middle- to high-latitude sites, it would be ideal if the relation could be assumed time-stable and used to reconstruct past temperatures over the breadth of timescales covered by tree-ring records. Unfortunately, this assumption is not always valid. Studies of $\delta^{18}O$ in meteoric water (Fricke and O'Neil, 1999; Moran et al., 2007; Birks and Edwards, 2009; Liu et al., 2011), proxy archives (Edwards et al., 1996, 2008; Hammarlund et al., 2002; Fisher et al., 2004; Feng et al., 2007) and numerical modelling experiments (Field et al., 2010; Sturm et al., 2010) clearly show that atmospheric circulation moderates the slope and intercept

of the $\delta^{18}O$-temperature relation, which can complicate the use of $\delta^{18}O$ as a simple first-order temperature proxy (Jouzel et al., 1997).

As discussed, the $\delta^{18}O$ of meteoric water is determined by a distillation process that is strongly controlled by temperature. Assuming the same moisture source and flow path, meteoric $\delta^{18}O$ for a given site should maintain a constant relation with temperature (Dansgaard, 1964). Changes in circulation, however, can impact the moisture source and trajectory, which can impact the initial $\delta^{18}O$ of the moist air and extent to which isotopic equilibriums are achieved through the entire distillation process, and, ultimately, this adds non-temperature-related noise to meteoric $\delta^{18}O$ (Sodemann et al., 2008a, 2008b; Sturm et al., 2010). A second complication is the potential for changes in precipitation seasonality. In high-latitude regions, tree-ring $\delta^{18}O$ is labelled by a mixture of isotopically-depleted snowmelt and relatively enriched summer rain, and will be seasonally-biased towards the months that contributed most water to the soil (Sturm et al., 2010). If circulation alters the proportion of isotopically-depleted/enriched snow/rain for a given site, the seasonal bias of the tree-ring $\delta^{18}O$ temperature signal may also change. This effect has been noted at some sites in continental Siberia where a steady rise in winter snows relative to annual precipitation led to a decline in tree-ring $\delta^{18}O$ over the 20th century, despite a rise in air temperature (Saurer et al., 2002). Variability in atmospheric circulation has been blamed for instabilities in the tree-ring $\delta^{18}O$-temperature response at several sites in Scandinavia (Seftigen et al., 2011), China (Liu et al., 2009), and Italy (Reynolds-Henne et al., 2007), although the ultimate cause(s), i.e., source/trajectory or precipitation seasonality, was not investigated.

Depending on how variable circulation patterns are over time, and how sensitive the meteoric $\delta^{18}O$-temperature relation at a given site is to circulation, the tree-ring $\delta^{18}O$-temperature signal may or may not vary substantially due to circulation changes. At sites where meteoric $\delta^{18}O$ is strongly influenced by circulation, tree-ring $\delta^{18}O$ may be a poor temperature proxy, but could potentially be used as a circulation proxy. Where circulation and temperature signals are equally strong, a simple paleoclimate interpretation may not be possible. But where circulation effects are weak compared to temperature effects, a temperature reconstruction may be possible.

The main source of meteoric water for the Mackenzie Delta and much of NWNA is the North Pacific (Burns, 1973; Wahl et al., 1987; Dyke, 2000), and the trajectory of this moisture is strongly influenced by the strength of the semi-permanent Aleutian Low (AL) pressure cell over the north Pacific (Trenberth and Hurrell, 1994; Serreze and Barry, 2005). For example, when the AL is in a deeper state, advected air tends to follow a more meridional trajectory which draws warm, moist southern air northward into NWNA, but also leads to enhanced rain shadowing towards the interior (Mock et al., 1998; L'Heureux et al., 2004; Rodionov et al., 2005). Conversely, a weak AL leads to more zonal air flow. Given the influence of AL on NWNA air flow trajectories, AL variability could impact meteoric $\delta^{18}O$ in the Mackenzie Delta and the robustness of tree-ring $\delta^{18}O$-temperature signals, although a direct assessment of this potential effect is not possible due to the near absence of meteoric $\delta^{18}O$ data from NWNA (Bowen and Revenaugh, 2003; IAEA/WHO, 2006). However, some proxy-based evidence appears to suggest that AL-$\delta^{18}O$ effects may be significant in parts of NWNA.

The Mt. Logan Prospector Russell Col (PRCol) ice-core $\delta^{18}O$ and Jellybean Lake lake-core calcite $\delta^{18}O$ records in S.W. Yukon, proxies for meteoric $\delta^{18}O$, both exhibit an abrupt depletion at ca. AD 1840 unlike any other since AD 800 (Fig. 2.7; Fisher et al., 2004; Anderson et al., 2005). This depletion is not consistent with a classical temperature effect since most biological temperature proxies from the area suggest that post-AD 1840 temperatures have been relatively warm (Davi et al., 2003; D'Arrigo et al., 2006; Viau et al., 2012). Instead, Fisher et al. (2004) interpreted the post-1840 depletion as a shift from zonal- to meridional-type circulation, consistent with an intensified AL. However, the occurrence of a major regime shift at this time is putative at best as it is not corroborated by other lake-core $\delta^{18}O$ records from interior Yukon (Anderson et al., 2007, 2011) or the Eclipse ice-core $\delta^{2}H$ record which is ca. 40 km N.W. from PRCol. Also, a well-verified North Pacific Index (a measure of AL strength) reconstruction by D'Arrigo et al. (2005), based on an extensive ring-width chronology network from coastal NWNA, indicates that AL variability was comparable between the pre- and post-AD 1840 eras and that a major regime shift likely did not occur at AD 1840 (Fig. 2.8). The physical basis for the tree-ring-NPI relation, presumably, manifests through the influence of AL on coastal climate, which in turn influences tree growth.

Given these disparate results, it is pre-mature to accept or refute the occurrence of the putative AD 1840 event, qualify it as a large-scale regime shift, or draw conclusions about the sensitivity of meteoric $\delta^{18}O$ in these areas to circulation. Additional proxy $\delta^{18}O$ records from NWNA are needed to address these uncertainties. This doctoral research looks for evidence of the AD 1840 event in the Mackenzie Delta by extending Porter et al.'s (2009) tree-ring $\delta^{18}O$ record from AD 1850 back to 1780. Furthermore, the stability

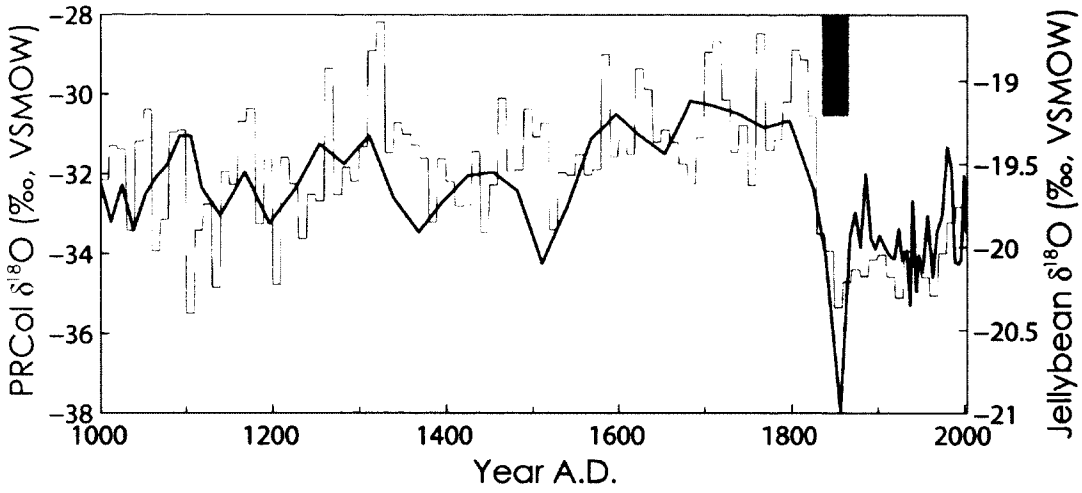

Figure 2.7. Comparison of the Mt. Logan PRCol ice-core $\delta^{18}O$ (red) and Jellybean Lake calcite $\delta^{18}O$ (black) records; time-series data provided by D. Fisher (Geological Survey of Canada) and L. Anderson (U.S. Geological Survey). Both records exhibit an anomalous shift at AD 1840 that is thought to reflect a shift in the strength of the Aleutian Low.

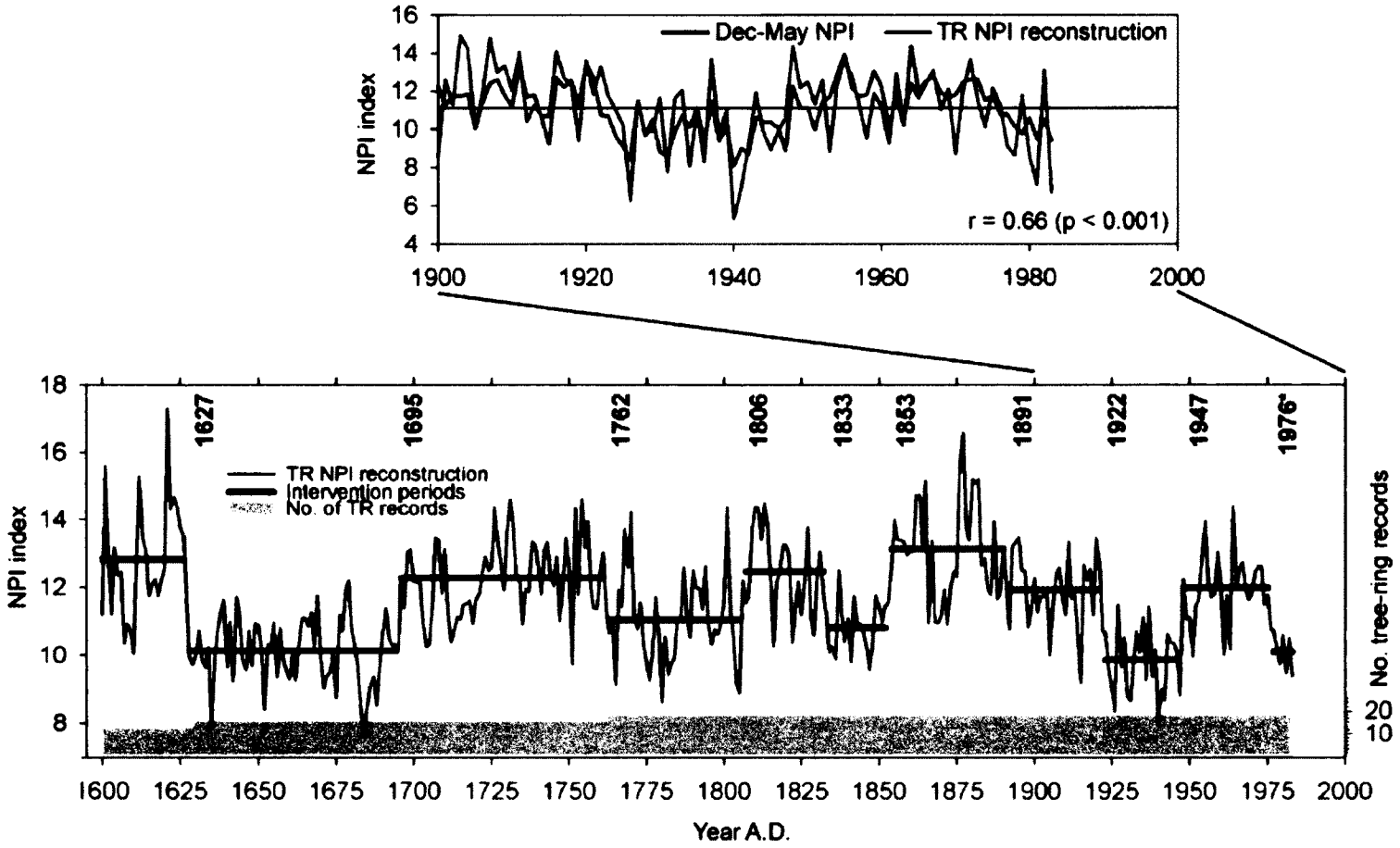

Figure 2.8. Adapted from D'Arrigo et al. (2005). A comparison of observed (red) and predicted (blue) Dec-May North Pacific Index. Predicted NPI is a tree-ring-based reconstruction from 18 ring-width chronologies along coastal NWNA. The reconstruction demonstrates that NPI variability over the 20th century has been comparable to the range of variability since AD 1600.

of the tree-ring temperature-$\delta^{18}O$ response over the period AD 1892-2003, a period that experienced a wide range of AL variability (D'Arrigo et al., 2005), is assessed and used as indirect evidence for the importance of circulation effects in the Mackenzie Delta.

In the absence of direct or proxy meteoric $\delta^{18}O$ records, numerical models could provide some insight into the 'expected' sensitivity of meteoric $\delta^{18}O$ to circulation for a given area (Jouzel et al., 1997; Sodemann et al., 2008a, 2008b; Field et al., 2010; Sturm et al., 2010). A relatively coarse scale (4° × 5° horizontal resolution) analysis for NWNA was carried out by Field et al. (2010) using the isotope-enabled general circulation model NASA-GISS ModelE (Schmidt et al., 2005, 2006). Field et al. found that variability in circulation likely has a significant impact on NWNA meteoric $\delta^{18}O$ for winter months, but not on a mean annual basis. Further, they found that a shift from zonal to meridional circulation would likely cause an increase in meteoric $\delta^{18}O$, not a decrease as suggested by Fisher et al. (2004). Field et al. (2010) did not specifically evaluate circulation effects in the Mackenzie Delta region, but their results appear to show that Mackenzie Delta meteoric $\delta^{18}O$ would be affected during winter months. However, Field et al. (2010) did not examine the spring-summer season, which is the seasonal bias of the Mackenzie Delta tree-ring $\delta^{18}O$ record. To better understand the potential impacts of circulation on the Mackenzie Delta tree-ring $\delta^{18}O$ record and potential to use this record as a first-order temperature proxy, this doctoral research also employs the ModelE to characterise the expected response of spring-summer meteoric $\delta^{18}O$ to AL variability.

CHAPTER THREE

TEMPERATURE-GROWTH DIVERGENCE IN WHITE SPRUCE FORESTS OF OLD CROW FLATS, YUKON TERRITORY, AND ADJACENT REGIONS OF NORTHWESTERN NORTH AMERICA[1]

3.1 INTRODUCTION

In high-latitude regions, dendroclimatic studies often report a positive relationship between summer temperatures and tree-ring width (e.g., Briffa et al., 1990; Szeicz and MacDonald, 1995; Gostev et al., 1996; D'Arrigo et al., 2006; Frank et al., 2007; Wilson et al., 2007; Youngblut and Luckman, 2008). This observed relation is intuitive for trees living at the cold northern margins of the boreal forest where tree growth is largely thought to be temperature-dependent; however, this is not always the case. In northwestern North America (NWNA), in particular, many white spruce (*Picea glauca* [Moench] Voss) stands are inversely correlated with previous-year summer temperature (e.g., Barber et al., 2000; Lloyd and Fastie, 2002; Wilmking et al., 2004; Pisaric et al., 2007; McGuire et al., 2010). At some of these sites, inverse relations may have persisted over the entire 20th century (Lloyd and Bunn, 2007), but at others they appear to be a recent phenomenon (Jacoby and D'Arrigo, 1995; D'Arrigo et al., 2004). Similar temperature response shifts are also found at high-latitude Eurasian sites (Briffa et al., 1998b; Jacoby et al., 2000). Collectively, these instances of transient temperature-growth

[1] A modified version of this chapter has been published in the journal Global Change Biology – Porter, T, & Pisaric, M, 2011: Temperature-growth divergence in white spruce forests of Old Crow Flats, Yukon Territory, and adjacent regions of northwestern North America. Global Change Biology, 17: 3418-3430.

responses are referred to as the Divergence Problem (hereafter 'divergence'; D'Arrigo et al., 2008).

In a paleoclimatology context, divergence complicates the use of affected tree-ring chronologies as temperature proxies since reconstructions depend on time-stable proxy-climate relations. However, because high-latitude tree-ring networks are an important data source for centennial- to millennial-length temperature reconstructions (Jansen et al., 2007), it is important to improve understandings of divergence and the extent to which past climate-growth relations can be considered time-stable.

Divergence is often observed as a low-frequency departure between summer temperature and ring-width occurring after the mid- to late-20th century (D'Arrigo et al., 2008), coinciding with the warmest period the Arctic has experienced in the last two millennia (Kaufman et al., 2009). Although the cause(s) of divergence are largely unknown, it has been suggested that the relatively warm late-20th century may be driving this non-linear behaviour by temperature-induced drought stress (Jacoby and D'Arrigo, 1995; Barber et al., 2000; Lloyd and Bunn, 2007; McGuire et al., 2010) or optimal biological temperature thresholds being surpassed (D'Arrigo et al., 2004; Wilmking et al., 2004). Other possible explanations for divergence include late-20th-century changes in snow cover (Vaganov et al., 1999), UV-B radiation (Briffa et al., 2004), and global dimming (D'Arrigo et al., 2008). However, current understandings of divergence are based on a small number of study sites, limiting one's ability to draw conclusions about its causes and the likelihood that past temperature-growth relations were also impacted.

Here, a new network of site-averaged ring-width chronologies from 23 white spruce sites in Old Crow Flats, Yukon Territory, Canada, is used to satisfy three

objectives: (1) expand the high-latitude tree-ring network into a region where this research has been absent; (2) examine the response of this network to temperature; and (3) determine if trees in this region were impacted by divergence. Further, comparisons are drawn between these results and a larger-scale network of white spruce sites across NWNA. Old Crow Flats hosts the northernmost extent of boreal treeline in Yukon Territory and is adjacent to interior Alaska, central Yukon, and the Mackenzie Delta, areas where divergence has been identified (D'Arrigo et al., 2004; Wilmking et al., 2004; Pisaric et al., 2007). The study site network is unique in NWNA due to its high density. This characteristic makes it possible to better identify regionally-significant growth patterns that are closely linked to regional-scale factors such as climate than any individual site chronology (Hughes, 2011).

3.2 MATERIALS AND METHODS

3.2.1 Study region

The Old Crow Flats region (Fig. 3.1) is a low-lying basin complex bounded by mountain ranges in Alaska and Yukon Territory. The region's surficial geology is primarily defined by a thick glaciolacustrine clay unit deposited by Glacial Lake Old Crow when it occupied the area from ca. 24,000-12,000 years BP (Hughes, 1972; Morlan, 1980; Thorson and Dixon, 1983; Dyke et al., 2002). Much of the region is poorly drained and covered by a vast mosaic of shallow lakes and peatlands (Ovenden and Brassard, 1989; Labrecque et al., 2009). Meandering channels incise the surficial clay and provide some drainage (Lauriol et al., 2002). Channel floodplains are well drained

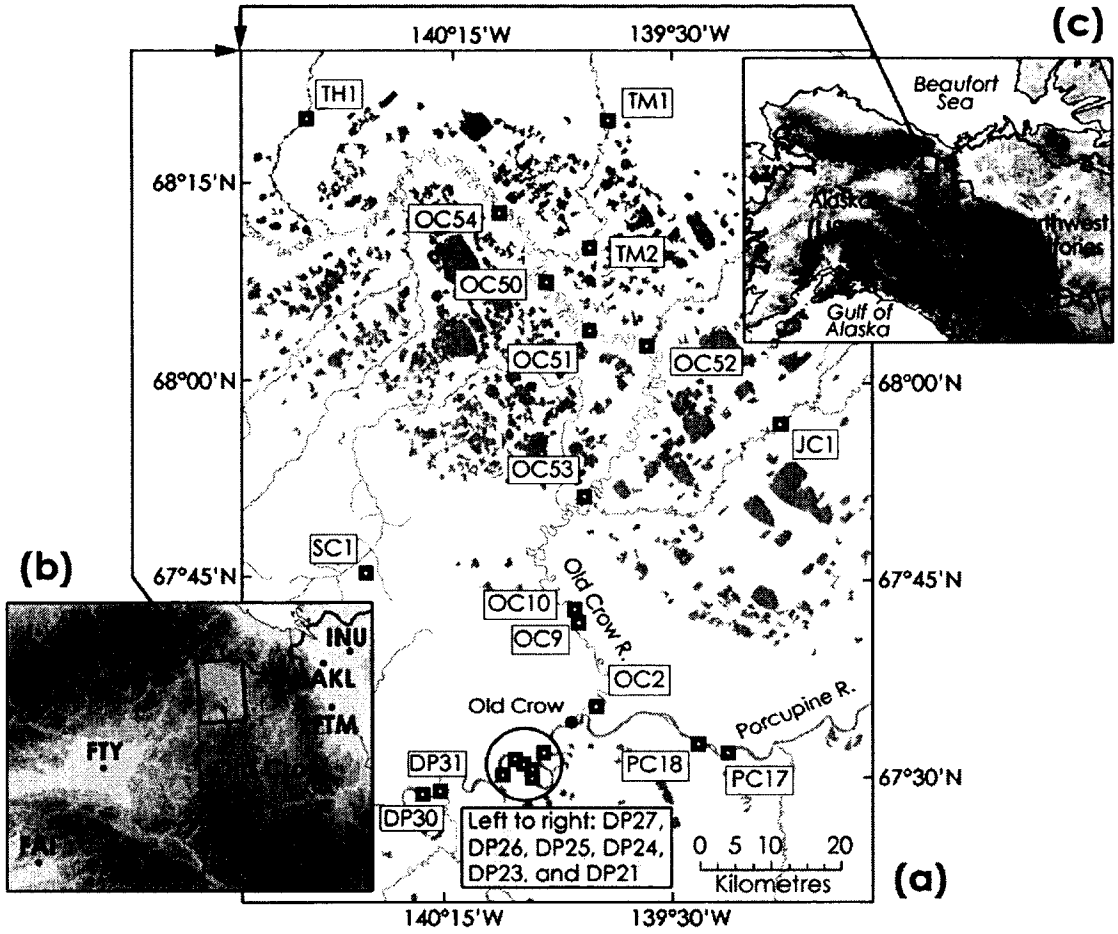

Figure 3.1. (a) White spruce sites sampled in Old Crow Flats (site codes indicated, see Table 3.1). Major lakes and channels are shaded grey. (b) Climate stations at Fairbanks (FAI), Fort Yukon (FTY), Inuvik (INU), Aklavik (AKL), and Fort McPherson (FTM). (c) Large-scale context of Old Crow Flats. Boreal treeline was delineated in (b) and (c) from the Circumpolar Arctic Vegetation Map dataset (Walker et al. 2005). The shaded relief in panels (b) and (c) is based on the GTOPO30 digital elevation model (U.S. Geological Survey; http://www1.gsi.go.jp/geowww/globalmap-gsi/gtopo30/gtopo30.html) and differentiates between low (light grey) and high (dark grey) elevations.

and covered by thick organic layers underlain by fine-to-coarse fluvial deposits (Hughes and Rampton, 1971). White spruce forests in the region are generally found on floodplains while black spruce (*Picea mariana* [Mill.] BSP) forests tend to occupy poorly drained areas amongst the lakes.

Old Crow Flats is in the continuous permafrost zone (Heginbottom et al., 1995). Climate is highly seasonal (Fig. 3.2) with dry, stable Arctic air dominating during winter, and relatively warm, moist air from the North Pacific and Beaufort Sea during summer (Dyke, 2000). Mean annual, winter (Dec-Feb), and summer (Jun-Aug) temperatures at Old Crow are -9.0°C, -28.6°C, and 12.6°C, respectively (http://www.climate.weatheroffice.gc.ca). Minimum (maximum) temperatures are below freezing for all months except June-August (May-September) (Fig. 3.2). Despite its abundance of lakes, annual precipitation at Old Crow Flats is low compared to other northern regions with only parts of the Canadian Arctic Archipelago and northern Greenland receiving less precipitation per annum (Serreze and Barry, 2005). Old Crow receives ca. 265 mm of precipitation annually, ca. 38 mm during winter, and ca. 119 mm in summer (Fig. 3.2).

3.2.2 Tree-ring data

Twenty-three white spruce stands were sampled in 2007 and 2008 (Fig. 3.1a); all sites are situated within 150 km of latitudinal treeline. General sampling locations were preselected so that sites would be distributed across the region. In the field, mature sites were preferentially sampled to maximize the length of resultant tree-ring chronologies. Mature sites were identified based on tree morphology and abundance of deadwood. All

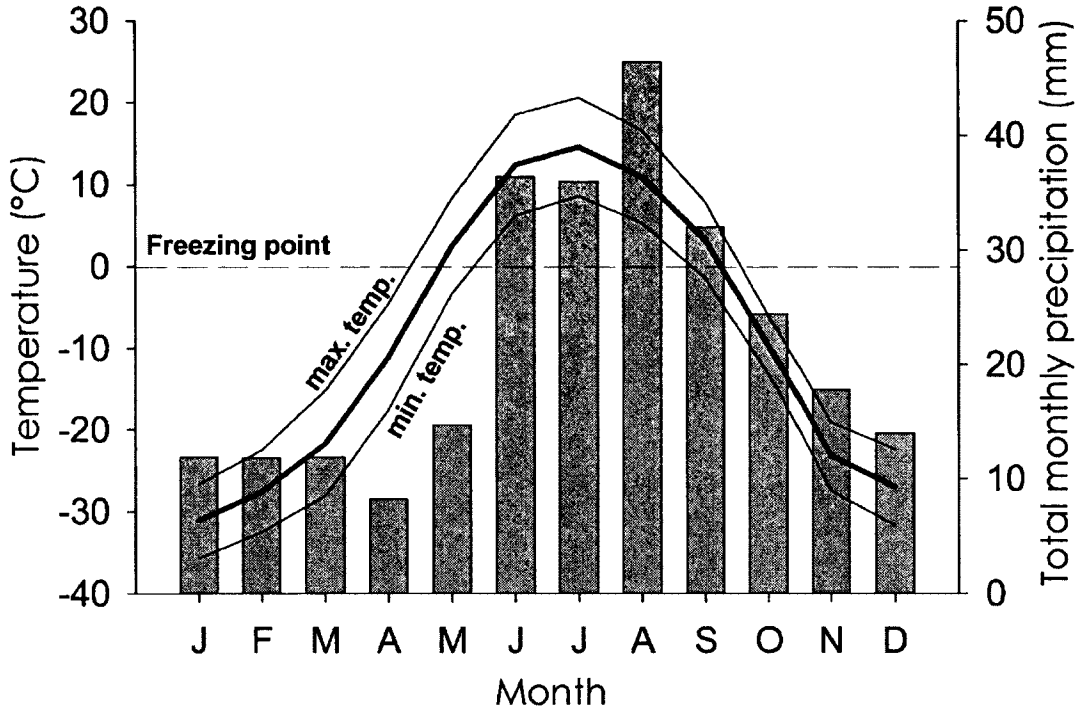

Figure 3.2. Monthly normals (1971-2000) for minimum, mean, and maximum temperatures (lines), and total precipitation (bars) at Old Crow, Yukon Territory (http://www.climate.weatheroffice.ec.gc.ca).

sites shared a similar open canopy structure such that light could easily penetrate to ground level, and a comparable assemblage of shrubs, mosses, grasses, and lichens. All sites except TM2 and SC1 are situated on channel floodplains. TM2 is situated on a hill known locally as Timber Hill and faces south-west; SC1 is a relatively high-elevation site (ca. 647 m a.s.l. compared to ca. 267 m a.s.l. on average for the other sites; Table 3.1) in the Old Crow Range and faces north-east. The remaining sites have no particular aspect.

On average, 33 trees were sampled per site, most of which (ca. 80%) were living. Increment cores were collected from living trees, and cookies were collected from dead trees. Standard techniques were used to collect and prepare tree-ring samples for ring-width measurement (Speer, 2010). Rings were visually cross-dated and measured using a Velmex tree-ring system (precise to 0.001 mm). Two radii per tree were measured in all but a few cases. Cross-dating accuracy was verified using the program COFECHA (Holmes, 1983). Age-related trends were removed using standard data-adaptive negative exponential or negative to zero slope linear curve fits (Fritts et al., 1969). A 'signal-free-enabled' version of the program ARSTAN (courtesy of Ed Cook, Lamont-Doherty Earth Observatory Tree-Ring Laboratory) was used to calculate standard tree-ring indices according to the 'signal-free standardisation' approach described by Melvin and Briffa (2008). Mean site chronologies were calculated using the robust bi-weight mean (Cook, 1985). Signal-free standardisation was used instead of traditional standardisation because it is ideally suited to avoid 'trend-distortion,' an effect that can distort the common climate signal in tree-ring series, especially toward the modern end of mean site chronologies (Melvin and Briffa, 2008). For some of the sites, trend distortion would be a valid concern if signal-free methods were not used (Appendix B, SI-Figs. 3.1 and 3.2).

Table 3.1. White spruce sites sampled in Old Crow Flats and corresponding tree-ring chronology information.

Site code	Lat. (°N)	Long. (°W)	Elev. (m)	No. series/ trees	First year	Last year	Mean series length (yrs)
DP21	67.53	139.93	251	67/35	1657	2007	199.7
DP23	67.50	139.96	249	46/24	1711	2007	216.1
DP24	67.51	139.96	249	42/22	1735	2006	208.7
DP25	67.52	139.99	251	43/22	1759	2006	163.7
DP26	67.52	140.02	243	36/20	1728	2006	200.5
DP27	67.50	140.06	243	57/29	1608	2007	150.0
DP30	67.48	140.33	244	71/36	1552	2007	247.2
DP31	67.48	140.26	245	80/41	1617	2007	240.6
JC1	67.95	139.14	286	73/37	1744	2007	157.0
OC2	67.59	139.75	258	67/35	1691	2007	149.7
$OC9_a$	67.70	139.81	267	54/27	1618	1846	183.8
$OC9_b$	67.70	139.81	267	50/26	1874	2007	109.2
OC10	67.72	139.82	259	61/32	1719	2006	111.7
OC50	68.13	139.93	282	45/25	1668	2007	184.8
OC51	68.07	139.78	272	84/43	1680	2007	186.6
OC52	68.05	139.59	269	59/31	1749	2007	158.9
OC53	67.86	139.79	265	82/44	1648	2007	189.3
OC54	68.22	140.09	292	42/21	1615	2007	140.3
PC17	67.55	139.41	251	94/49	1803	2006	159.2
PC18	67.53	139.32	251	60/33	1686	2006	203.4
SC1	67.76	140.52	647	56/29	1537	2007	214.4
TH1	68.33	140.75	339	97/50	1650	2007	225.4
TM1	68.34	139.72	315	94/48	1631	2007	223.6
TM2	68.17	139.78	305	77/41	1522	2007	217.4

N.B. – $OC9_a$ and $OC9_b$ belong to the same site, but do not overlap because of a stand replacing fire that occurred just prior to circa A.D. 1850; $OC9_a$ represents a population of trees that died before or during the fire and $OC9_b$ represents the post-burn population.

3.2.3 Temperature-growth analysis

The Old Crow climate record is relatively short (1951-2007) and incomplete. To support a longer comparison with the tree-ring data, a regional composite temperature record was developed from stations in Fairbanks and Fort Yukon in Alaska, and Inuvik, Aklavik, and Fort McPherson from the Mackenzie Delta region of Northwest Territories (Fig. 3.1b). These records compare well with the Old Crow record in terms of trend and interannual variability, and can be used to estimate regional temperatures for Old Crow Flats. Alaskan data were provided by the Alaska Climate Research Center (M. Shulski, 2008, pers. comm.) and Canadian data were obtained from Environment Canada (www.climate.weatheroffice.ec.gc.ca). The records were averaged by region for interior Alaska and the Mackenzie Delta (following normalization), and the regional means were then scaled to the Old Crow record and averaged to create a monthly minimum, mean, and maximum temperature record for the larger region centered on Old Crow Flats. The regional composite spans 1930-2007 (pre-1930 data were not used due to limited spatial coverage). For the average month, regional minimum, mean, and maximum temperatures are well correlated with minimum, mean, and maximum temperatures recorded at Old Crow ($r = 0.88$, 0.91, and 0.88, respectively; $p \leq 0.001$).

Growth-year and previous-year May-August temperatures (1930-2007) were compared to each of the 23 site chronologies to determine their dominant response to temperature. Pearson's Product-Moment Correlation Coefficients (r-values) were used to quantify these relations. Sites that shared a common temperature response were averaged into mean regional chronologies to enhance the common signal and then examined for signs of divergence as observed in neighbouring regions.

3.3 RESULTS

3.3.1 Temperature-growth relations in Old Crow Flats

Correlations between the 23 mean site chronologies and the regional temperature record reveal two primary, and distinctly opposite responses to summer temperature (Table 3.2). In general, all sites are best correlated with June or July temperatures, but roughly half correlate negatively and the other half correlate positively with June or July temperatures (Table 3.2). The negatively correlated sites are most strongly correlated with previous year maximum July temperatures, while the positively correlated sites exhibit their strongest correlations with minimum June temperatures of the growth year. Sites with the negative/positive temperature response are hereafter referred to as 'Group 1'/'Group 2' sites (Table 3.2). Only one site, DP21, had a 'mixed' temperature relation, albeit weak, and could not be differentiated as either Group 1 or Group 2 (Table 3.2). Since the primary focus of this study is regionally-significant growth responses to temperature, the Group 1 and Group 2 chronologies, which are of greater regional importance, are examined further.

3.3.2 Group 1/Group 2 regional growth patterns

The distinction between Group 1 and Group 2 sites is clear in terms of correlation with summer temperature (Table 3.2). In terms of growth index, there are many notable differences and similarities (Fig. 3.3a, b) which are emphasized by comparing the mean Group 1 and Group 2 chronologies (Fig. 3.3c; calculated for all years defined by 2 or more site chronologies). Mean Group 1 and Group 2 chronologies are highly coherent

Table 3.2. Correlations between the 23 Old Crow Flats site chronologies and previous-year June/July maximum temperatures (left) and growth-year June/July minimum temperatures (right) (see Appendix B, SI-Table 3.1 for May-August correlations); only correlations significant at $p \leq 0.05$ (two-tailed) are presented; sites are classed as Group 1/Group 2 if negatively/positively correlated with June/July temperatures.

	Previous year max. temperatures		Growth year min. temperatures	
	June	July	June	July
Mixed				
DP21	-	-0.29	0.31	-
Group 1				
DP27	-0.45	-0.58	-0.28	-0.41
DP30	-0.28	-0.43	-	-
OC9	-0.50	-0.54	-0.42	-0.41
OC10	-0.24	-0.48	-	-
OC50	-0.42	-0.40	-	-
OC52	-0.41	-0.57	-	-0.25
OC53	-0.25	-0.48	-	-
OC54	-0.41	-0.58	-0.31	-0.35
PC18	-0.35	-0.54	-	-0.23
TM1	-	-0.41	-	-
TM2	-0.41	-0.62	-	-
Group 2				
DP23	-	-	0.41	-
DP24	0.35	-	0.54	0.43
DP25	0.35	0.24	0.54	0.48
DP26	0.33	-	0.52	0.38
DP31	-	-	0.48	0.27
JC1	-	-	0.39	-
OC2	-	-	0.44	0.26
OC51	0.24	-	0.57	0.45
PC17	0.38	0.25	0.54	0.41
SC1	0.34	-	0.53	0.43
TH1	0.24	-	0.58	0.42
Regional means				
Group 1	-0.42	-0.61	-	-0.24
Group 2	0.28	-	0.57	0.40

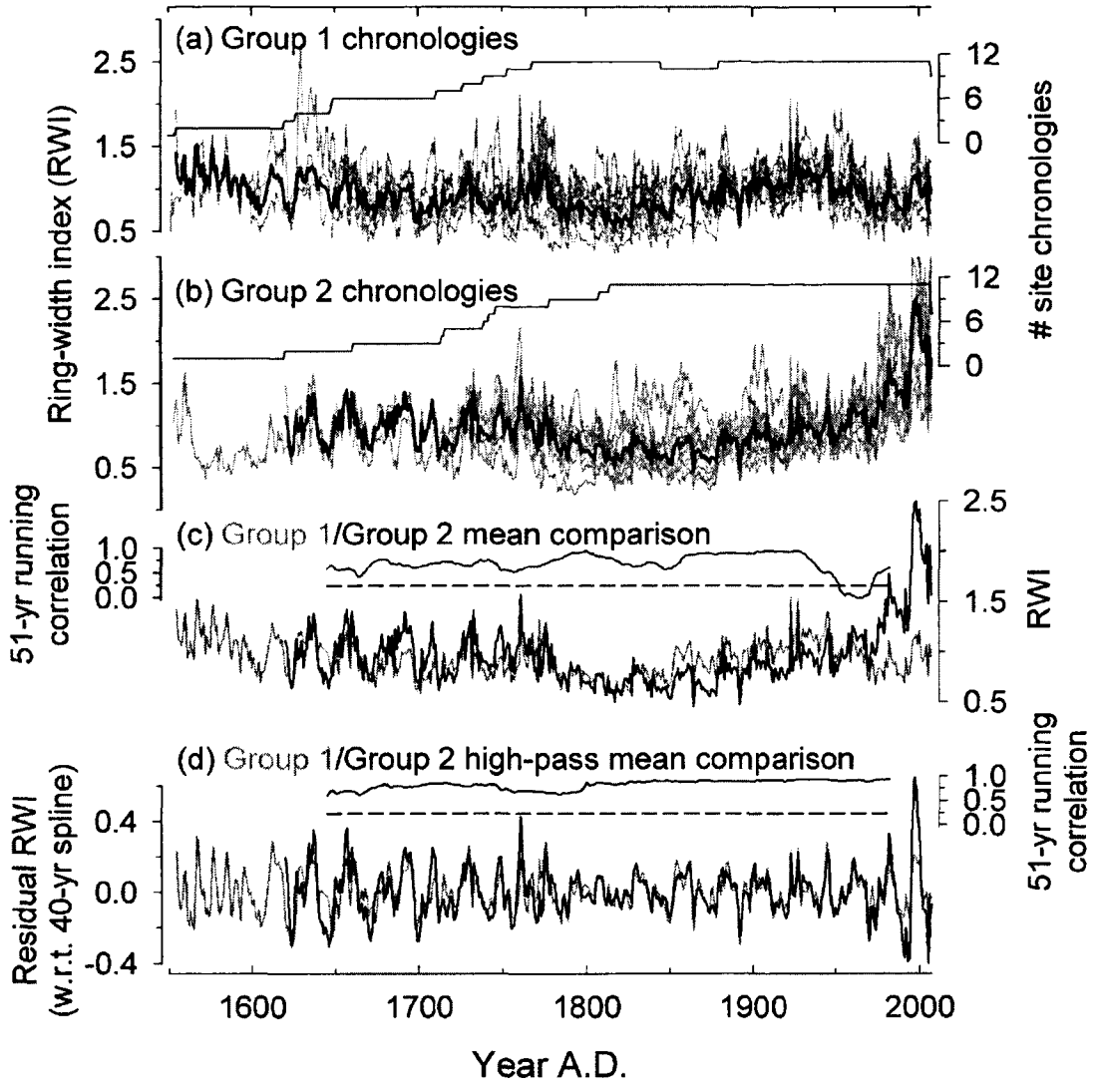

Figure 3.3. (a/b) Group 1/Group 2 site chronologies (grey lines); all site chronologies are defined by ≥ 4 series (≥ 2 trees). The mean Group 1/Group 2 chronologies (black lines) were calculated using a robust bi-weight mean for all years defined by 2 or more site chronologies. Sample depth curves are indicated above each plot. (c) A comparison of the mean Group 1 (1555-2007) and Group 2 (1620-2007) chronologies. The running 51-year correlation (above plot) indicates coherence between the chronologies (dashed line is $p \leq 0.05$ level). (d) High-pass filtered (40-year cubic smoothing spline, 50% frequency cut-off; Cook and Peters 1981) comparison of the mean Group 1 and Group 2 chronologies; the high-pass series were smoothed with a 3-year cubic-smoothing spline for ease of comparison.

over the period 1620-1800, as demonstrated by a strong running correlation coefficient (Fig. 3.3c; see also Appendix B, SI-Fig. 3.3a for a magnified comparison).

Both groups began the 19th century at their lowest index values on record and maintained similar growth levels until ca. 1850 before following an upward trend into the 20th century (Fig. 3.3c). However, Group 1 began its upward trend slightly before Group 2 (as early as ca. 1825/1875 for Group 1/Group 2) causing a systematic offset between them until the mid-20th century (Fig. 3.3c; see Appendix B, SI-Fig. 3.3b for a magnified comparison). The significance of these differences was tested using a running 2-sample t-test (see Appendix B, SI-Note 3.1). Significant ($p \leq 0.05$) differences between the Group 1 and Group 2 chronologies are found during 63% of years from 1866-1948. However, despite these growth differences, their respective linear trends were indistinguishable over the period 1866-1948 (+0.043/+0.042 index values per decade for Group 1/Group 2) leading to a strong, stable running correlation (Fig. 3.3c; mean $r = 0.82$).

Important differences emerge after the 1930s. Group 1 reaches its highest growth values on record in the 1930s (Appendix B, SI-Fig. 3.3; 1926-1935 mean index = 1.2) and then declines towards low values in the 1980s. Conversely, Group 2 maintains a positive trend throughout the 20th century and reaches record high growth values at present (Appendix B, SI-Fig. 3.3; 1998-2007 mean index = 2.0). Effectively, this opposing behaviour equates to a 'growth-trend divergence' that is evident in the running correlation which drops below the $p \leq 0.05$ significance level in 1953, reaching its lowest point ($r = -0.02$) in 1966 (Fig. 3.3c). Group 1 growth trends become positive after the 1980s contributing to a small rise in correlation with Group 2. By 1972, correlations become significant again, but remain low relative to pre-1930 correlations (Fig. 3.3c).

While the Group 1 and Group 2 chronologies are very different in the 'low-frequency' domain since the 1930s, the two groups are coherent at higher-frequencies over all periods. To demonstrate this, high-pass filtered mean Group 1 and Group 2 chronologies (40-year cubic smoothing spline; see Cook and Peters, 1981) were compared. The comparison shows that both groups exhibited the same high-frequency growth variations over the last 400 years, even after the post-1930s growth trend divergence described above (Fig. 3.3d).

3.3.3 Group 1/Group 2 vs. temperature

As with their constituent site chronologies, the mean Group 1 and Group 2 chronologies are most strongly correlated with previous-year July maximum and growth-year June minimum temperatures, respectively (Table 3.2). A visual comparison of the mean group chronologies versus their most closely associated temperature index shows no apparent signs of temperature-growth divergence during recent decades of the 20th century (Fig. 3.4), as observed in other parts of NWNA. From the 1930s to 1980s, Group 1 growth declined as July maximum temperatures increased, but rebounded from the 1980s to present as July temperatures cooled slightly (Fig. 3.4). Contrary to July maximum temperatures, June minimum temperatures have increased steadily since the 1930s, a trend that is matched by the Group 2 growth response (Fig. 3.4).

3.3.4 Larger-scale significance of Group 1/Group 2

To determine if the contrasting Group 1 and Group 2 growth patterns are a local phenomenon or reflective of larger-scale growth patterns, long white spruce ring-width

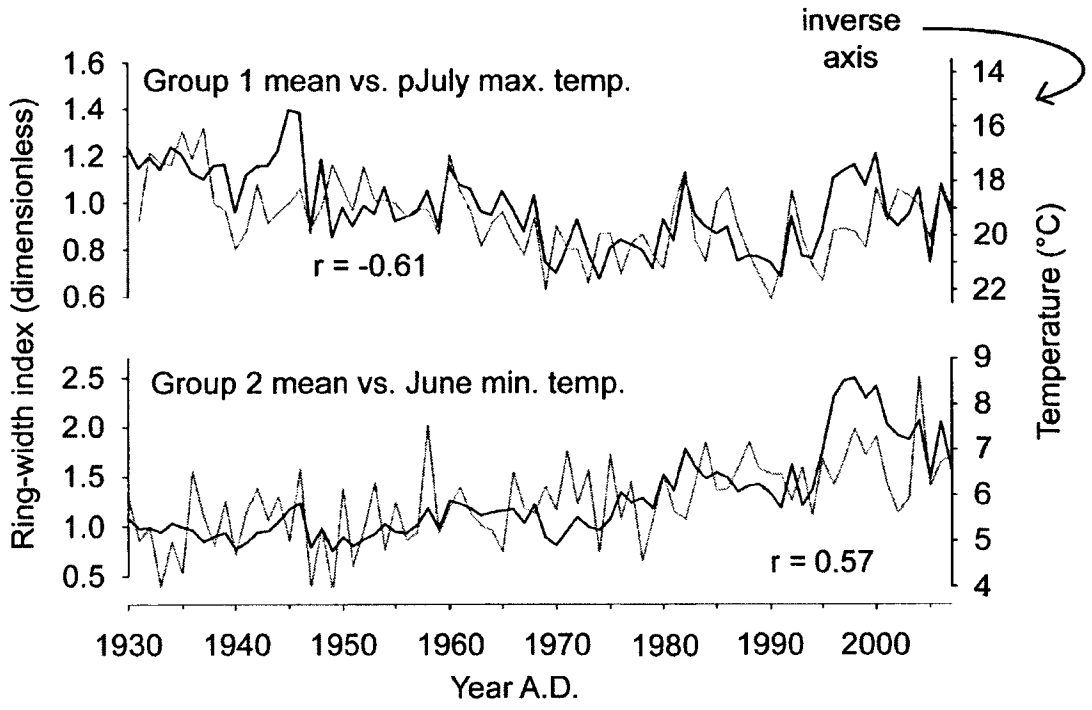

Figure 3.4. Comparisons between mean Group 1/Group 2 (black lines) and previous-year July maximum/growth-year June minimum temperatures (grey lines); correlations are significant at $p \leq 0.001$.

series from adjacent parts of NWNA (Fig. 3.5) were obtained from the International Tree Ring Databank (ITRDB; http://www.ncdc.noaa.gov/paleo/treering.html) and other sources (Table 3.3), and compared to the mean Group 1 and Group 2 chronologies. Only chronologies spanning 1700-1975 were considered in order to assess long-term growth coherence. Also, a number of spatial criteria were considered to determine which sites were used. To avoid sites with a strong maritime climate (e.g., Gulf of Alaska coastline; see L'Heureux et al., 2004; Serreze and Barry, 2005), only sites above 65°N were used. The longitudinal range of sites extends eastward from the west coast of Alaska to 115°W. This spatial range coincides with sites near boreal treeline where tree growth is expected to be temperature-limited. The ITRDB has 26 chronologies matching the spatiotemporal criteria (Fig. 3.5; Table 3.3). Further, 2 'sub-population' chronologies developed from hundreds of white spruce trees at several sites in the Mackenzie Delta (Pisaric et al., 2007; Fig. 3.5; Table 3.3) were used. All 28 'NWNA chronologies' were processed using signal-free standardisation as outlined in the Methods section.

The NWNA chronologies were considered comparable to Group 1 and Group 2 if they met the following criteria: (1) correlates positively and significantly ($p \leq 0.01$) with both Group 1 and Group 2 from 1850-1930; and (2) correlates positively and significantly with only one of Group 1 or Group 2 from 1930-present. Based on these criteria, 14 NWNA chronologies are not similar to Group 1 or Group 2 (Table 3.3; sites 02-03, 05-13, 15, 18, & 25), 11 of which (sites 02-03, & 05-13) are clustered in a small area (ca. 8 km radius) on the Seward Peninsula, Alaska. Of the remaining 14 NWNA chronologies, 7 are similar to Group 1: sites 14, 17, 19-21, & 23-24 (Table 3.4); hereafter, these chronologies, including the mean Group 1 chronology, are referred to as

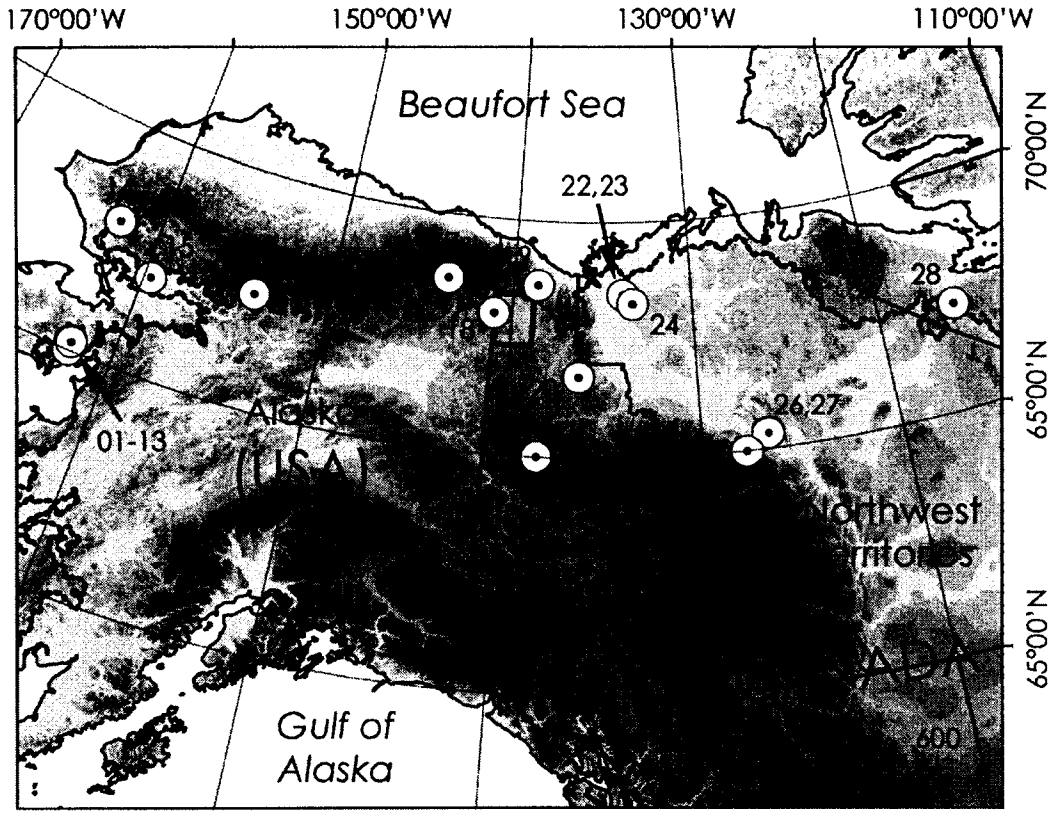

Figure 3.5. Locations of all NWNA site chronologies compared to the mean Group 1/Group 2 chronologies (site numbers indicated, refer to Table 3.3). The shaded relief is based on the GTOPO30 global digital elevation model (U.S. Geological Survey; http://www1.gsi.go.jp/geowww/globalmap-gsi/gtopo30/gtopo30.html) and differentiates between low (light grey) and high (dark grey) elevations.

Table 3.3. List of 300+ year white spruce ring-width chronologies from upper NWNA (65-70°N, 115-170°W) that were compared to the mean Group 1 (G1)/Group 2 (G2) chronologies from Old Crow Flats. Correlations with G1/G2 were calculated for all years of overlapping data for the periods 1850-1930 and 1930-2003; only positive correlations significant at $p \leq 0.01$ (one-tailed) are provided. Site no. corresponds to the map of NWNA sites (Fig. 3.5). Mean chronologies for each NWNA site were calculated from raw ring-width data using signal-free standardisation as outlined in the Methods section. All ring-width files were downloaded from the ITRDB unless stated otherwise.

Site no.	Site name, ITRDB code	Temporal coverage	Correlation with G1/G2			
			1850-1930		1930-2003	
			G1	G2	G1	G2
01	Almond Butter Lower, AK057	1607-2002	0.26	0.32	-	0.58
02	Almond Butter Upper, AK058	1406-2002	-	-	-	-
03	Alpine View, AK059	1542-2002	-	-	-	-
04	Burnt Over, AK060	1621-2002	0.27	0.29	-	0.46
05	Bye Rosanne, AK061	1575-2002	-	-	0.47	-
06	Death Valley, AK062	1358-2002	-	-	-	-
07	Echo Slope, AK063	1590-2002	-	-	-	-
08	Frost Valley, AK064	1611-2002	-	-	0.31	-
09	Gordon's Cat, (AK065	1400-2002	-	-	-	-
10	Hey Bear, AK066	1533-2002	-	-	-	-
11	Hey Bear Upper, AK067	1383-2002	-	-	-	-
12	Mt. Mole, AK068	1550-2002	-	-	-	-
13	Windy Ridge, AK070	1556-2002	-	-	-	-
14	[a]Four-Twelve with Revisit, AK031	1515-1990	0.55	0.51	0.63	-
15	[b]Kobuk/Noatak, AK046	978-1992	-	-	0.36	0.29
16	[a]Arrigetch, AK032	1585-1990	0.41	0.39	-	0.50
17	Sheenjek River and Flats, AK033	1296-1979	0.41	0.37	0.51	-
18	[c]Firth River, AK047	1676-2002	0.71	0.71	-	-
19	Spruce Creek, CANA029	1570-1977	0.34	0.26	0.48	-
20	[d]Richardson Mountain, CANA121	1547-1992	0.64	0.65	0.59	-
21	[a]Twisted Tree Heartrot Hill, CANA157	1459-1999	0.65	0.66	0.69	-
22	[e]MDEC Positive Responders	1516-2003	0.77	0.82	-	0.86
23	[e]MDEC Negative Responders	1501-2003	0.72	0.73	0.82	-
24	[f]Campbell Dolomite Upland, CANA138	1060-1992	0.56	0.45	0.67	-
25	Mackenzie Mountains, CANA156	1509-1984	-	-	0.69	-
26	Franklin Mountains, CANA154	1621-1984	0.39	0.34	-	0.45
27	[d]Discovery Ridge, CANA117	1429-1991	0.35	0.26	-	0.63
28	[a]Coppermine River, CANA153	1046-2003	0.53	0.59	-	0.29

Data contributors by site #: Church and Fritts (19); D'Arrigo, Mashig, Frank, Wilson, and Jacoby (01-13); Jacoby, D'Arrigo, and Buckley (14, 16-17, 21, 25-26, and 28); King and Graumlich (15); Pisaric (22-23); Szeicz and MacDonald (27); Szeicz, MacDonald, and Lundberg (20 and 24); Wilmking (18).

[a]Updated versions of sites 14, 16, 21, and 28 (not yet available on ITRDB) were provided by R. D'Arrigo (pers. comm.).

[b]Kobuk/Noatak is a regional (ca. 24,000 km^2 area) composite developed from hundreds of trees in the Kobuk and Noatak River basins.

[c]Cross-dating verification using COFECHA indicated that two of the Firth River series (BRFR49 & 88) should be adjusted -1 year. The possibility these series were misaligned was confirmed by M. Wilmking (pers. comm., Sept. 2010). Adjusting these series increased their correlation with the BRFR49/88 master chronologies from 0.03/0.11 to 0.40/0.41.
[d]As per Szeicz and MacDonald (1995), only 200+/100+ year series for Discovery Ridge/Richardson Mountain were used.
[e]MDEC (Mackenzie Delta East Channel) represents several sites in the Mackenzie Delta whose individual series were pooled into 'positive- or negative-responder' chronologies (Pisaric et al. 2007). The Positive and Negative Responder chronologies used here are modified versions of the originals used by Pisaric et al. (2007); see Appendix B, SI-Note 3.2 for more details.
[f]A subset (11 trees) of samples collected by Szeicz, MacDonald, and Lundberg from Campbell Dolomite Upland was developed into a separate 'Campbell Dolomite Upland B' chronology by F. Schweingruber and is available on the ITRDB. Here only the Szeicz, MacDonald, and Lundberg version was used because of its much larger sample depth.

'NWNA 1 chronologies' (Fig. 3.6a). The other 7 NWNA chronologies are similar to Group 2: sites 01, 04, 16, 22, & 26-28 (Table 3.4). These chronologies, plus the mean Group 2 chronology, are now referred to as 'NWNA 2 chronologies' (Fig. 3.6b).

A comparison of the mean NWNA 1 and NWNA 2 chronologies reveals the same general observation seen with the Old Crow Flats tree-ring data. NWNA 1 and NWNA 2 had a coherent growth pattern from AD 1550 until the mid-20th century, after which the mean chronologies diverge from one another (Fig. 3.6c). This is reflected in the strong running correlation from 1550-1930 and the subsequent decline to non-significant values by 1957 (Fig. 3.6c). Unlike with Group 1 and Group 2, NWNA 1 and NWNA 2 have very little offset from 1866-1948 (Fig. 3.6c); only 10% of the years over this period are significantly different based on a running 2-sample t-test (Appendix B, SI-Note 3.1). A second important difference between the Old Crow Flats and the NWNA chronologies is that the timing of mid-20th-century divergence differs slightly. NWNA 1 sites do not peak until ca. 1950s, which is roughly 2 decades later than the Group 1 sites in Old Crow Flats. Lastly, as was found in Old Crow Flats, high-frequency growth patterns at the NWNA-scale were coherent over all periods (Fig. 3.6d) suggesting that growth trend divergence is exclusively a low-frequency phenomenon.

3.3.5 NWNA 1/ NWNA 2 vs. temperature

Given their similarity to Group 1/Group 2, it seems plausible that NWNA 1/NWNA 2 may also represent negative/positive responses to 20th-century summer temperature. Indeed, this idea is supported by independent climate-growth analyses for

Table 3.4. NWNA chronologies that meet the following two similarity criteria: (1) correlates positively and significantly ($p \leq 0.01$) with both Group 1 and Group 2 from 1850-1930; and (2) correlates positively and significantly with only one of Group 1 or Group 2 from 1930-present. Chronologies that meet these criteria and are most closely associated with Group 1/Group 2 during 1930-2003 are classed as NWNA 1/NWNA 2 chronologies.

NWNA 1 chronologies
Campbell Dolomite Upland
Four-Twelve with Revisit
MDEC Negative Responders
Richardson Mountain
Sheenjek River and Flats
Spruce Creek
Twisted Tree Heartrot Hill
NWNA 2 chronologies
Almond Butter Lower
Arrigetch
Burnt Over
Coppermine River
Discovery Ridge
Franklin Mountains
MDEC Positive Responders

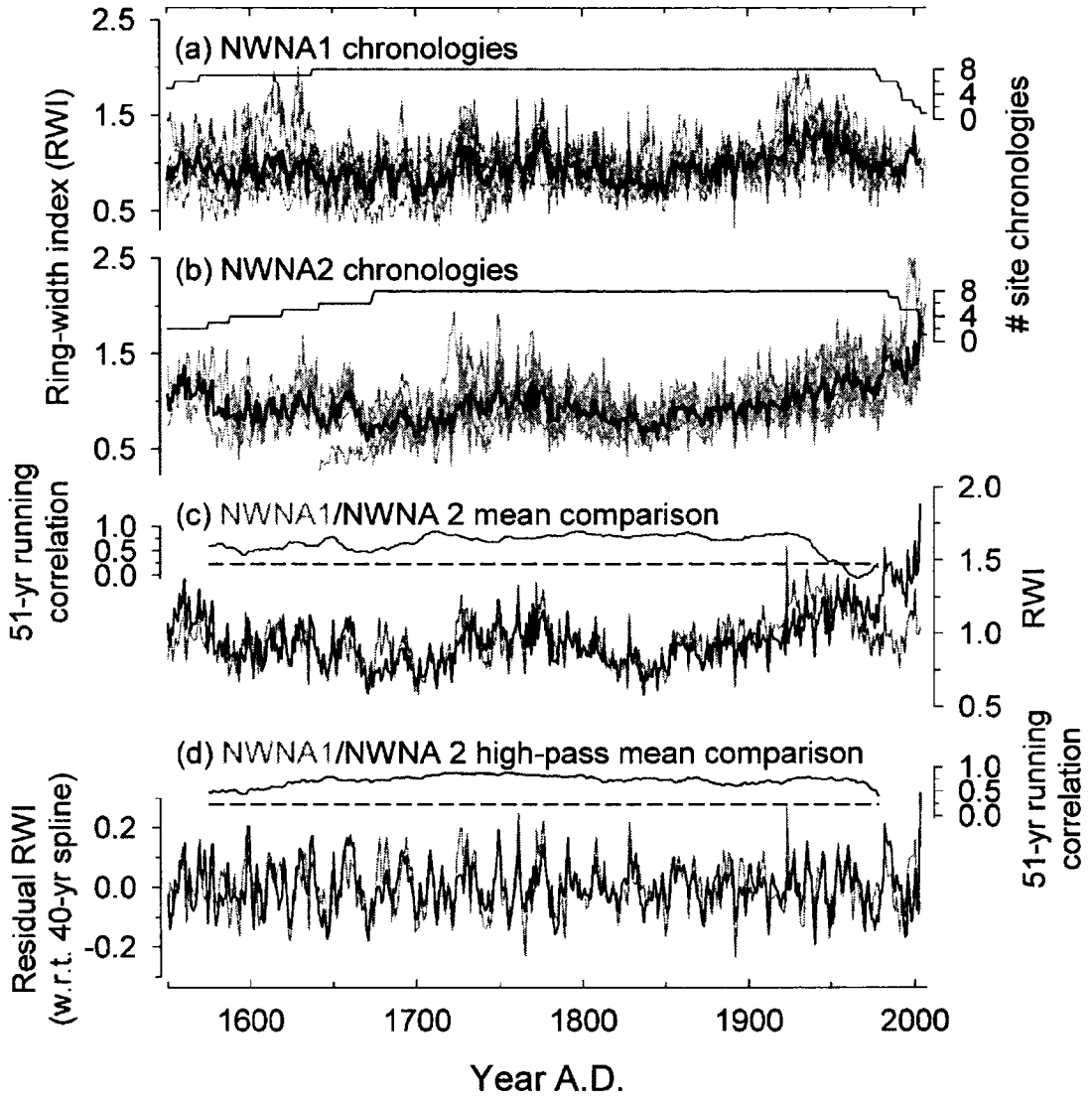

Figure 3.6. (a/b) NWNA 1/NWNA 2 site chronologies (Table 3.4; including the mean Group 1/Group 2 chronologies) (grey lines); all site chronologies are defined by a minimum of 4 series from at least two different trees. The mean NWNA 1/NWNA 2 chronologies (black lines) were calculated using a robust bi-weight mean for all years defined by a minimum of two site chronologies. Sample depth curves are indicated above each plot. (c) A comparison of the mean NWNA 1 and NWNA 2 chronologies. The running 51-year correlation (above plot) indicates coherence between the chronologies (dashed line is $p \leq 0.05$ level). (d) High-pass filtered (40-year cubic smoothing spline, 50% frequency cut-off; Cook and Peters 1981) comparison of the mean NWNA 1 and NWNA 2 chronologies; the high-pass series were smoothed with a 3-year cubic-smoothing spline for ease of comparison.

several of the NWNA 1/NWNA 2 site chronologies (Szeicz and MacDonald, 1994, 1996; D'Arrigo et al., 2004; Pisaric et al., 2007; Visser et al., 2010). At broader scales, this is supported by correlations between the mean NWNA 1/NWNA 2 chronologies and a composite of gridded mean monthly temperatures for the greater NWNA region derived from the CRUTEM3v dataset (Brohan et al., 2006; see Appendix B, SI-Note 3.3 for details on the composite).

Overall, NWNA 1 sites were most strongly and negatively correlated with previous-year July temperatures over the last century (1900-2003), as with Group 1 in Old Crow Flats (Table 3.5). However, NWNA 1's temperature-growth relation was not stable over the 20th century as demonstrated by a split-period analysis (Table 3.5). NWNA 1 sites shared a significant positive relation with growth-year June/July average temperatures in the early-20th century (1900-1950), and a significant inverse relation with prior-year July temperatures in the late-20th century (1951-2003) (Table 3.5). This transition from a positive to negative temperature response is effectively illustrated with a plot of NWNA 1 versus June/July temperatures (Fig. 3.7). However, because of the gradual, low-frequency nature of the change, and of the temperature-growth relation itself, it is difficult to pinpoint the timing of temperature-growth divergence with any precision. Based on a visual inspection of the data, the early-1960s appear to be a reasonable approximation (Fig. 3.7). Conversely, NWNA 2 sites responded positively to growth-year June/July temperatures during both the early- and late-20th century (Table 3.5; Fig. 3.7).

Table 3.5. Correlations between the mean NWNA 1/NWNA 2 chronologies and regional mean monthly CRUTEM3v temperatures (Brohan et al. 2006; see Appendix B, SI-Note 3.3); correlations for May-August of the prior and current growth years are provided for three periods: 1900-2003, 1900-1950, and 1951-2003; all correlations are significant at $p \leq 0.05$ (two-tailed); underlined coefficients are significant at $p \leq 0.01$.

		NWNA1			NWNA2		
		1900-2003	1900-1950	1951-2003	1900-2003	1900-1950	1951-2003
Year t-1	May	-	-	-	0.34	-	-
	Jun	-	-	-	0.41	-	0.40
	Jul	-0.36	-	-0.40	0.29	-	-
	Aug	-	-	-	0.21	-	-
Year t	May	-0.20	-	-0.30	0.20	-	-
	Jun	-	0.53	-	0.54	0.47	0.46
	Jul	-	0.39	-	0.54	0.41	0.36
	Aug	-	0.20	-	0.21	-	-

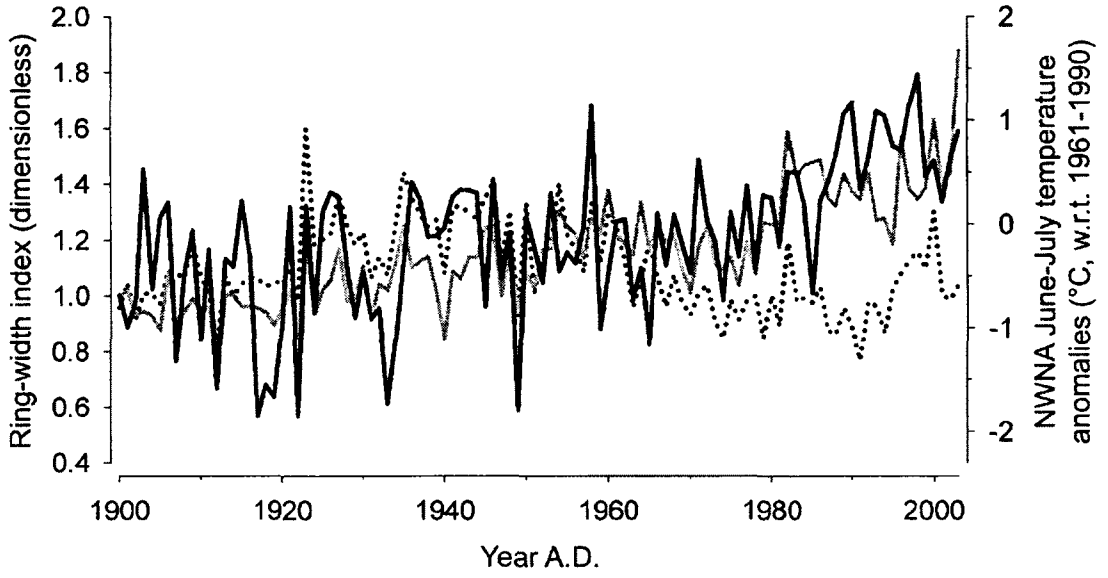

Figure 3.7. Comparison between the mean NWNA 1 (dotted)/NWNA 2 (grey) chronologies and NWNA-scale June/July instrumental temperature anomalies (solid black line). Temperature anomalies were calculated from the CRUTEM3v dataset (Brohan et al., 2006).

3.3.6 Long-term temperature-growth relations in NWNA

As both NWNA 1 and NWNA 2 had a positive temperature response before the mid-20th century, it seems likely that the NWNA 1 growth pattern represents an anomalous temperature response. Although, this idea lacks long-term verification from NWNA instrumental data which are largely restricted to the 20th century. Alternatively, a simple comparison against the mean of 6 Northern Hemisphere (NH) temperature reconstructions since AD 1300 provides independent verification (Fig. 3.8a and 3.8b). NWNA 1 and NWNA 2 track NH temperatures well before the mid-20th century (Fig. 3.8b) suggesting their pre-divergence growth was a positive function of temperature. It is important to note that some site chronologies that constitute the mean NWNA chronologies were also used in some of the NH reconstructions; however, the contribution of the shared chronologies to the overall variance of the NH reconstructions is negligible. In other words, virtually all of the coherence between NWNA 1/NWNA 2 and NH temperatures is from independent data. Finally, as was the case with NWNA 1 versus NWNA temperatures (Fig. 3.7), NWNA 1 failed to track NH temperatures since the mid-20th century (Fig. 3.8).

3.4 DISCUSSION

3.4.1 Implications and timing of growth trend divergence

Evidence of widespread growth trend divergence in NWNA is presented above. The Group 1 and Group 2 chronologies showed similar growth patterns prior to the 1930s, but one of two contrasting patterns since then. This growth trend divergence (negative/positive trends) is the main distinction between Group 1 and Group 2 since the

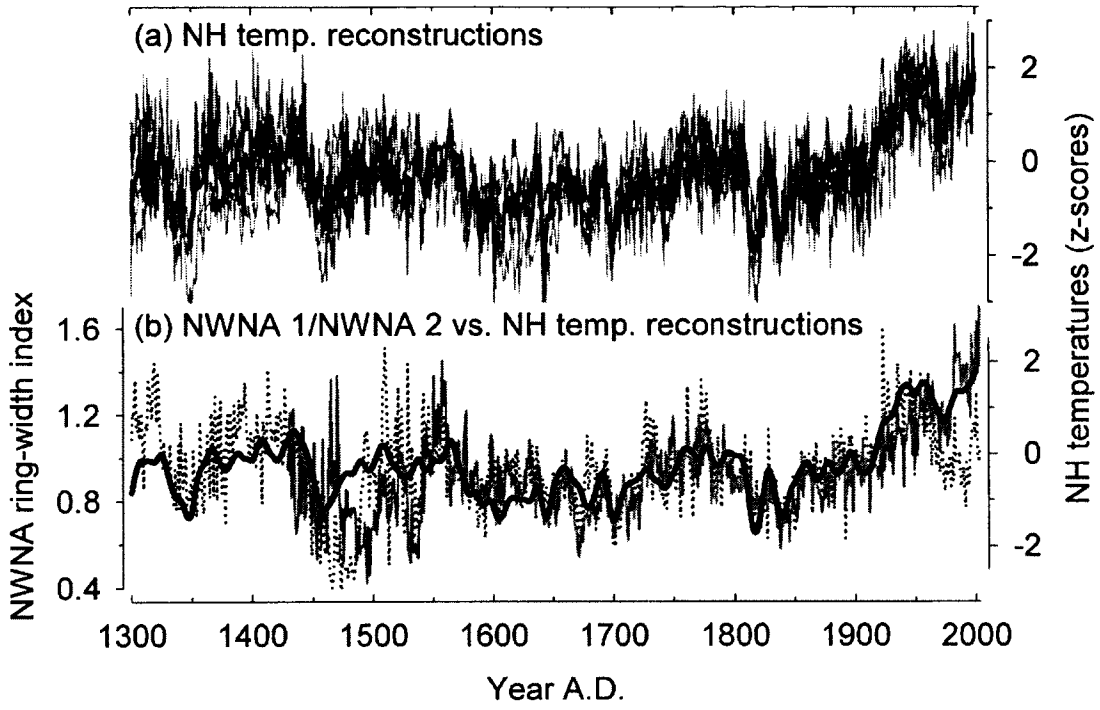

Figure 3.8. (a) Northern Hemisphere (NH) temperature reconstructions by Jones et al. (1998), Briffa (2000), Esper et al. (2002), D'Arrigo et al. (2006), Wahl and Ammann (2007), Wilson et al. (2007) (grey lines); mean reconstruction (black line). The reconstructions were expressed as z-scores relative to the common period of overlap (1750-1980). (b) Comparison of the mean NH temperature reconstruction (thick black line; smoothed with 15-year cubic smoothing spline, Cook and Peters 1981) against the mean NWNA 1 (dotted)/NWNA 2 (grey line) chronologies. The mean NWNA chronologies are defined by a minimum of 2 site chronologies.

1930s. At larger scales, this growth trend divergence was replicated using 14 white spruce chronologies across NWNA, although the timing of divergence was the 1950s. The coherence of these chronologies before divergence implies that they were responding to a similar regional climatic factor; however, their contrasting behaviour since implies that one of the groups diverged from its former response to climate.

Due to the instrumental data limitations in Old Crow Flats it was not possible to directly assess the implied climate-growth response change for Group 1/Group 2 sites. Yet, the NWNA-scale analysis did reveal that NWNA 1 sites transitioned from a positive to negative temperature response in the mid-20th century, while NWNA 2 sites maintained a stable positive temperature response throughout the 20th century. A comparison against reconstructed Northern Hemisphere temperatures confirmed that all sites, including NWNA 1 sites, shared a positive temperature response prior to 20th-century divergence.

The more recent negative temperature response shared by NWNA 1 trees is contrary to expectations of trees in temperature limited environments, and appears to suggest that temperature is now negatively influencing growth. A possible explanation for this negative response could be temperature-induced drought stress, as suggested by others (Jacoby and D'Arrigo, 1995; Barber et al., 2000; Wilmking et al., 2004; McGuire et al., 2010), where recent climate warming may be causing a moisture shortage due to enhanced evapotranspiration, which then limits tree-ring growth. Another observation that deserves attention is the fact that the negative temperature-growth response is strongest in July of the previous growing season. The biological origin of this 'previous year' response may be manifest through a photosynthate carryover effect, whereby

favourable growing conditions during the previous year translate into a surplus of photosynthates, which are then cached in roots and other tissues to augment growth during the following growing season (Mooney and Billings, 1960; Kozlowski, 1992). If the negative temperature-growth response is due to temperature-induced drought stress, warmer years could in fact reduce the carryover of photosynthates from one year to the next.

As reported elsewhere (Jacoby and D'Arrigo, 1995; Briffa et al., 1998b; Cook et al., 2004; D'Arrigo et al., 2004, 2008), the NWNA results largely support the idea that temperature-growth divergence is a mid-20th-century phenomenon. However, there does appear to be some variability in timing. For example, in Old Crow Flats, Group 1/Group 2 sites began to trend in opposite directions as early as the 1930s. Briffa et al. (1998) and Pisaric et al. (2007) also found that some regions may have diverged in the 1930s.

On a more cautious note, there is some indication that Group 1 sites began to separate from Group 2 sites in terms of temperature sensitivity during the 19th century given their offset index values thereafter. At the NWNA-scale, this offset was less apparent, but it was evident. Similarly, sub-population (i.e., intra-site dynamics) studies in Alaska have also found evidence of growth pattern divergence during the 19th century (Wilmking et al., 2004). However, in Old Crow Flats, this offset may not represent a true temperature-growth divergence given that Group 1 and Group 2 have virtually identical linear trends over their period of offset. This parallel behaviour suggests Group 1 and Group 2 responded to climate in the same manner over this period, but that they had slight differences in terms of climatic sensitivity. Furthermore, the possibility it is a detrending artefact should not be discounted, due to the difficulty in separating age-

related trend from two very different externally-forced 20th-century growth patterns, one peaking in the 1930s and another with a strong late-century increase. Regardless of its nature, the offset does not imply a major change in temperature-growth response. By contrast, 20th-century growth trend divergence implies a temperature-growth response reversal for some sites.

3.4.2 Long-term stability of temperature-growth relations

Divergence has been the subject of on-going research for nearly two decades (D'Arrigo et al., 2008). From a paleoclimatology perspective, it is important to better understand the spatiotemporal extent of the phenomenon, its causes, and the likelihood it has impacted past growth. In turn, such insight would help determine the extent to which affected chronologies can be used to provide robust estimates of past temperature. Current understandings of divergence remain tenuous due to the limited number of datasets affected by divergence and the co-linearity of potential contributing environmental factors (D'Arrigo et al., 2008). However, a growing body of evidence suggests that divergence may be caused by the anomalously warm temperatures of the 20th century (Jacoby and D'Arrigo, 1995; Barber et al., 2000; D'Arrigo et al., 2004; Wilmking et al., 2004; Pisaric et al., 2007) which likely have been unmatched in the last 2000 years (Kaufman et al., 2009).

The idea that divergence is unique to the 20th century does have some empirical support. Based on their comparison of divergent northern site chronologies with a number of other temperature-sensitive hemispheric chronologies, Cook et al. (2004) concluded that 20th-century divergence is unique in the context of the last 1100 years.

Similarly, the comparison of the NWNA chronologies to reconstructed NH temperatures suggests that 20th-century divergence is unique in the context of the last 700 years, at least. In fact, the coherence between the NWNA 1/NWNA 2 chronologies and NH temperatures prior to divergence is remarkable considering the spatial-scale differences (i.e., NWNA vs. NH) and the well documented regional-heterogeneity of NH temperatures over past centuries (D'Arrigo et al., 2006; Mann et al., 2009). One notable exception occurs during the late 1400s when the NWNA chronologies indicate a cool period. This period corresponds with the well known Spörer minimum (Stuiver, 1961; Bard et al., 2000), one of the longest and most pronounced solar minima of the past millennium. It is possible that regional climate differences occurred during this period, which may explain the temporary departure between the NWNA chronologies and the hemispheric mean.

3.4.3 Large-scale drivers of divergence

The results support the notion that divergence in NWNA is unique to the 20th century suggesting that it was caused by a large-scale environmental or climatic change that is also unique to the 20th century. Several large-scale factors have been proposed including: temperature-induced drought stress (Jacoby and D'Arrigo, 1995; Barber et al., 2000; Lloyd and Fastie, 2002; Wilmking and Juday, 2005; McGuire et al., 2010), biological temperature thresholds (D'Arrigo et al., 2004; Wilmking et al., 2004), snow cover changes (Vaganov et al., 1999), UV-B changes (Briffa et al., 2004), and global dimming (D'Arrigo et al., 2008). Depending on the region, divergence may have been caused by one, all, or a combination of these factors. However, negative temperature-

growth relations in NWNA have been linked to regional moisture gradients (Wilmking and Juday, 2005; Lloyd and Bunn, 2007) implying that the divergence may be caused by moisture stress. NWNA is already limited in terms of its annual precipitation budget, and the strong 20th-century warming in this region (ACIA, 2005) has likely placed an even greater moisture limitation on these forests.

Another large-scale factor that may have contributed to divergence in NWNA but that has been absent in most published discussions of the phenomenon is Pacific-derived moisture. Directional warming was one of the most prominent climate system changes following the mid-19th century in high-latitude regions (Overpeck et al., 1997; Kaufman et al., 2009). However, in NWNA, this warming was accompanied by important moisture changes towards interior NWNA (Anderson et al., 2007, 2011) due to a major atmospheric circulation reorganisation linked to the strength of the Aleutian Low (Fisher et al., 2004; Anderson et al., 2005). This transition led to a relatively dry 20th century in many parts of interior NWNA compared to the last 1200 years (Fisher et al., 2004; Anderson et al., 2011). This reorganisation appears to have been widespread as it coincides with several other large climate system changes in the Pacific basin (Thompson et al., 1986; Mann et al., 2000; Hendy et al., 2002). Although it remains unclear which large-scale factor ultimately caused some sites to diverge, several moisture related factors may be involved including temperature-induced drought stress and reduced Pacific-derived moisture since the mid-19th century.

3.4.4 The role of small-scale factors

Because divergence is found across such a large portion of NWNA, it is clear that it was caused by a large-scale forcing. However, not all sites were affected, some of which are found within a few kilometres of sites that were affected (e.g., DP30 vs. DP31, or DP23-26 vs. DP27; Appendix B, SI-Fig. 3.4). Therefore, it is also clear that site-specific factors determine how each site has been impacted by the putative large-scale forcing that caused divergence. Ecological factors may be particularly important. For example, Wilmking and Juday (2005) reported that sites with lower tree densities tended to have a greater proportion of trees that responded positively to temperature, presumably related to soil moisture competition.

Organic layer thickness may also be important. At a white spruce stand in the Mackenzie Delta, King (2009) found that trees with a positive temperature-growth response were linked to thicker surficial organic layers that maintain cooler active layers and limit direct evaporative moisture loss from the soil. Negative temperature responses were linked to a thinner organic layer and warmer active layer. A larger-scale study of black spruce in western Quebec, Canada, by Drobyshev et al. (2010) also supports the notion that surficial organic layer thickness may lead to contrasting climate-growth responses (see also Nilsson and Wardle, 2005, and Turetsky et al., 2010 on the importance of the organic layer in boreal ecosystem functioning). The contribution of such site-level (or intra-site) factors to divergence has not been examined in detail, but presents an exciting research opportunity to better understand the spatial complexity of tree growth responses in high-latitude boreal ecosystems.

3.5 CONCLUDING REMARKS

Divergence has been an ongoing issue for dendroclimatologists working in high-latitude regions for the past 16 years. Because of the limited number of datasets affected by divergence, progress in characterizing and advancing current understandings of it has been slow. In this study, a sizeable contribution to the high-latitude tree-ring network was made, adding 23 new white spruce chronologies from Old Crow Flats, northern Yukon. Furthermore, comparisons between these sites and 14 other long white spruce chronologies from across NWNA were made, which shed new light on potential causes of divergence. The results suggest that white spruce temperature-growth divergence in NWNA largely began in the 1950s, and as early as the 1930s in Old Crow Flats. A long-term comparison of NWNA chronologies against reconstructed Northern Hemisphere temperatures provides good independent verification of the idea that these chronologies responded positively to temperature since AD 1300, and that divergence in NWNA is probably restricted to the 20th century.

The large spatial extent of sites that were impacted by divergence suggests a large-scale forcing was the cause. As divergence occurs during the warmest period of the last 2000 years (Kaufman et al., 2009) it is likely temperature-induced drought stress is involved. A strengthened Aleutian Low since the mid-19th century (Fisher et al., 2004; Anderson et al., 2005), which led to anomalously dry 20th-century conditions in interior NWNA (Anderson et al., 2011), may also be a contributing factor. However, considering the proximity of divergent and non-divergent sites in the network, it was speculated that site-specific factors (e.g., organic layer thickness; King, 2009; Drobyshev et al., 2010) have an overarching role in determining the susceptibility of trees to divergence.

CHAPTER FOUR

A RECONSTRUCTION OF JUNE-JULY MINIMUM TEMPERATURES SINCE AD 1245 FROM WHITE SPRUCE TREE-RINGS IN THE MACKENZIE DELTA, NORTHWESTERN CANADA

4.1 INTRODUCTION

The circumpolar north has experienced rapid climate warming in recent decades (ACIA, 2005), which has stimulated a broad range of ecosystem-level changes (Tape et al., 2006; Bunn et al., 2007; Turetsky et al., 2011). Climate change across the Arctic is being characterised based on a sparse network of instrumental climate records that are mostly shorter than 100 years in duration (Lawrimore et al., 2011). Although such a network is suitable for characterising recent, broad-scale climate changes, it is of limited value for evaluating regional variability and the long-term context for recent changes. Proxy records can be used to improve the spatiotemporal coverage of northern climate datasets (Jones et al., 2009). Tree-ring chronologies are ideal because they are annually-resolved and are, thus, comparable to instrumental climate records (Hughes, 2011). Of particular interest to this study is the development of millennial-length tree-ring-based climate reconstructions, which can be used to characterise natural climate variability and the sensitivity of climate to pre-industrial forcings, and test the performance of general circulation models over a wide range of climatic conditions (Jansen et al., 2007; Jones et al., 2009). However, millennial-length chronologies are not possible in all regions either because living trees are too short-lived or environmental conditions are unsuitable for the preservation of deadwood. Millennial-length chronologies have been developed for some

parts of northern Eurasia, but are virtually absent in northern North America (Jansen et al., 2007). This study focuses on the Mackenzie Delta region, northwestern Canada, which hosts Canada's northernmost boreal treeline extent and has proven potential for the development of multi-centennial to millennial-length, climatically-sensitive tree-ring chronologies (Szeicz and MacDonald, 1996; Bégin et al., 2000; Pisaric et al., 2007).

A 29-site network of temperature-sensitive white spruce (*Picea glauca* [Moench] Voss) ring-width series, compiled from 10 existing and 19 new sites (Fig. 4.1), is used to develop a regional chronology and reconstruct June-July minimum temperatures back to AD 1245. Most trees in this network have an unstable temperature-growth response during the 20th century (Pisaric et al., 2007) which is largely consistent with the 'divergence problem' discussed by D'Arrigo et al. (2008). D'Arrigo et al. (2008) define the divergence problem (hereafter 'divergence') as "the tendency for tree growth at some previously temperature-limited northern sites to demonstrate a weakening in mean temperature response in recent decades, with the divergence being expressed as a loss in climate sensitivity and/or a divergence in trend." However, divergence in the Mackenzie Delta began in the early 20th century (Pisaric et al., 2007), which is much earlier than in most other regions, and methods to avoid this bias in the regional chronology are documented herein.

The regional chronology improves upon two long, independent site chronologies by Szeicz and MacDonald (1996) and Bégin et al. (2000) as it represents a regional network of trees, which provided an opportunity to isolate regionally-coherent growth patterns linked to climate and attenuate site- and tree-specific noise (Hughes, 2011). The quality of the reconstruction is demonstrated based on standard calibration-verification

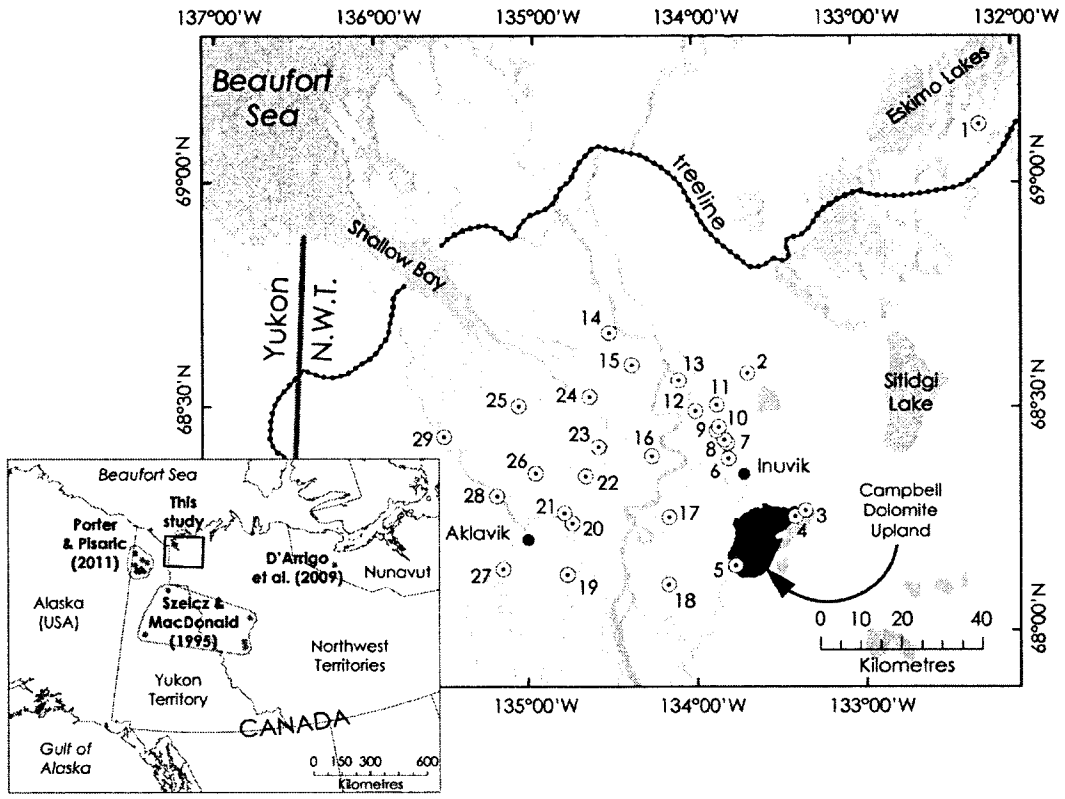

Figure 4.1. White spruce study sites in the Mackenzie Delta region are marked by white dotted circles; site numbers correspond to Table 4.1; water bodies are shaded grey; boreal treeline is delineated from the Circumpolar Arctic Vegetation Map (Walker et al., 2005). White spruce sites from other studies (inset map) are marked by grey dotted circles; site networks from the same study are bounded together.

tests (Cook and Kairiukstis, 1990) over the instrumental period, and long-term coherence with several independent temperature proxy records from neighbouring regions, and circum-Arctic- and hemispheric-scale networks. The dataset makes a substantial contribution to the high-latitude tree-ring network, often sampled for larger-scale temperature reconstructions (Esper et al., 2002; D'Arrigo et al., 2006), and provides a long, high-resolution context for evaluating the significance of recent climate warming in the Mackenzie Delta region.

4.2 BACKGROUND

Three notable ring-width studies on white spruce have been published from the Mackenzie Delta region: Szeicz and MacDonald (1996), Bégin et al. (2000), and Pisaric et al. (2007). Szeicz and MacDonald (1996) and Bégin et al. (2000) developed the longest chronologies back to AD 1060 and 1172, respectively. The Bégin et al. (2000) chronology was developed from living trees and deadwood snags (i.e., resting on the surface) from an isolated stand in the Eskimo Lakes district, north of treeline (site 1 – Fig. 4.1). As is typical of trees living in cold, high-latitude regions, their chronology was positively correlated with summer temperatures and was used to reconstruct past temperatures. Conversely, Szeicz and MacDonald (1996) sampled trees from rocky outcrops at Campbell Dolomite Upland (CDU; site 3 – Fig. 4.1) and found that their chronology was moisture-sensitive due to its inverse correlation with prior-summer temperatures and positive correlation with annual precipitation. More recently, the CDU chronology has been interpreted as a summer temperature proxy (Esper et al., 2002; Frank et al., 2007; Porter and Pisaric, 2011). Comparisons with other temperature-

sensitive proxies suggest the CDU chronology had responded positively to temperature prior to the 20th century, but shifted to a negative temperature response in the 20th century (Porter and Pisaric, 2011). Similarly, temperature-growth divergence is found at several other white spruce stands in northwestern North America (NWNA) (Jacoby and D'Arrigo, 1995; D'Arrigo et al., 2004; Wilmking et al., 2004; Pisaric et al., 2007; Porter and Pisaric, 2011).

Pisaric et al. (2007) were the first to examine the climatic response of individual trees at inner-delta sites (sites 6-13, Fig. 4.1). They too found that divergence was widespread, but that a subset of trees from several sites maintained a constant, positive temperature response over the full 20th century. They showed that the mean chronologies of divergent and divergence-free trees (termed 'negative- and positive-responders' by Pisaric et al., 2007) began to exhibit contrasting growth patterns as early as ca. AD 1900. Prior to the point of divergence, divergent and divergence-free trees shared a common growth pattern that was a positive function of temperature based on long comparisons with other temperature-sensitive proxies (Porter and Pisaric, 2011).

While many trees in NWNA, including the Mackenzie Delta, were susceptible to divergence, others were not (Bégin et al., 2000; Wilmking et al., 2004; Pisaric et al., 2007; Porter and Pisaric, 2011). The spatiotemporal coverage of NWNA tree-ring and climate records remain limitations to understanding the cause(s) of divergence and likelihood that it occurred in the past (D'Arrigo et al., 2008), with implications for tree-ring-based climate reconstructions (Jansen et al., 2007), but mounting evidence suggests that it is unique to the 20th century (Cook et al., 2004; Porter and Pisaric, 2011) and was likely caused by a large-scale climatic forcing. In NWNA, drought-stress is commonly

blamed (Jacoby and D'Arrigo, 1995; Barber et al., 2000; McGuire et al., 2010) and proxy records do support the idea that the 20th century has been anomalously warm (D'Arrigo et al., 2006) and dry (Anderson et al., 2007, 2011) in the context of the last millennium. However, because not all trees were affected (Wilmking et al., 2004; Pisaric et al., 2007; Porter and Pisaric, 2011), local factors likely explain why some trees have been more susceptible to divergence than others (Porter and Pisaric, 2011). For example, if drought is the main driver, variability in stand density or surficial organic layer thickness (Wilmking et al., 2004; King, 2009; Drobyshev et al., 2010; Yarie and Van Cleve, 2010), which moderate soil hydroclimate, or regional precipitation gradients (Wilmking and Juday, 2005) could alleviate or exacerbate drought stress.

Regardless, if divergence is unique to the 20th century and has not affected all trees, it should be possible to develop robust temperature reconstructions in divergence-affected regions by careful selection of tree-ring data (Wilson et al., 2007). Here the aforementioned tree-ring data from the study region (Fig. 4.1) are re-examined to develop a divergence-free temperature reconstruction. This 29-site network is one of the densest ever examined in NWNA, and this provided the opportunity to combine tree-ring data from multiple sites to enhance regional growth patterns linked to climate and suppress tree- and site-specific noise.

4.3 METHODS

4.3.1 Study area

The physical environment of the Mackenzie Delta region is well documented in the literature (Mackay, 1963; Burn and Kokelj, 2009). Here a brief description is given of

the delta plain and uplands where the study sites are found (Fig. 4.1). The Mackenzie Delta plain is an alluvial feature of Holocene origin comprised of Mackenzie and Peel River sediments (Mackay, 1963). White spruce forests dominate the delta plain and grow in well-drained alluvium typically underlain by permafrost (Smith, 1976; Nguyen et al., 2009). Most of the delta plain sites studied here (sites 6-29, Fig. 4.1) approximate the open-canopy, white spruce/lichen-crowberry stand type described by Pearce et al. (1988) which have an abundance of mature living trees, deadwood, and a reflective lichen cover (e.g., *Cladonia rangiferina*; *Caldina mitis*; Appendix C, SI-Fig. 4.1). Over many years, development of ice-rich permafrost has elevated these well-drained alluvial surfaces above the regular level of spring flooding (Kokelj and Burn, 2005), which has helped prevent rot and preserve deadwood. The general absence of extensive wildfires in the delta also helps to preserve centuries-old trees and deadwood, making the area well suited for dendroclimatic research.

Five upland sites examined here (sites 1-5, Fig. 4.1), not located within the Mackenzie Delta, are broadly consistent with the delta plain sites in terms of canopy and understory structure, but they differ in terms of surficial geology. Three of these sites (CDU, CDU1, and CDU2) are found on Campbell Dolomite Upland (Appendix C, SI-Fig. 4.2), a dolomite, quartzite, and shale outcrop of Precambrian to Lower Devonian age (Norris, 1981). The outcrop was overridden by Laurentide ice at some time between 14 and 21 ^{14}C ka BP (Dyke et al., 2002). Forested sites have only a shallow mineral soil layer, presumably from weathered parent material or glacial till. The other two upland sites (ESK and NL1) are isolated tundra stands on hummocky, rolling moraine deposits (Rampton, 1988).

Regional climate is highly seasonal with temperature and precipitation peaking in mid-summer. Mean temperature normals (AD 1971-2000) at Inuvik for winter (DJF), spring (MAM), summer (JJA), and fall (SON) are -26.7, -11.9, 12.2, and -8.5°C, respectively; the same normals for total precipitation are 41.1, 38.5, 95.2, and 73.8 mm (http://climate.weatheroffice.gc.ca). Synoptic climate is influenced by Arctic high-pressure that dominates most of the year and summertime intrusions of warm-moist cyclonic systems from the Pacific as the cool, dry Arctic air retreats (Burns, 1973).

4.3.2 Tree-ring data

In the summers of 2007 and 2008, 19 white spruce stands (Table 4.1) were sampled using standard dendrochronology methods (Speer, 2010). General sampling areas were preselected so the sites would be evenly distributed across the region. Mature sites with abundant snags were targeted to maximize the length of tree-ring chronologies. On average, 45 trees were sampled per site, most of which (ca. $\geq$ 80%) were living. A single bark-to-bark core passing through or near the pith was collected from living trees at waist height; 'cookies' were cut from snags. All samples were sanded to a smooth finish so that the rings could be visually cross-dated and measured using a Velmex tree-ring measuring system (0.001 mm precision). Two radii were measured for each tree in nearly all cases. The cross-dating accuracy was verified with the computer program COFECHA (Holmes, 1983).

These 19 sites are supplemented by 10 previously-developed sites (Table 4.1): the 8 eastern delta sites by Pisaric et al. (2007); the Eskimo Lakes 'ESK' site by Bégin et al. (2000); the Campbell Dolomite Upland 'CDU' site by Szeicz and MacDonald (1996).

Table 4.1. White spruce sites in the Mackenzie Delta region; 'Site no.' indicates the site's location on Fig. 4.1.

Site no.	Site code	Lat. (°N)	Long. (°W)	No. trees	First year	Last year	Mean series length (yrs)
1	[a]ESK	69.13	132.22	25	1172	1990	266
2	*NL1	68.59	133.68	49	1653	2006	202
3	[b]CDU	68.28	133.34	64	1060	1992	261
4	*CDU1	68.27	133.41	39	1158	2007	205
5	*CDU2	68.16	133.76	49	1118	2007	239
6	[c]TM	68.40	133.80	35	1529	2003	225
7	[c]DW	68.43	133.81	39	1483	2003	306
8	[c]BB	68.45	133.85	75	1501	2006	258
9	[c]MP	68.46	133.87	59	1545	2003	232
10	[c]M	68.47	133.85	29	1398	2003	234
11	[c]FT	68.52	133.86	44	1332	2003	244
12	[c]MS	68.51	134.00	42	1611	2003	262
13	[c]HL	68.58	134.10	27	1563	2003	340
14	*AC1	68.68	134.52	52	1579	2006	277
15	*AM1	68.61	134.38	39	1435	2007	254
16	*NC2	68.41	134.26	40	1687	2007	232
17	*KC2	68.27	134.16	42	1596	2007	259
18	*KC1	68.12	134.16	52	1445	2007	225
19	*ES1	68.14	134.77	51	1607	2007	272
20	*AK1	68.26	134.74	46	1631	2006	230
21	*AK2	68.28	134.79	13	1716	2006	235
22	*SC1	68.36	134.66	54	1603	2007	240
23	*NC1	68.43	134.58	46	1580	2007	229
24	*PC1	68.54	134.64	59	1499	2007	256
25	*JA2	68.52	135.07	45	1453	2007	241
26	*JA1	68.37	134.97	42	1587	2007	255
27	*PE1	68.15	135.16	37	1615	2007	257
28	*WC2	68.32	135.20	51	1474	2007	232
29	*WC1	68.45	135.52	41	1591	2006	260

Further information on each site: [a]Bégin et al. (2000); [b]Szeicz and MacDonald (1996); [c]Pisaric et al. (2007); *this study.

Raw data for the eastern delta sites were provided by M. Pisaric. The ESK data (Appendix C, SI-Note 4.1) were provided by C. Bégin (Geological Survey of Canada). The CDU data (independent from 'CDU1' and 'CDU2') were obtained from two sources: the original Szeicz and MacDonald (1996) dataset was obtained from the International Tree-Ring Databank (file CANA138); an additional 11 trees sampled by Szeicz and MacDonald, but not published until Esper et al. (2002; see also Frank et al., 2007), were also included. These additional CDU series were provided by D. Frank (Swiss Federal Research Institute, WSL).

Age-related trends were removed from ring-width series using standard data-adaptive negative-exponential or linear negative-to-zero slope curves (Fritts et al., 1969) following the 'signal-free standardisation' approach described by Melvin and Briffa (2008). Signal-free standardisation is an improvement on traditional detrending methods as it helps avoid distortion caused by climate signals embedded in raw series. Ideally, an expected growth curve should reflect the growth that would occur assuming an unvarying climate (i.e., the age-related growth trend). However, when data-adaptive curves are used, they are unavoidably distorted (referred to as 'trend distortion') by the climate signal and removing these curves from the raw series will, therefore, remove some of the original climate signal. Since data-adaptive curves (determined by the least squares solution) are most strongly influenced by series ends, trend distortion is also most severe at the series ends. In the case of mean chronologies where the modern ends of many standardised series terminate on the same year (i.e., living trees) and are averaged together, a large trend distortion may occur (Melvin and Briffa, 2008) and could lead to an artificial mismatch between tree-ring and climate series (Esper and Frank, 2009).

Signal-free standardisation attempts to avoid trend distortion by first estimating and removing the common climate signal from each series, based on the iterative procedure outlined by Melvin and Briffa (2008), resulting in 'signal-free measurements' that can be used to better characterise age-related trends.

A signal-free-enabled version of the program ARSTAN (provided by E. Cook, Lamont-Doherty Earth Observatory) was used to calculate the standardised ring-width indices. Indices belonging to the same tree were averaged into mean 'tree indices' (Appendix C, SI-Fig. 4.3). Mean site chronologies were calculated using the robust bi-weight mean (Cook, 1985).

4.3.3 Climate data

To allow the longest possible comparisons between local climate and the tree-ring data, regional composites of monthly minimum, mean and maximum temperatures and total precipitation were developed from several nearby climate station datasets (Appendix C, SI-Fig. 4.4; refer to SI-Note 4.2 for details about the raw data and how the regional composite records were developed). The temperature composites span the period AD 1892-2007, but are continuous only from AD 1910-2007 for most months (Appendix C, SI-Figs. 4.5-4.7). The precipitation composites span the period AD 1926-2007, and are continuous over the full period for most months (Appendix C, SI-Fig. 4.8). Temperatures in the Mackenzie Delta region exhibit a high degree of spatial coherence (Burn and Kokelj, 2009), as demonstrated by the relatively strong mean inter-station correlations (Appendix C, SI-Figs. 4.5-4.7). Conversely, total precipitation is more spatially heterogeneous in the study region (Burn and Kokelj, 2009), as demonstrated by the

relatively weak mean inter-station correlations (Appendix C, SI-Fig. 4.8), suggesting the precipitation composites may be less representative of the study region compared to the temperature composites. Therefore, correlations between the tree-ring and precipitation data, or lack thereof, should be interpreted with some caution.

4.4 RESULTS AND DISCUSSION

4.4.1 Regional growth patterns and divergence

Tree-ring series from the network span the period AD 1060-2007 (Table 4.1). More than 70% of the sites yielded samples that extend into the 16th century, more than 40% extend into the 15th century, and just over 20% extend into the 14th century or earlier. The oldest samples are from the upland sites ESK, CDU, CDU1, and CDU2, which extend into the 11th or 12th centuries. All sites share a large amount of common variability suggesting a regional growth-limiting factor such as climate. This is demonstrated by a comparison of each site chronology against a regional mean defined by the remaining trees from the network (Fig. 4.2). Each site is well correlated with its corresponding regional mean. The most strongly correlated sites (e.g., DW, BB, MP, M, FT, etc.) are delta plain sites. Nevertheless, the majority of upland sites (e.g., ESK, NL1, CDU, and CDU2) are also well correlated regionally. The unexplained variability with respect to regional growth likely reflects site-specific factors (e.g., micro-topography, organic layer thickness, stand density, flood susceptibility, drainage, etc.) that impact climate-growth sensitivity and response, highlighting the value of a network-based approach to dendroclimatic research (Hughes, 2011).

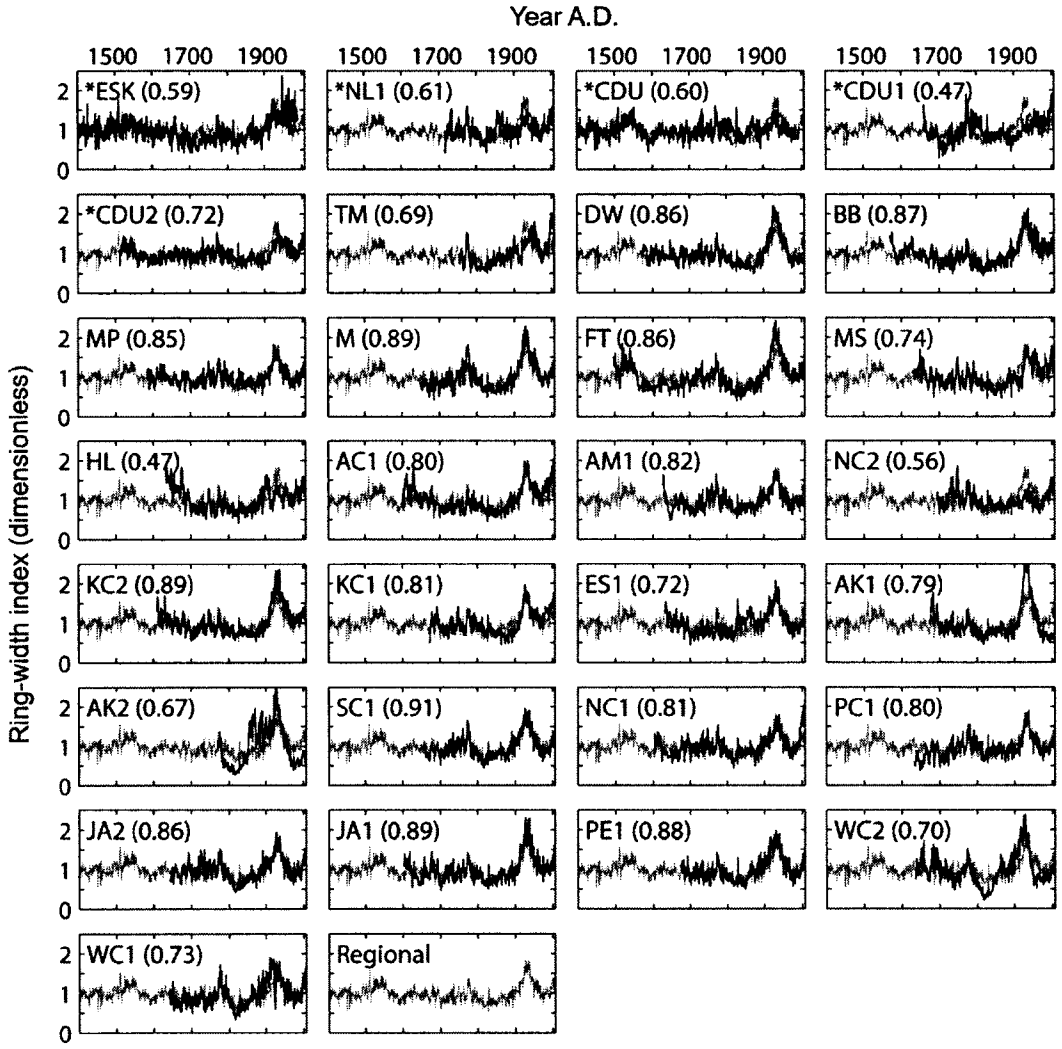

Figure 4.2. Comparisons between each of the 29 site chronologies (black lines; calculated for all years defined ≥ 6 trees) and regional mean chronologies (grey lines; the mean of all other trees from the remaining 28 sites). Upland sites are denoted by an '*'; all other sites are delta plain sites. Inter-series correlations are in brackets; all correlations are significant at $p \leq 0.001$.

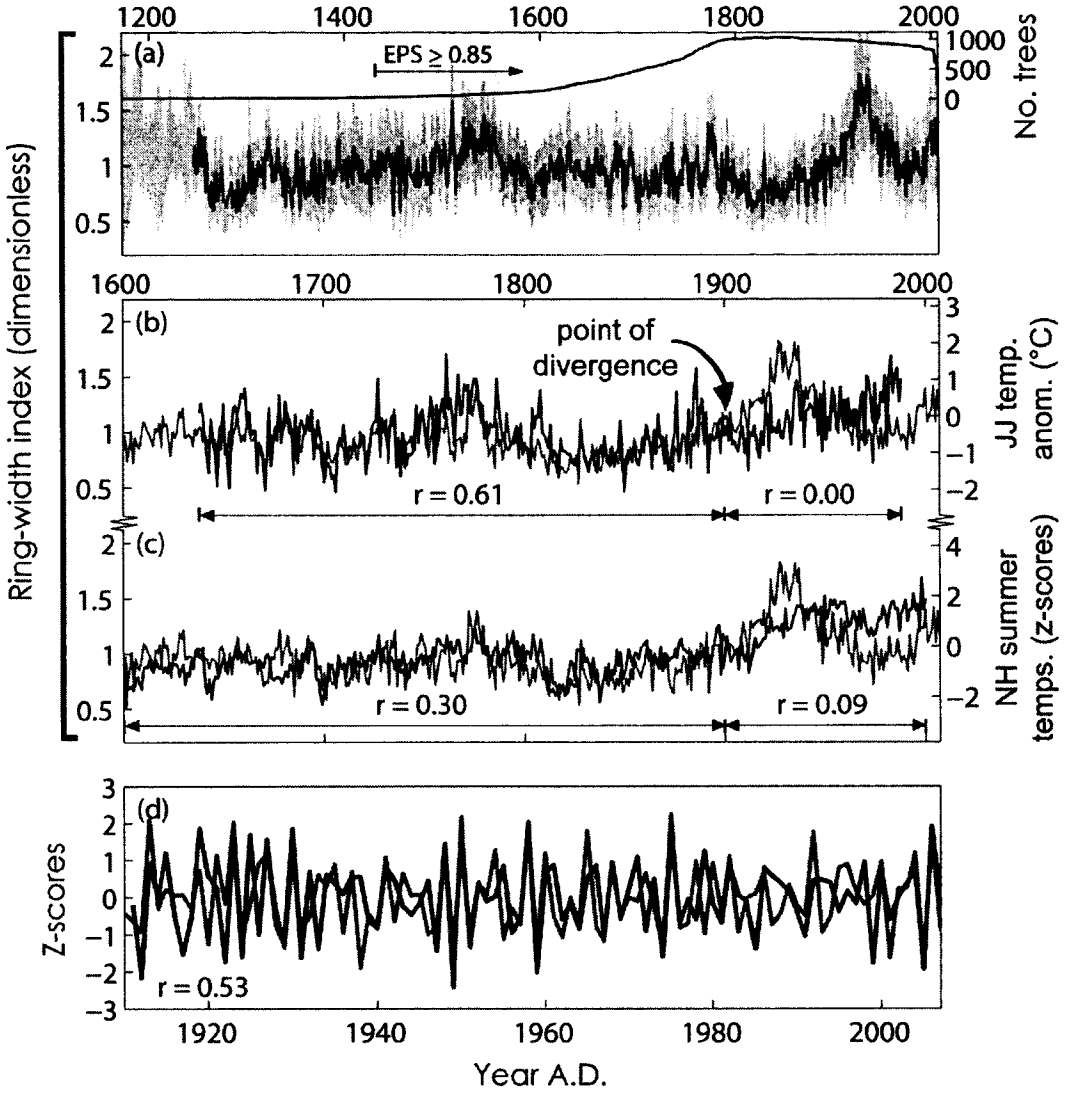

Figure 4.3. (a) The Mackenzie Delta Regional Chronology (AD 1245-2007; dark grey line); the MDRC is shown for years with an Expressed Population Signal (EPS) ≥ 0.7; EPS ≥ 0.85 is indicated; the 5-95 (light grey) and 25-75 (medium grey) percentile ranges for all tree indices are indicated; the number of trees defining the MDRC (black line). (b) Comparison of the MDRC (grey) and reconstructed mean June-July temperatures (black) by Szeicz and MacDonald (1995; see Appendix C, SI-Note 4.3). (c) Comparison of the MDRC (grey) and a composite of 6 hemispheric-scale temperature reconstructions (black; see Appendix C, SI-Note 4.4). (d) Comparison of first-differenced June-July temperatures (black) and the mean of all first-differenced tree indices (grey). Note that the time axes differ between plots (a), (b-c) and (d).

All tree indices were averaged into a regional chronology (Fig. 4.3a; hereafter the Mackenzie Delta Regional Chronology, or 'MDRC') to isolate the common regional growth pattern and assess its climate response. The MDRC was calculated for the period AD 1245-2007 only. This period is characterised by an Expressed Population Signal (EPS; Wigley et al., 1984) above 0.7 (i.e., 70% signal, 30% noise), except during the years AD 1399 and 1405-1408 when EPS is 0.66-0.69. The EPS was estimated using a 51-year inter-correlation window. EPS drops well below 0.5 prior to AD 1245 due to the low number of trees ($\leq$ 15 trees) available. The MDRC was not weighted by site, but it is important to note that a site-weighted MDRC is virtually identical (AD 1245-2007, $r = 0.97$, $p << 0.001$).

The strong regional growth coherence indicates a regional forcing such as climate, but does not necessarily imply that the average tree's response to this forcing has been time-stable (Pisaric et al., 2007). The MDRC strongly emulates the divergent growth pattern reported by Pisaric et al. (2007) in the Mackenzie Delta, and is similar to divergent growth patterns found at other white spruce sites across NWNA (Porter and Pisaric, 2011). Pisaric et al.'s (2007) analysis showed that divergence in the Mackenzie Delta occurs much earlier than in other parts of NWNA (divergence is often considered a late-20th century phenomenon; D'Arrigo et al., 2008), but that a minority of trees across the region were not susceptible to divergence. Pisaric et al. (2007) demonstrated that divergent and divergence-free trees had the same growth pattern before ca. AD 1900, suggesting that all trees responded to the same climate variable in the same way before the 20th century, but that divergent trees failed to track summer temperatures during the 20th century, at least at lower-frequencies. Multi-centennial comparisons against

reconstructed hemispheric-scale temperatures confirm that divergent and divergence-free trees had a positive temperature response prior to AD 1900, but that divergent trees have since diverged from this response (Porter and Pisaric, 2011).

Here this point is reiterated with a comparison of the MDRC against a well-verified ring-width-based June-July temperature reconstruction (AD 1638-1988) by Szeicz and MacDonald (1995) from a network of five high-elevation white spruce sites from the middle-Mackenzie Valley, and parts of central and northern Yukon (all within ca. 500 km of the Mackenzie Delta – Fig. 4.1). This comparison (Fig. 4.3b) shows that the average Mackenzie Delta tree was coupled to reconstructed June-July temperatures from AD 1638 to the start of the 20th century, but then diverged from this response at ca. AD 1900, roughly a half century before divergence occurs in most other parts of NWNA (D'Arrigo et al., 2008; Porter and Pisaric, 2011). This same general result is found when the MDRC is compared with reconstructed Northern Hemisphere-scale temperatures (Fig. 4.3c), in spite of the large spatial-scale differences.

Another unique feature of divergence in the Mackenzie Delta is that it occurs in two phases. The first phase spans ca. AD 1900-1950 when tree growth overestimates summer temperatures, and the second phase follows when tree growth underestimates temperatures (Figs. 4.3b and 4.3c). The first phase is not common to most other cases of divergence in NWNA, but the second phase is (D'Arrigo et al., 2008; Porter and Pisaric, 2011). The observation that a collection of sites across NWNA responded negatively to late-20th century temperatures, a period of exceptional warmth in the last two millennia (Kaufman et al., 2009), has led some to speculate that divergence may be a negative response to drought stress that has been exacerbated by late-20th century warming

(Jacoby and D'Arrigo, 1995; Barber et al., 2000; McGuire et al., 2010; Porter and Pisaric, 2011). However, the first phase of divergence in the Mackenzie Delta, a period of accelerated growth, is clearly a response to favourable not adverse conditions. Therefore, drought stress likely is not the cause of early-20th century divergence, but could be partly responsible for the depressed growth values in the late-20th century.

Since AD 1900, the MDRC followed a sinusoidal growth pattern that rises to record high values in the AD 1930s, declines to lower values in the AD 1980s, and rises to higher values to end the record (Fig. 4.3a). This low-frequency pattern is not consistent with reconstructed temperatures (Fig. 4.3b). A correlation analysis between the MDRC and instrumental monthly temperatures (AD 1892-2007) and total precipitation (AD 1926-2007) finds no significant correlations (except a weak inverse correlation with December precipitation) (Table 4.2). However, a second correlation analysis based on first-differenced data (i.e., high-frequency variability only) demonstrates that the average tree had a significant, positive correlation with June and July temperatures during the 20th century (see '1st diff.', Table 4.2). These correlations are strongest for minimum and mean temperatures, and slightly weaker for maximum temperatures. A time-series comparison of first-differenced June-July mean temperatures and ring-width for the period AD 1911-2007 (Fig. 4.3d) shows that the association has been stable over the 20th century (n.b., first-differenced June-July temperatures were not available prior to AD 1911). This point is supported by similar inter-series correlations for the first (AD 1911-1959, $r = 0.57$, $p \leq 0.01$) and second (AD 1960-2007, $r = 0.47$, $p \leq 0.01$) halves of the comparison period. The overall correlation is $r = 0.53$ ($p \leq 0.01$), a level of agreement

Table 4.2. Correlations between monthly climate variables and tree-ring width indices: MDRC (Fig. 3a); '1st diff.' (mean of all 1st differenced tree indices; Fig. 3d); and 'DFRC' (Divergence Free Regional Chronology; Fig. 4f). Only correlations significant at $p \leq 0.05$ (two-tailed) are shown; correlations significant at $p \leq 0.01$ (two-tailed) are in bold font.

		Sep	Oct	Nov	Dec	Jan	Feb	Mar	Apr	May	Jun	Jul	Aug
Total	MDRC	·	·	·	-0.24	·	·	·	·	·	·	·	·
Precip.	1st diff.	·	·	·	·	·	-0.24	·	**0.30**	·	·	·	·
	DFRC	0.22	·	·	·	·	·	·	·	·	·	·	·
Min.	MDRC	·	·	·	·	·	·	·	·	·	·	·	·
Temp.	1st diff.	·	·	·	·	-0.20	·	·	·	·	**0.48**	**0.35**	·
	DFRC	**0.30**	·	·	**0.32**	0.24	**0.29**	0.22	0.25	·	**0.56**	**0.43**	0.23
Mean	MDRC	·	·	·	·	·	·	·	·	·	·	·	·
Temp.	1st diff.	·	·	·	·	-0.20	·	·	·	·	**0.49**	**0.35**	·
	DFRC	·	·	·	0.22	·	0.23	·	·	·	**0.51**	0.23	·
Max.	MDRC	·	·	·	·	·	·	·	·	·	·	·	·
Temp.	1st diff.	·	·	·	·	·	·	·	·	·	**0.43**	**0.33**	·
	DFRC	·	·	·	·	·	·	·	·	·	**0.41**	·	·

which is typical of interannual temperature-growth relations for some Alaskan white spruce (e.g., Andreu-Hayles et al., 2011).

The results presented thus far show that divergence in the Mackenzie Delta is mostly restricted to the post-AD 1900 era and the low-frequency domain. However, as previously demonstrated by Pisaric et al. (2007), and as is shown next, not all trees in the study region were affected by divergence and this provides the opportunity to develop a robust regional chronology that can be used to reconstruct past temperatures.

4.4.2 Developing a divergence-free regional chronology

Large-scale (e.g., hemispheric) climate-proxy reconstructions are typically developed from extensive networks of site chronologies that are well correlated and have a time-stable relation with the target climate variable (Briffa et al., 2002; D'Arrigo et al., 2006). In some high-latitude regions, tree-ring-based temperature reconstructions have been most successful when tree-ring records were screened for divergence (Wilson et al., 2007). Here the same principles are applied to a local-scale network to develop a 'divergence-free' chronology. However, rather than excluding divergent records altogether, only the divergent (i.e., post-AD 1900) portions of these records are excluded as the pre-divergence portions are not in question based on previous analyses and the discussion above.

Divergent versus divergence-free records can be separated based on their correlation with summer temperature, but as Esper and Frank (2009) suggest, this approach is circular and would surely lead to a mean chronology that is tuned to the temperature index chosen for the correlation analysis. Alternatively, growth-trend

(positive vs. negative) could be used as a sorting criterion. At the NWNA-scale, Porter and Pisaric (2011) found that most divergent and divergence-free records have consistent growth trends over all periods except ca. AD 1950-1980. During the AD 1950-1980 period, divergent records tend to have a negative growth trend while divergence-free trees have a positive trend. However, in areas such as Old Crow Flats (Porter and Pisaric, 2011) and the Mackenzie Delta (Pisaric et al., 2007) the contrasting growth trend period begins slightly earlier, ca. AD 1930-1980.

All 1286 tree indices from the 29 sites were examined and sorted based on growth trend from AD 1930-1980. Trees with a negative trend were sorted as 'Group 1', and trees with a positive trend were sorted as 'Group 2'. The Group 1 and Group 2 trees were then averaged into regional chronologies (Figs. 4.4a and 4.4b). The regional chronologies are only given for years with an EPS above 0.7, as was done for the MDRC. Deadwood ring-width indices that did not cover the AD 1930-1980 period were left unsorted and were averaged into a 'Snag' regional chronology (Fig. 4.4c). Of the sorted trees, most are Group 1 (Table 4.3). Three sites did not have any Group 2 trees (i.e., FT, AK1, and AK2). Of the 26 sites that had both responses, the majority of trees (82% at the average site) were Group 1. The dominance of Group 1 trees was observed at all sites except ESK and CDU1. Group 2 trees represent 20-30% of the population at some sites including NL1, CDU2, TM, MS, HL, AC1, NC2, KC1, and WC1. Regionally, there is no statistical difference between the mean series lengths of Group 1 and Group 2 trees (261 vs. 263 years; 1σ = 76 vs. 79 years), suggesting that the contrasting growth responses are not a function of age. Rather, these growth differences are likely due to local-scale ecological factors (Porter and Pisaric, 2011).

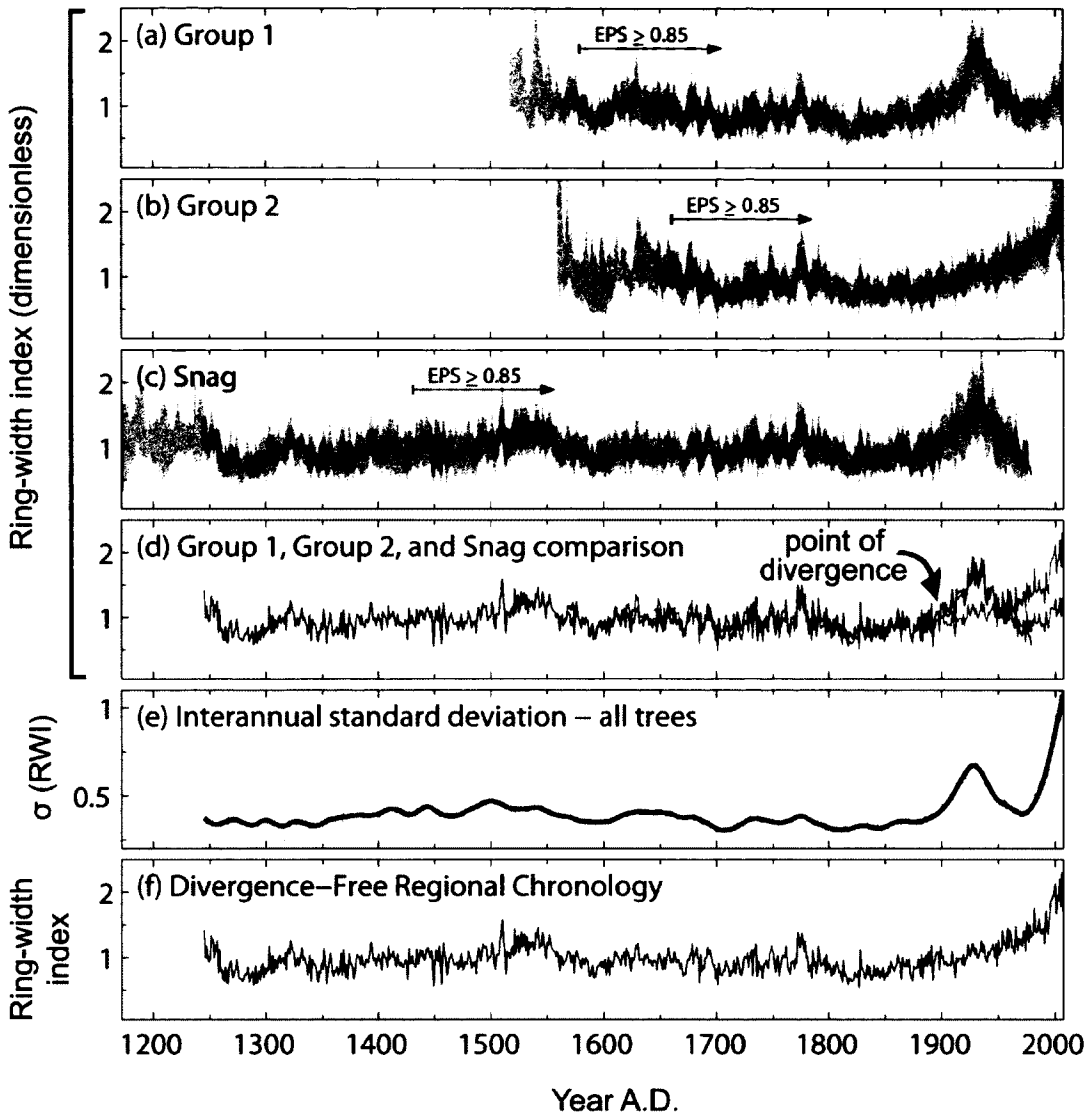

Figure 4.4. (a-c) Regional averages of Group 1 (blue), Group 2 (red), and Snag (black) ring-width indices; regional averages are shown for all years with an EPS $\geq$ 0.7 (EPS $\geq$ 0.85 is indicated); the 5-95 (light grey) and 25-75 (medium grey) percentile ranges are given. (d) Comparison of the Group 1, Group 2, and Snag regional chronologies. (e) Interannual standard deviations (grey) of all ring-width indices; a 41-year cubic smoothing spline (green) is used to highlight the low-frequency trend. (f) Divergence-Free Regional Chronology.

Table 4.3. The frequency, percentage, and mean and median age (years) of Group 1 and Group 2 trees at each site.

Site	Group 1				Group 2			
	freq. trees	% of trees	Mean age	Median age	freq. trees	% of trees	Mean age	Median age
ESK	2	15.4	329	329	11	84.6	274	263
NL1	31	81.6	207	227	7	18.4	214	238
CDU	24	85.7	272	238	4	14.3	290	265
CDU1	13	46.4	184	189	15	53.6	209	192
CDU2	24	80.0	231	225	6	20.0	278	267
TM	28	80.0	225	222	7	20.0	223	222
DW	23	95.8	333	359	1	4.2	406	406
BB	48	87.3	288	281	7	12.7	213	214
MP	19	95.0	276	255	1	5.0	340	340
M	15	93.8	263	241	1	6.3	183	183
FT	18	100.0	261	270	0	0.0	n/a	n/a
MS	30	78.9	254	242	8	21.1	282	259
HL	18	66.7	336	358	9	33.3	348	367
AC1	30	81.1	307	327	7	18.9	308	288
AM1	27	96.4	266	253	1	3.6	258	258
NC2	17	68.0	254	258	8	32.0	259	258
KC2	23	85.2	282	258	4	14.8	247	254
KC1	24	66.7	234	224	12	33.3	242	254
ES1	39	92.9	273	298	3	7.1	328	332
AK1	37	100.0	249	245	0	0.0	n/a	n/a
AK2	12	100.0	241	235	0	0.0	n/a	n/a
SC1	38	90.5	251	242	4	9.5	222	214
NC1	24	92.3	261	250	2	7.7	284	284
PC1	48	98.0	258	245	1	2.0	211	211
JA2	30	85.7	243	251	5	14.3	258	255
JA1	23	92.0	276	266	2	8.0	289	289
PE1	23	95.8	289	303	1	4.2	233	233
WC2	37	94.9	233	234	2	5.1	318	318
WC1	24	77.4	259	266	7	22.6	304	297
Average site*	25.8	81.7	263.2	261.6	5.2	18.3	269.9	267.6

*based on sites that have both response types (i.e., all sites except ft, ak1, and ak2)

A comparison of the regionally-averaged Group 1, Group 2, and Snag chronologies shows that all trees, regardless of grouping, share a common growth pattern from AD 1644 until 1900, the point of divergence (Fig. 4.4d). The mean inter-series correlation between the three chronologies during this period is 0.87 ($p \leq 0.001$). After AD 1900, Group 1 trees had a sharp upward trend to ca. AD 1930, then a decline to ca. AD 1980. As would be expected, the Snag chronology closely follows the Group 1 chronology post-AD 1900 as it is an unsorted chronology and likely defined mostly by Group 1 trees which are most common regionally. Conversely, Group 2 trees had a consistently positive trend since AD 1900.

A running standard deviation of the ring-width indices for all trees (Fig. 4.4e) was calculated as further evidence that all trees, regardless of grouping, had similar growth patterns prior to AD 1900 but increasingly variable growth patterns ever since. The regional standard deviation was relatively stable during AD 1245-1900, with smoothed (41-year cubic smoothing spline with a 50% frequency cut-off; Cook and Peters, 1981) values ranging between 0.30 and 0.47 (mean = 0.37). Subsequently, the regional standard deviation increases sharply to a local maximum of ca. 0.66 in the AD 1930s, a period when the Group 1 and Group 2 regional chronologies exhibit considerable differences. During the mid-20th century, the regional standard deviation returns to pre-AD 1900 levels, which is explained by the fact that Group 1 and Group 2 indices are similar during the mid-20th century as they cross each other trending in opposite directions. Finally, the regional standard deviation increases sharply to finish the record above 1.0, indicating that ring-width indices across the region are most variable during this period. Again, these differences are evident between the Group 1 and Group 2 regional chronologies.

Based on the idea that divergence in NWNA is restricted to the 20th century (Porter and Pisaric, 2011), a Divergence-Free Regional Chronology (DFRC; Fig. 4.4f) was calculated from the robust bi-weight mean (Cook, 1985) of all ring-width indices before the point of divergence (AD 1900) and only Group 2 indices since AD 1900, thereby excluding divergent signals. The DFRC was calculated for the period AD 1245-2007, defined by an EPS of 0.7 or greater (except during the years AD 1399 and 1405-1408 when EPS is 0.66-0.69). EPS is greater than 0.85 following AD 1431. An EPS of 0.85 is often recommended for dendroclimatic studies (Wigley et al., 1984), but is a subjective threshold. Here, the more liberal EPS $\geq$ 0.7 threshold is used to facilitate a longer interpretation, but more caution should be used when interpreting the AD 1245-1431 portion of the DFRC.

4.4.3 Calibration, verification, and reconstruction

The DFRC was correlated with the monthly climate data to determine its most optimal climate response (Table 4.2). The strongest and most significant correlations were observed for June and July minimum and maximum temperatures, as was noted earlier for the first-differenced data. Comparatively, maximum June and July temperatures were not as well correlated. The finding that June and July minimum and mean temperatures are well correlated with tree growth at both high- and low-frequencies helps to provide some confidence that these relations are not spurious.

June-July (or June-August in some cases) is a common season of influence for temperature-sensitive chronologies from high-latitude and -elevational sites in North America and Eurasia (e.g., Szeicz and MacDonald, 1995; Gostev et al., 1996; Büntgen et

al., 2005; Wilson et al., 2007; Youngblut and Luckman, 2008; D'Arrigo et al., 2009; Esper et al., 2010; Porter and Pisaric, 2011; Flower and Smith, 2012). However, few other studies have explored correlations with minimum (night time) and maximum (day time) temperature. Rather, most studies examine mean temperature correlations only. In this study, considerable differences between minimum, mean, and maximum temperature correlations are noted. The June correlation is similar between minimum ($r = 0.56$, $p \leq 0.01$) and mean ($r = 0.51$, $p \leq 0.01$) temperatures, but the July correlation is much stronger for minimum ($r = 0.43$, $p \leq 0.01$) compared to mean ($r = 0.23$, $p \leq 0.01$) temperatures. Recent work by Wilson and Luckman (2003; see also Luckman and Wilson, 2005; Youngblut and Luckman, 2008) has demonstrated that maximum temperatures are more strongly associated with tree-growth in some cases in western Canada. Wilson and Luckman (2003) suggested that this may be due to the fact that most photosynthesis occurs in the day time and, presumably, day time temperatures are more likely to influence photosynthesis than night time temperatures. However, in this study, the DFRC is more closely associated with minimum June-July temperatures ($r = 0.60$, $p \leq 0.01$) than mean or maximum June-July temperatures ($r = 0.46$ and 0.31, respectively, $p \leq 0.01$). As for Wilson and Luckman's (2003) hypothesis, it is not possible to refute their logic as it applies to their sites, but it is unfair to assume night time temperatures do not influence photosynthesis in other cases. For example, early-June night time temperatures in the Mackenzie Delta region can approach the freezing point and, thus, can have a significant influence on biological activity.

Based on the correlation analysis, June-July minimum temperature is the optimal climate index for the DFRC. The potential to reconstruct June-July minimum

temperatures from the DFRC was evaluated using a standard split-period calibration-verification procedure commonly employed in dendroclimatic research (Cook and Kairiukstis, 1990). Two 53-year calibration periods were defined: AD 1893-1954 (Split 1) and 1955-2007 (Split 2). The Split 1 calibration period spans 62 calendar years, but contains only 53 years of June-July minimum temperature measurements due to the discontinuities in the early portion of the regional temperature record (Appendix C, SI-Fig. 4.5). Also, 3 of the 53 years (AD 1893, 1900, and 1908) in Split 1 contain measurements for June but not July, and 2 of the 53 years (AD 1895 and 1896) contain measurements for July but not June. In order to calculate June-July averages for these years, the missing June or July measurements were estimated from the arithmetic mean of the 4 closest years of June or July measurements.

For each calibration period, the DFRC and the June-July minimum temperature records were compared and the following statistics were calculated to evaluate the relation: Pearson's Product Moment Correlation Coefficient (R), coefficient of determination (R^2), adjusted R^2, standard error of the estimate (SE), Durbin-Watson (DW), and sign-test (Table 4.4). Calibration models were verified over all years excluded from the calibrations. The verification periods were: AD 1955-2007 (Split 1) and 1893-1954 (Split 2). For each verification period, the following statistics were calculated to evaluate the stability of the calibration relation: Pearson's R, Reduction of Error (RE), and Coefficient of Efficiency (CE) (Table 4.4).

Modelled temperatures explain between 18 and 23% (adj-R^2) of observed temperatures for Splits 1 and 2, and 35% for the full period model (Table 4.4). Values in this range are typical of high-latitude ring-width networks which express temperature

Table 4.4. Split-period calibration/verification and full-period (AD 1893-2007) calibration statistics for linear regression models of June-July minimum temperatures as a function of the DFRC.

	Split 1	Split 2	Full period
Calibration			
Period	1893-1954	1955-2007	1893-2007
N	53	53	106
Slope	3.27	1.69	2.07
Intercept	2.17	4.06	3.46
R	0.44	0.49	0.60
R^2	0.20	0.24	0.36
Adj-R^2	0.18	0.23	0.35
SE	0.81	0.88	0.86
DW	1.78	1.84	1.86
Sign (+/-)	34/18*	32/21	65/40*
Verification			
Period	1955-2007	1893-1954	n/a
N	53	53	n/a
R	0.49	0.44	n/a
RE	0.39	0.57	n/a
CE	-0.15	0.08	n/a

N.B., Temperature data for June (1895 and 1896) and July (1893, 1900, and 1908) were not available. To allow the calculation of June-July averages for these years, the missing data points were estimated by the mean of the four closest years of data. The calibration/verification period 1893-1954 (62 years) contains only 53 years of valid data points, and 9 years of missing data. All correlations are significant at $p \leq 0.001$ (one-tailed); sign-test result significant at $^{*}p \leq 0.05$.

signals best at lower frequencies (Cook et al., 2004; D'Arrigo et al., 2006). As expected, the explained variance of the full period model increases with smoothing (e.g., adj-R^2 = 0.66 for the period AD 1910-2007 if a 9-year smoothing spline is used). For Splits 1 and 2, and the full period model, the DW statistic is always close to a value of 2.0 indicating low autocorrelation in model residuals, and the SE has a narrow range from 0.81-0.88 suggesting the magnitude of unexplained variance is stationary. The Split 1 and full period calibration models pass a sign-test at the 95% confidence level, but Split 2 does not. Despite the weaker Split 2 sign-test result, the overall sign-test results are encouraging given the lower-frequency nature of the temperature signals in high-latitude ring-width series, and suggest that some inter-annual temperature variability is recorded in the tree-rings. This is also evident from the comparison of first-differenced ring-width and June-July temperatures (Fig. 4.3d).

The verification statistics indicate that the calibration relations are robust and time-stable (Table 4.4). The most informative statistics are the RE and CE which are always above zero, except for the CE of Split 1. By definition, any model with an RE or CE above zero demonstrates some skill and is predictively-superior to a model defined by the observed mean climatology of the calibration (for RE) and verification (for CE) periods. Based on the RE results alone, both calibration models are skilful.

The DFRC passes most of the standard calibration-verification tests, which suggests it can be used as a proxy for June-July minimum temperatures. The full-period model (Table 4.4; Fig. 4.5a) was used to reconstruct June-July minimum temperatures since AD 1245 (Fig. 4.5h). The 2σ confidence interval for the reconstruction is 1.72°C (2

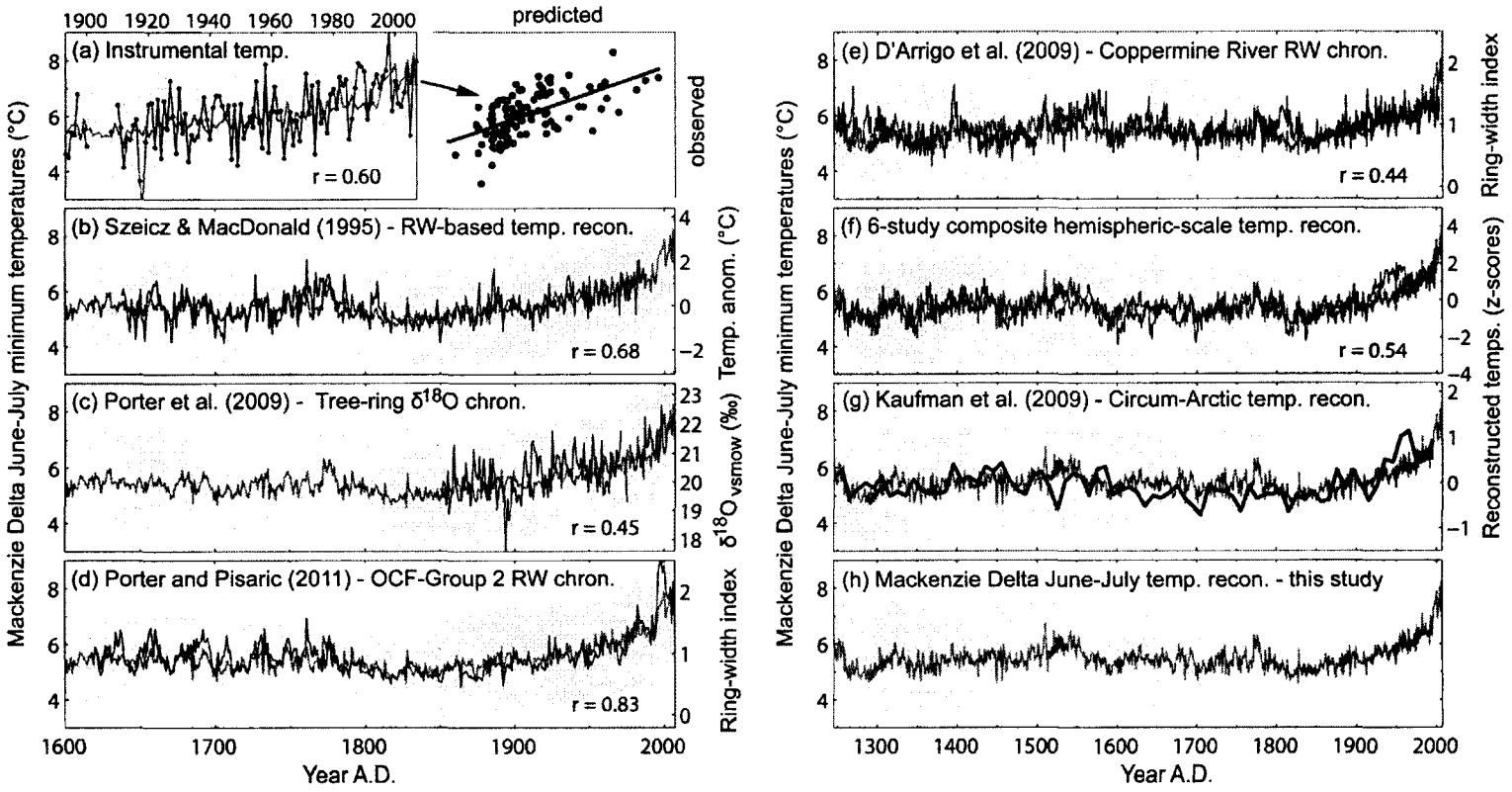

Figure 4.5. Mackenzie Delta regional June-July minimum temperature reconstruction (dark grey; 2×SE interval light grey) versus: (a) instrumental (observed) June-July minimum temperatures; (b) Szeicz and MacDonald (1995) ring-width-based June-July mean temperature reconstruction; (c) Porter et al. (2009) tree-ring $\delta^{18}O$ record, March-July minimum temperature proxy; (d) Porter and Pisaric (2011) OCF-Group-2 ring-width chronology, June minimum temperature proxy; (e) D'Arrigo et al. (2009) Coppermine River ring-width chronology, June-July temperature proxy; (f) 6-study composite hemispheric-scale reconstructed temperatures; (g) Kaufman et al. (2009) circum-Arctic temperature reconstruction. (h) The Mackenzie Delta regional June-July minimum temperature reconstruction from this study. Correlations represent the period of overlap between the Mackenzie Delta reconstruction and the comparison series; all correlations are significant at $p \leq 0.001$. Refer to SI-Note 5 (Appendix C) for details on each comparison series, some of which are modified from their original published form. Note that time axes differ between plots (a), (b-d), and (e-h).

× SE), which does not account for changes in sample depth or model parameter uncertainties. As such, 1.72°C probably underestimates the true 2σ confidence interval.

From AD 1910-2007, reconstructed and observed June-July minimum temperatures (Fig. 4.5a) had positive warming trends of 0.2°C/decade or a total change of 1.96°C. Comparatively, mean June-July temperatures for this region increased by only 1.46°C, which is more than double the global trend of ca 0.70°C for the same period (HadCRUT3 land and sea surface temperatures; Brohan et al., 2006). The Mackenzie Delta and other regions of NWNA have experienced some of the most rapid warming trends in recent decades (ACIA, 2005), which can be explained in part by major reductions of summer sea ice in the Beaufort and Chukchi Seas (Serreze et al., 2009).

Over longer time-scales, the reconstruction indicates that the most recent decade (AD 2000-2009) was the warmest decade on record since AD 1245, and ca. 1.4°C warmer than any other decade prior to the mid-20th century (Table 4.5). Six of the top ten warmest decades are in the 20th and 21st centuries. The other four warmest decades are the 1520s, 1530s, 1540s, and 1770s. Consistent with the IPCC's Fourth Assessment Report, the reconstruction also shows that the most recent 50-year period has been the warmest 50-year period in the last 500 years (Jansen et al., 2007), and since AD 1245. These results confirm the study region is currently experiencing a warm period that is unparalleled in eight centuries.

Four of the ten coldest decades in the reconstruction span AD 1810-1849 (Table 4.5), corresponding to the Dalton solar minimum (Bard et al., 2000), a cool period expressed in several temperature-sensitive tree-ring chronologies in NWNA (Luckman and Wilson, 2005; D'Arrigo et al., 2006; Porter and Pisaric, 2011). Four of the other six

Table 4.5. Rankings of the ten warmest and ten coolest reconstructed decade-averaged minimum temperatures since AD 1245.

Warm Decades	°C	Cool decades	°C
2000-2009	*7.4	1810-1819	4.9
1990-1999	6.9	1280-1289	4.9
1980-1989	6.4	1820-1829	5.0
1970-1979	6.2	1270-1279	5.0
1960-1969	6.0	1830-1839	5.0
1520-1529	6.0	1290-1299	5.0
1540-1549	6.0	1840-1849	5.0
1950-1959	6.0	1260-1269	5.1
1770-1779	5.9	1700-1709	5.1
1530-1539	5.9	1340-1349	5.1

*Based on AD 2000-2007 reconstructed and AD 2008-2009 observed temperatures.

coldest decades span the period AD 1260-1299, corresponding with the onset of the Wolfe solar minimum, but not its peak (Bard et al., 2000). The other two coldest decades are the 1340s and 1700s, corresponding with the Wolfe and Maunder minima, respectively (Bard et al., 2000). As found elsewhere, the results suggest that solar output has been an important driver of summer temperatures prior to the 20th century, while the more recent warming is congruent with anthropogenic forcing (IPCC, 2007) and Arctic amplification (Serreze et al., 2009).

4.4.4 Long-term, regional-scale validation

The reconstruction is validated at the regional-scale by several independent temperature-proxy records (Fig. 4.1). The Szeicz and MacDonald (1995) June-July temperature reconstruction (AD 1638-1988) is well correlated ($r = 0.68$, $p \leq 0.001$) with the reconstruction and generally shares the same low-frequency trends (Fig. 4.5b). This strong coherence is mutually corroborative (Jones et al., 2009) and demonstrates that both tree-ring networks responded to the same regional climatic factor; in the Lower Mackenzie Valley and adjacent parts of NWNA, temperature is likely the only climate variable so coherent across such distances (Burn and Zhang, 2009; Porter and Pisaric, 2011).

A tree-ring $\delta^{18}O$ record (AD 1850-2003) developed by Porter et al. (2009) from the Mackenzie Delta also correlates well ($r = 0.45$, $p \leq 0.001$) with the reconstruction (Fig. 4.5c). Porter et al. (2009) found that the $\delta^{18}O$ record was a first-order proxy for March-July minimum temperatures due to the temperature-dependence of $\delta^{18}O$ in meteoric water. Despite the seasonal differences in the temperature signals of the $\delta^{18}O$

record and DFRC (March-July vs. June-July), the $\delta^{18}O$ record is strongly correlated with the reconstruction. This result is especially meaningful because the $\delta^{18}O$-temperature signal originates from a completely different process compared to the DFRC temperature signal. For example, the $\delta^{18}O$-temperature signal is due to the use of meteoric water that has been isotopically labelled by atmospheric temperatures, i.e., a passive $\delta^{18}O$-temperature signal. Conversely, the ring-width temperature signal likely results from a combination of many biological processes and phenological constraints that are directly and indirectly influenced by temperature. Both records show cool conditions during the mid-1800s followed by a general rise to peak warmth in recent decades. Differences between the two records occur mainly at decadal-frequencies, which can be explained by the fact that spring temperatures are more energetic at decadal frequencies than summer temperatures in NWNA (Hartmann and Wendler, 2005).

The OCF-Group 2 ring-width chronology (AD 1620-2007) is a composite of 11 white spruce site chronologies from Old Crow Flats in northern Yukon (Fig. 4.1) which do not show any signs of divergence (Porter and Pisaric, 2011). The OCF-Group 2 chronology is strongly correlated ($r = 0.83$, $p \leq 0.001$) with the Mackenzie Delta reconstruction (Fig. 4.5d). This strong association is related to the early-summer temperature sensitivity of both tree-ring networks, and the fact that temperatures are highly inter-correlated between the two regions (Porter and Pisaric, 2011). This long-term coherence demonstrates that both regions shared similar temperature histories over the last four centuries.

Finally, the Coppermine River ring-width chronology (AD 1046-2003) by D'Arrigo et al. (2009) from a stand of white spruce in western Nunavut (Fig. 4.1) is also

well correlated ($r = 0.44$, $p \leq 0.001$) with the reconstruction (Fig. 4.5e). The temperature-dependence of this chronology was affirmed in several studies (D'Arrigo et al., 2009; Visser et al., 2010; Porter and Pisaric, 2011). Since AD 1245, the Coppermine chronology has tracked the low-frequency trends expressed in the reconstruction, with coherence being especially strong since AD 1600 ($r = 0.57$, $p \leq 0.01$). Reduced coherence before AD 1600 may reflect a combination of factors such as lower sample depth for both records, differences in regional-representativeness (i.e., the DFRC reconstruction represents a 29 site network, while the Coppermine chronology represents only a single site and may contain more site-specific growth signals unrelated to climate), and regional temperature differences.

4.4.5 Long-term, hemispheric- and circumpolar-scale validation

The reconstruction is also well matched by temperature reconstructions at much larger spatial scales. A composite of six hemispheric-scale temperature reconstructions (Appendix C, SI-Note 4.4), largely tree-ring-based and representative of the Northern Hemisphere, was compared to the Mackenzie Delta reconstruction (Fig. 4.5f). The inter-series coherence is strongest at lower-frequencies, as would be expected (Jones et al., 2009), and the overall correlation ($r = 0.54$, $p \leq 0.001$) is encouraging given the differences in spatial-scale, and spatial-heterogeneity of temperatures over the past millennium (D'Arrigo et al., 2006; Mann et al., 2009). Further, the hemispheric records were produced mainly from tree-ring data detrended by regional-curve standardisation, in comparison to the DFRC which was produced by signal-free standardisation. Despite the spatial and data-processing differences, these records are well matched over the last 8

centuries suggesting that they are responding to the same climatic variable, i.e., warm-season temperature. One notable difference is a relatively warm early-20th century expressed in the hemispheric-scale composite. This early-20th century warmth (centered on ca. AD 1940) is a common feature of instrumental temperature records for the Northern Hemisphere as a whole (Brohan et al., 2006), however, it was not well expressed in NWNA (Porter and Pisaric, 2011) or the Mackenzie Delta region (Fig. 4.5a). Rather, the Mackenzie Delta experienced a more subdued warming trend during the early-20th century followed by accelerated warming in recent decades as is shown in the reconstruction (Fig. 4.5h).

Lastly, the Mackenzie Delta reconstruction agrees well with a multi-proxy composite reconstruction of temperatures based on a circum-Arctic network of sites (Fig. 4.5g) by Kaufman et al. (2009). The composite was calculated based on Kaufman et al.'s ice- and lake-core proxy records only (Appendix C, SI-Note 4.5). Although its temporal resolution is relatively coarse (10-year) compared to the Mackenzie Delta reconstruction, both records generally share the same low-frequency trends. Following AD 1245, both records transition from warm to cool conditions by the late-13th century, followed by a general warming to the ca. AD 1500s, although the circum-Arctic composite has a brief cooling at ca. AD 1525. Subsequently, both records exhibit a long-term cooling trend leading into the early-19th century, followed by a strong warming to present. This qualitative agreement suggests that the broader circum-Arctic region and the Mackenzie Delta have shared similar temperature histories over the last eight centuries with a very strong warming trend in recent decades that is exceptional in this long-term context.

4.5 CONCLUDING REMARKS

A new ring-width chronology, DFRC, is presented for the Mackenzie Delta region and used to reconstruct warm-season temperatures since AD 1245. The DFRC is unique compared to most temperature-sensitive tree-ring chronologies in NWNA because it was developed from a network of sites that largely exhibited divergent temperature-growth responses during the 20th century. Divergence in NWNA is a widespread phenomenon (D'Arrigo et al., 2008), but one that appears to be restricted to the 20th century (Cook et al., 2004) and has not affected all trees (Porter and Pisaric, 2011). In the Mackenzie Delta region, affected tree-ring records begin to diverge from their normal positive temperature response at ca. AD 1900. From AD 1930-1980, divergent and divergence-free records differentiate strongly in terms of growth trend with divergent records exhibiting a strong negative trend while divergence-free records exhibit a positive growth trend. This growth trend distinction is observed in other parts of NWNA (Porter and Pisaric, 2011) and was used here as a criterion to identify and exclude divergent records (post-AD 1900) from the DFRC. The reconstruction shows several cool intervals corresponding with the Wolfe, Maunder, and Dalton solar minima. These cool periods are interrupted by warm periods that are consistent with early-20th century warmth, but the late-20th century is by far the warmest period on record. The reconstruction reflects a rapidly warming Arctic in recent decades, in accordance with other long temperature-proxies, and supports the notion that late-20th century warming is anomalous in the context of the last eight centuries (ACIA, 2005; Jansen et al., 2007; Kaufman et al., 2009).

The DFRC is not well defined prior to AD 1245 ($\leq$ 15 trees, EPS $\leq$ 0.7) which is a limitation to extending the reconstruction further back in time. However, there is a need for annual-resolution temperature-proxy reconstructions spanning the full millennium (Jansen et al., 2007; Jones et al., 2009) and it may be possible to satisfy this goal in the Mackenzie Delta region. Millennial-length records are necessary to improve existing knowledge of the putative Medieval Climate Anomaly, which is not yet well constrained at global- and hemispheric-scales (D'Arrigo et al., 2006; Mann et al., 2009). With this objective in mind, future dendroclimatic investigations in the Mackenzie Delta region should focus on the development of long sub-fossil chronologies that are potentially found in the many shallow lakes that mark this region, as has already been well demonstrated for parts of northern Europe (e.g., Grudd et al., 2002; Linderholm and Gunnarson, 2005).

CHAPTER FIVE

ON ESTIMATING THE PRECISION OF STABLE ISOTOPE RATIOS IN PROCESSED TREE-RINGS[2]

5.1 INTRODUCTION

Stable isotope ratios (δ) in tree-rings are a valuable resource for dendrochronologists addressing both climatic (e.g., Treydte et al., 2006; Porter et al., 2009) and ecophysiological (e.g., Feng, 1999; Waterhouse et al., 2004) questions. Since stable isotope dendrochronology was first demonstrated (Craig, 1954), standard methods have been adopted and improved over the years (McCarroll and Loader, 2004), and continue to be refined even today (e.g., Laumer et al., 2009; Gagen et al., 2011). The focus of this study is on the reproducibility or precision of tree-ring δ values and, specifically, how it is estimated for samples processed from whole wood to various end products such as cellulose-nitrate, α-cellulose, or cellulose intermediates; the term 'processed tree-rings' is used to refer to such samples. This discussion applies mainly to stable isotopes that vary between whole wood and processed tree-rings due to isotopic biases of various wood compounds (i.e., $\delta^{13}C$), or exchange of loosely-bound H/O atoms with ambient H_2O or adhesion of ambient H_2O (i.e., $\delta^{2}H/\delta^{18}O$). A standard method is proposed for estimating the δ precision of processed tree-rings that accounts for

[2] A modified version of this chapter has been published in the journal Dendrochronologia – Porter, T, & Middlestead, M, 2012: On estimating the precision of stable isotope ratios in processed tree-rings. Dendrochronologia, 30: 239-242.

analytical uncertainties associated with sample processing. At present, many tree-ring isotope studies do not control for such uncertainties, or report that they do.

5.2 BACKGROUND

Stable isotope ratio measurements are subject to analytical uncertainties associated with the mass spectrometer, combustion or pyrolysis system, and sample amount and purity (Werner and Brand, 2001). These uncertainties lead to variability in measured δ values of samples which can be significant compared to variability between tree-rings and, thus, it is standard practice to report the 2σ (2 standard error) precision. *Ceteris paribus*, δ precisions of ca. ±2.5‰, ±0.1‰, and ±0.3‰ are typical for continuous-flow analysis of wood δ^2H, $\delta^{13}C$, and $\delta^{18}O$, respectively (McCarroll and Loader, 2004). Typically, δ precision is estimated from a long-term, running standard deviation of δ values measured for a Quality Assurance (QA) standard analysed along with each batch of samples introduced to the mass spectrometer; δ values for samples and the QA standard are calibrated against 2 or more internal reference standards that are also analysed along with each batch of samples, and whose δ values with respect to an internationally-accepted reference scale (e.g., VSMOW or VPDB) are well known. Ideally, the samples, QA standard, and reference standards are all of the same matrix (e.g., α-cellulose; Boettger et al., 2007; Brand et al., 2009).

For routine δ analysis of processed tree-rings, bulk quantities of the reference standards and QA standard are typically purchased commercially or developed in-house from whole wood using the same processing method applied to samples, consistent with

the Identical Treatment or 'IT' principle (Werner and Brand, 2001). However, in the case of the QA standard, the use of such 'ready-made' QA standards is not advised as they do not reflect uncertainties associated with sample processing that can impact upon the purity and δ of samples, mainly operator-related errors. Operator errors are inadvertent and unrealised, for if they were realised the compromised samples should not be analysed. These errors may include, but are not limited to, contamination from airborne particulates, processing irregularities (e.g., reactions were not always carried out to completion due to insufficient/variable solution strengths, heating, and reaction times; inadequate rinsing of chemical residues; etc.), and insufficient desiccation prior to $\delta^2H/\delta^{18}O$ analysis. Such errors are likely rare for an experienced operator. However, many tree-ring δ projects are carried out by senior undergraduate and graduate students, some of whom are learning these methods for the first time and may have limited laboratory experience. Operator error may occur more often in such cases, and the proposed method provides a system to monitor inter-batch reproducibility and identify potentially compromised results.

5.3 PROPOSED METHOD

To estimate the δ precision of processed tree-rings, the IT principle must be respected by exposing the QA standard to the same chemical processing steps that sample tree-rings undergo. Ideally, a bulk reserve (e.g., enough for several years of analysis) of homogeneous whole wood particles, of roughly the same consistency as a sample, should be prepared by milling a piece of wood into smaller particles and used as the QA standard. Alternatively, bulk quantities of wood flour or shavings can be purchased

commercially. Aliquots of the QA standard, consistent in mass to a typical sample, should be processed along with each batch of samples so that the QA standard is exposed to the same potential errors a sample is exposed to, which would be reflected in its δ value and the overall precision estimate.

To ensure that δ variability in the processed QA standard is not influenced by sampling error, it is critical that all aliquots are isotopically representative of the bulk reserve from which they were sampled. For large or small aliquots, a representative aliquot can be assured if the QA standard is a homogeneous mixture of fine-grained particles, e.g., approaching the consistency of fine sand. However, fine-grained particles are only appropriate for cellulose extraction methods that process samples individually in test tubes (e.g., Brendel et al., 2000). For 'batch-processing' methods that require samples to be cut into coarse-granules or slivers (e.g., Leavitt and Danzer, 1993; Loader et al., 1997), a coarse-grained QA standard should be used. Granular particles are ideal to facilitate a well-mixed bulk reserve. To avoid homogeneity issues with a coarse-grained QA standard, larger aliquots should be taken since individual granules may have a wide range of δ values; experimentation may be needed to determine the appropriate aliquot size.

During processing, all reasonable efforts should be exercised to ensure that samples and QA standards are treated equally (i.e., all reactions carried out to completion; samples and QA standards are rotated in the heating block or bath; etc.) to avoid potential systematic differences in the purity and δ of samples and QA standards. Once processing is complete, samples and QA standards should be sub-sampled for δ analysis. Sub-sampling is required to ensure the amount of sample, or QA standard,

introduced to the mass spectrometer system is constant as variability in sample amount can contribute variability to measured δ values. Fine-grained samples and QA standards can be readily sub-sampled as they are homogeneous, while coarse-grained materials must first be homogenised by mechanical milling or ultrasonic breaking (Laumer et al., 2009).

Precision can be estimated by characterising the 2σ range of a given series of δ values for the QA standard, although the number of QA data points included in the estimate will vary from one laboratory to the next based on internal protocols and, of course, the purpose of the estimate. In any case, there is no universal number of QA data points that must be used, as δ precision is a statistical estimate that accounts for sample size, but Bessel's correction (degrees of freedom = n-1) should be used to err on the side of caution, especially with small sample sizes. If the purpose of the estimate is to quantify long-term δ reproducibility for a given laboratory, then the estimate would likely contain hundreds to thousands of QA data points that span several years of routine analysis. However, if the purpose is to quantify δ reproducibility associated with a given project (e.g., tree-ring series), then it is more appropriate to use only QA data points from that project. Regardless, δ precision reporting should be unambiguous by stating whether or not the QA standard was processed along with samples, if the estimate is project-specific or a long-term average for the laboratory that conducted the analysis, and how many QA data points were used.

Lastly, it should be noted that the proposed method provides an opportunity to monitor inter-batch δ reproducibility and identify batches that have potentially been compromised during sample processing, which may be of considerable value in cases

where inexperienced operators are involved. For example, if the δ value for a QA standard falls outside the acceptable range of δ values (as per internal laboratory protocols; e.g., 99% confidence interval), then the batch that the QA standard belonged to should be scrutinised. If upon a second analysis the QA standard δ value is still found to be an outlier, the entire batch should be reprocessed or excluded. The final course of action, however, should be dictated by internal laboratory protocols.

5.4 PILOT STUDY

The proposed method was used in a recent tree-ring $\delta^{18}O$ project carried out at the G.G. Hatch Stable Isotope Lab. The objective was to measure the $\delta^{18}O$ of 210 tree-rings from white spruce (*Picea glauca* [Moench] Voss) trees sampled at 'Timber' site (Porter et al., 2009) near boreal treeline in the Mackenzie Delta, northern Canada. For the QA standard, a homogeneous mixture of fine-grained wood particles, from a large diameter core collected from the study site, was used. The samples and the QA standard were homogenised using a Retsch-Brinkmann MM200 Mixer Mill. The 210 samples plus 14 QA standard aliquots (ca. 70 mg) were processed in batches of 16 over 14 days. Each batch was processed from whole wood to α-cellulose in a single day using the rapid extraction method outlined by Brendel et al. (2000), but modified to include an alkaline hydrolysis step as suggested by Gaudinski et al. (2005). After processing, the samples and QA standards were placed in a drying oven at 50°C overnight, and then stored in a vacuum-sealed desiccator with Drierite, a gypsum-based desiccant.

Samples and QA standards were weighed (ca. 150-250 μg material) into silver capsules, returned to the desiccator for a minimum of 24 hours, and then loaded into a Costech zero-blank auto-sampler carousel. The auto-sampler was put under vacuum and purged with dry helium for 5 minutes before the $\delta^{18}O$ analysis began. A Thermo-Finnigan TC-EA and DeltaXP IRMS were used for the analysis (system parameters: pyrolysis tube at 1400°C; 5Å GC column at 90°C; 100 mL/min flow rate). Samples and QA standards were analysed in the order they were processed. Each QA $\delta^{18}O$ value reported here (Table 5.1) represents a single pyrolysis.

Sample and QA $\delta^{18}O$ values were calibrated using 3 α-cellulose reference standards with $\delta^{18}O_{VSMOW}$ values of 20.3, 27.5, and 32.8‰. Ideally, the $\delta^{18}O$ range of the reference standards should bracket the $\delta^{18}O$ values of the unknown samples; however, the QA standard (whose $\delta^{18}O$ was unknown before the analysis) was found to be depleted by ca. 3‰ compared to the most negative reference standard (i.e., 20.3‰). However, this is understandable since tree-rings in the Mackenzie Delta are labelled by some of the most isotopically-depleted precipitation in the Northern Hemisphere (Bowen and Revenaugh, 2003), and there are few sources of natural wood cellulose as depleted, high-arctic shrubs being one exception (Welker et al., 2005). Nevertheless, the 3-point calibration curve was quite linear ($r^2 \geq 0.99$) over the range 20.3-32.8‰, and extrapolation by ca. 3‰ is reasonable.

The 14 QA standards had a $\delta^{18}O_{VSMOW}$ range of 17.1-17.5‰, a mean of 17.3‰, and a 2σ precision of 0.3‰ (Table 5.1). As discussed above, a precision of 0.3‰ is typical for continuous-flow analysis of tree-ring $\delta^{18}O$, suggesting that the samples and QA standards were consistently processed to the same end product and probably did not

Table 5.1. $\delta^{18}O_{VSMOW}$ values for the 14 QA standards. Each value represents a single pyrolysis. The analysis took place over several weeks from July 12 to August 30, 2010.

QA std.	$\delta^{18}O$ (‰)	Date
W01	17.5	Jul-12
W02	17.1	Jul-12
W03	17.4	Jul-14
W04	17.5	Aug-13
W05	17.5	Aug-16
W06	17.2	Aug-17
W07	17.4	Aug-18
W08	17.1	Aug-18
W09	17.3	Aug-24
W10	17.5	Aug-25
W11	17.4	Aug-26
W12	17.2	Aug-27
W13	17.4	Aug-30
W14	17.2	Aug-30

Mean (W01-W14) = 17.3‰; 2σ = 0.3‰

accumulate much error in excess of what can be explained by uncertainties associated with the mass spectrometer, pyrolysis environment, and specifics of α-cellulose.

However, had caution not been used in treating all samples and QA standards the same, the δ precision estimate could have been very different. To demonstrate this point, 2 additional QA aliquots were prepared to α-cellulose and purposely not desiccated prior to analysis. As α-cellulose is a hygroscopic compound, it was expected that exposure to ambient humidity would contribute error to the $\delta^{18}O$ value. The 2 purposely-compromised QA standards were analysed on 2 separate days, both having a $\delta^{18}O$ value of 18.2‰. This compromised $\delta^{18}O$ value is greater than +7σ from the mean of the desiccated QA standards, thereby demonstrating how improper storage of samples, or even a leak in the desiccator, could lead to error in the $\delta^{18}O$ of samples. If such an error did occur during routine analysis, and the QA standard was not processed using the proposed method, it might not be possible to identify the error *post facto*.

5.5 CONCLUDING REMARKS

There are many sources of uncertainty that could influence the δ of processed tree-rings before samples are introduced to the mass spectrometer. To better characterize the δ precision of processed samples, QA standards must be treated as if they are samples. In isotope laboratories that specialize in tree-ring analysis and offer the service of preparing tree-ring cellulose, their in-house protocols could be revised fairly easily. However, in cases where the tree-ring researcher is responsible for preparing their own samples before sending them to an isotope laboratory, the onus is on the researcher to

provide the QA standards. In such cases, the isotope laboratory may recognize the merit of using the proposed method and waive the costs associated with analyzing additional QA standards. Again, the onus is on the researcher to inquire about such details.

CHAPTER SIX

APRIL-JULY MINIMUM TEMPERATURES SINCE AD 1780 RECONSTRUCTED FROM STABLE OXYGEN ISOTOPE RATIOS IN WHITE SPRUCE TREE-RINGS FROM THE MACKENZIE DELTA, NORTHWESTERN CANADA

6.1 INTRODUCTION

Instrumental climate data for most regions globally is limited to the last hundred years, and the duration and spatial-density of these records decreases pole ward (Lawrimore et al., 2011). Improved spatiotemporal coverage is needed to better characterise natural climate variability, especially at higher latitudes, evaluate the sensitivity of climate to pre-industrial forcings, and provide initialisation and verification datasets for climate models needed to forecast regional impacts. In place of missing instrumental records, natural proxies can be used to fill gaps in the global climate network (Jones et al., 2009; Bradley, 2011).

Tree-ring chronologies are especially useful because they are annually-resolved and, thus, comparable to instrumental climate records. The most climatically-sensitive tree-ring growth (e.g., ring-width or -density) chronologies are found at the margins of a tree's ecological range where climate is the primary limiting factor (Briffa et al., 2002). Arctic treeline is one such marginal environment where tree-ring growth chronologies are temperature-limited and have provided valuable insights on climate over the past millennium (Briffa et al., 1992; Esper et al., 2002; D'Arrigo et al., 2006; Wahl and Ammann, 2007). However, in more recent decades some white spruce stands in

northwestern Canada and interior Alaska have exhibited non-linear temperature-growth responses (Jacoby and D'Arrigo, 1995; D'Arrigo et al., 2004; Wilmking et al., 2004; Pisaric et al., 2007; McGuire et al., 2010; Porter and Pisaric, 2011), known as the 'Divergence Problem' (hereafter 'divergence'; D'Arrigo et al., 2008). Divergence in tree-ring studies has raised concerns over the ability to use affected chronologies in reconstructions of past climate (Jansen et al., 2007).

In light of these concerns, Porter et al. (2009) explored the potential of tree-ring stable oxygen isotope ratios ($\delta^{18}O$) as an alternative proxy in the Mackenzie Delta, a region where divergence is widespread (Pisaric et al., 2007). Porter et al. (2009) developed tree-ring $\delta^{18}O$ records (AD 1850-2003) from three white spruce trees at a site unofficially named 'Timber' (Fig. 6.1). Comparison with the nearest climate record at Inuvik showed that Timber $\delta^{18}O$ was significantly correlated with March-July minimum temperatures over the AD 1957-2003 period, suggesting a first-order link to temperature-dependent isotopic labelling of local precipitation (Dansgaard, 1964). However, this relation has yet to be rigorously assessed for climate reconstruction purposes. The main purpose of the present study is to evaluate the robustness of the Timber $\delta^{18}O$-temperature signal as a basis for developing an extended temperature reconstruction.

One factor that could complicate temperature signals in tree-ring $\delta^{18}O$, or any terrestrial $\delta^{18}O$ archive, is atmospheric circulation variability (Edwards et al., 1996, 2008; Birks and Edwards, 2009; Liu et al., 2011; Saurer et al., 2012). Changing circulation can alter the source region or rain-out history of atmospheric moisture, and the seasonality of precipitation, potentially affecting the stationarity of temperature signals in $\delta^{18}O$ archives (Dansgaard, 1964; Jouzel, 1999; Sodemann et al., 2008b; Sturm et al., 2010). For the

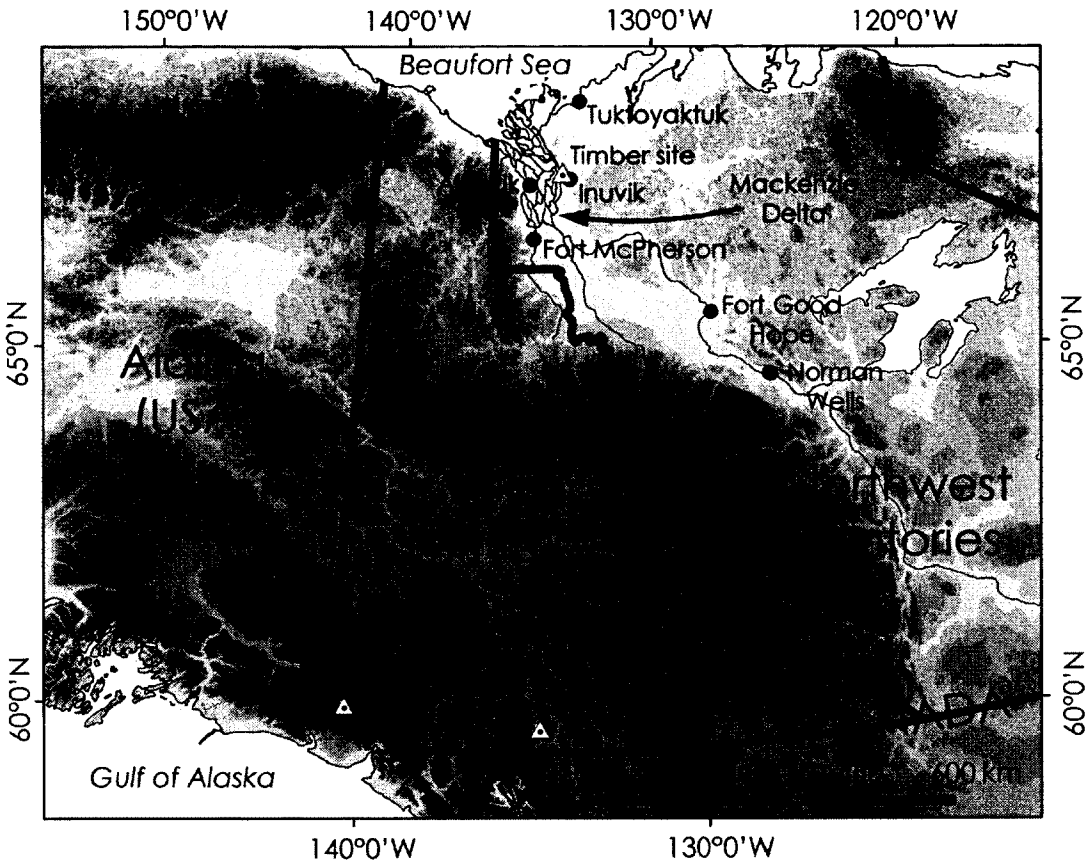

Figure 6.1. Map of study sites (triangles) and climate stations (solid dots) of interest. The shaded relief is based on the GTOPO30 digital elevation model (U.S. Geological Survey; http://www1.gsi.go.jp/geowww/globalmap-gsi/gtopo30/gtopo30.html) and differentiates between low (light grey) and high (dark grey) elevations.

study region and greater northwestern North America (NWNA) in general, the semi-permanent Aleutian Low (AL) positioned over the North Pacific is the primary pressure center driving atmospheric circulation and moisture advection to the interior (Burns, 1973; Wahl et al., 1987; Dyke, 2000; Serreze and Barry, 2005).

Because AL variability could conceivably influence the Timber $\delta^{18}O$-temperature relation, it is important to test the relation over a time period that experienced a wide range of circulation patterns before it is considered for reconstruction purposes. Here, the relation was evaluated using a newly compiled instrumental temperature record from six local stations that extends over the past century. Over the analysis period, AL strength has varied significantly at interannual and decadal frequencies, as quantified by the North Pacific Index (NPI; Trenberth and Hurrel, 1994), and it is important to note that this range of variability appears to be representative of its range over the last 400 years according to a well-verified NPI reconstruction by D'Arrigo et al. (2005). Therefore, the period of analysis seems appropriate for assessing the stability of the temperature-$\delta^{18}O$ relation under a wide range of circulation patterns.

However, evidence from two independent $\delta^{18}O$ records in southwestern Yukon (Fig. 6.1) (Mt. Logan PRCol ice-core [Fisher et al., 2004] and Jellybean Lake sediment-core [Anderson et al., 2005]) suggests an AL regime shift may have occurred at ca. AD 1840 that is unprecedented since at least AD 800 when a similar event is thought to have occurred (Fisher et al., 2004). The AD 1840 event was represented by a marked decrease in both records in spite of a general warming since AD 1840 indicated by a number of biological proxies from the area (Szeicz and MacDonald, 1995; Davi et al., 2003; D'Arrigo et al., 2006; Viau et al., 2012) which should have caused an $\delta^{18}O$ increase in the

PRCol and Jellybean records if they were dictated by a classical temperature effect. As such, the two records were thought to be circulation-sensitive, and it was speculated that the AD 1840 shift represented a transition from a zonal to meridional circulation regime consistent with an intensified AL (Fisher et al., 2004; Anderson et al., 2005). Results from simulations with an isotope-enabled general circulation model, however, suggested that enhanced meridional circulation would likely increase meteoric $\delta^{18}O$ (Field et al., 2010). Regardless, if a regime change did occur at AD 1840, it might have affected $\delta^{18}O$ archives across interior NWNA, and this would complicate the interpretation of $\delta^{18}O$-temperature signals from these archives. To explore this possibility in the Mackenzie Delta, Porter et al.'s (2009) tree-ring $\delta^{18}O$ record was extended to AD 1780 to look for anomalous variability at ca. AD 1840 as evidence of a regime shift.

Finally, model simulations were carried out using the NASA-GISS ModelE isotope-enabled general circulation model (Schmidt et al., 2005, 2006) as an additional line of inquiry to better understand the potential impact of circulation on meteoric and tree-ring $\delta^{18}O$ in the study region. This modelling exercise provides novel insights that are pertinent to the selection of sites for paleoclimate-$\delta^{18}O$ studies in NWNA.

6.2 MATERIALS AND METHODS

6.2.1 Tree-ring $\delta^{18}O$ data

The mean climatology, site characteristics, and existing tree-ring $\delta^{18}O$ series for Timber site are described by Porter et al. (2009). New cores for this study were collected from white spruce trees in 2008 and 2009 using a Haglof increment borer (12 mm internal diameter). A single bark-to-bark core passing through or near the pith was

collected from mature white spruce trees, providing 2 radii from each tree. Cores from three of the trees were selected for isotope analysis. The three cores were selected on the basis of tree longevity and ring-width. Tree longevity was a criterion to ensure the $\delta^{18}O$ series from each core would extend several decades prior to the putative AD 1840 event. Ring-width was a criterion to ensure a sufficient sample amount for analysis. Trees at Timber have narrow rings during the early-19th century which presented technical challenges for separating individual rings, and ensuring enough α-cellulose after processing. To overcome this challenge, cores with relatively wide rings during problem years were selected. This same criterion was used by Porter et al. (2009) due to the narrowness of late-20th century rings.

Tree-ring growth patterns of the sample cores were first visually cross-dated, measured using a Velmex tree-ring measuring system, and verified against the Timber master tree-ring chronology using the computer program COFECHA (Holmes, 1983). Sample rings were then separated under magnification using a scalpel. Duplicate rings from opposite radii of the same tree (i.e., representing the same year) were pooled. The sampled rings from each tree were analysed independently. Samples from two of the trees span the years AD 1790-1865 and samples from the third tree span AD 1780-1870. The samples were milled to fine wood particles, approximating the consistency of a fine sand, and processed to α-cellulose using Brendel et al.'s (2000) method but modified to include an alkaline hydrolysis step to ensure complete removal of non-α-cellulose compounds (Gaudinski et al., 2005; Boettger et al., 2007). In contrast, Porter et al.'s (2009) samples were processed using a Jayme-Wise-type α-cellulose extraction method described by Green (1963; see also Sternberg, 1989). The two methods differ in terms of the oxidants

used to remove hemicelluloses. However, given the same wholewood, both methods produce chemically-identical α-cellulose when fine-particle samples are used (Gaudinski et al., 2005).

The $\delta^{18}O$ analysis for this study was completed at the G.G. Hatch Stable Isotope Laboratory, University of Ottawa. The system specifications and reference standards used are outlined by Porter and Middlestead (2012). In contrast, Porter et al. (2009) completed their analysis at the Environmental Isotope Laboratory, University of Waterloo. Because equipment and laboratory protocols used in the two studies are not identical, isotopic offsets between the two datasets can occur. A recent inter-laboratory comparison by Boettger et al. (2007) demonstrated this effect showing that $\delta^{18}O$ results from the same samples analysed at 9 different laboratories were systematically offset by as much as 1‰, and this was attributed to differences in sample storage and low- vs. high-temperature pyrolysis. A possible analytical offset between the Porter et al. (2009) and new $\delta^{18}O$ series was assessed by comparing their median chronologies over their common period of overlap (AD 1850-1870). A mean offset of 0.7‰ was observed, likely due to inter-laboratory factors, and was corrected by adjusting the new series by +0.7‰. Adjusting the new series, however, is an arbitrary choice as it is difficult to say which dataset is more accurate with respect to the VSMOW (Vienna Standard Mean Ocean Water) scale.

To evaluate the $\delta^{18}O$ precision of the samples, Quality Assurance (QA) standards were prepared according to the identical treatment method outlined by Porter and Middlestead (2012). Fourteen QA standards were processed along with 210 of the 243 samples in equal batches (i.e., 1 QA standard + 15 samples per batch). The $\delta^{18}O$ precision estimate based on these QA standards was ±0.3‰, which is typical for non-processing-

related uncertainties alone (McCarroll and Loader, 2004). Given this result, it is likely that the samples were consistently processed to the same α-cellulose purity. In comparison, the $\delta^{18}O$ precision for the Porter et al. (2009) data was ±0.4‰.

Tukey's bi-weight robust mean is commonly used in dendrochronology research when merging independent tree-ring series into a mean chronology if sample size is greater than six, and the median function is used when sample size is less than or equal to six (Cook, 1985). Both measures of central tendency help to guard against outlier data points that can strongly affect the mean chronology when sample size is low. Here, sample size is always less than or equal to six, and so the median function is used to calculate the master Timber $\delta^{18}O$ chronology.

The Expressed Population Signal statistic (Wigley et al., 1984) was used to estimate the signal-to-noise ratio of the $\delta^{18}O$ series:

(1) $EPS = (N \times rbar)/(1 + (N - 1) \times rbar)$

where rbar is the mean inter-correlation between all tree-ring series over a given window length, and N is the number of series involved in the calculation. The EPS used here is calculated based on a 31 year window length. Because all Timber $\delta^{18}O$ series do not cover the same period, and some are not internally-continuous (e.g., many null data points in the 1970s due to narrow rings; refer to Porter et al., 2009), the EPS calculation was given some flexibility to allow up to a third of the 31 years for each tree to contain null data points. In these cases, N is not a discrete number and was defined as the mean number of trees available over the 31 year period.

6.2.2 Regional temperature record

A regional composite temperature record (AD 1892-2010) was used to assess the long-term temperature-dependence of the master Timber $\delta^{18}O$ chronology. The composite record was developed using monthly temperature data from several local stations including Tuktoyaktuk (1970-2007), Inuvik (1957-2006), Aklavik (1926-2007), Fort McPherson (1892-1977), Fort Good Hope (1908-2007), and Normal Wells (1943-2010) (Fig. 6.1). Raw temperature data were obtained from Environment Canada (http://climate.weatheroffice.gc.ca). As mean temperatures between the stations are biased by their geographic position, the mean and variance of each record were adjusted to match the Inuvik record before calculating the regional means (Appendix D, SI-Fig. 6.1). The regional composite record is discontinuous from AD 1892-1909 for most months, and continuous from AD 1910-2010.

6.2.3 Calibration and verification

Correlation analysis was used to evaluate the relation between the Timber $\delta^{18}O$ master chronology and monthly minimum, mean, and maximum temperatures. Monthly temperatures that shared a strong relation with Timber $\delta^{18}O$ were averaged into an optimal seasonal index. The robustness of the optimal temperature-$\delta^{18}O$ relation was assessed using a standard split-period calibration/verification analysis (Cook and Kairiukstis, 1990). The calibration statistics included Pearson's R, R^2, adjusted-R^2, Standard Error (SE), Durbin-Watson (DW), and a sign-test. The verification statistics included the Reduction of Error (RE) and Coefficient of Efficiency (CE).

6.2.4 Isotope-enabled general circulation modelling

The expected response between meteoric $\delta^{18}O$ and NPI (calculated as the mean sea-level pressure for the area 30°N-65°N, 160°E-140°W; Trenberth and Hurrel, 1994) was assessed using two model runs from NASA-GISS ModelE (2° × 2.5° horizontal grid resolution, 40 vertical levels; Schmidt et al., 2005, 2006) at a higher spatial resolution than Field et al. (2010). Run 1 (AD 1969-2009) was based on a free-running atmosphere, and Run 2 (AD 1970-2009) had its horizontal winds prescribed towards NCEP/NCAR Reanalysis (Kalnay et al., 1996). Both runs were forced using the same monthly sea-surface temperature (SST) field (Rayner et al., 2003). Although not entirely independent due to the common SST field, analysis of two simulations provides some indication of whether the model results are realization-specific.

Spatial correlations between NPI and modelled meteoric $\delta^{18}O$ were examined for fall-winter (Nov-Feb) and spring-summer (April-July) months. Seasonal $\delta^{18}O$ means computed from monthly means were weighted by monthly precipitation amount. Since the AL has a strong and significant influence on regional temperatures across NWNA (Mock et al., 1998), the effects of temperature were first removed from the meteoric $\delta^{18}O$ field (linear temperature-$\delta^{18}O$ relation was quantified by linear regression for each grid point and subtracted) to isolate $\delta^{18}O$ variability that may be related to changes in moisture source and trajectory. The residual $\delta^{18}O$ field was then correlated against NPI, yielding, in effect, a partial-correlation analysis. Finally, the modelled precipitation-NPI relation was explored to determine the potential for changes in precipitation seasonality, which could influence the seasonal bias of bulk soil water $\delta^{18}O$ for a given site.

6.3 RESULTS AND DISCUSSION

6.3.1 Timber $\delta^{18}O$ chronology

Over their common period of overlap (AD 1850-1870) the median $\delta^{18}O$ records from this study and Porter et al. (2009) are well correlated, demonstrating a common environmental signal and supports combining all series into a master chronology (Fig. 6.2). The master chronology spans the period AD 1780-2003 and is defined by one to six trees depending on the year (overall mean is 2.9 trees/year). Although the average sample size is relatively low compared to most traditional dendrochronology studies, the EPS results indicate a relatively high signal-to-noise ratio. The mean EPS for the entire record is 0.84, which is just below the 0.85 threshold (i.e., 85% signal, 15% noise) recommended by Wigley et al. (1984) for dendroclimatic research. EPS values are at their lowest in the following 12 years: AD 1963-1971, 1978-1979, and 1982; during these years EPS varies from 0.66-0.75. These low values are due to reduced sample depth in the late-1970s and early-80s, caused by extremely narrow rings as discussed by Porter et al. (2009). However, for all other years (94% of years), EPS ranges from 0.75-0.92 with a mean EPS of 0.85 and supports the use of this chronology for paleoclimatic research.

6.3.2 The putative AD 1840 event

Based on the Timber $\delta^{18}O$ master chronology (Fig. 6.2), there is no evidence for the AD 1840 event in the Mackenzie Delta region. Overall, the Timber chronology exhibits a gradual rising trend from AD 1780 to the late-19th century. There are no abrupt shifts from enriched to depleted values at ca. AD 1840. One fluctuation in the Timber $\delta^{18}O$ record that is a departure from normal variability is the temporary dip in AD 1893;

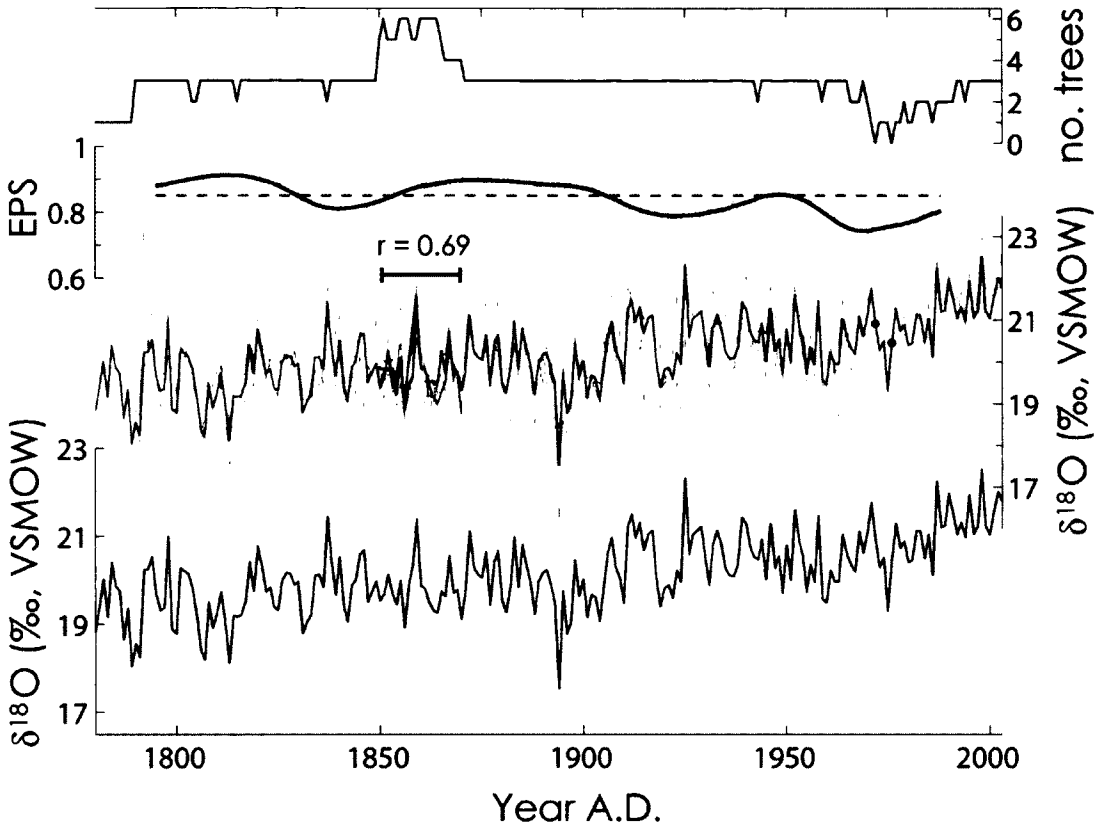

Figure 6.2. Timber site $\delta^{18}O$ tree-ring data: individual series (grey); median of Porter et al. (2009) data (blue) and new data from this study (red); the master Timber chronology (black); interpolated $\delta^{18}O$ values for the years 1972 and 1976 (black dots); inter-correlation between Porter et al. (2009) and new data during the period of overlap (1850-1870) is highly significant ($p \leq 0.001$). Expressed Population Signal (EPS) and sample depth (no. trees) are indicated; a 31-year cubic smoothing spline with a 50% frequency cut-off (Cook and Peters, 1981) is used to illustrate general EPS trends.

however, this has been related to an extremely cold spring recorded in the Fort McPherson record (Porter et al., 2009). Assuming that the Timber $\delta^{18}O$ chronology is an archive for meteoric $\delta^{18}O$, these results appear to suggest that no large-scale regime shift occurred at AD 1840 or that Timber $\delta^{18}O$ is insensitive to circulation regime changes.

At the Pacific-basin scale, the putative AD 1840 event corresponds well with important changes in the equatorial trade winds (Thompson et al., 1986; Hendy et al., 2002) and ENSO-event duration (Mann et al., 2000), suggesting possible large-scale teleconnections. However, it is not well-replicated in NWNA. For example, the event is not found in the NPI reconstruction by D'Arrigo et al. (2005), or other lake-core $\delta^{18}O$ records from interior Yukon (Anderson et al., 2011). At more local scales, it is also missing from the Eclipse $\delta^{2}H$ ice-core record (Fisher et al., 2004), ca. 40 km from the PRCol site. Further, it is notable that ice accumulation shifts are found in the PRCol and Eclipse ice-cores during the mid-19th century, but in opposite directions under, presumably, the same circulation regime (Fisher et al., 2004). Given these disparate results, it may be that the AD 1840 event found in the PRCol and Jellybean Lake records was not caused by a large-scale regime shift, but perhaps it represents a more subtle change in atmospheric flow that was amplified by complex topography and the extreme elevation of the St. Elias Mountains. A relative increase in depleted winter snows should not be ruled out either (Field et al., 2010).

Conversely, the absence of the AD 1840 event in Timber $\delta^{18}O$ record could also indicate that the Mackenzie Delta region is insensitive to AL variability. This possibility was evaluated using the ModelE simulations based on a correlation analysis of modelled NPI versus meteoric $\delta^{18}O$ (with the effects of temperature removed) (Fig. 6.3), and

modelled NPI versus precipitation amount (Fig. 6.4). The large-scale correlation patterns vary greatly between November-February (NDJF) and April-July (AMJJ), as would be expected since AL is a prominent feature mainly during the cold-season and starts to break down in April (Serreze and Barry, 2005), but some generalizations can be made. For Timber and adjacent areas, NPI-$\delta^{18}O$ correlations are mostly insignificant for Runs 1 and 2 in both seasons, but especially in AMJJ (Fig. 6.3). In general, NPI-$\delta^{18}O$ correlations are weak and insignificant for interior NWNA. A higher spatial density of significant, weak or moderate correlations occurs along the Pacific coast of NWNA and further inland to the northeast. Of particular interest, Run 2 NPI-$\delta^{18}O$ correlations are inverse and significant for PRCol suggesting that a deeper AL (i.e., enhanced meridional flow) would cause a positive shift in meteoric $\delta^{18}O$, as suggested by Field et al. (2010).

For the Timber area, NPI-precipitation correlations are also rather weak and insignificant overall, but with a greater spatial-density of significant correlations during NDJF (Fig. 6.4; see also Appendix D, SI-Fig. 6.2). Regardless, Timber $\delta^{18}O$ is more closely associated with AMJJ (Porter et al., 2009), a season when precipitation levels are increased in the region (Burn and Kokelj, 2009). Overall, AMJJ NPI-precipitation correlations are weak and insignificant in the Mackenzie Delta and interior NWNA. Considering the NPI-precipitation and NPI-$\delta^{18}O$ correlation results in tandem, it seems unlikely that AL variability would strongly affect Timber $\delta^{18}O$, implying that this record may be of considerable value as a first-order temperature proxy. Therefore, the absence of an AD 1840 shift in the Timber $\delta^{18}O$ record should not be considered evidence that an AD 1840 event did not occur, as is suggested by the PRCol and Jellybean Lake records.

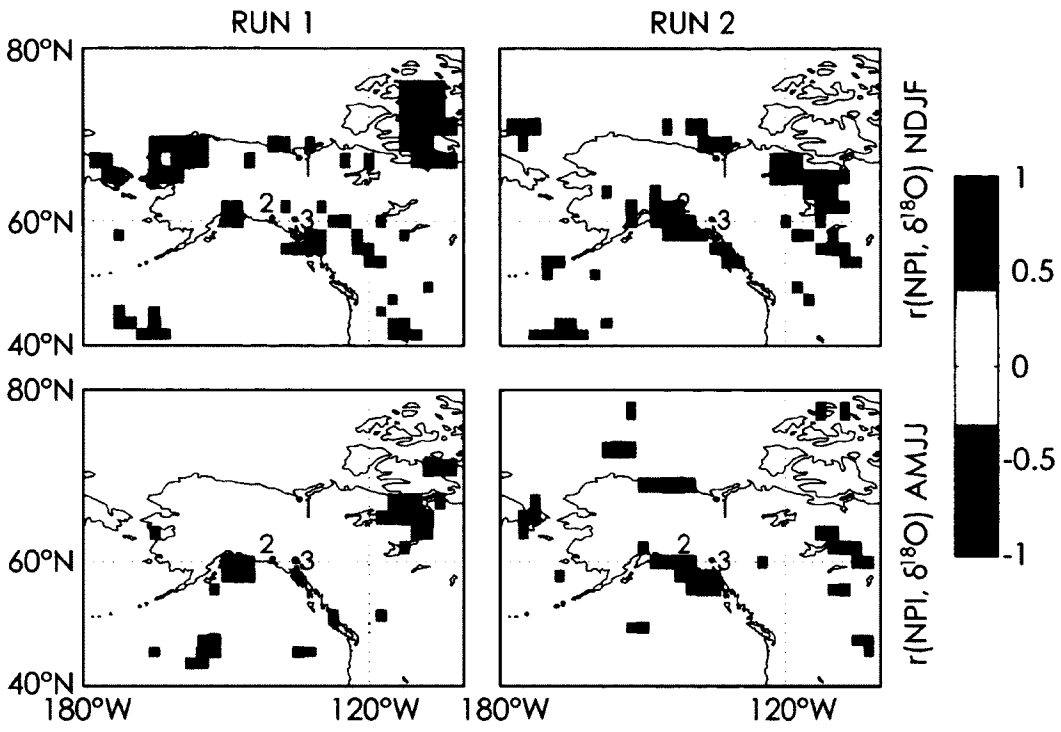

Figure 6.3. A correlation analysis between NPI and simulated meteoric $\delta^{18}O$ (influence of temperature on $\delta^{18}O$ removed) for fall-winter (NDJF; top) and spring-summer (AMJJ; bottom) months. Results from Runs 1 (left) and 2 (right) are compared. Points 1, 2, and 3 are Timber, PRCol, and Jellybean Lake, respectively.

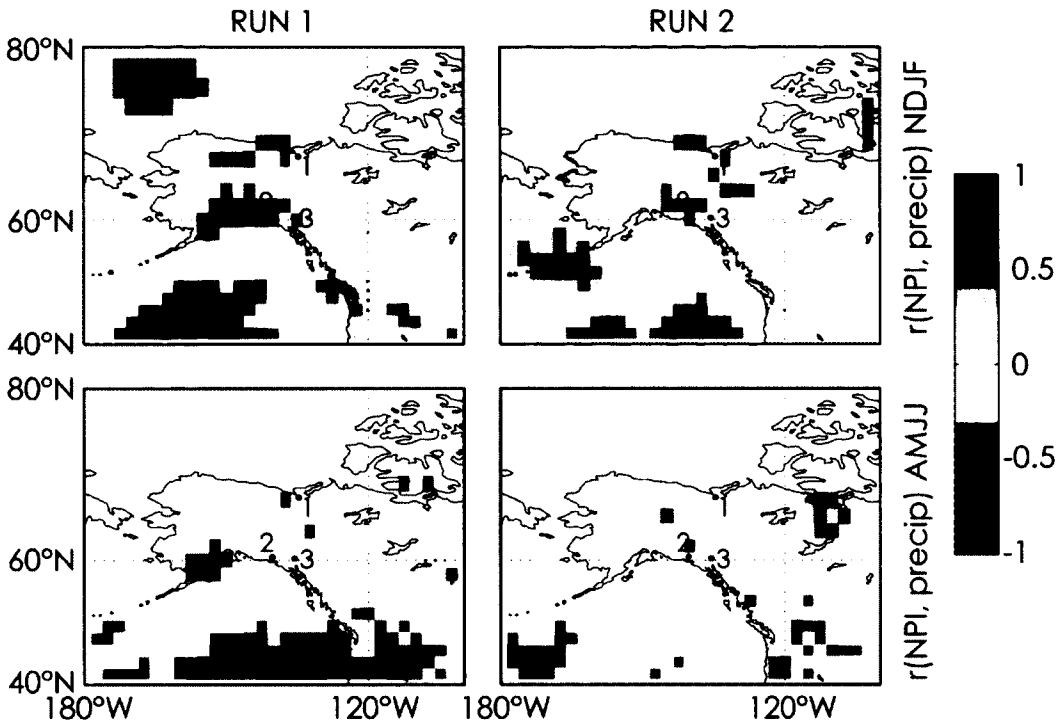

Figure 6.4. A correlation analysis between NPI and precipitation amount for fall-winter (NDJF; top) and spring-summer (AMJJ; bottom) months. Results from Runs 1 (left) and 2 (right) are compared. Points 1, 2, and 3 are Timber, PRCol, and Jellybean Lake, respectively. These correlation patterns were also assessed using the longer NCEP/NCAR Reanalysis (1948-2009; Kalnay et al., 1996) and ERA-40 Reanalysis (1958-2002; Uppala et al., 2005) datasets, and are provided in Appendix D (SI-Fig. 6.2).

As for PRCol and Jellybean Lake, the NPI-precipitation correlations for Runs 1 and 2 are also quite weak and insignificant during AMJJ (Fig. 6.4; see also Appendix D, SI-Fig. 6.2). However, the annual water budget for coastal southwestern Yukon is cold-season dominated (NCEP/NCAR Reanalysis data; Kalnay et al., 1996), and so NPI-precipitation associations during NDJF are likely much more important. The NDJF NPI-precipitation correlations are inverse and significant for PRCol (Runs 1 and 2) and Jellybean Lake (Run 1 only), implying that a deeper AL would lead to increased precipitation (n.b., strengthened NJDF correlation patterns are well replicated using the longer NCEP/NCAR and ERA-40 Reanalysis datasets – Appendix D, SI-Fig. 6.2). Therefore, the AD 1840 shift from enriched to depleted $\delta^{18}O$ could represent a disproportional increase in winter precipitation, possibly due to enhanced meridional flow as suspected by Fisher et al. (2004). However, the net change in $\delta^{18}O$ archives for S.W. Yukon is more complex due to the opposing effects of moisture source/trajectory on isotope distillation (Fig. 6.3) and precipitation seasonality (Fig. 4; Appendix D, SI-Fig. 6.2), which cancel to some extent. A more sophisticated analysis is needed to determine which factor is likely to dominate; however, that is beyond the scope of this study.

6.3.3 Timber $\delta^{18}O$-temperature reconstruction

Monthly (prior-year September to growth-year August) correlations between the master Timber $\delta^{18}O$ chronology and the regional temperature record were assessed over the period AD 1892-2003. Consistent with Porter et al. (2009), Timber $\delta^{18}O$ is closely associated with spring-summer minimum temperatures (Table 6.1), but one minor difference is that April-July is shown here to be the optimal seasonal index, whereas

Porter et al. (2009) found it was March-July based on their analysis using the shorter Inuvik temperature record (i.e., AD 1957-2003).

The robustness of the April-July minimum temperature-$\delta^{18}O$ relation was evaluated using a split-period calibration/verification analysis (Table 6.2). The calibration periods were 1893-1953 (Split 1) and 1954-2003 (Split 2); verification periods are the opposites of the calibration periods. The results demonstrate that the association between Timber $\delta^{18}O$ and April-July minimum temperatures is robust. For Splits 1 and 2, Timber $\delta^{18}O$ accounts for 35% and 16% of temperature variability, respectively. The weaker Split 2 adjusted-R^2 is likely due to the fact that the master chronology is not as well defined during the 1970s and 1980s due to lower sample depth. For Splits 1 and 2, the Durbin-Watson statistic is close to a value of 2.0, indicating very little autocorrelation in the residuals. The standard error is slightly less for Split 1 (1.05°C) than Split 2 (1.36°C), indicating slightly more error in the residuals during the latter period, as would be expected given the sample depth differences.

Results for the sign-test, a high-frequency test, are mixed. For the Split 1 calibration, the sign-test result is highly significant suggesting that the sign of interannual Timber $\delta^{18}O$ changes largely matches changes in April-July minimum temperature. However, Split 2 does not pass the sign-test. Again, this likely relates to the low number of samples defining the master chronology during the 1970s and '80s. Despite this shortfall, it is encouraging that Timber $\delta^{18}O$ is associated with temperatures as strongly as it is considering the many potential sources of non-temperature-related noise, e.g., white noise from analytical uncertainties (Werner and Brand, 2001; Porter and Middlestead, 2012), minor evaporative-enrichment effects (Roden et al., 2000), residual soil water

Table 6.1. Monthly and seasonal correlations between regional-composite minimum temperatures and the Timber mean $\delta^{18}O$ chronology (AD 1891-2003). Correlations significant at $p \leq 0.01$ (one-tailed) are bolded.

		r-value
Year t-1	Sept	0.05
	Oct	0.16
	Nov	0.11
	Dec	0.15
Year t	Jan	**0.24**
	Feb	0.22
	Mar	0.22
	Apr	**0.47**
	May	**0.44**
	Jun	**0.32**
	Jul	**0.28**
	Aug	0.13
Season	AMJJ*	**0.54**
	AMJ*	**0.53**
	AM	**0.51**

*N.B., Fort McPherson temperature data for June (1896) and July (1893, 1900, and 1908) were unavailable; to allow the calculation of April-July seasonal values for these years, the missing June and July data points were estimated using the closest four years of available data.

Table 6.2. Calibration/verification and full-period (AD 1893-2003) calibration statistics for linear regression models of April-July minimum temperatures as a function of the mean Timber $\delta^{18}O$ chronology.

	Split 1	Split 2	Full period
Calibration			
Period	1893-1953	1954-2003	1893-2003
N	51	50	101
Slope	0.97	0.87	1.01
Intercept	-23.60	-20.92	-24.10
SE	1.05	1.36	1.24
DW	1.47	2.19	1.97
R	0.60	0.42	0.55
R^2	0.37	0.17	0.30
Adj-R^2	0.35	0.16	0.29
Sign (+/-)	36/14[§]	23/26	60/40*
Verification			
Period	1954-2003	1893-1953	n/a
N	50	51	n/a
RE	0.31	0.46	n/a
CE	0.08	0.21	n/a

N.B., the period 1893-1953 contains only 51 years of valid data points; sign-test results significant at $^{\S}p \leq 0.01$ and $*p \leq 0.1$; all correlations are significant at $p \leq 0.01$ (one-tailed).

from previous years and occasional flooding (Kokelj and Burn, 2005), and uncertainties in the meteoric $\delta^{18}O$-temperature response (Dansgaard, 1964; Fricke and O'Neil, 1999).

The verification reduction of error and coefficient of efficiency results are always above zero for Splits 1 and 2, indicating that both calibration models are more skilful than the mean climatologies of the calibration and verification periods, respectively. These verification results indicate that Timber $\delta^{18}O$ is a suitable first-order proxy for April-July minimum temperatures. A full-period (AD 1893-2003) calibration model, explaining 29% of the observed temperature variability, was used to predict April-July minimum temperatures back to AD 1780 (Table 6.2). The full-period model has a Durbin-Watson statistic of 1.97, standard error of 1.24°C, and a sign-test result of 60 agreements and 40 disagreements that is significant at $p \leq 0.057$.

Predicted and observed temperatures were compared to demonstrate coherence (Fig. 6.5a). 'Local' temperatures in the comparison are the regionally-averaged temperature data for the Mackenzie Delta region (Appendix D, SI-Fig. 6.1). Temperature estimates from the 20th Century V2 Reanalysis (20CR) project (Compo et al., 2011) were used for additional verification. The 20CR are synthetic data generated by a numerical weather prediction model constrained by observed surface pressure, sea-surface temperatures, and sea-ice extent. For the study region and neighbouring areas (60-70°N, 130-140°W), 20CR temperatures for April-July provide a good approximation of local temperatures (Appendix D, SI-Fig. 6.3) and were used to gap fill missing data points in the local temperature record from AD 1871-1909 (Fig. 6.5a).

The local-20CR composite and $\delta^{18}O$-predicted temperatures are well matched over the full period of overlap (AD 1871-2003), especially at lower frequencies (e.g., R =

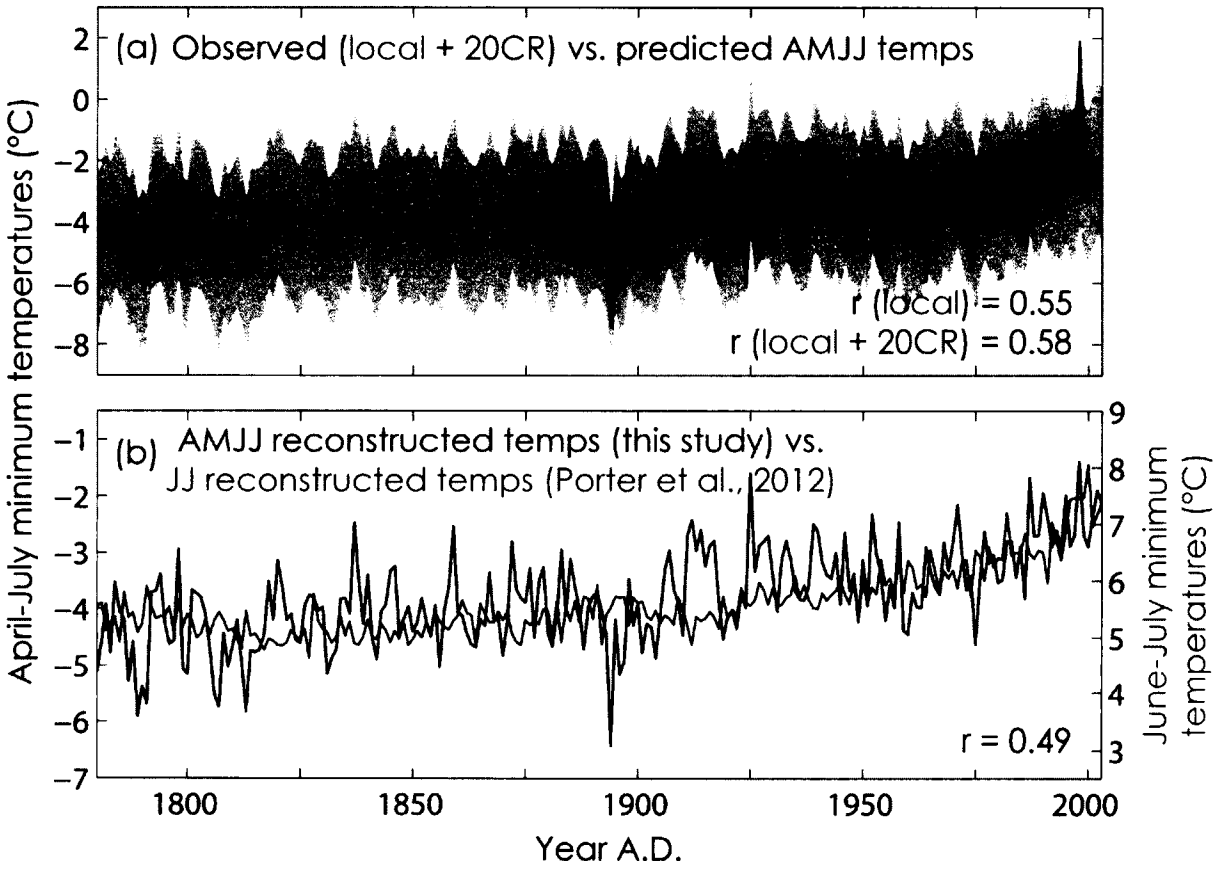

Figure 6.5. (a) Comparison between observed (colour) and predicted (black) April-July minimum temperatures since AD 1871; the observed temperature data are a composite of local temperature (Appendix D, SI-Fig. 6.1) and 20CR (Appendix D, SI-Fig. 6.3) data; the shaded confidence interval represents two standard errors of the prediction (± 2.48°C). (b) Comparison of the $\delta^{18}O$- temperature reconstruction (this study) and ring-width-inferred June-July temperatures for the Mackenzie Delta region (Porter et al., 2012). All correlations are significant at $p \leq 0.001$.

0.78/0.88 when both series are smoothed with a 5-year/10-year cubic-smoothing spline; Cook and Peters, 1981). From AD 1871-1893, both records show a brief cooling trend to a low in AD 1893, warming to the ca. 1940s, slight cooling to the ca. 1960s, and a further warming trend to present. According to the reconstruction, April-July temperatures today are likely the warmest they have been in the last 230 years. Qualitatively, it is encouraging that the reconstruction captures the sharp cooling event in AD 1893, but it does not fully capture the AD 1998 warm event, corresponding with the 1997/98 El-Niño (van Oldenborgh, 2000) which had a major impact on global climate. However, given the many sources of noise that could influence the temperature signal, it is not surprising that some extreme events are not well reconstructed.

On a final point of verification, the $\delta^{18}O$-temperature reconstruction was compared to a June-July temperature reconstruction for the Mackenzie Delta by Porter et al. (2012) based on a regional-scale network of 'divergence-free' ring-width chronologies. Aside from the fact that one reconstruction is $\delta^{18}O$-based and the other is ring-width-based, a second important difference is that they are tuned to slightly different seasons. As a general rule, the coherence of temperatures within a region will be best during and between cold-season months, but tends to improve for all seasons over longer time periods (e.g., multi-decadal to centennial; Jones et al., 2009). Therefore, the two reconstructions are expected to be least similar at shorter-frequencies (e.g., interannual to decadal). One apparent discrepancy is found in the ca. 1940s when April-July minimum temperatures seem to be anomalously warm compared to June-July minimum temperatures (Fig. 6.5). In this region, the 1940s was a warm period for most months

except summer (Appendix D, SI-Fig. 6.1), and so the apparent discrepancy is actually evidence that the reconstructions are behaving as they should.

As expected, the reconstructions share the same underlying trends characterised by lower temperatures in the early- to late-19th century followed by a strong 20th century warming trend, consistent with broad-scale instrumental and proxy-based evidence for a rapidly warming Arctic (ACIA, 2005; Kaufman et al., 2009). Another important point regarding the coherence of these reconstructions is that their temperature signals result from entirely different physical processes (i.e., temperature-effect for $\delta^{18}O$ and, presumably, temperature-driven biological constraints for ring-width) and, thus, their agreement provides independent verification and added confidence to each other. For the purpose of intra-regional verification of proxy reconstructions, Jones et al. (2009) highlighted the need for new proxy types in all parts of the world. At least in the Mackenzie Delta region, $\delta^{18}O$ appears to be an excellent candidate for this purpose.

6.4 CONCLUDING REMARKS

There have been many case studies exploring the paleoclimatic 'potential' of tree-ring $\delta^{18}O$ for various locales of the world (McCarroll and Loader, 2004); however, in nearly all cases the $\delta^{18}O$ chronologies were limited to the modern instrumental climate data period, rather than developing long $\delta^{18}O$ chronologies for reconstruction purposes, which was a criticism of Gagen et al. (2011). This study has moved beyond potential and demonstrated the first tree-ring $\delta^{18}O$-temperature reconstruction for a high-latitude site in northwestern North America, and one of a few worldwide. The statistical and visual diagnostics for the reconstruction provide strong evidence that tree-ring $\delta^{18}O$ is a viable

temperature proxy for the Mackenzie Delta, which offers promise for much longer reconstructions given that millennial-length tree-ring chronologies are found in this region (Szeicz and MacDonald, 1996; Bégin et al., 2000; Porter et al., 2012).

The fact that the Timber $\delta^{18}O$-temperature signal is as much a function of spring (April-May) temperature as it is of summer (June-July) temperature also deserves some attention. For the circumpolar boreal forest, the more traditional tree-ring indicators such as ring-width are often biased towards the warm season (Garfinkel and Brubaker, 1980; Jacoby and D'Arrigo, 1989; Briffa et al., 1998b; Barber et al., 2000; Davi et al., 2003; Treydte et al., 2006; Wilson et al., 2007; D'Arrigo et al., 2009; Esper et al., 2010; Andreu-Hayles et al., 2011), which imparts a warm-season bias on large-scale reconstructions based heavily on high-latitude ring-width data (Jansen et al., 2007). Although seasonal (e.g., warm- vs. cold-season) differences are less important when multi-decadal to centennial climate variability is of interest (Jones et al., 2009), there remains a need for proxies with a variety of seasonal biases to improve knowledge of seasonal and mean annual climate dynamics at regional- and global-scales. Improved knowledge of past seasonal dynamics could serve several purposes, including the ability to providing more refined datasets for calibrating and verifying GCMs, and diagnosing the natural origins of climate anomalies. Regarding the latter, climatic variations linked to solar or volcanic forcings might be expected to be coherent across all seasons, whereas internal forcings linked to Pacific ocean-atmosphere dynamics, for example, tend to be expressed mostly during the cool season. At least in the Mackenzie Delta, tree-ring $\delta^{18}O$ is sensitive to a broader seasonal window of climate than tree-ring width and, together,

these proxies can potentially be used to tease apart temperature differences between spring and summer conditions.

The well-known relation between temperature and meteoric $\delta^{18}O$, especially for higher-latitude sites, presents an obvious opportunity to use $\delta^{18}O$ archives to reconstruct temperatures. This relation has been most popularly applied to the Greenland and Antarctica ice-cores (Jouzel et al., 1987; Dansgaard et al., 1993; Johnsen et al., 2001; Augustin et al., 2004). However, atmospheric circulation variability can potentially complicate the interpretation of more continental $\delta^{18}O$ records as first-order temperature proxies (Sturm et al., 2010), and the importance of these effects for most parts of the world is not well understood, partly due to the paucity of the global meteoric $\delta^{18}O$ records (Bowen and Revenaugh, 2003). Alternatively, isotope-enabled general circulation models can be used as practical tools for understanding the importance of circulation effects for various regions, as was demonstrated here. Further, it would seem there is potential to use these models to guide in site selection for tree-ring $\delta^{18}O$ research. For example, if the research objective is to develop a reconstruction of temperature, sites where circulation effects are predicted to be strong should be avoided. Conversely, if circulation is the target variable, areas that are most strongly affected by circulation could be sampled.

CHAPTER SEVEN

CONCLUSIONS AND OUTLOOK

7.1 KEY FINDINGS

This research completed several objectives pertinent to the use of tree-ring width and $\delta^{18}O$ as paleoclimatic archives in NWNA. Furthermore, one methodological contribution specific to the analysis of stable isotopes in processed tree-rings was made. The key findings are reviewed here.

1) Insights on temperature-growth divergence in NWNA

Chapter 3 provided new insights on the, hitherto, poorly-understood boreal forest Divergence Problem which has affected many northern tree-rings chronologies, especially in NWNA. A 23-site network of white spruce ring-width chronologies was established in Old Crow Flats, near boreal treeline, where dendroclimatic research has been largely absent. The site density of this network is unparalleled by other divergence studies in NWNA, which provided a unique opportunity to identify regionally-coherent growth patterns linked to climate. The analysis revealed two primary growth patterns in the region, one that diverged from temperatures since the early-20th century and one that did not. These two patterns are widespread across NWNA, confirming that divergence was caused by a large-scale forcing, such as climate. It was speculated that anomalously dry conditions during the 20th century, exacerbated by recent warming, have caused some trees to respond negatively to increased warming. Divergence across NWNA appears to be unique to the 20th century in the context of the last seven centuries, at least, implying

that tree-ring-based temperature reconstructions over this period are possible if divergent growth trends are excluded when calibrating temperature-growth transfer functions. The reason that only some sites/trees are affected, however, remains poorly understood. Since divergent and divergence-free sites/trees are found in close proximity to each another, it was speculated that ecological factors that regulate local soil moisture availability, rather than absolute precipitation differences, may pre-dispose some sites to be more susceptible to drought-stress and divergence than others.

2) Divergence-free temperature reconstruction, AD 1245-2007

Chapter 4 introduced a new 29-site network of white spruce chronologies for the Mackenzie Delta region. Most of the trees (ca. 82% for the average site) exhibit a divergent temperature-growth response, similar to what has been observed in other parts of NWNA. Based on the premise that divergence is unique to the 20th century, a divergence-free regional chronology was developed by excluding the divergent portions of the affected records from the regional mean. Divergent records were distinguished from divergence-free records based on growth trend during the period AD 1930-1980, divergent/divergence-free records having a negative/positive trend. The divergence-free chronology expressed a robust temperature signal over the instrumental period (AD 1892-2007) and was used to infer June-July minimum temperatures since AD 1245. The reconstruction was validated by several other temperature proxies from nearby regions and circum-Arctic/hemispheric site networks. The divergence-free reconstruction indicates cool conditions in the late-13th, early-18th, and early-19th centuries that coincide with known solar minima. These cooler periods are separated by warmer periods that, in

some cases, equal the warmth of the early-20th century. However, the late-20th century is by far the warmest period on record. Each of the last six decades, AD 1950-2009, ranks in the top ten warmest decades since AD 1245, the last four being the warmest. The latest decade is estimated be 1.4°C warmer than any decade before the mid-20th century. Recent warming in the Mackenzie Delta is anomalous in the context of the last eight centuries.

3) The δ precision estimate for processed tree-rings

Chapter 5 draws attention to the *status quo* method for estimating the precision of stable isotope ratios (δ) in 'processed tree-rings'. The *status quo* method is appropriate for estimating δ precision due to analytical uncertainties associated with the combustion or pyrolysis environment, mass spectrometer, and analyte specifics, but does not account for uncertainties associated with the processing of whole wood samples to various forms of cellulose, mainly due to operator-related errors. A new method is proposed to account for processing-related uncertainties, and is demonstrated for the Mackenzie Delta $\delta^{18}O$ data introduced in Chapter 6.

4) $\delta^{18}O$-based temperature reconstruction, AD 1780-2003

Chapter 6 examined the potential to use the Timber tree-ring $\delta^{18}O$ chronology as a reliable temperature proxy. One potential complication for the robustness of temperature signals in any natural $\delta^{18}O$ record labelled by meteoric water is atmospheric circulation variability. The Timber $\delta^{18}O$-temperature relation was demonstrated to be robust over the period AD 1871-2003, a period that experienced a wide range of atmospheric circulation variability which is thought to equal the range of variability since AD 1600. Because the

$\delta^{18}O$-temperature relation is robust over the period AD 1871-2003, it can be assumed that it was robust over periods with a similar range of atmospheric circulation variability, i.e., since AD 1600. The $\delta^{18}O$ record was used to infer April-July minimum temperatures over the period AD 1780-2003, and is well verified by the divergence-free reconstruction from Chapter 4. The equal spring-summer seasonal bias of the $\delta^{18}O$ temperature reconstruction is unique compared to most high-latitude ring-width-based temperature reconstructions which are often solely a function of summer temperatures.

Evidence for a putative circulation regime shift at AD 1840, inferred by two $\delta^{18}O$ records from southwestern Yukon, was not found in the Timber $\delta^{18}O$ record suggesting either that no such event occurred or that tree-ring $\delta^{18}O$ in the Mackenzie Delta region is insensitive to circulation variability. Based on simulated $\delta^{18}O$ data from the NASA-GISS ModelE isotope-enabled general circulation model (isoGCM), and the observed stability in the Timber temperature-$\delta^{18}O$ relation since AD 1871, it does not seem likely that atmospheric circulation would have a strong impact on average meteoric or tree-ring $\delta^{18}O$ in the Mackenzie Delta region. Therefore, the lack of evidence for the AD 1840 event in the Timber $\delta^{18}O$ record should not be considered as evidence that such an event did not occur.

7.2 FUTURE RESEARCH

The findings in Chapters 3, 4, and 6 have yielded important new insights on the value of tree-ring width and $\delta^{18}O$ as paleoclimatic archives in NWNA, and as would be expected, these new insights have pointed to new questions and opportunities for future research. Several considerations for future research are provided here.

1) Why some trees diverge and others do not

In Old Crow Flats and the Mackenzie Delta, it was demonstrated that divergence affects only some sites within a region, or some trees within a site. The physical reasons behind the spatial intricacies of divergence may be related to local-scale ecological factors that regulate the retention of soil moisture. In particular, it was hypothesized that stand density and surficial organic layer (SOL) thickness are important. For example, a greater canopy and sub-canopy plant density equates to less water per tree compared to a lower stand density, given the same amount of water inputs. SOL thickness is also an important variable. Thicker SOLs reduce soil temperatures during summer, which limits evaporative water loss from the soil. Water resources are expected to be more limited for trees with a higher density of neighbouring trees or a thin SOL, and this may be why some trees are more prone to drought stress and divergence. This hypothesis could be tested by re-sampling trees from a subset of sites in Old Crow Flats and the Mackenzie Delta, measuring the ecological variables of interest around each tree, and evaluating if certain ecological conditions favour one growth response over the other. Evaluating the physical reasons for divergence is an important avenue for future research, and is critical to a more conclusive assessment of the likelihood divergence has or has not occurred in the past.

2) Extend the Mackenzie Delta temperature reconstructions

Tree-ring width and $\delta^{18}O$ are valuable temperature proxies in the Mackenzie Delta region and were used to reconstruct June-July and April-July temperatures back to AD 1245 and 1780, respectively. There is potential to extend both reconstructions further

back in time using sub-fossil wood, and this would serve two main purposes. Since both proxies adopt their temperature signals from completely different processes, they can be used to provide independent, mutual verification. By extending the $\delta^{18}O$-based reconstruction to AD 1245 and comparing it with the ring-width-based reconstruction, the conclusions that (i) *divergence is likely restricted to the 20th century* and (ii) *the temperature-$\delta^{18}O$ relation is time-stable prior to the 20th century* could be further verified. If the reconstructions were coherent from AD 1245-present (especially at multi-decadal to centennial timescales), this would imply that both temperature-proxy relations were time-stable, which would provide an additional layer of confidence to the reconstructed temperature history for this region. However, if little coherency was observed, this would imply that one or both of the temperature-proxy relations were unstable, which would warrant further investigation.

A second reason to extend the reconstructions is to improve knowledge of earlier climate anomalies in this region, e.g., the putative Medieval Warm Period (ca. AD 700-1200), which remains poorly constrained by high-resolution proxy records in most parts of the world, a limitation to diagnosing its origin(s). Such an effort requires development of new tree-ring chronologies that span earlier time periods, which may be a formidable challenge in the Mackenzie Delta region. As discussed in Chapter 4, the oldest tree-ring records from the region are found in the Campbell Dolomite Uplands and Eskimo Lakes localities, which extend into the 11th and 12th centuries, respectively. Future efforts to develop longer chronologies should target these localities and explore the possibility of recovering sub-fossil wood from lake bottoms, a strategy that has been successfully used in some parts of northwestern Europe to develop multi-millennial-length chronologies.

3) IsoGCM-guided sampling for tree-ring $\delta^{18}O$ research

IsoGCMs can be used to identify areas where meteoric $\delta^{18}O$ is likely strongly influenced by atmospheric circulation, or where the temperature effect is likely strongest and circulation has a negligible effect. Such information would be of considerable value to stable isotope dendroclimatologists seeking to develop a tree-ring $\delta^{18}O$ chronology for the purposes of reconstructing circulation or temperature, as it could be used as a general guide in the site selection process for identifying which sites to target and which to avoid. Therefore, a novel avenue for future research would be to develop a global map based on isoGCM output that delineates the relative importance of temperature versus circulation effects.

WORKS CITED

ACIA (2005) *Arctic Climate Impact Assessment*. New York, NY, USA: Cambridge University Press, 1042.

Anderson L, Abbott MB, Finney BP and Burns SJ (2005) Regional atmospheric circulation change in the North Pacific during the Holocene inferred from lacustrine carbonate oxygen isotopes, Yukon Territory, Canada. *Quaternary Research* 64: 21–35.

Anderson L, Abbott MB, Finney BP and Burns SJ (2007) Late Holocene moisture balance variability in the southwest Yukon Territory, Canada. *Quaternary Science Reviews* 26: 130–141.

Anderson L, Finney BP and Shapley MD (2011) Lake carbonate-$\delta^{18}O$ records from the Yukon Territory, Canada: Little Ice Age moisture variability and patterns. *Quaternary Science Reviews* 30: 887–898.

Anderson PM and Brubaker LB (1994) Vegetation history of northcentral Alaska: A mapped summary of late-quaternary pollen data. *Quaternary Science Reviews* 13: 71–92.

Andreu-Hayles L, D'Arrigo R, Anchukaitis KJ, Beck PSA, Frank D and Goetz S (2011) Varying boreal forest response to Arctic environmental change at the Firth River, Alaska. *Environmental Research Letters* 6: doi:10.1088/1748-9326/6/4/045503.

Anisimov OA, Vaughan DG, Callaghan TV, Furgal C, Marchant H, Prowse TD, Vilhjálmsson H and Walsh JE (2007) Polar regions (Arctic and Antarctic). In: Parry ML, Canziani OF, Palutikof JP, van der Linden PJ and Hanson CE (eds) *Climate Change 2007: Impacts, Adaptation and Vulnerability. Contribution of Working Group II to the Fourth Assessment Report of the Intergovernmental Panel on Climate Change.* Cambridge, United Kingdom: Cambridge University Press, 653–685.

Augustin L, Barbante C, Barnes PRF, Barnola JM, Bigler M, Castellano E, Cattani O, Chappellaz J, Dahl-Jensen D, Delmonte B, Dreyfus G, Durand G, Falourd S, Fischer H, Flückiger J, Hansson ME, Huybrechts P, Jugie G, Johnsen SJ, Jouzel J, Kaufmann P, Kipfstuhl J, Lambert F, Lipenkov VY, Littot GC, Longinelli A, Lorrain R, Maggi V, Masson-Delmotte V, Miller H, Mulvaney R, Oerlemans J, Oerter H, Orombelli G, Parrenin F, Peel DA, Petit J-R, Raynaud D, Ritz C, Ruth U, Schwander J, Siegenthaler U, Souchez R, Stauffer B, Steffensen JP, Stenni B, Stocker TF, Tabacco IE, Udisti R, Van De Wal RSW, Van Den Broeke M, Weiss J, Wilhelms F, Winther J-G, Wolff EW and Zucchelli M (2004) Eight glacial cycles from an Antarctic ice core. *Nature* 429: 623–628.

Ballantyne AP, Greenwood DR, Sinninghe-Damsté JS, Csank AZ, Eberle JJ and Rybczynski N (2010) Significantly warmer Arctic surface temperatures during the Pliocene indicated by multiple independent proxies. *Geology* 38: 603–606.

Ballantyne AP, Rybczynski N, Baker PA, Harrington CR and White D (2006) Pliocene Arctic temperature constraints from the growth rings and isotopic composition of fossil larch. *Palaeogeography, Palaeoclimatology, Palaeoecology* 242: 188–200.

Barber VA, Juday GP and Finney BP (2000) Reduced growth of Alaskan white spruce in the twentieth century from temperature-induced drought stress. *Nature* 405: 668–673.

Barber VA, Juday GP, Finney BP and Wilmking M (2004) Reconstruction of summer temperatures in interior Alaska from tree-ring proxies: Evidence for changing synoptic climate regimes. *Climatic Change* 63: 91–120.

Barbour MM, Andrews TJ and Farquhar GD (2001) Correlations between oxygen isotope ratios of wood constituents of *Quercus* and *Pinus* samples from around the world. *Australian Journal of Plant Physiology* 28: 335–348.

Barbour MM, Cernusak LA and Farquhar GD (2005) Factors Affecting the Oxygen Isotope Ratio of Plant Organic Material. In: Flanagan LB, Ehleringer JR and Pataki DE (eds) *Stable Isotopes and Biosphere-Atmosphere Interactions: Processes and Biological Controls.* San Diego, California, USA: Elsevier Academic Press, 9–28.

Bard E, Raisbeck G, Yiou F and Jouzel J (2000) Solar irradiance during the last 1200 years based on cosmogenic nuclides. *Tellus B* 52: 985–992.

Bégin C, Michaud Y and Archambault S (2000) Tree-ring evidence of recent climate changes in the Mackenzie Basin, Northwest Territories. *Geological Survey of Canada Bulletin* 547: 65–77.

Bintanja R, Graversen RG and Hazeleger W (2011) Arctic winter warming amplified by the thermal inversion and consequent low infrared cooling to space. *Nature Geoscience* 4: 758–761.

Birks SJ and Edwards TWD (2009) Atmospheric circulation controls on precipitation isotope-climate relations in western Canada. *Tellus B* 61: 566–576.

Boettger T, Haupt M, Knöller K, Weise SM, Waterhouse JS, Rinne KT, Loader NJ, Sonninen E, Jungner H, Masson-Delmotte V, Stievenard M, Guillemin M-T, Pierre M, Pazdur A, Leuenberger M, Filot M, Saurer M, Reynolds CE, Helle G and Schleser GH (2007) Wood cellulose preparation methods and mass spectrometric analyses of $\delta^{13}C$, $\delta^{18}O$, and nonexchangeable $\delta^{2}H$ values in cellulose, sugar, and starch: an interlaboratory comparison. *Analytical Chemistry* 79: 4603–4612.

Bowen GJ and Revenaugh J (2003) Interpolating the isotopic composition of modern meteoric precipitation. *Water Resources Research* 39: doi:10.1029/2003WR002086.

Bradley RS (1999) *Paleoclimatology: Reconstructing Climates of the Quaternary.* San Diego, CA: Academic Press, 610.

Bradley RS (2011) High-resolution paleoclimatology. In: Hughes MK, Swetnam TW and Diaz H (eds) *Dendroclimatology: Progress and Prospects*. New York, USA: Springer, 3–15.

Bradley RS and Jones PD (1993) "Little Ice Age" summer temperature variations: their nature and relevance to recent global warming trends. *The Holocene* 3: 367–376.

Brand WA, Coplen TB, Aerts-Bijma AT, Böhlke JK, Gehre M, Geilmann H, Gröning M, Jansen HG, Meijer HAJ, Mroczkowski SJ, Qi H, Soergel K, Stuart-Williams H, Weise SM and Werner RA (2009) Comprehensive inter-laboratory calibration of reference materials for $\delta^{18}O$ versus VSMOW using various on-line high-temperature conversion techniques. *Rapid Communications in Mass Spectrometry* 23: 999–1019.

Brendel O, Iannetta PPM and Stewart D (2000) A rapid and simple method to isolate pure alpha-cellulose. *Phytochemical Analysis* 11: 7–10.

Briffa KR (2000) Annual climate variability in the Holocene: interpreting the message of ancient trees. *Quaternary Science Reviews* 19: 87–105.

Briffa KR, Bartholin TS, Eckstein D, Jones PD, Karlén W, Schweingruber FH and Zetterberg P (1990) A 1,400-year tree-ring record of summer temperatures in Fennoscandia. *Nature* 346: 434–439.

Briffa KR, Jones PD, Bartholin TS, Eckstein D, Schweingruber FH, Karlén W, Zetterberg P and Eronen M (1992) Fennoscandian summers from AD 500: temperature changes on short and long timescales. *Climate Dynamics* 7: 111–119.

Briffa KR, Jones PD, Pilcher JR and Hughes MK (1988) Reconstructing summer temperatures in northern Fennoscandinavia back to A.D. 1700 using tree-ring data from Scots pine. *Arctic and Alpine Research* 20: 385–394.

Briffa KR, Osborn TJ and Schweingruber FH (2004) Large-scale temperature inferences from tree rings: a review. *Global and Planetary Change* 40: 11–26.

Briffa KR, Osborn TJ, Schweingruber FH, Jones PD, Shiyatov SG and Vaganov EA (2002) Tree-ring width and density data around the Northern Hemisphere: Part 1, local and regional climate signals. *The Holocene* 12: 737–757.

Briffa KR, Schweingruber FH, Jones PD, Osborn TJ, Harris I, Shiyatov SG, Vaganov EA and Grudd H (1998a) Trees tell of past climates: but are they speaking less clearly today? *Philosophical Transactions of the Royal Society, Biological Sciences* 353: 65–73.

Briffa KR, Schweingruber FH, Jones PD, Osborn TJ, Shiyatov SG and Vaganov EA (1998b) Reduced sensitivity of recent tree-growth to temperature at high northern latitudes. *Nature* 391: 678–682.

Brohan P, Kennedy JJ, Haris I, Tett SFB and Jones PD (2006) Uncertainty estimates in regional and global observed temperature changes: A new data set from 1850. *Journal of Geophysical Research* 111: doi:10.1029/2005JD006548.

Bryson RA (1966) Air masses, streamlines, and the boreal forest. *Geographical Bulletin* 8: 228–269.

Bunn AG, Goetz SJ, Kimball JS and Zhang K (2007) Northern high-latitude ecosystems respond to climate change. *EOS, Transactions, American Geophysical Union* 34: 333–335.

Burk RL and Stuiver M (1981) Oxygen isotope ratios in trees reflect mean annual temperature and humidity. *Science* 211: 1417–1419.

Burn CR and Kokelj SV (2009) The environment and permafrost of the Mackenzie Delta area. *Permafrost and Periglacial Processes* 20: 83–105.

Burn CR and Zhang Y (2009) Permafrost and climate change at Herschel Island (Qikiqtaruq), Yukon Territory, Canada. *Journal of Geophysical Research* 114: doi:10.1029/2008JF001087.

Burns BM (1973) *The Climate of the Mackenzie Valley-Beaufort Sea*. Toronto: Environment Canada, 227.

Büntgen U, Esper J, Frank D, Nicolussi K and Schmidhalter M (2005) A 1052-year tree-ring proxy for Alpine summer temperatures. *Climate Dynamics* 25: 141–153.

Büntgen U, Frank DC, Schmidhalter M, Neuwirth B, Seifert M and Esper J (2006) Growth/climate response shift in a long subalpine spruce chronology. *Trees* 20: 99–110.

Christensen JH, Hewitson B, Busuioc A, Chen A, Gao X, Held I, Jones R, Kolli RK, Kwon WT, Laprise R, Magana Rueda V, Mearns L, Menéndez CG, Räisänen J, Rinke A, Sarr A and Whetton P (2007) Regional Climate Projections. In: Solomon S, Qin D, Manning M, Chen Z, Marquis M, Averyt KB, Tignor M and Miller HL (eds) *Climate Change 2007: The Physical Science Basis. Contribution of Working Group I to the Fouth Assessment Report of the Intergovernmental Panel on Climate Change*. Cambridge, United Kingdom and New York, NY, USA: Cambridge University Press, 847–940.

Clark PU, Nicklas GP, Stocker TF and Weaver AJ (2002) The role of the thermohaline circulation in abrupt climate change. *Nature* 415: 863–869.

Compo GP, Whitaker JS, Sardeshmukh PD, Matsui N, Allan RJ, Yin X, Gleason BE, Vose RS, Rutledge G, Bessemoulin P, Brönnimann S, Brunet M, Crouthamel RI, Grant AN, Groisman PY, Jones PD, Kruk MC, Kruger AC, Marshall GJ, Maugeri M, Mok HY, Nordli Ø, Ross TF, Trigo RM, Wang XL, Woodruff SD and Worley SJ (2011) The

Twentieth Century Reanalysis Project. *Quarterly Journal of the Royal Meteorological Society* 137: 1–28.

Cook ER (1985) *A Time Series Analysis Approach to Tree Ring Standardization. PhD dissertation*. Tuscon, USA: University of Arizona, 171.

Cook ER, Briffa KR, Meko DM, Graybill DA and Funkhouser G (1995) The "segment length curse" in long tree-ring chronology development for paleoclimatic studies. *The Holocene* 5: 229–237.

Cook ER, Esper J and D'Arrigo RD (2004) Extra-tropical Northern Hemisphere land temperature variability over the past 1000 years. *Quaternary Science Reviews* 23: 2063–2074.

Cook ER and Kairiukstis LA (1990) *Methods of Dendrochronology: Applications in the Environmental Sciences*. Boston: Kluwer Academic Publishers, 394.

Cook ER and Peters K (1981) The smoothing spline: a new approach to standardizing forest interior tree-ring width series for dendroclimatic studies. *Tree-Ring Bulletin* 41: 45–53.

Craig H (1954) Carbon-13 variations in Sequoia rings and the atmosphere. *Science* 119: 141–3.

Craig H and Gordon LI (1965) Deuterium and oxygen 18 variations in the ocean and the marine atmosphere. In: Tongiorgi E (ed) *Proceedings of a Conference on Stable Isotopes in Oceanographic Studies and Paleotemperatures*. Spoleto, Italy, 9–130.

Cropper JP and Fritts HC (1981) Tree-ring width chronologies from the North American Arctic. *Arctic and Alpine Research* 13: 245–260.

Crowley TJ (2000) Causes of climate change over the past 1000 years. *Science* 289: 270–277.

Csank AZ, Patterson WP, Eglington BM, Rybczynski N and Basinger JF (2011) Climate variability in the Early Pliocene Arctic: Annually resolved evidence from stable isotope values of sub-fossil wood, Ellesmere Island, Canada. *Palaeogeography, Palaeoclimatology, Palaeoecology* 308: 339–349.

Cwynar LC and Spear RW (1995) Paleovegetation and paleoclimatic changes in the Yukon at 6 ka BP. *Géographie physique et Quaternaire* 49: 29–35.

Dansgaard W (1953) The abundance of ^{18}O in atmospheric water and water vapour. *Tellus* 5: 461–469.

Dansgaard W (1954) The ^{18}O abundance in fresh water. *Geochimica et Cosmochimica Acta* 6: 241–260.

Dansgaard W (1964) Stable isotopes in precipitation. *Tellus* 16: 436–468.

Dansgaard W, Johnsen SJ, Gundestrup NS, Hammer CU, Hvidberg CS, Steffensen JP, Sveinbjörnsdottir AE, Jouzel J and Bond G (1993) Evidence for general instability of past climate from a 250-kyr ice-core record. *Nature* 364: 218–220.

Dansgaard W, Johnsen SJ, Møller J and Langway CC (1969) One thousand centuries of climatic record from Camp Century on the Greenland ice sheet. *Science* 166: 377–80.

Davi NK, Jacoby GC and Wiles GC (2003) Boreal temperature variability inferred from maximum latewood density and tree-ring width data, Wrangell Mountain region, Alaska. *Quaternary Research* 60: 252–262.

DeNiro MJ and Epstein S (1981) Isotopic composition of cellulose from aquatic organisms. *Geochimica et Cosmochimica Acta* 45: 1885–1894.

Dongmann G, Nurnberg HW, Förstel H and Wagener K (1974) On the enrichment of $H_2{}^{18}O$ in the leaves of transpiring plants. *Radiation and Environmental Biophysics* 11: 41–52.

Douglass AE (1919) *Climatic Cycles and Tree Rings Growth.* Washington D.C.: Carnegie Institute Washington Publication 289.I, 30–37.

Driscoll WW, Wiles GC, D'Arrigo R and Wilmking M (2005) Divergent tree growth response to recent climatic warming, Lake Clark National Park and Preserve, Alaska. *Geophysical Research Letters* 32: doi:10.1029/2005GL024258.

Drobyshev I, Simard M, Bergeron Y and Hofgaard A (2010) Does soil organic layer thickness affect climate–growth relationships in the black spruce boreal ecosystem? *Ecosystems* 13: 556–574.

Dyke AS, Andrews JT, Clark PU, England JH, Miller GH, Shaw J and Veillette JJ (2002) The Laurentide and Innuitian ice sheets during the Last Glacial Maximum. *Quaternary Science Reviews* 21: 9–31.

Dyke LD (2000) Climate of the Mackenzie River valley. In: Dyke LD and Brooks GR (eds) *The Physical Environment of the Mackenzie Valley, Northwest Territories: A Baseline for the Assessment of Environmental Change.* Ottawa, Ontario: Geological Survey of Canada, 21–30.

D'Arrigo R, Jacoby G, Buckley B, Sakulich J, Frank D, Wilson R, Curtis A and Anchukaitis K (2009) Tree growth and inferred temperature variability at the North American arctic treeline. *Global and Planetary Change* 65: 71–82.

D'Arrigo R, Kaufmann RK, Davi N, Jacoby GC, Laskowski C, Myneni RB and Cherubini P (2004) Thresholds for warming-induced growth decline at elevational tree line in the Yukon Territory, Canada. *Global Biogeochemical Cycles* 18: doi:10.1029/2004GB002249.

D'Arrigo R, Wilson R, Deser C, Wiles G, Cook E, Villalba R, Tudhope A, Cole J and Linsley B (2005) Tropical-North Pacific climate linkages over the past four centuries. *Journal of Climate* 18: 5253–5265.

D'Arrigo R, Wilson R and Jacoby G (2006) On the long-term context for late twentieth century warming. *Journal of Geophysical Research* 111: doi:10.1029/2005JD006352.

D'Arrigo R, Wilson R, Liepert B and Cherubini P (2008) On the "Divergence Problem" in northern forests: A review of the tree-ring evidence and possible causes. *Global and Planetary Change* 60: 289–305.

Earle CJ, Brubaker LB, Lozhkin AV and Anderson PM (1994) Summer temperature since 1600 for the upper Kolyma region, northeastern Russia, reconstructed from tree rings. *Arctic and Alpine Research* 26: 60–65.

Earles S (2008) *Dendrochronological Studies of White Spruce in the Northern Yukon, Canada. Unpublished MSc Thesis*. London, Ontario: University of Western Ontario, 147.

Edwards TWD, Birks SJ, Luckman BH and MacDonald GM (2008) Climatic and hydrologic variability during the past millennium in the eastern Rocky Mountains and northern Great Plains of western Canada. *Quaternary Research* 70: 188–197.

Edwards TWD and Fritz P (1986) Assessing meteoric water composition and relative humidity from ^{18}O and ^{2}H in wood cellulose: paleoclimatic implications for southern Ontario, Canada. *Applied Geochemistry* 1: 715–723.

Edwards TWD, Graf W, Trimborn P, Stichler W, Lipp J and Payer HD (2000) $\delta^{13}C$ response surface resolves humidity and temperature signals in trees. *Geochimica et Cosmochimica Acta* 64: 161–167.

Edwards TWD, Wolfe BB and MacDonald GM (1996) Influence of changing atmospheric circulation on precipitation $\delta^{18}O$-temperature relations in Canada during the Holocene. *Quaternary Research* 46: 211–218.

Epstein S and Mayeda T (1953) Variations of the O^{18} content of waters from natural sources. *Geochimica et Cosmochimica Acta* 4: 213–224.

Esper J, Cook ER, Krusic PJ and Peters K (2003) Tests of the RCS method for preserving low-frequency variability in long tree-ring chronologies. *Tree-Ring Research* 59: 81–98.

Esper J, Cook ER and Schweingruber FH (2002) Low-frequency signals in long tree-ring chronologies for reconstructing past temperature variability. *Science* 295: 2250–2253.

Esper J and Frank D (2009) Divergence pitfalls in tree-ring research. *Climatic Change* 94: 261–266.

Esper J, Frank D, Büntgen U, Verstege A, Hantemirov RM and Kirdyanov AV (2010) Trends and uncertainties in Siberian indicators of 20th century warming. *Global Change Biology* 16: 386–398.

Farquhar GD and Lloyd J (1993) Carbon and oxygen isotope effects in the exchange of carbon dioxide between terrestrial plants and the atmosphere. In: Ehleringer JR, Hall AE and Farquhar GD (eds) *Stable Isotopes and Plant Carbon-Water Relations*. San Diego, California, USA: Academic Press, 47–70.

Feng X (1999) Trends in intrinsic water-use efficiency of natural trees for the past 100–200 years: A response to atmospheric CO_2 concentration. *Geochimica et Cosmochimica Acta* 63: 1891–1903.

Feng X, Reddington AL, Faiia AM, Posmentier ES, Shu Y and Xu X (2007) The changes in North American atmospheric circulation patterns indicated by wood cellulose. *Geology* 35: 163–166.

Field RD, Moore GWK, Holdsworth G and Schmidt GA (2010) A GCM-based analysis of circulation controls on $\delta^{18}O$ in the southwest Yukon, Canada: Implications for climate reconstructions in the region. *Geophysical Research Letters* 37: doi:10.1029/2009GL041408.

Fisher DA, Wake C, Kreutz K, Yalcin K, Steig E, Mayewski P, Anderson L, Zheng J, Rupper S, Zdanowicz C, Demuth M, Waszkiewicz M, Dahl-Jensen D, Goto-Azuma K, Bourgeois JB, Koerner RM, Sekerka J, Osterberg E, Abbott MB, Finney BP and Burns SJ (2004) Stable isotope records from Mount Logan, Eclipse ice cores and nearby Jellybean Lake. Water cycle of the North Pacific over 2000 years and over five vertical kilometers: Sudden shifts and tropical teleconnections. *Géographie physique et Quaternaire* 58: 337–352.

Flower A and Smith DJ (2012) A dendroclimatic reconstruction of June–July mean temperature in the northern Canadian Rocky Mountains. *Dendrochronologia* 29: 55–63.

Foley JA, Kutzbach JE, Coe MT and Levis S (1994) Feedbacks between climate and the boreal forests during the Holocene epoch. *Nature* 371: 52–54.

Frank D, Esper J and Cook ER (2007) Adjustment for proxy number and coherence in a large-scale temperature reconstruction. *Journal of Geophysical Research* 34: L16709, doi:10.1029/2007GL030571.

Fricke HC and O'Neil JR (1999) The correlation between $^{18}O/^{16}O$ ratios of meteoric water and surface temperature: its use in investigating terrestrial climate change over geologic time. *Earth and Planetary Science Letters* 170: 181–196.

Fritts HC (1976) *Tree-Rings and Climate*. Caldwell, New Jersey: The Blackburn Press, 567.

Fritts HC, Moismann JE and Bottorff CP (1969) A revised computer program for standardizing tree-ring series. *Tree-Ring Bulletin* 29: 15–20.

Gagen M, McCarroll D, Jalkanen R, Loader NJ, Robertson I and Young GHF (2012) A rapid method for the production of robust millennial length stable isotope tree ring series for climate reconstruction. *Global and Planetary Change* 82-83: 96–103.

Gagen M, McCarroll D, Loader NJ and Robertson I (2011) Stable isotopes in dendroclimatology: Moving beyond "potential." In: Hughes MK, Swetnam TW and Diaz HF (eds) *Dendroclimatology: Progress and Prospects*. New York: Springer, 147–172.

Garfinkel HL and Brubaker LB (1980) Modern climate-tree-growth relationships and climatic reconstruction in sub-Arctic Alaska. *Nature* 286: 872–874.

Gaudinski JB, Dawson TE, Quideau S, Schuur EAG, Roden JS, Trumbore SE, Sandquist DR, Oh S-W and Wasylishen RE (2005) Comparative analysis of cellulose preparation techniques for use with ^{13}C, ^{14}C, and ^{18}O isotopic measurements. *Analytical Chemistry* 77: 7212–24.

Giddings JL (1938) Recent tree-ring work in Alaska. *Tree-Ring Bulletin* 5: 16.

Giddings JL (1943) Some climatic aspects of tree growth in Alaska. *Tree-Ring Bulletin* 9: 26–32.

Giddings JL (1954) Tree-ring dating in the American arctic. *Tree-Ring Bulletin* 30: 23–25.

Gostev M, Wiles G, D'Arrigo R, Jacoby G and Khomentovsky P (1996) Early summer temperatures since 1670 A.D. for Central Kamchatka reconstructed based on a Siberian larch tree-ring width chronology. *Canadian Journal of Forest Research* 26: 2048–2052.

Gray J and Thompson P (1976) Climatic information from $^{18}O/^{16}O$ ratios of cellulose in tree rings. *Nature* 262: 481–482.

Graybill DA and Shiyatov SG (1992) Dendroclimatic evidence from the northern Soviet Union. In: Bradley RS and Jones PD (eds) *Climate Since A.D. 1500*. New York: Routledge, 393–414.

Green JW (1963) Wood cellulose. In: Whistler RL (ed) *Methods in Carbohydrate Chemistry, III.* New York: Academic Press, 9–21.

Gregory RA and Wilson BF (1968) A comparison of cambial activity of white spruce in Alaska and New England. *Canadian Journal of Botany* 46: 733–734.

Grudd H, Briffa KR, Karlén W, Bartholin TS, Jones PD and Kromer B (2002) A 7400-year tree-ring chronology in northern Swedish Lapland: natural climatic variability expressed on annual to millennial timescales. *The Holocene* 12: 657–665.

Hammarlund D, Barnekow L, Birks HJB, Buchardt B and Edwards TWD (2002) Holocene changes in atmospheric circulation recorded in the oxygen-isotope stratigraphy of lacustrine carbonates from northern Sweden. *The Holocene* 12: 339–351.

Hansen J, Ruedy R, Sato M and Lo K (2010) Global surface temperature change. *Reviews of Geophysics* 48: doi:10.1029/2010RG000345.

Hare FK (1950) Climate and zonal divisions of the boreal forest formation in eastern Canada. *Geographical Review* 40: 615–635.

Hare FK (1951) Some climatological problems of the Arctic and sub-Arctic. In: Malone TE (ed) *Compendium of Meteorology*. Boston: American Meteorological Society, 952–964.

Hare FK and Ritchie JC (1972) The boreal bioclimates. *Geographical Review* 62: 333–365.

Hartmann B and Wendler G (2005) The significance of the 1976 Pacific climate shift in the climatology of Alaska. *Journal of Climate* 18: 4824–4839.

Heginbottom JA, Dubreuil MA and Harker PA (1995) Canada - Permafrost. *National Atlas of Canada, 5th Edition. Plate 2.1, scale 1:7,500,000 (MCR 4177).* Ottawa, Canada: Natural Resources Canada.

Hendy EJ, Gagen MK, Alibert CA, McColloch MT, Lough JM and Isdale PJ (2002) Abrupt decrease in tropical Pacific sea surface salinity at the end of the Little Ice Age. *Science* 295: 1511–1514.

Hinzman LD, Bettez ND, Bolton WR, Chapin FS, Dyurgerov MB, Fastie CL, Griffith B, Hollister RD, Hope A, Huntington HP, Jensen AM, Jia GJ, Jorgenson T, Kane DL, Klein DR, Kofinas G, Lynch AH, Lloyd AH, McGuire AD, Nelson FE, Oechel WC, Osterkamp TE, Racine CH, Romanovsky VE, Stone RS, Stow DA, Sturm M, Tweedie CE, Vourlitis GL, Walker MD, Walker DA, Webber PJ, Welker JM, Winker KS and Yoshikawa K (2005) Evidence and implications of recent climate change in Northern Alaska and other Arctic regions. *Climatic Change* 72: 251–298.

Holmes RL (1983) Computer-assisted quality control in tree-ring dating and measurement. *Tree-Ring Bulletin* 43: 69–78.

Hughes MK (2011) Dendroclimatology in high-resolution paleoclimatology. In: Hughes MK, Swetnam TW and Diaz HF (eds) *Dendroclimatology: Progress and Prospects*. New York: Springer, 17–34.

Hughes OL (1972) Surficial geology of northern Yukon Territory and northwestern District of Mackenzie, Northwest Territories. *Geological Survey of Canada Paper 69-36:* 11. Ottawa, Canada: Geological Survey of Canada.

Hughes OL and Rampton VN (1971) Northern Yukon Territory, and Northwestern District of Mackenzie. *Surficial Geology Map 1319A (1:500,000)*. Ottawa, Canada: Geological Survey of Canada.

IAEA/WHO (2006) Global Network of Isotopes in Precipitation. *The GNIP Database*. Available at: http://www.iaea.org/water.

IPCC (2007) *Climate Change 2007: The Physical Science Basis, Contribution of Working Group I to the Fourth Assessment Report of the Intergovernmental Panel on Climate Change*. New York, NY, USA: Cambridge University Press, 996.

Jacoby GC, Brubaker LB, Garfinkel HL, Lawson MP and Kuivinen KC (1982) The Arctic. In: Hughes MK, Kelly PM, Pilcher JR and LaMarche VC (eds) *Climate from Tree-Rings*. New York: Cambridge University Press, 107–117.

Jacoby GC and Cook ER (1981) Past temperature variations inferred from a 400-year tree-ring chronology from Yukon Territory, Canada. *Arctic and Alpine Research* 13: 409–418.

Jacoby GC, Cook ER and Ulan LD (1985) Reconstructed summer degree days in central Alaska and northwestern Canada since 1524. *Quaternary Research* 23: 18–26.

Jacoby GC and D'Arrigo R (1989) Reconstructed northern hemisphere annual temperature since 1671 based on high-latitude tree-ring data from North America. *Climatic Change* 14: 39–59.

Jacoby GC and D'Arrigo RD (1995) Tree ring width and density evidence of climatic and potential forest change in Alaska. *Global Biogeochemical Cycles* 9: 227–234.

Jacoby GC, Lovelius NV, Shumilov OI, Raspopov OM, Karbainov JM and Frank DC (2000) Long-Term Temperature Trends and Tree Growth in the Taymir Region of Northern Siberia. *Quaternary Research* 53: 312–318.

Jacoby GC and Ulan LD (1982) Reconstruction of past ice conditions in a Hudson Bay estuary using tree-rings. *Nature* 298: 637–639.

Jansen E, Overpeck J, Briffa KR, Duplessy JC, Joos F, Masson-Delmotte V, Olago D, Otto-Bliesner B, Peltier WR, Rahmstorf S, Ramesh R, Raynaud D, Rind D, Solomina O, Villalba R, Zhang D and Jensen EJ (2007) Palaeoclimate. In: Solomon S, Qin D, Manning M, Chen Z, Marquis M, Averyt KB, Tignor M and Miller HL (eds) *Climate Change 2007: The Physical Science Basis, Contribution of Working Group I to the Fourth Assessment Report of the Intergovernmental Panel on Climate Change.* Cambridge, United Kingdom and New York, USA: Cambridge University Press, 433–497.

Johnsen SJ, Dahl-Jensen D, Gundestrup N, Steffensen JP, Clausen HB, Miller H, Masson-Delmotte V, Sveinbjörnsdottir AE and White J (2001) Oxygen isotope and palaeotemperature records from six Greenland ice-core stations: Camp Century, Dye-3, GRIP, GISP2, Renland and NorthGRIP. *Journal of Quaternary Science* 16: 299–307.

Johnson EA (1992) *Fire and Vegetation Dynamics: Studies from the North American Boreal Forest.* Cambridge: Cambridge University Press, 129.

Johnstone JF, Chapin III F, Hollingsworth TN, Mack MC, Romanovsky VE and Turetsky MR (2010) Fire, climate change, and forest resilience in interior Alaska. *Canadian Journal of Forest Research* 40: 1302–1312.

Jones PD, Briffa KR, Barnett TP and Tett SFB (1998) High-resolution palaeoclimatic records for the last millennium: interpretation, integration and comparison with General Circulation Model control-run temperatures. *The Holocene* 8: 455–471.

Jones PD, Briffa KR, Osborn TJ, Lough JM, van Ommen TD, Vinther BM, Luterbacher J, Wahl ER, Zwiers FW, Mann ME, Schmidt GA, Ammann CM, Buckley BM, Cobb KM, Esper J, Goosse H, Graham N, Jansen E, Kiefer T, Kull C, Küttel M, Mosley-Thompson E, Overpeck JT, Riedwyl N, Schulz M, Tudhope AW, Villalba R, Wanner H, Wolff E and Xoplaki E (2009) High-resolution palaeoclimatology of the last millennium: a review of current status and future prospects. *The Holocene* 19: 3–49.

Jouzel J (1999) Calibrating the isotopic paleothermometer. *Science* 286: 910–911.

Jouzel J, Alley RB, Cuffey KM, Dansgaard W, Grootes P, Hoffmann G, Johnsen SJ, Koster RD, Peel D, Shuman CA, Stievenard M, Stuiver M and White J (1997) Validity of the temperature reconstruction from water isotopes in ice cores. *Journal of Geophysical Research* 102: 471–487.

Jouzel J, Lorius C, Petit JR, Genthon C, Barkov NI, Kotlyakov VM and Petrov VM (1987) Vostok ice core: a continuous isotope temperature record over the last climatic cycle (160,000 years). *Nature* 329: 403–408.

Kalnay E, Kanamitsu M, Kistler R, Collins W, Deaven D, Gandin L, Iredell M, Saha S, White G, Woollen J, Zhu Y, Leetmaa A, Reynolds R, Chelliah M, Ebisuzaki W, Higgins W, Janowiak J, Mo KC, Ropelewski C, Wang J, Jenne R and Joseph D (1996) The

NCEP/NCAR 40-Year Reanalysis Project. *Bulletin of the American Meteorological Society* 77: 437–471.

Kaufman D (2004) Holocene thermal maximum in the western Arctic (0–180°W). *Quaternary Science Reviews* 23: 529–560.

Kaufman DS, Schneider DP, McKay NP, Ammann CM, Bradley RS, Briffa KR, Miller GH, Otto-Bliesner BL, Overpeck JT, Vinther BM and Arctic Lakes 2k Project Members (2009) Recent warming reverses long-term Arctic cooling. *Science* 325: 1236–1239.

King GM (2009) *Factors influencing the growth of white spruce (Picea glauca) in the Mackenzie Delta, NT. Unpublished MSc thesis*. Ottawa, Canada: Carleton University, 159.

Kokelj SV and Burn CR (2005) Near-surface ground ice in sediments of the Mackenzie Delta, Northwest Territories, Canada. *Permafrost and Periglacial Processes* 16: 291–303.

Körner C (1998) A re-assessment of high elevation treeline positions and their explanation. *Oecologia* 115: 445–459.

Kozlowski TT (1992) Carbohydrate sources and sinks in woody plants. *The Botanical Review* 58: 107–222.

Kozlowski TT and Pallardy SG (1997) *Physiology of Woody Plants, 2nd Edition*. San Diego: Academic Press, 411.

Krebs JA and Barry RG (1970) The Arctic Front and the tundra-taiga boundary in Eurasia. *Geographical Review* 60: 548–554.

Labrecque S, Lacelle D, Duguay CR, Lauriol B and Hawkings J (2009) Contemporary (1951-2001) evolution of lakes in the Old Crow Basin, northern Yukon, Canada: Remote sensing, numerical modelling, and stable isotope analysis. *Arctic* 62: 225–238.

Lageard JGA, Thomas PA and Chambers FM (2000) Using fire scars and growth release in subfossil Scots pine to reconstruct prehistoric fires. *Palaeogeography, Palaeoclimatology, Palaeoecology* 164: 87–99.

Laumer W, Andreu L, Helle G, Schleser GH, Wieloch T and Wissel H (2009) A novel approach for the homogenization of cellulose to use micro-amounts for stable isotope analyses. *Rapid Communications in Mass Spectrometry* 23: 1934–1940.

Lauriol B, Duguay CR and Riel A (2002) Response of the Porcupine and Old Crow rivers in northern Yukon, Canada, to Holocene climatic change. *The Holocene* 12: 27–34.

Lawrimore JH, Menne MJ, Gleason BE, Williams CN, Wuertz DB, Vose RS and Rennie J (2011) An overview of the Global Historical Climatology Network monthly mean temperature data set, version 3. *Journal of Geophysical Research* 116: doi:10.1029/2011JD016187.

Leavitt SW and Danzer SR (1993) Method for batch processing small wood samples to holocellulose for stable-carbon isotope analysis. *Analytical Chemistry* 65: 87–89.

Libby LM and Pandolfi LJ (1974) Temperature dependence of isotope ratios in tree rings. *Proceedings of the National Academy of Sciences of the United States of America* 71: 2482–2486.

Libby LM, Pandolfi LJ, Payton PH, Marshall III J, Becker B and Giertz-Sienbenlist V (1976) Isotopic tree thermometers. *Nature* 261: 284–288.

Linderholm HW and Gunnarson BE (2005) Summer temperature variability in central Scandinavia during the last 3600 years. *Geografiska Annaler* 87: 231–241.

Liu X, Shao X, Liang E, Chen T, Qin D, An W, Xu G, Sun W and Wang Y (2009) Climatic significance of tree-ring $\delta^{18}O$ in the Qilian Mountains, northwestern China and its relationship to atmospheric circulation patterns. *Chemical Geology* 268: 147–154.

Liu Z, Kennedy CD and Bowen GJ (2011) Pacific/North American teleconnection controls on precipitation isotope ratios across the contiguous United States. *Earth and Planetary Science Letters* 310: 319–326.

Lloyd AH and Bunn AG (2007) Responses of the circumpolar boreal forest to 20th century climate variability. *Environmental Research Letters* 2: doi:10.1088/1748–9326/2/4/045013.

Lloyd AH and Fastie CL (2002) Spatial and temporal variability in the growth and climate response of treeline trees in Alaska. *Climatic Change* 52: 481–509.

Loader NJ, Robertson I, Barker AC, Switsur VR and Waterhouse JS (1997) An improved technique for the batch processing of small wholewood samples to α-cellulose. *Chemical Geology* 136: 313–317.

Luckman BH and Wilson RJS (2005) Summer temperatures in the Canadian Rockies during the last millennium: a revised record. *Climate Dynamics* 24: 131–144.

L'Heureux ML, Mann ME, Cook BI, Gleason BE and Vose RS (2004) Atmospheric circulation influences on seasonal precipitation patterns in Alaska during the latter 20th century. *Journal of Geophysical Research* 109: doi:10.1029/2003JD003845.

MacDonald GM, Szeicz JM, Claricoates J and Dale KA (2000a) Responses of the central Canadian treeline to recent climatic changes. *Annals of the Association of American Geographers* 88: 183–208.

MacDonald GM, Velichko AA, Kremenetski CV, Borisova OK, Goleva AA, Andreev AA, Cwynar LC, Riding RT, Forman SL, Edwards TWD, Aravena R, Hammarlund D, Szeicz JM and Gattaulin VN (2000b) Holocene treeline history and climate change across northern Eurasia. *Quaternary Research* 53: 302–311.

Mack MC, Bret-Harte MS, Hollingsworth TN, Jandt RR, Schuur EAG, Shaver GR and Verbyla DL (2011) Carbon loss from an unprecedented Arctic tundra wildfire. *Nature* 475: 489–492.

Mackay JR (1963) The Mackenzie Delta area, N.W.T. *Geographical Branch Memoir.* Ottawa, Ontario: Department of Mines and Technical Surveys, 202.

Mann ME, Bradley RS and Hughes MK (1998) Global-scale temperature patterns and climate forcing over the past six centuries. *Nature* 392: 779–787.

Mann ME, Bradley RS and Hughes MK (2000) Long-term variability in El-Niño-Southern Oscillation and associated teleconnections. In: Diaz HF and Markgraf V (eds) *El Niño and the Southern Oscillation.* New York, USA: Cambridge University Press, 357–412.

Mann ME, Zhang Z, Rutherford S, Bradley RS, Hughes MK, Shindell D, Ammann C, Faluvegi G and Ni F (2009) Global signatures and dynamical origins of the Little Ice Age and Medieval Climate Anomaly. *Science* 326: 1256–1260.

McCarroll D and Loader NJ (2004) Stable isotopes in tree rings. *Quaternary Science Reviews* 23: 771–801.

McCullough DG, Werner RA and Neumann D (1998) Fire and insects in northern and boreal forest ecosystems of North America. *Annual Review of Entomology* 43: 107–127.

McGuire AD, Ruess RW, Lloyd A, Yarie J, Clein JS and Juday GP (2010) Vulnerability of white spruce tree growth in interior Alaska in response to climate variability: dendrochronological, demographic, and experimental perspectives. *Canadian Journal of Forest Research* 40: 1197–1209.

Meehl GA, Stocker TF, Collins WD, Friedlingstein P, Gaye AT, Gregory JM, Kitoh A, Knutti R, Murphy JM, Noda A, Raper SCB, Watterson IG, Weaver AJ and Zhao ZC (2007) Global Climate Projections. In: Solomon S, Qin D, Manning M, Chen Z, Marquis M, Averyt KB, Tignor M and Miller HL (eds) *Climate Change 2007: The Physical Science Basis. Contribution of Working Group I to the Fouth Assessment Report of the Intergovernmental Panel on Climate Change.* Cambridge, United Kingdom and New York, NY, USA: Cambridge University Press, 747–846.

Melvin TM and Briffa KR (2008) A "signal-free" approach to dendroclimatic standardisation. *Dendrochronologia* 26: 71–86.

Mock CJ, Bartlein PJ and Anderson PM (1998) Atmospheric circulation patterns and spatial climatic variations in Beringia. *International Journal of Climatology* 18: 1085–1104.

Mooney HA and Billings WD (1960) The annual carbohydrate cycle of alpine plants as related to growth. *American Journal of Botany* 47: 594–598.

Moran TA, Marshall SJ, Evans EC and Sinclair KE (2007) Altitudinal gradients of stable isotopes in lee-slope precipitation in the Canadian Rocky Mountains. *Arctic, Antarctic, and Alpine Research* 39: 455–467.

Morlan RE (1980) Taphonomy and archaeology in the upper Pleistocene of the northern Yukon Territory: a glimpse of the peopling of the New World. *Archaeological Survey of Canada, Paper 94* 398.

NASA-GISS (2012) *GISS surface temperature analysis (GISTEMP): combined land-surface air and sea-surface water temperature anomalies.* Available at: http://data.giss.nasa.gov/gistemp/.

Nguyen TN, Burn CR, King DJ and Smith SL (2009) Estimating the extent of near-surface permafrost using remote sensing, Mackenzie Delta, Northwest Territories. *Permafrost and Periglacial Processes* 20: 141–153.

Nilsson MC and Wardle DA (2005) Understorey vegetation as a forest ecosystem driver: evidence from the northern Swedish boreal forest. *Frontiers in Ecology and the Environment* 3: 421–428.

Norris DK (1981) Aklavik, District of Mackenzie. *Geology Map 1517A (1:250,000).* Ottawa, Canada: Geological Survey of Canada.

Oswalt W (1949) Dated houses at Squirrel River, Alaska. *Tree-Ring Bulletin* 16: 7–8.

Oswalt W (1960) The growing season of Alaskan spruce. *Tree-Ring Bulletin* 23: 3–9.

Ovenden J and Brassard GR (1989) Wetland vegetation near Old Crow, northern Yukon. *Canadian Journal of Botany* 67: 954–960.

Overpeck J, Hughen KA, Hardy D, Bradley R, Case R, Douglas M, Finney B, Gajewski K, Jacoby G, Jennings A, Lamoureux S, Lasca A, MacDonald G, Moore J, Retelle M, Smith S, Wolfe A and Zielinski G (1997) Arctic environmental change of the last four centuries. *Science* 278: 1251–1256.

Pearce CM, McLennan D and Cordes LD (1988) The evolution and maintenance of white spruce woodlands on the Mackenzie Delta, N.W.T., Canada. *Holarctic Ecology* 11: 248–258.

Pisaric MFJ, Carey SK, Kokelj SV and Youngblut D (2007) Anomalous 20th century tree growth, Mackenzie Delta, Northwest Territories, Canada. *Geophysical Research Letters* 34: doi:10.1029/2006GL029139.

Pisaric MFJ, MacDonald GM, Velichko AA and Swynar LC (2000) The lateglacial and postglacial vegetation history of the northwestern limits of Beringia, based on pollen, stomate and tree stump evidence. *Quaternary Science Reviews* 20: 235–245.

Porter TJ and Middlestead P (2012) On estimating the precision of stable isotope ratios in processed tree-rings. *Dendrochronologia* 30: 239–242.

Porter TJ and Pisaric MFJ (2011) Temperature-growth divergence in white spruce forests of Old Crow Flats, Yukon Territory, and adjacent regions of northwestern North America. *Global Change Biology* 17: 3418–3430.

Porter TJ, Pisaric MFJ, Kokelj SV and DeMontigny P (2012) A reconstruction of June-July minimum temperatures since AD 1245 from white spruce tree-rings in the Mackenzie Delta region, northwestern Canada. *Unpublished manuscript.*

Porter TJ, Pisaric MFJ, Kokelj SV and Edwards TWD (2009) Climatic signals in $\delta^{13}C$ and $\delta^{18}O$ of tree-rings from white spruce in the Mackenzie Delta region, northern Canada. *Arctic, Antarctic, and Alpine Research* 41: 497–505.

Rampton VN (1988) Quaternary geology of the Tuktoyaktuk Coastlands, Northwest Territories. *Memoir 423.* Ottawa, Canada: Geological Survey of Canada.

Rayner NA, Parker DE, Horton EB, Folland CK, Alexander LV, Rowell DP, Kent EC and Kaplan A (2003) Global analyses of sea surface temperature, sea ice, and night marine air temperature since the late nineteenth century. *Journal of Geophysical Research* 108: doi:10.1029/2002JD002670.

Rebetez M, Saurer M and Cherubini P (2003) To what extent can oxygen isotopes in tree rings and precipitation be used to reconstruct past atmospheric temperature? A case study. *Climatic Change* 61: 237–248.

Reynolds-Henne CE, Siegwolf RTW, Treydte KS, Esper J, Henne S and Saurer M (2007) Temporal stability of climate-isotope relationships in tree rings of oak and pine (Ticino, Switzerland). *Global Biogeochemical Cycles* 21: doi:10.1029/2007GB002945.

Ritchie JC (1977) The modern and late Quaternary vegetation of the Campbell-Dolomite uplands, near Inuvik, N.W.T. Canada. *Ecological Monographs* 47: 401–423.

Ritchie JC and Hare FK (1971) Late Quaternary vegetation and climate near the Arctic treeline of northwestern North America. *Quaternary Research* 1: 331–342.

Robertson I, Leavitt SW, Loader NJ and Buhay W (2008) Progress in isotope dendroclimatology. *Chemical Geology* 252: EX1–EX4.

Robertson I, Waterhouse JS, Barker AC, Carter AHC and Switsur VR (2001) Oxygen isotope ratios of oak in east England: implications for reconstructing the isotopic composition of precipitation. *Earth and Planetary Science Letters* 191: 21–31.

Roden JS, Lin G and Ehleringer JR (2000) A mechanistic model for interpretation of hydrogen and oxygen isotope ratios in tree-ring cellulose. *Geochimica et Cosmochimica Acta* 64: 21–35.

Rodionov SN, Overland JE and Bond NA (2005) The Aleutian Low and winter climatic conditions in the Bering Sea. Part I: classification. *Journal of Climate* 18: 160–177.

Rossi S, Deslauriers A, Anfodillo T, Morin H, Saracino A, Motta R and Borghetti M (2006) Conifers in cold environments synchronize maximum growth rate of tree-ring formation with day length. *The New Phytologist* 170: 301–10.

Rossi S, Deslauriers A, Griçar J, Seo J-W, Rathgeber CB, Anfodillo T, Morin H, Levanic T, Oven P and Jalkanen R (2008) Critical temperatures for xylogenesis in conifers of cold climates. *Global Ecology and Biogeography* 17: 696–707.

Rozanski K, Araguas-Araguas L and Gonfiantini R (1993) Isotopic patterns in modern global precipitation. In: Swart PK, McKenzie J, Lohmann KC and Savin S (eds) *Climate Change in Continental Isotopic Records*. Washington D.C.: American Geophysical Union, 1–37.

Rozanski K, Araguás-Araguás L and Gonfiantini R (1992) Relation between long-term trends of oxygen-18 isotope composition of precipitation and climate. *Science* 258: 981–985.

Saurer M, Aellen K and Siegwolf R (1997a) Correlating $\delta^{13}C$ and $\delta^{18}O$ in cellulose of trees. *Plant, Cell and Environment* 20: 1543–1550.

Saurer M, Borella S and Leuenberger M (1997b) $\delta^{18}O$ of tree rings of beech (*Fagus silvatica*) as a record of $\delta^{18}O$ of the growing season precipitation. *Tellus B* 49: 80–92.

Saurer M, Kress A, Leuenberger M, Rinne KT, Treydte KS and Siegwolf RTW (2012) Influence of atmospheric circulation patterns on the oxygen isotope ratio of tree rings in the Alpine region. *Journal of Geophysical Research* 117: doi:10.1029/2011JD016861.

Saurer M, Schweingruber FH, Vaganov EA, Shiyatov SG and Siegwolf R (2002) Spatial and temporal oxygen isotope trends at the northern tree-line in Eurasia. *Geophysical Research Letters* 29: doi:10.1029/2001GL013739.

Schmidt GA, Hoffmann G, Shindell DT and Hu Y (2005) Modeling atmospheric stable water isotopes and the potential for constraining cloud processes and stratosphere-troposphere water exchange. *Journal of Geophysical Research* 110: doi:10.1029/2005JD005790.

Schmidt GA, Ruedy R, Hansen JE, Aleinov I, Bell N, Bauer M, Bauer S, Cairns B, Canuto V, Cheng Y, Del Genio A, Faluvegi G, Friend AD, Hall TM, Hu Y, Kelley M, Kiang NY, Koch D, Lacis AA, Lerner J, Lo KK, Miller RL, Nazarenko L, Oinas V, Perlwitz J, Perlwitz J, Rind D, Romanou A, Russell GL, Sato M, Shindell DT, Stone PH, Sun S, Tausnev N, Thresher D and Yao M-S (2006) Present-day atmospheric simulations using GISS ModelE: Comparison to in situ, satellite, and reanalysis data. *Journal of Climate* 19: 153–192.

Schulman E (1944) Tree-ring work in Scandinavia. *Tree-Ring Bulletin* 11: 2–6.

Schuur EAG and Abbott B (2011) Climate change: High risk of permafrost thaw. *Nature* 480: 32–33.

Schweingruber FH and Briffa KR (1996) Tree-ring density networks for climate reconstruction. In: Jones PD, Bradley RS and Jouzel J (eds) *Climatic Variations and Forcing Mechanisms of the Last 2000 Years*. Berlin: Springer, 43–66.

Seftigen K, Linderholm HW, Loader NJ, Liu Y and Young GHF (2011) The influence of climate on $^{13}C/^{12}C$ and $^{18}O/^{16}O$ ratios in tree ring cellulose of *Pinus sylvestris* L. growing in the central Scandinavian Mountains. *Chemical Geology* 286: 84–93.

Serreze MC, Barrett AP, Stroeve JC, Kindig DN and Holland MM (2009) The emergence of surface-based Arctic amplification. *The Cryosphere* 3: 11–19.

Serreze MC and Barry RG (2005) *The Arctic Climate System*. Cambridge, United Kingdom: Cambridge University Press, 385.

Shakhova N, Semiletov I, Salyuk A, Yusupov V, Kosmach D and Gustafsson O (2010) Extensive methane venting to the atmosphere from sediments of the East Siberian Arctic Shelf. *Science* 327: 1246–1250.

Smith MW (1976) Permafrost in the Mackenzie Delta, Northwest Territories. *Paper 75-2*. Ottawa, Canada: Geological Survey of Canada.

Smol JP, Wolfe AP, Birks HJB, Douglas MSV, Jones VJ, Korhola A, Rienitz R, Rühland K, Sorvari S, Antoniades D, Brooks SJ, Fallu MA, Hughes M, Keatley BE, Laing TE, Michelutti N, Nazarova L, Nyman M, Paterson AM, Perren B, Quinlan R, Rautio M,

Saulnier-Talbot É, Siitonen S, Solovieva N and Weckström J (2005) Climate-driven regime shifts in the biological communities of arctic lakes. *Proceedings of the National Academy of Sciences of the Unites States of America* 102: 4397–4402.

Sodemann H, Masson-Delmotte V, Schweirz C, Vinther BM and Wernli H (2008a) Interannual variability of Greenland winter precipitation sources: 2. Effects of North Atlantic Oscillation variability on stable isotopes in precipitation. *Journal of Geophysical Research* 113: doi:10.1029/2007JD009416.

Sodemann H, Schweirz C and Wernli H (2008b) Interannual variability of Greenland winter precipitation sources: Lagrangian moisture diagnostic and North Atlantic Oscillation influence. *Journal of Geophysical Research* 113: doi:10.1029/2007JD008503.

Speer JH (2010) *Fundamentals of Tree-Ring Research*. Tucson, Arizona: University of Arizona Press, 252.

Sternberg L, DeNiro M and Savidge R (1986) Oxygen isotope exchange between metabolites and water during biochemical reactions leading to cellulose synthesis. *Plant Physiology* 82: 423–427.

Sternberg LSL (1989) Oxygen and hydrogen isotope measurements in plant cellulose analysis. In: Linskens HF and Jackson JF (eds) *Modern Methods of Plant Analysis: Plant Fibers*. New York: Springer-Verlag, 89–99.

Stuiver M (1961) Variations in radiocarbon concentration and sunspot activity. *Journal of Geophysical Research* 66: 273–276.

Sturm C, Zhang Q and Noone D (2010) An introduction to stable water isotopes in climate models: benefits of forward proxy modelling for paleoclimatology. *Climate of the Past* 6: 115–129.

Szeicz JM and MacDonald GM (1994) Age-dependent tree-ring growth responses of subarctic white spruce to climate. *Canadian Journal of Forest Research* 24: 120–132.

Szeicz JM and MacDonald GM (1995) Dendroclimatic reconstruction of summer temperatures in northwestern Canada since A.D. 1638 based on age-dependent modelling. *Quaternary Research* 44: 257–266.

Szeicz JM and MacDonald GM (1996) A 930-year ring-width chronology from moisture-sensitive white spruce (*Picea glauca* Moench) in northwestern Canada. *The Holocene* 6: 345–351.

Tape K, Sturm M and Racine C (2006) The evidence for shrub expansion in northern Alaska and the Pan-Arctic. *Global Change Biology* 12: 686–702.

Thompson LG, Mosely-Thompson E, Dansgaard W and Grootes PM (1986) The Little Ice Age as recorded in the stratigraphy of the tropical Quelccaya Ice Cap. *Science* 234: 354–361.

Thorson RM and Dixon EJ (1983) Alluvial history of the Porcupine River, Alaska: role of glacial-lake overflow from northwest Canada. *Geological Society of America* 94: 576–589.

Tranquillini W (1979) *Physiological Ecology of the Alpine Timberline: Tree Existence at High Altitudes with Special Reference to the European Alps*. Berlin: Springer-Verlag, 137.

Trenberth KE and Hurrell JW (1994) Decadal atmosphere-ocean variations in the Pacific. *Climate Dynamics* 9: 303–319.

Trenberth KE and Otto-Bliesner BL (2006) Toward integrated reconstruction of past climates. *Science* 300: 589–591.

Treydte K, Frank D, Esper J, Andreu L, Bednarz Z, Berninger F, Boettger T, D'Alessandro CM, Etien N, Filot M, Grabner M, Guillemin MT, Gutierrez E, Haupt M, Helle G, Hilasvuori E, Jungner H, Kalela-Brundin M, Krapiec M, Leuenberger M, Loader NJ, Masson-Delmotte V, Pazdur A, Pawelczyk S, Pierre M, Planells O, Pukiene R, Reynolds-Henne CE, Rinne KT, Saracino A, Saurer M, Sonninen E, Stievenard M, Switsur VR, Szczepanek M, Szychowska-Krapiec E, Todaro L, Waterhouse JS, Weigl M and Schleser GH (2007) Signal strength and climate calibration of a European tree-ring isotope network. *Geophysical Research Letters*. American Geophysical Union 34: doi:10.1029/2007GL031106.

Treydte KS, Schleser GH, Helle G, Frank DC, Winiger M, Haug GH and Esper J (2006) The twentieth century was the wettest period in northern Pakistan over the past millennium. *Nature* 440: 1179–1182.

Turetsky MR, Kane ES, Harden JW, Ottmar RD, Manies KL, Hoy E and Kasischke ES (2011) Recent acceleration of biomass burning and carbon losses in Alaskan forests and peatlands. *Nature Geoscience* 4: 27–31.

Turetsky MR, Mack MC, Hollingsworth TN and Harden JW (2010) The role of mosses in ecosystem succession and function in Alaska's boreal forest. *Canadian Journal of Forest Research* 40: 1237–1264.

Uppala SM, Kållberg PW, Simmons AJ, Andrae U, Bechtold VDC, Fiorino M, Gibson JK, Haseler J, Hernandez A, Kelly GA, Li X, Onogi K, Saarinen S, Sokka N, Allan RP, Andersson E, Arpe K, Balmaseda MA, Beljaars ACM, Berg LVD, Bidlot J, Bormann N, Caires S, Chevallier F, Dethof A, Dragosavac M, Fisher M, Fuentes M, Hagemann S, Hólm E, Hoskins BJ, Isaksen L, Janssen PAEM, Jenne R, Mcnally AP, Mahfouf J-F, Morcrette J-J, Rayner NA, Saunders RW, Simon P, Sterl A, Trenberth KE, Untch A,

Vasiljevic D, Viterbo P and Woollen J (2005) The ERA-40 re-analysis. *Quarterly Journal of the Royal Meteorological Society* 131: 2961–3012.

Vaganov EA, Hughes MK, Kirdyanov AV, Schweingruber FH and Silkin PP (1999) Influence of snowfall and melt timing on tree growth in subarctic Eurasia. *Nature* 400: 149–151.

van Oldenborgh GJ (2000) What caused the onset of the 1997–98 El Niño? *Monthly Weather Review* 128: 2601–2607.

Viau AE, Ladd M and Gajewski K (2012) The climate of North America during the past 2000 years reconstructed from pollen data. *Global and Planetary Change* 84-85: 75–83.

Visser H, Büntgen U, D'Arrigo R and Petersen AC (2010) Detecting instabilities in tree-ring proxy calibration. *Climate of the Past Discussions* 6: 225–255.

Wahl ER and Ammann CM (2007) Robustness of the Mann, Bradley, Hughes reconstruction of Northern Hemisphere surface temperatures: Examination of criticisms based on the nature and processing of proxy climate evidence. *Climatic Change* 85: 33–69.

Wahl HE, Fraser DB, Harvey RC and Maxwell JB (1987) *Climate of Yukon. Climatological Studies, Vol. 40.* Ottawa, Canada: Environment Canada, 323.

Walker DA, Raynolds MK, Daniëls FJA, Einarsson E, Elvebakk A, Gould WA, Katenin AE, Kholod SS, Markon CJ, Melnikov ES, Moskalenko NG, Talbot SS and and the other members of the CT (2005) The Circumpolar Arctic vegetation map. *Journal of Vegetation Science* 16: 267–282.

Waterhouse JS, Switsur VR, Barker AC, Carter AHC, Hemming DL, Loader NJ and Robertson I (2004) Northern European trees show a progressively diminishing response to increasing atmospheric carbon dioxide concentrations. *Quaternary Science Reviews* 23: 803–810.

Welker JM, Rayback S and Henry GHR (2005) Arctic and North Atlantic Oscillation phase changes are recorded in the isotopes ($\delta^{18}O$ and $\delta^{13}C$) of *Cassiope tetragona* plants. *Global Change Biology* 11: 997–1002.

Werner RA and Brand WA (2001) Referencing strategies and techniques in stable isotope ratio analysis. *Rapid Communications in Mass Spectrometry* 15: 501–519.

Wigley TML, Briffa KR and Jones PD (1984) On the average value of correlated time series, with applications in dendroclimatology and hydrometeorology. *Journal of Climate and Applied Meteorology* 23: 201–213.

Wilmking M and Juday GP (2005) Longitudinal variation of radial growth at Alaska's northern treeline—recent changes and possible scenarios for the 21st century. *Global and Planetary Change* 47: 282–300.

Wilmking M, Juday GP, Barber VA and Zald HSJ (2004) Recent climate warming forces contrasting growth responses of white spruce at treeline in Alaska through temperature thresholds. *Global Change Biology* 10: 1724–1736.

Wilson R, D'Arrigo R, Buckley B, Büntgen U, Esper J, Frank D, Luckman B, Payette S, Vose R and Youngblut D (2007) A matter of divergence: tracking recent warming at hemispheric scales using tree ring data. *Journal of Geophysical Research* 112: doi:10.1029/2006JD008318.

Wilson R and Luckman B (2003) Dendroclimatic reconstruction of maximum summer temperatures from upper tree-line sites in interior British Columbia. *The Holocene* 13: 853–863.

Yarie J and Van Cleve K (2010) Long-term monitoring of climatic and nutritional affects on tree growth in interior Alaska. *Canadian Journal of Forest Research* 40: 1325–1335.

Youngblut D and Luckman B (2008) Maximum June-July temperatures in the southwest Yukon over the last 300 years reconstructed from tree rings. *Dendrochronologia* 25: 153–166.

APPENDIX A

SAMPLE AND DATA STORAGE

For the foreseeable future, the physical samples collected for this thesis will be cared for by Dr. Michael Pisaric at Brock University, St. Catharines, Ontario, Canada. Contact Dr. Pisaric (mpisaric@brocku.ca or 905-688-5550 ext. 6152) to arrange access to these samples. Ring-width data for the Old Crow Flats samples can be downloaded via the Polar Data Catalogue (http://www.polardata.ca/). All data will soon be archived on the International Tree-Ring Databank (http://www.ncdc.noaa.gov/paleo/treering.html), hosted by the National Oceanic and Atmospheric Administration.

APPENDIX B

CHAPTER 3 SUPPORTING INFORMATION

SI-Note 3.1. A running 2-sample t-test was used to test the null hypothesis that the Group 1 and 2 site chronologies are derived from the same normal distribution with equal means and variance ($p \leq 0.05$). The null hypothesis was tested for each year both groups had four or more site chronologies. The t-test result was calculated using the 'ttest2' function (Statistics Toolbox) in Matlab 7.4.

SI-Note 3.2. The MDEC negative-responder (neg) and positive-responder (pos) used here are modified versions of the "negative- and positive-responder" chronologies by Pisaric et al. (2007). The main difference is that the modified MDEC-neg and -pos chronologies do not contain Campbell Dolomite Upland series (Szeicz and MacDonald, 1996). CDU series were excluded from MDEC neg and MDEC pos to ensure that the Group 1/Group 2 correlations with CDU, MDEC neg, and MDEC pos would be independent of each other.

SI-Note 3.3. The mean NWNA 1/NWNA 2 chronologies were compared to a regional average of CRUTEM3v gridded temperatures (Brohan et al., 2006). The regional average includes 22 (5° x 5°) grid cells bounded by 60-70°N and 170-115°W; only 2 grid cells (65-70°N/160-155°W and 65-70°N/150-145°W) did not contain any data.

Temperature data before 1900 were not used as spatial coverage is limited. The number of grid cells with data for the year 1900 is 5; the number of grid cells increases steadily to more than 10 by the early-1920's, more than 15 by the early-1940's, and a high of 20 by 1959.

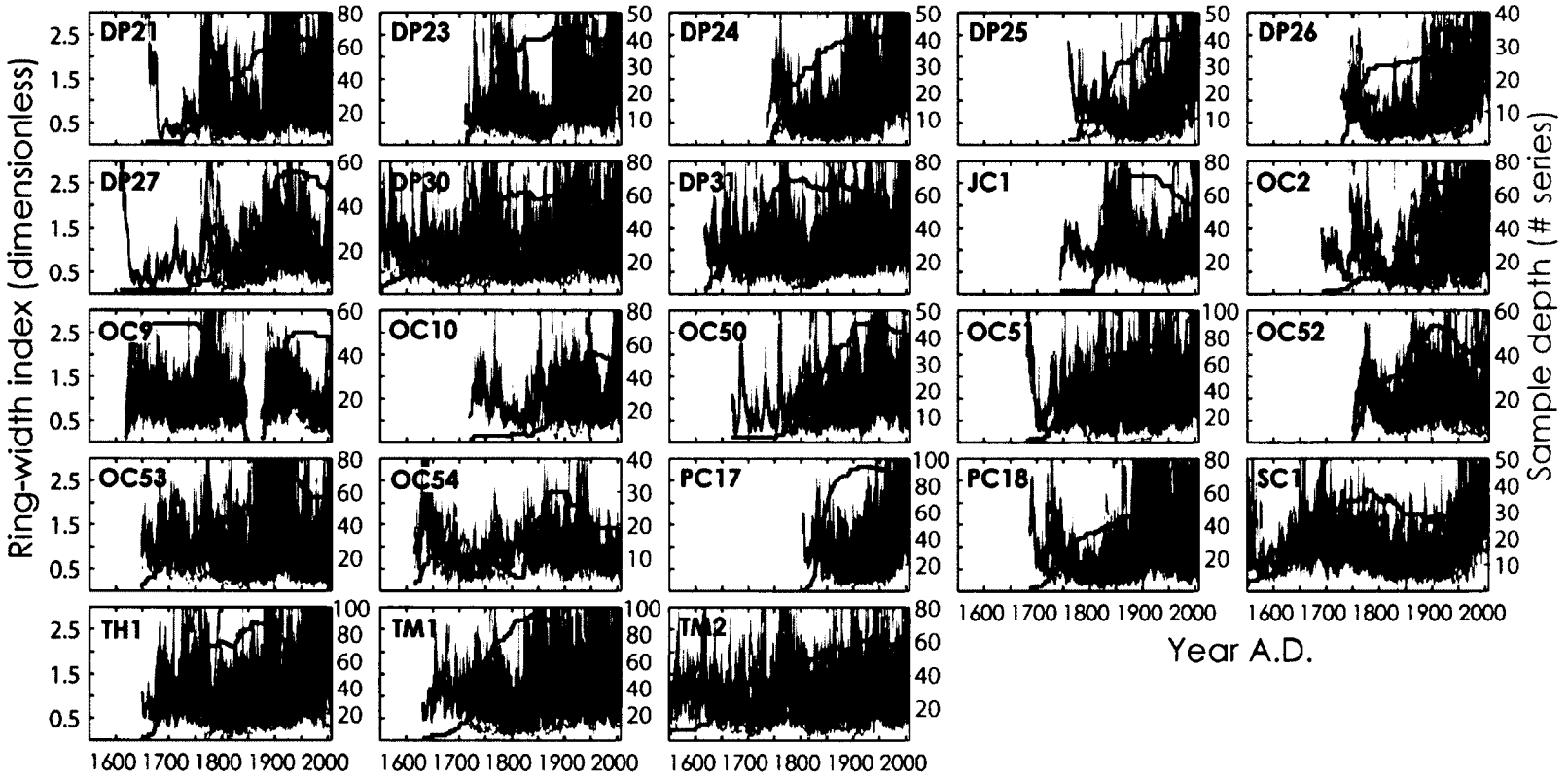

SI-Figure 3.1. Standardized ring-width indices (grey lines) and mean site chronologies (black lines) for each site in Old Crow Flats based on signal-free standardisation (Melvin and Briffa, 2008) using data-adaptive 'negative exponential' or 'negative-to-zero slope linear' curve fits (Fritts et al., 1969). Sample depth (red lines) indicates the number of series defining the mean chronology. The mean chronologies were calculated with a robust bi-weight mean (Cook, 1985); more details on each chronology are provided in Table 3.1.

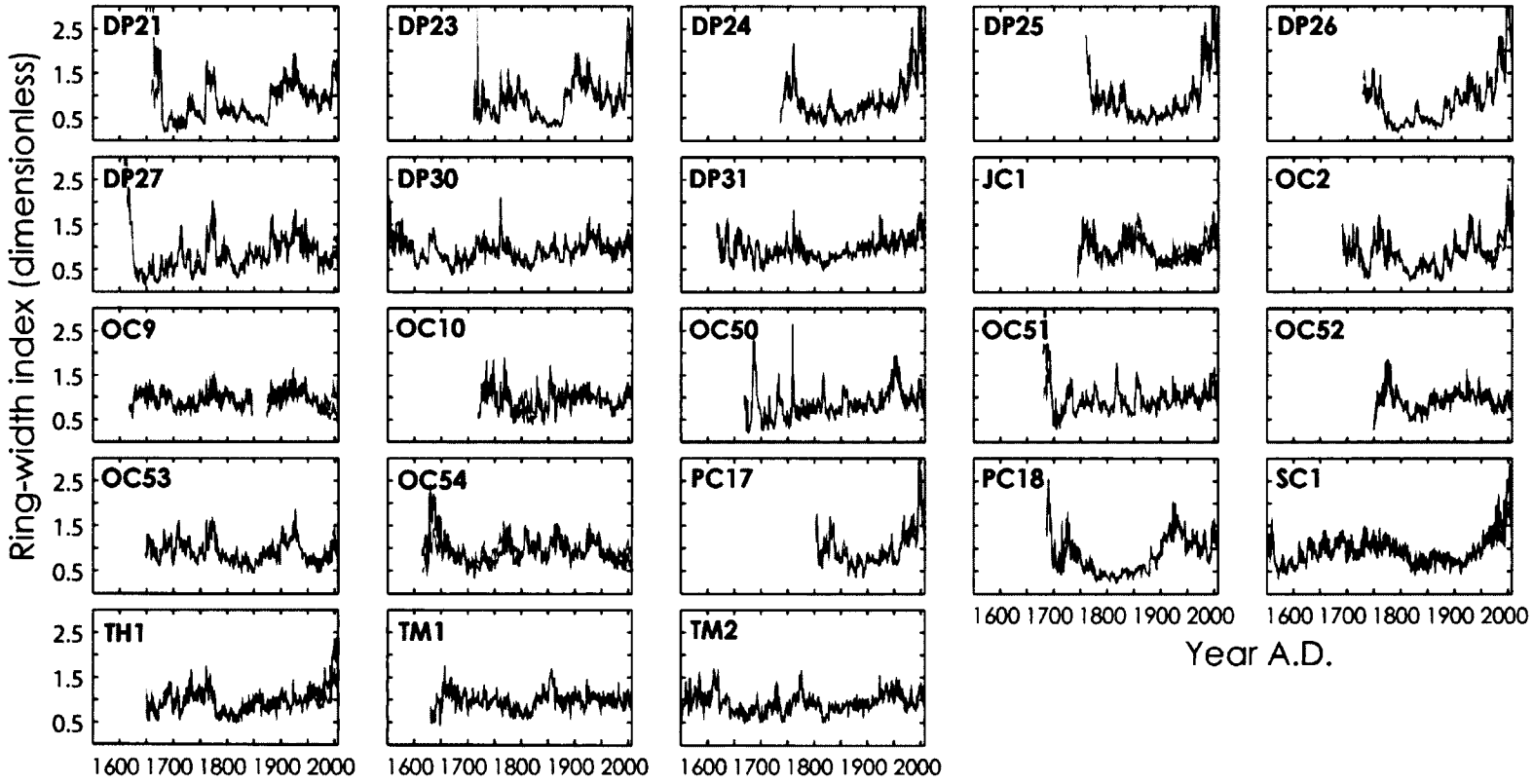

SI-Figure 3.2. A comparison of each mean site chronology produced using 'signal-free' (black lines) and non-signal-free (red lines) methods. Inter-series differences can be considered the result of 'trend distortion' (Melvin and Briffa, 2008). Due to differences in non-age-related growth (i.e., forced by climate, disturbance, etc.) between sites, trend distortion effects are more pronounced in some chronologies (e.g., JC1, OC9, OC54, SC1, and TH1) than in others (e.g., DP26, OC50, OC52, TM1, and TM2).

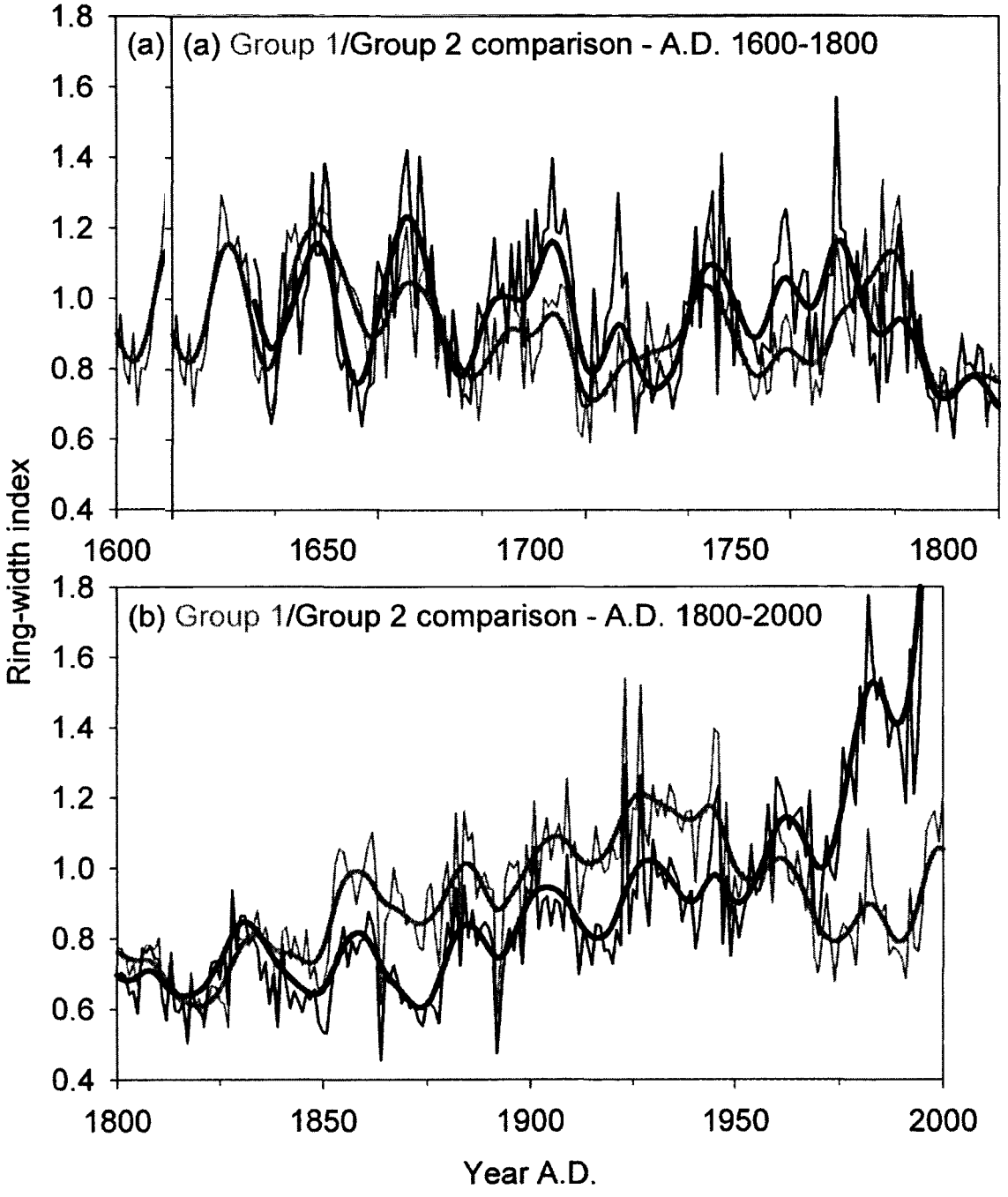

SI-Figure 3.3. Magnified comparison of the mean Group 1 and Group 2 chronologies during (a) 1600-1800 and (b) 1800-2000. Smoothed chronologies were calculated using a 15-year cubic smoothing spline with a 50% frequency cut-off (Cook and Peters, 1981).

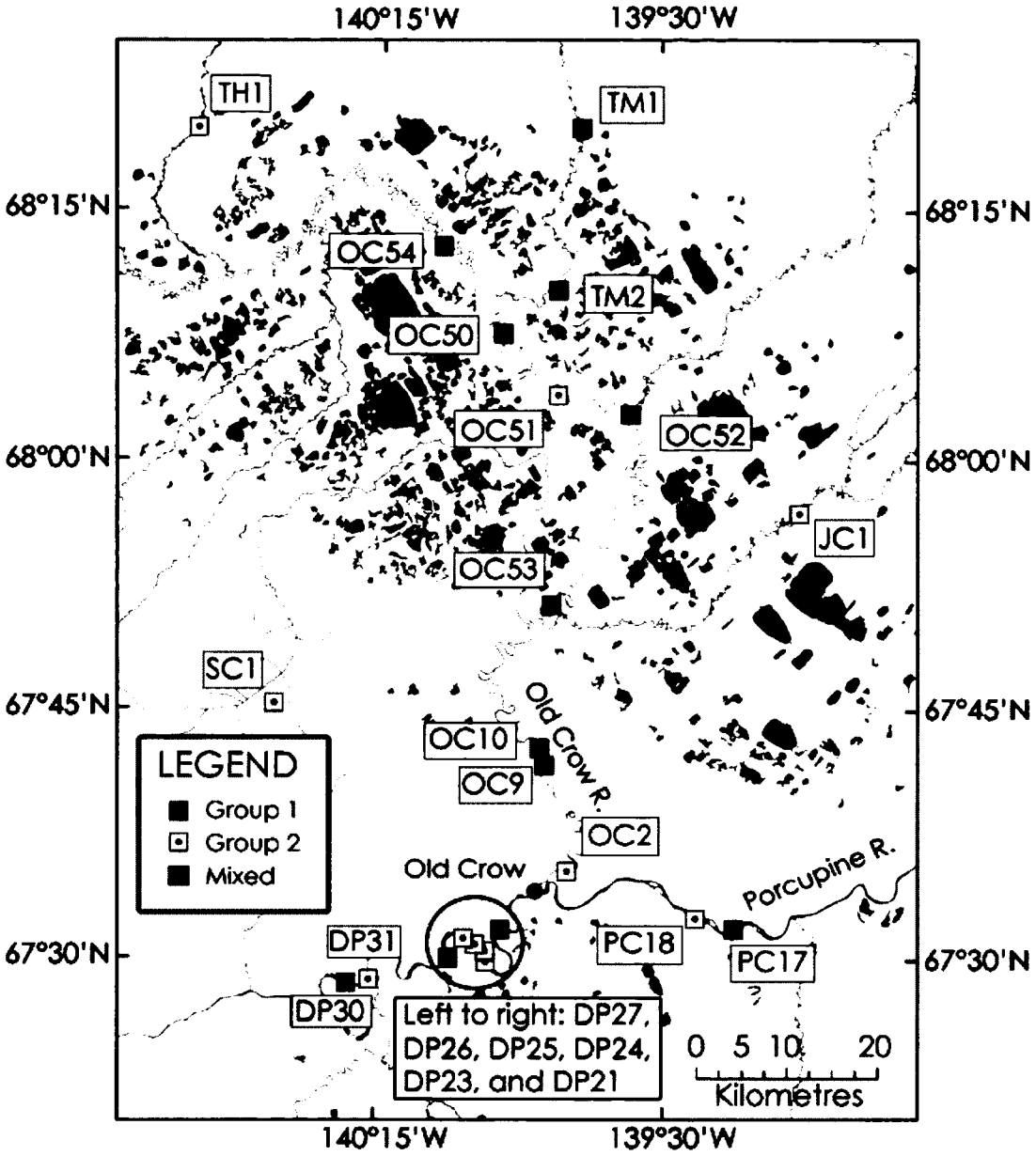

SI-Figure 3.4. Old Crow Flats sites: Group 1 (negative temperature response), Group 2 (positive temperature response), and Mixed (mixed negative/positive temperature response).

SI-Table 3.1. Correlations between the 23 Old Crow Flats site chronologies and minimum/maximum temperatures from May-August of the growth year and previous growth year; only correlations significant at $p \leq 0.05$ (two-tailed) are presented.

	Minimum temperatures								Maximum temperatures							
	Previous growth year				Growth year				Previous growth year				Growth year			
	May	Jun	Jul	Aug	May	Jun	Jul	Aug	May	Jun	Jul	Aug	May	Jun	Jul	Aug
DP21						0.31					-0.29					
DP23		0.32				0.41										
DP24	0.29	0.45	0.38			0.54	0.43	0.27	0.30	0.35				0.41	0.28	
DP25	0.33	0.46	0.42	0.23	0.25	0.54	0.48	0.31	0.31	0.35	0.24			0.38	0.29	
DP26	0.27	0.46	0.36		0.24	0.52	0.38	0.24	0.24	0.33				0.34		
DP27		-0.38	-0.43		-0.35	-0.28	-0.41	-0.23	-0.27	-0.45	-0.58	-0.40	-0.43	-0.39	-0.41	-0.32
DP30										-0.28	-0.43	-0.33	-0.27		-0.34	-0.34
DP31	0.29			0.27		0.48	0.27		0.28					0.31		
JC1	0.27	0.36				0.57	0.45			0.24				0.34		
OC2	0.24	0.26				0.39										
OC9	-0.33	-0.53	-0.52	-0.35	-0.34	-0.42	-0.41	-0.24	-0.34	-0.50	-0.54	-0.41	-0.36	-0.46	-0.42	-0.34
OC10										-0.24	-0.48	-0.24			-0.27	-0.24
OC50		-0.34	-0.26		-0.26					-0.42	-0.40		-0.31		-0.24	
OC51	0.26					0.44	0.26									
OC52		-0.36	-0.47		-0.36		-0.25	-0.23		-0.41	-0.57	-0.34	-0.41	-0.25	-0.35	-0.34
OC53										-0.25	-0.48	-0.29	-0.25		-0.34	-0.39
OC54	-0.25	-0.42	-0.53	-0.40	-0.36	-0.31	-0.35	-0.30	-0.28	-0.41	-0.58	-0.47	-0.44	-0.40	-0.43	-0.45
PC17	0.30	0.46	0.36		0.23	0.54	0.41		0.32	0.38	0.25			0.42	0.29	
PC18		-0.24	-0.34		-0.24		-0.23			-0.35	-0.54	-0.34	-0.32	-0.24	-0.38	-0.37
SC1	0.36	0.45	0.28	0.27		0.53	0.43		0.33	0.34				0.37	0.25	
TH1	0.35	0.41	0.26	0.27		0.58	0.42		0.26	0.24				0.35		
TM1			-0.38		-0.35						-0.41		-0.37			
TM2		-0.31	-0.42		-0.32					-0.41	-0.62	-0.30	-0.39		-0.35	-0.29

WORKS CITED – APPENDIX B

Brohan P, Kennedy JJ, Haris I, Tett SFB and Jones PD (2006) Uncertainty estimates in regional and global observed temperature changes: A new data set from 1850. *Journal of Geophysical Research* 111: doi:10.1029/2005JD006548.

Cook ER (1985) *A Time Series Analysis Approach to Tree Ring Standardization. PhD dissertation.* Tuscon, USA: University of Arizona, 171.

Cook ER and Peters K (1981) The smoothing spline: a new approach to standardizing forest interior tree-ring width series for dendroclimatic studies. *Tree-Ring Bulletin* 41: 45–53.

Fritts HC, Moismann JE and Bottorff CP (1969) A revised computer program for standardizing tree-ring series. *Tree-Ring Bulletin* 29: 15–20.

Melvin TM and Briffa KR (2008) A "signal-free" approach to dendroclimatic standardisation. *Dendrochronologia* 26: 71–86.

Pisaric MFJ, Carey SK, Kokelj SV and Youngblut D (2007) Anomalous 20th century tree growth, Mackenzie Delta, Northwest Territories, Canada. *Geophysical Research Letters* 34: doi:10.1029/2006GL029139.

Szeicz JM and MacDonald GM (1996) A 930-year ring-width chronology from moisture-sensitive white spruce (*Picea glauca* Moench) in northwestern Canada. *The Holocene* 6: 345–351.

APPENDIX C

CHAPTER 4 SUPPORTING INFORMATION

SI-Note 4.1. The program COFECHA (Holmes, 1983) was used to assess the cross-dating quality of the ESK raw data; 9 of the 49 ESK series contained continuous sections (decades to centuries) of 'B-type' errors at the ends of the series indicating that they were potentially misaligned with respect to the master series. The remaining portions of these series were not in question as they were strongly correlated with the master series. As the physical samples were not available, it was not possible to re-measure the problem sections and assess the cause of these errors (e.g., reaction growth, locally absent rings, etc.). To ensure these potential errors would not bias the mean ESK chronology, the problem sections were excluded from further analysis.

SI-Note 4.2. For the regional temperature composites (SI-Figs. 4.5-4.7), monthly temperature records for Tuktoyaktuk, Inuvik, Aklavik, Fort McPherson, Norman Wells, and Fort Good Hope (SI-Fig. 4.4) were downloaded from Environment Canada (http://climate.weatheroffice.gc.ca/). The Fort McPherson record consists of data from the original 'Fort McPherson' station (AD 1892-1977) and the newer 'Fort McPherson A' station (AD 1981-2007) ca. 3 km from the original station (É. Mekis, Environment Canada, pers. comm.); only the AD 1892-1977 data are used due to a high number of estimated, missing, or incomplete data points in the new station record. Furthermore, there is no overlap between the new and old stations, making it impossible to identify and

adjust for systematic biases due to geographical position. The Fort Good Hope record is a composite of data from the original 'Fort Good Hope 2' station (AD 1897-1966; temperature data available since AD 1908) and the 'Fort Good Hope A' station (AD 1944-2007) ca. 1 km from the original station. The mean and variance of the Fort Good Hope 2 record were adjusted to the Fort Good Hope A record to account for systematic differences due to location, and combined into a mean record. The Mackenzie Delta regional temperature composites (SI-Figs. 4.5-4.7) were developed by first adjusting the mean and variance of each station record to that of the Inuvik record, and then averaging all records to create regional monthly composites.

The regional precipitation composites (SI-Fig. 4.8) were developed from Inuvik, Aklavik, and Fort McPherson data only. The reason only these stations were used is because precipitation is highly variable over short distances in the study region (Burn and Kokelj, 2009), and including stations that are more distant from the site network would diminish the representativeness of the regional composites with respect to the sampled trees. Inuvik, Aklavik, and Fort McPherson are the most proximal stations to and are likely most representative of the site network. Precipitation data for Inuvik (1957-2007) and Fort McPherson (1932-2007) were downloaded from the Adjusted and Homogenised Canadian Climate Database (http://ec.gc.ca/dccha-ahccd/), which are adjusted for gauge changes and trace snow and rainfall events (Mekis and Vincent, 2011). Trace events (< 0.2 mm rain, < 0.2 cm snow) cannot be accurately measured, and are assigned a value of zero and flagged in raw climate records. In Arctic regions, trace events can account for a large proportion of the total monthly precipitation budget, and trace-adjusted data are an

attempt to better reflect actual precipitation amounts. Only raw monthly data were available for Aklavik (AD 1926-2007; http://climate.weatheroffice.gc.ca/). However, over the 81 year period of station operation, 432 monthly observations were reported and just 10 of the observations were flagged as trace events. These 10 trace events were excluded from the Aklavik record to make it more comparable to the Inuvik and Fort McPherson records. The Aklavik record was as well correlated with the Inuvik record as the Fort McPherson record ($r = 0.43$ and 0.36, respectively, for the average month; $p \leq 0.05$) suggesting it is as regionally-representative as the Fort McPherson record. The Mackenzie Delta regional precipitation composites (SI-Fig. 4.8) were developed by first adjusting the mean and variance of the Aklavik and Fort McPherson records to that of the Inuvik record, and averaging the three records to create regional monthly composites.

SI-Note 4.3. The Szeicz and MacDonald (1995) June-July temperature reconstruction (AD 1638-1988) was obtained from NOAA's Paleoclimatology Program archive (http://www.ncdc.noaa.gov/paleo/recons.html) and converted to anomalies with respect to its mean value over the period AD 1638-1988.

SI-Note 4.4. The 6-study hemispheric-scale composite temperature reconstruction consists of the following reconstructions: Jones et al. (1998); Briffa (2000); Esper et al. (2002); D'Arrigo et al. (2006); Wahl and Ammann (2007); Wilson et al. (2007). The reconstructions were obtained from NOAA's Paleoclimatology Program archive (http://www.ncdc.noaa.gov/paleo/recons.html, accessed June 2011). The reconstructions are largely tree-ring based, and overall the composite reconstruction is weighted towards

samples from the Northern Hemisphere. Z-scores were calculated for each reconstruction based on their common period of overlap (AD 1750-1980) and averaged into the composite index using a robust bi-weight mean. It should be noted that the Szeicz and MacDonald (1996) 'CDU' chronology used in the Mackenzie Delta regional chronology was used by Esper et al. (2002); however, the overall contribution of CDU to the Esper et al.(2002) reconstruction is small, and negligible to the hemispheric-scale composite. As such, the regional chronology and the hemispheric-composite can be considered almost entirely independent of each another.

SI-Note 4.5. Details on each comparison in Fig. 4.5:

(a) See SI-Note 4.2;

(b) June-July mean temperature reconstruction by Szeicz and MacDonald (1995) (see SI-Note 4.3);

(c) Unaltered mean $\delta^{18}O$ tree-ring chronology by Porter et al. (2009); average of 3 white spruce trees from 'TM' site (site 6, Fig. 4.1), Mackenzie Delta;

(d) Unaltered OCF-Group 2 ring-width chronology by Porter and Pisaric (2011); regional mean of 11 site-chronologies in Old Crow Flats, northern Yukon Territory, Canada;

(e) A 'signal-free' version of the Coppermine River ring-width chronology by D'Arrigo et al. (2009), from western Nunavut, Canada. The signal-free chronology was calculated by Porter and Pisaric (2011);

(f) Six-study composite hemispheric-scale temperature reconstruction (see SI-Note 4.4);

(g) Circum-Arctic, multi-proxy temperature reconstruction by Kaufman et al. (2009); the original Kaufman et al. (2009) reconstruction uses 23 proxy records, 4 that are tree-ring-

based. Only the 19 non-tree-ring series (lake and ice cores) were used to calculate the circum-Arctic reconstruction shown in Fig. 4.5g. The Kaufman et al. (2009) dataset was downloaded from the National Oceanic and Atmospheric Administration's Paleoclimatology Program archive (http://www.ncdc.noaa.gov/paleo/recons.html). Z-scores for the 19 series were calculated based on their common period of overlap (AD 995-1795) and averaged into a composite index using the robust bi-weight mean (Cook, 1985).

(h) The Mackenzie Delta regional June-July minimum temperature reconstruction, this study.

SI-Figure 4.1. An overhead view of a 'white spruce/crowberry-lichen' forest site (Pearce et al., 1988) which is representative of most of the delta plain sites sampled in this study. These sites are easy to spot from overhead due to their sparse canopies and abundance of reflective lichen.

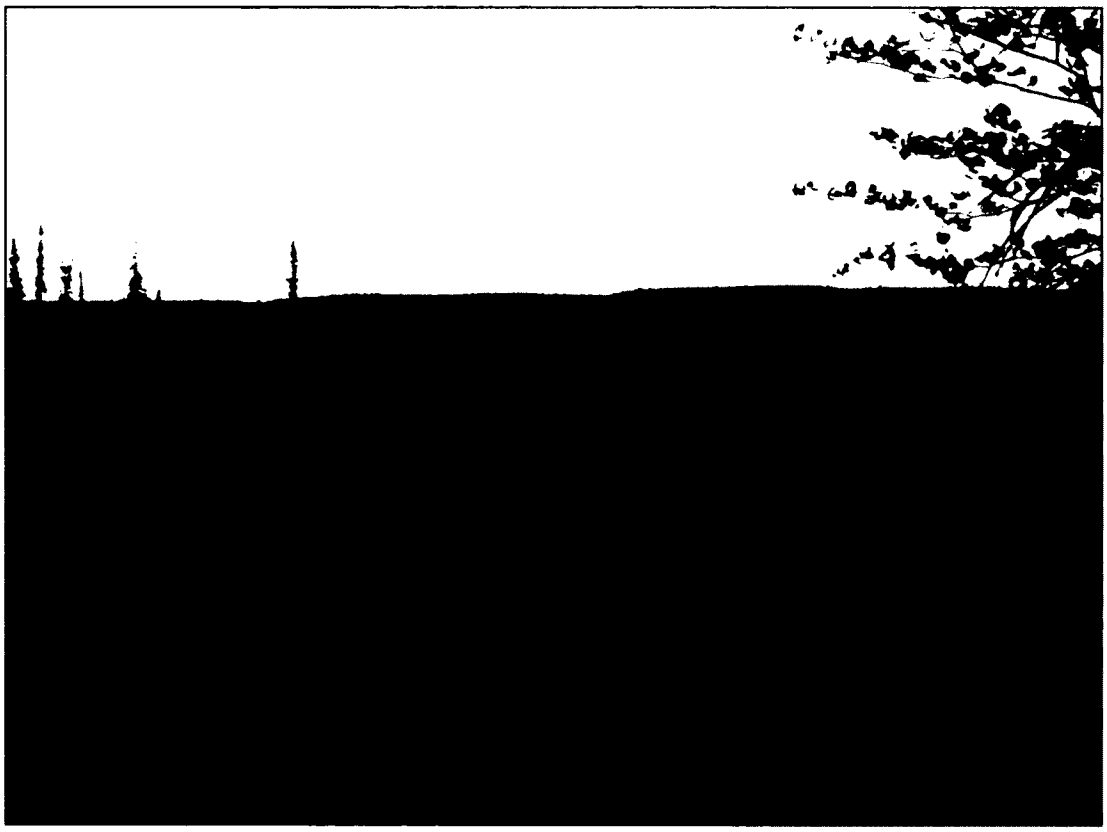

SI-Figure 4.2. A representative view of 'CDU2'. This site is characterised by an open-canopy, thick understory of mosses and lichens, and an irregular, rocky terrain. These site characteristics are also shared by 'CDU' and 'CDU1' (see Szeicz and MacDonald, 1996, for photographs of CDU).

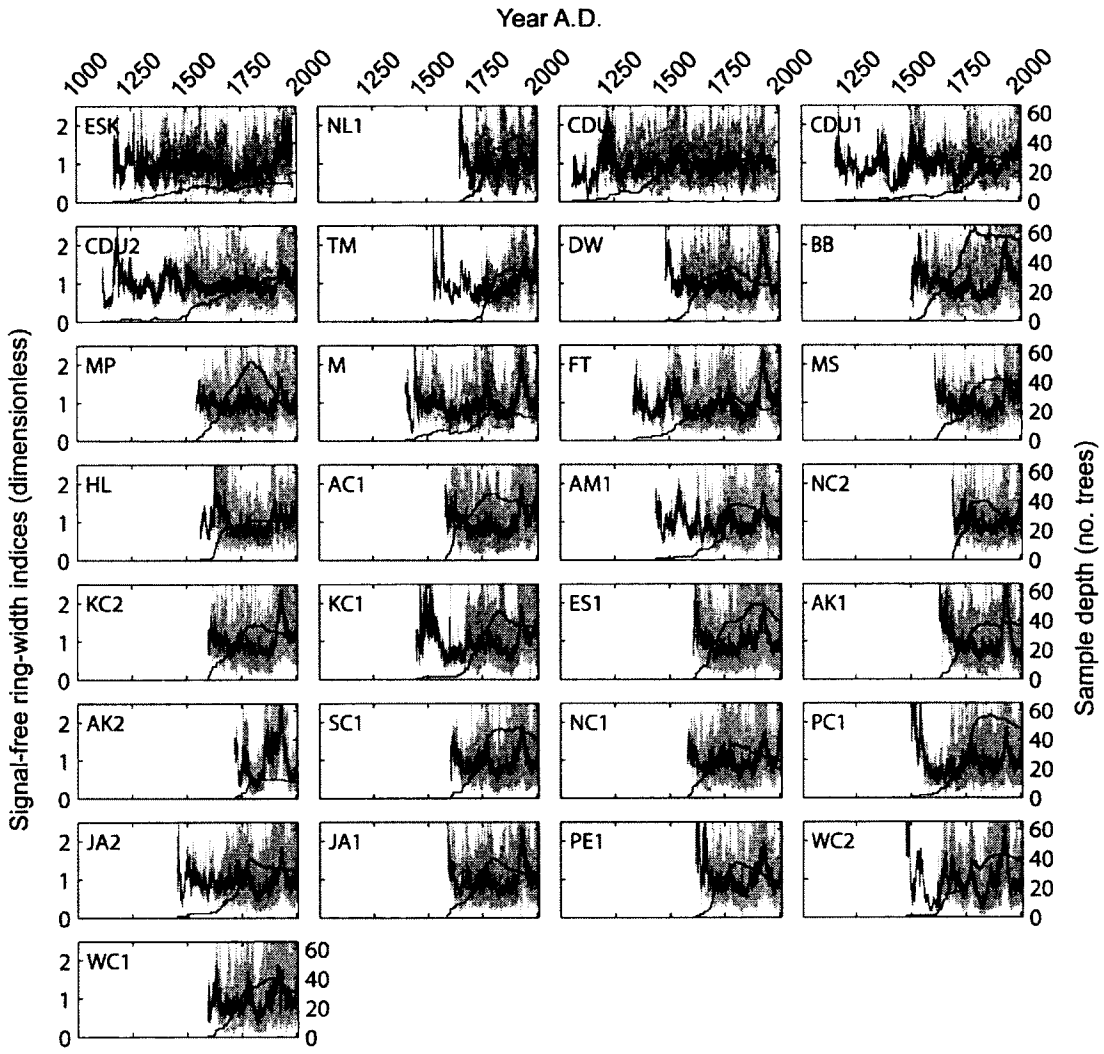

SI-Figure 4.3. Tree-averaged ring-width indices (light grey) and mean site chronologies (dark grey) for all 29 sites; the number of trees defining each year of the mean site chronologies is indicated (black).

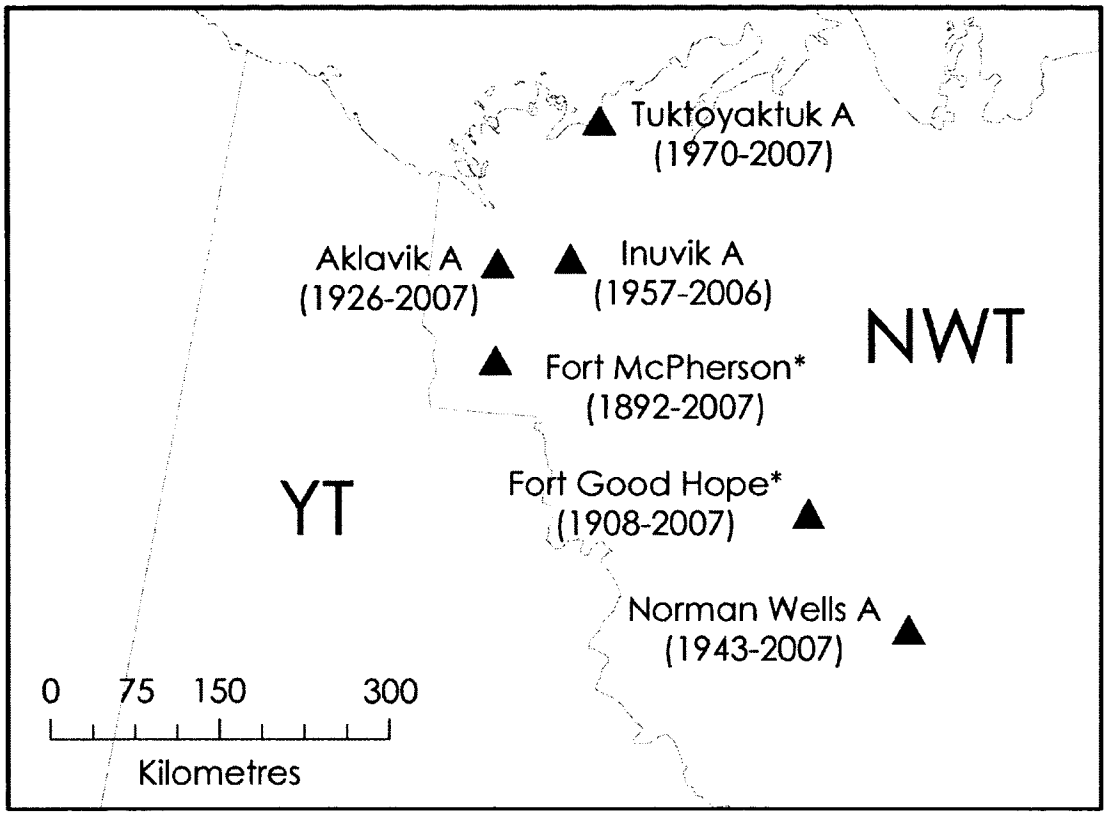

SI-Figure 4.4. Climate stations included in the regional temperature and precipitation composites. Periods of station operation are indicated (n.b., data are not available for all years of operation). 'Fort McPherson*' represents two non-overlapping station records: 'Fort McPherson' (1892-1977) and 'Fort McPherson A' (1981-2007). 'Fort Good Hope*' is a merged record representing 'Fort Good Hope 2' (1897-1966) and 'Fort Good Hope A' (1944-2007).

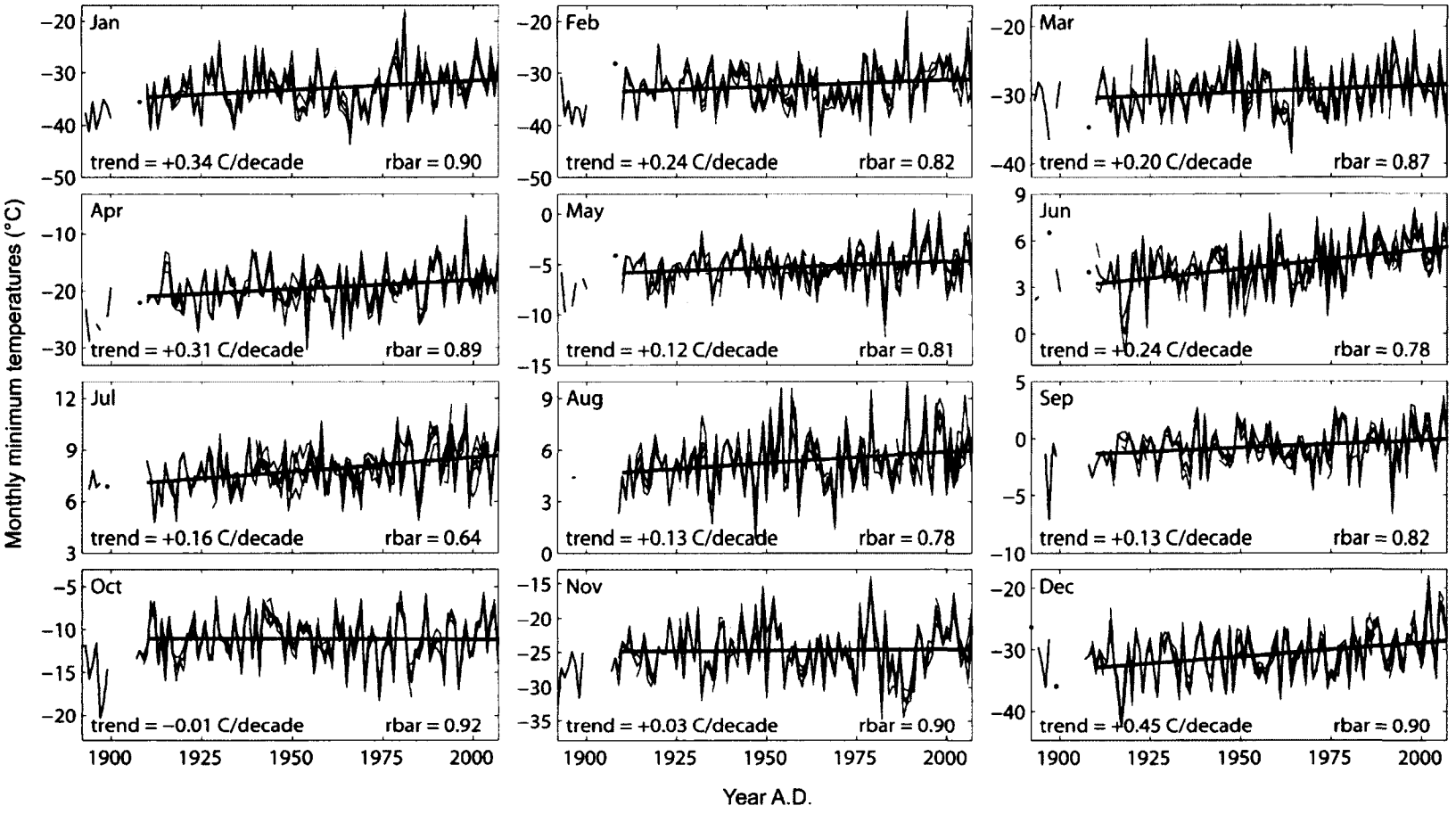

SI-Figure 4.5. Comparison of monthly minimum temperatures from Tuktoyaktuk, Inuvik, Aklavik, Fort McPherson, Norman Wells, and Fort Good Hope (red lines); regional means (black lines). 'rbar' is the mean inter-series correlation (all are significant at $p \leq 0.001$). 'trend' is the slope of the regional mean from AD 1910-2007, a period defined by two or more stations in most cases. See SI-Note 4.2 for more details.

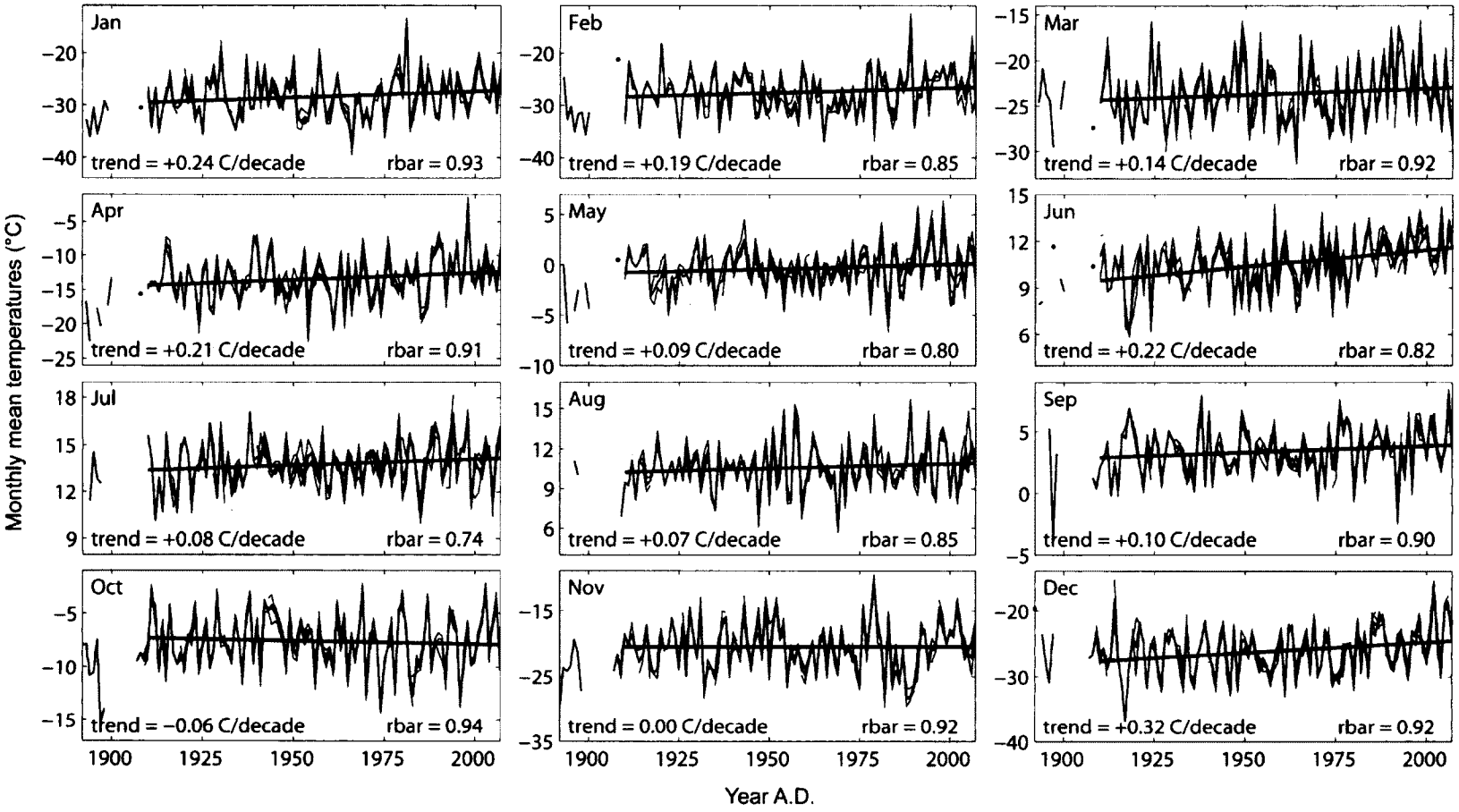

SI-Figure 4.6. Comparison of monthly mean temperatures from Tuktoyaktuk, Inuvik, Aklavik, Fort McPherson, Norman Wells, and Fort Good Hope (red lines); regional means (black lines). 'rbar' is the mean inter-series correlation (all are significant at $p \leq 0.001$). 'trend' is the slope of the regional mean from AD 1910-2007, a period defined by two or more stations in most cases. See SI-Note 4.2 for more details.

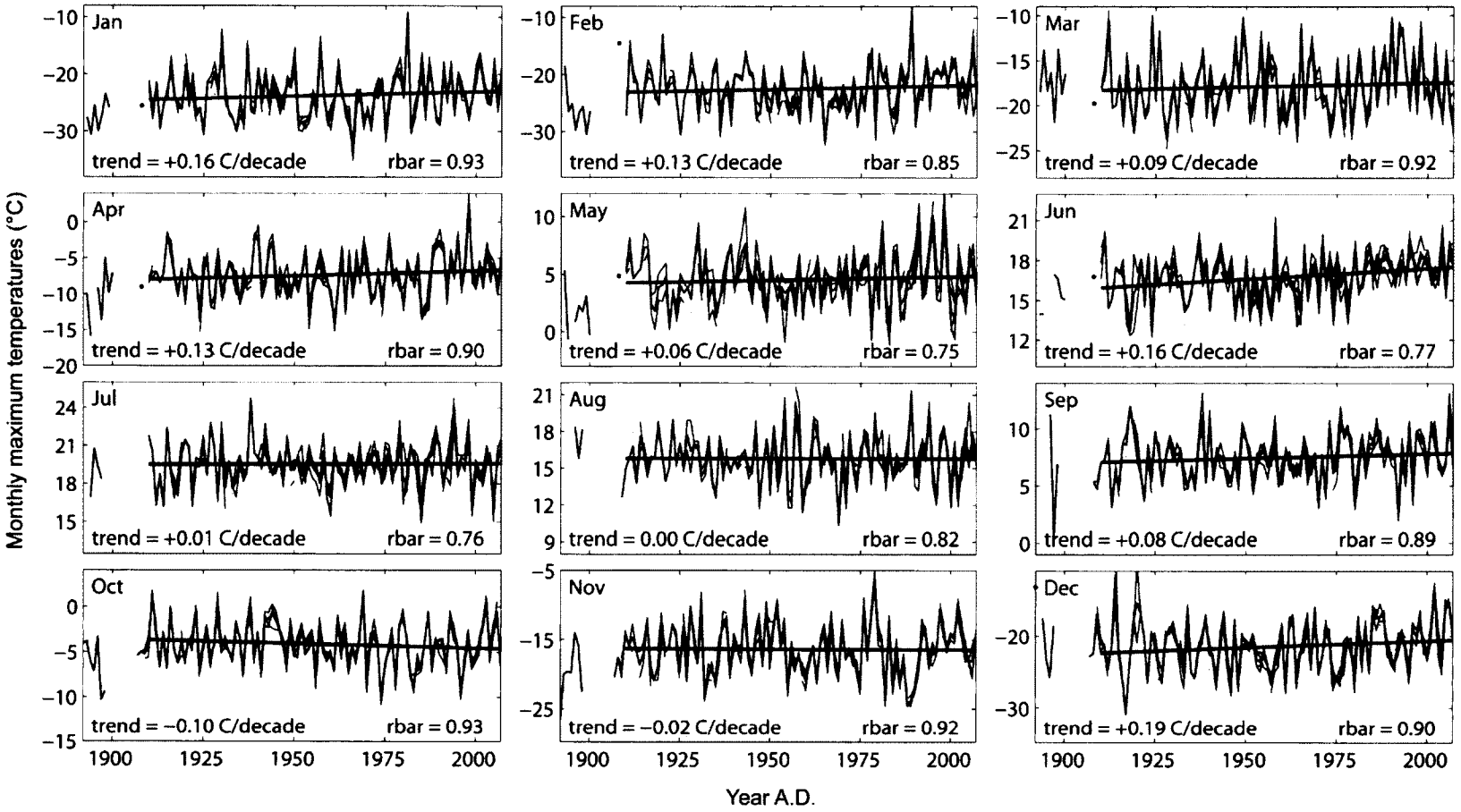

SI-Figure 4.7. Comparison of monthly maximum temperatures from Tuktoyaktuk, Inuvik, Aklavik, Fort McPherson, Norman Wells, and Fort Good Hope (red lines); regional means (black lines). 'rbar' is the mean inter-series correlation (all are significant at $p \leq 0.001$). 'trend' is the slope of the regional mean from AD 1910-2007, a period defined by two or more stations in most cases. See SI-Note 4.2 for more details.

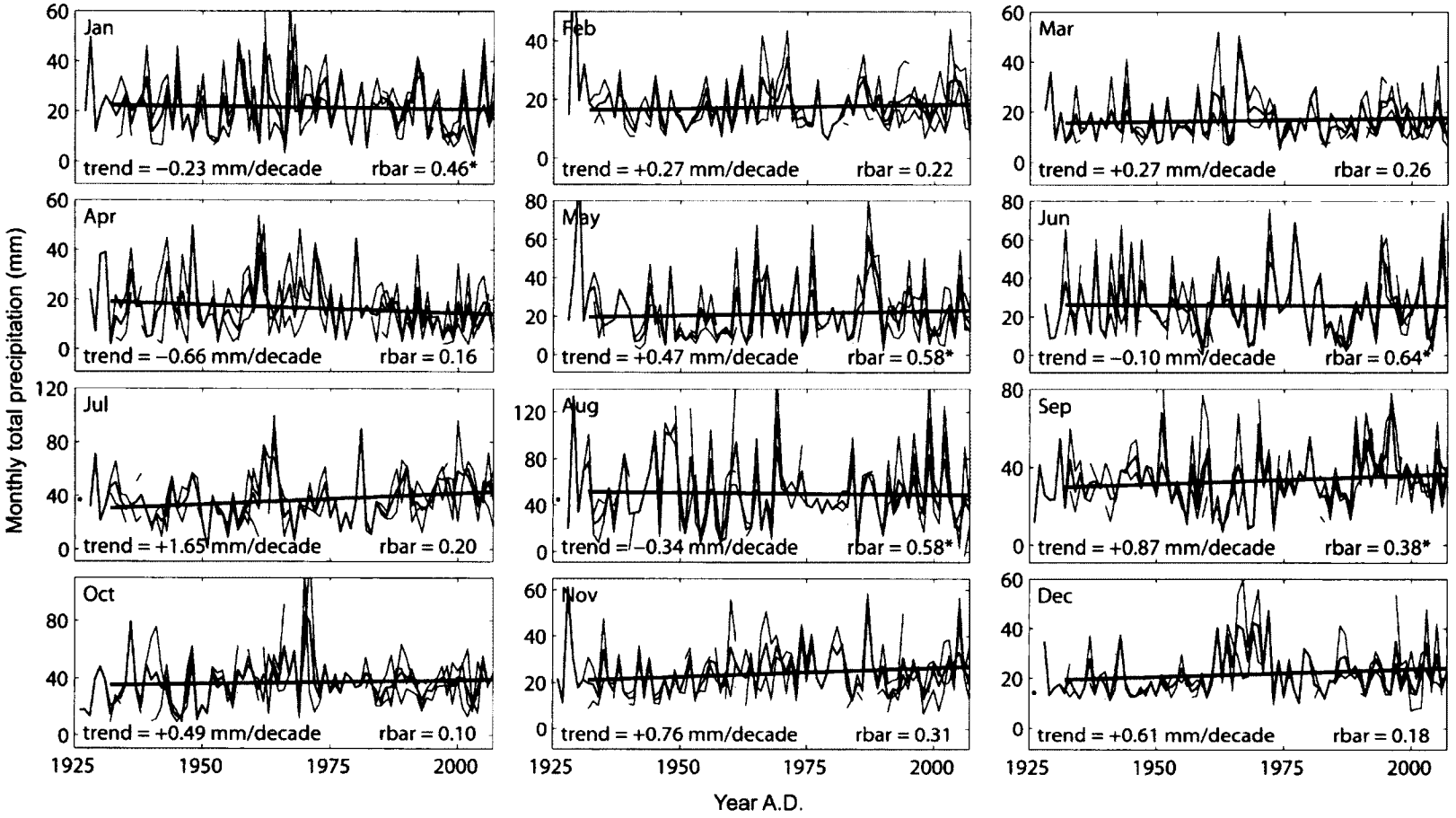

SI-Figure 4.8. Comparison of total monthly precipitation from Inuvik, Aklavik, and Fort McPherson (red lines); regional means (black line). 'rbar' is the mean inter-series correlation (*$p \leq 0.05$). 'trend' is the slope of the regional mean from AD 1932-2007, a period defined by two or more stations in most cases. See SI-Note 4.2 for more details.

WORKS CITED – APPENDIX C

Briffa KR (2000) Annual climate variability in the Holocene: interpreting the message of ancient trees. *Quaternary Science Reviews* 19: 87–105.

Burn CR and Kokelj SV (2009) The environment and permafrost of the Mackenzie Delta area. *Permafrost and Periglacial Processes* 20: 83–105.

Cook ER (1985) *A Time Series Analysis Approach to Tree Ring Standardization. PhD dissertation*. Tuscon, USA: University of Arizona, 171.

D'Arrigo R, Jacoby G, Buckley B, Sakulich J, Frank D, Wilson R, Curtis A and Anchukaitis K (2009) Tree growth and inferred temperature variability at the North American arctic treeline. *Global and Planetary Change* 65: 71–82.

D'Arrigo R, Wilson R and Jacoby G (2006) On the long-term context for late twentieth century warming. *Journal of Geophysical Research* 111: doi:10.1029/2005JD006352.

Esper J, Cook ER and Schweingruber FH (2002) Low-frequency signals in long tree-ring chronologies for reconstructing past temperature variability. *Science* 295: 2250–2253.

Holmes RL (1983) Computer-assisted quality control in tree-ring dating and measurement. *Tree-Ring Bulletin* 43: 69–78.

Jones PD, Briffa KR, Barnett TP and Tett SFB (1998) High-resolution palaeoclimatic records for the last millennium: interpretation, integration and comparison with General Circulation Model control-run temperatures. *The Holocene* 8: 455–471.

Kaufman DS, Schneider DP, McKay NP, Ammann CM, Bradley RS, Briffa KR, Miller GH, Otto-Bliesner BL, Overpeck JT, Vinther BM and Arctic Lakes 2k Project Members (2009) Recent warming reverses long-term Arctic cooling. *Science* 325: 1236–1239.

Mekis É and Vincent LA (2011) An overview of the second generation adjusted daily precipitation dataset for trend analysis in Canada. *Atmosphere-Ocean* 49: 163–177.

Pearce CM, McLennan D and Cordes LD (1988) The evolution and maintenance of white spruce woodlands on the Mackenzie Delta, N.W.T., Canada. *Holarctic Ecology* 11: 248–258.

Porter TJ and Pisaric MFJ (2011) Temperature-growth divergence in white spruce forests of Old Crow Flats, Yukon Territory, and adjacent regions of northwestern North America. *Global Change Biology* 17: 3418–3430.

Porter TJ, Pisaric MFJ, Kokelj SV and Edwards TWD (2009) Climatic signals in $\delta^{13}C$ and $\delta^{18}O$ of tree-rings from white spruce in the Mackenzie Delta region, northern Canada. *Arctic, Antarctic, and Alpine Research* 41: 497–505.

Szeicz JM and MacDonald GM (1995) Dendroclimatic reconstruction of summer temperatures in northwestern Canada since A.D. 1638 based on age-dependent modelling. *Quaternary Research* 44: 257–266.

Szeicz JM and MacDonald GM (1996) A 930-year ring-width chronology from moisture-sensitive white spruce (*Picea glauca* Moench) in northwestern Canada. *The Holocene* 6: 345–351.

Wahl ER and Ammann CM (2007) Robustness of the Mann, Bradley, Hughes reconstruction of Northern Hemisphere surface temperatures: Examination of criticisms based on the nature and processing of proxy climate evidence. *Climatic Change* 85: 33–69.

Wilson R, D'Arrigo R, Buckley B, Büntgen U, Esper J, Frank D, Luckman B, Payette S, Vose R and Youngblut D (2007) A matter of divergence: tracking recent warming at hemispheric scales using tree ring data. *Journal of Geophysical Research* 112: doi:10.1029/2006JD008318.

APPENDIX D

CHAPTER 6 SUPPORTING INFORMATION

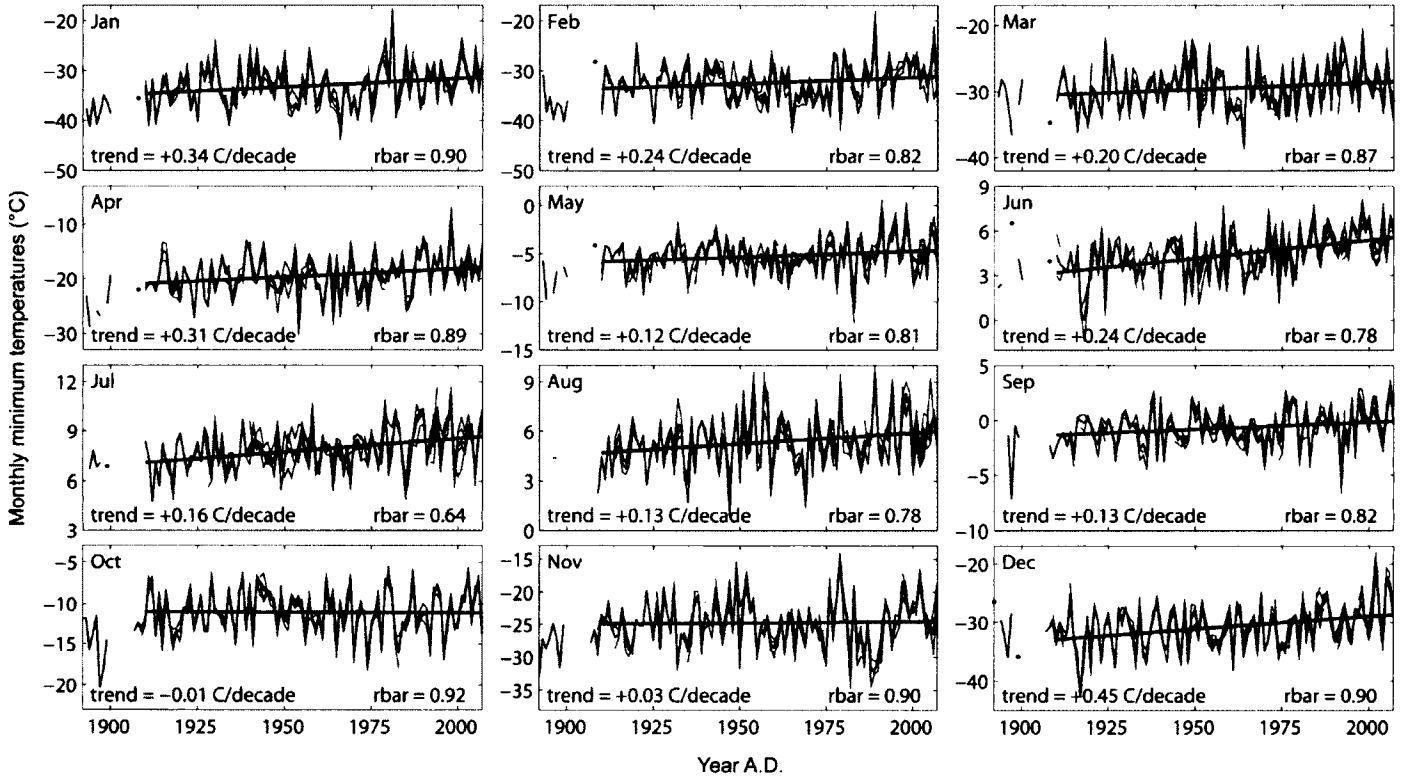

SI-Figure 6.1. Comparison of monthly minimum temperatures from Tuktoyaktuk, Inuvik, Aklavik, Fort McPherson, Norman Wells, and Fort Good Hope (red lines); regional means (black lines). 'rbar' is the mean inter-series correlation (all are significant at $p \leq 0.001$). 'trend' is the slope of the regional mean from AD 1910-2007, a period defined by two or more stations in most cases.

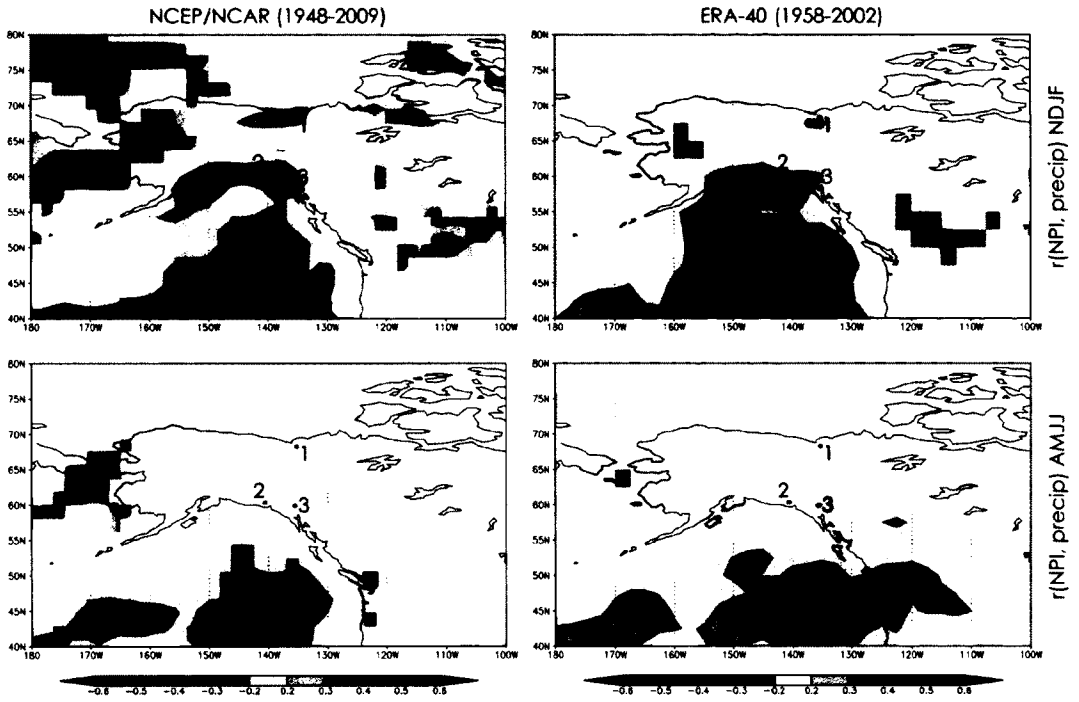

SI-Figure 6.2. A correlation analysis between NPI and precipitation amount for fall-winter (NDJF; top) and spring-summer (AMJJ; bottom) months. Both the NCEP/NCAR Reanalysis (Kalnay et al., 1996; left) and ERA-40 Reanalysis (Uppala et al., 2005; right) datasets were used. The correlation maps were plotted using the KNMI Climate Explorer (http://climexp.knmi.nl); correlations significant at $p < 0.05$ are in bold colour, non-significant correlations are in light colour. Points 1, 2, and 3 are Timber, PRCol, and Jellybean Lake, respectively.

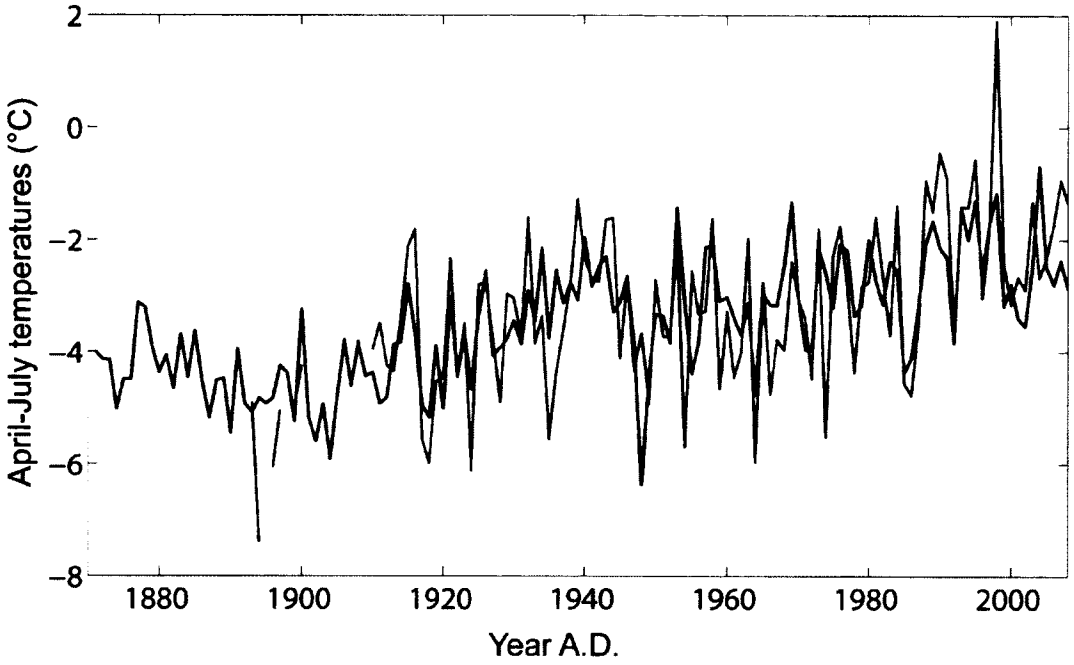

SI-Figure 6.3. Comparison April-July minimum temperatures for the Mackenzie Delta region (red) and 20CR (20th Century V2 Reanalysis; Compo et al., 2011) April-July mean temperatures for the area 60-70°N, 130-140°W; the mean and variance of the 20CR data were adjusted to the local temperature data by linear scaling; the inter-correlation is 0.69 ($p \leq 0.001$).

WORKS CITED – APPENDIX D

Compo GP, Whitaker JS, Sardeshmukh PD, Matsui N, Allan RJ, Yin X, Gleason BE, Vose RS, Rutledge G, Bessemoulin P, Brönnimann S, Brunet M, Crouthamel RI, Grant AN, Groisman PY, Jones PD, Kruk MC, Kruger AC, Marshall GJ, Maugeri M, Mok HY, Nordli Ø, Ross TF, Trigo RM, Wang XL, Woodruff SD and Worley SJ (2011) The Twentieth Century Reanalysis Project. *Quarterly Journal of the Royal Meteorological Society* 137: 1–28.

Kalnay E, Kanamitsu M, Kistler R, Collins W, Deaven D, Gandin L, Iredell M, Saha S, White G, Woollen J, Zhu Y, Leetmaa A, Reynolds R, Chelliah M, Ebisuzaki W, Higgins W, Janowiak J, Mo KC, Ropelewski C, Wang J, Jenne R and Joseph D (1996) The NCEP/NCAR 40-Year Reanalysis Project. *Bulletin of the American Meteorological Society* 77: 437–471.

Uppala SM, Kållberg PW, Simmons AJ, Andrae U, Bechtold VDC, Fiorino M, Gibson JK, Haseler J, Hernandez A, Kelly GA, Li X, Onogi K, Saarinen S, Sokka N, Allan RP, Andersson E, Arpe K, Balmaseda MA, Beljaars ACM, Berg LVD, Bidlot J, Bormann N, Caires S, Chevallier F, Dethof A, Dragosavac M, Fisher M, Fuentes M, Hagemann S, Hólm E, Hoskins BJ, Isaksen L, Janssen PAEM, Jenne R, Mcnally AP, Mahfouf J-F, Morcrette J-J, Rayner NA, Saunders RW, Simon P, Sterl A, Trenberth KE, Untch A, Vasiljevic D, Viterbo P and Woollen J (2005) The ERA-40 re-analysis. *Quarterly Journal of the Royal Meteorological Society* 131: 2961–3012.

VITA

Name:	Trevor John Porter
Birthplace & date:	Ottawa, Ontario; December 21, 1980
Education:	B.Sc. in Physical Geography, Highest Honours, Carleton University, 2006
Experience:	Izaak Walton Killam Memorial Postdoctoral Fellowship, Department of Earth and Atmospheric Sciences, University of Alberta, 2012-2014
	Lab Coordinator and Teaching Assistant, Department of Geography and Environmental Studies, Carleton University, 2005-2012
	Research Assistant, Carleton University Paleoecology Laboratory, 2004-2006
Awards:	Graduate Scholarship in Northern Research, Carleton University, 2011
	Canadian Standards Association Pat Keindel Graduate Scholarship in Climate Change, Carleton University, 2011
	Graduate Studies Research Bursary, Carleton University, 2006, '07, '08, '09, '10, & '11
	Best Ph.D. Student Paper Award, Association of American Geographers Paleoenvironmental Change Specialty Group, 2010
	NSERC Alexander Graham Bell Canada Graduate Scholarship, Doctoral, 2008 & '09
	Northern Scientific Training Program Grant, Aboriginal Affairs and Northern Development Canada, 2005, '07, & '08
	NSERC Post Graduate Scholarship, Masters and Doctoral, 2006 & '07
	Ontario Graduate Scholarship, 2006 (Declined)
	Senate Medal for Outstanding Academic Achievement, Carleton University, 2006

J. Peter Johnson Award, Department of Geography, Carleton University, 2006

Deans' Honour List, Carleton University, 2003, '04, '05, & '06

NSERC Undergraduate Student Research Award, 2004 & '05

Canada Millennium Excellence Award, 2004 & '05

Publications:

Porter, T, & Middlestead, P, 2012: On estimating the precision of stable isotope ratios in processed tree-rings. *Dendrochronologia*, 30: 239-242.

Porter, T, & Pisaric, M, 2011: Temperature-growth divergence in white spruce forests of Old CrowFlats, Yukon Territory, and adjacent regions of northwestern North America. *Global Change Biology*, 17: 3418-3430.

Wolfe, B, Humphries, M, Pisaric, M, Balasubramaniam, A, Burn, C, Chan, L, Cooley, D, Froese, D, Graupe, S, Hall, R, Lantz, T, **Porter, T**, Roy-Leveillee, P, Turner, K, Wesche, S, & Williams, M, 2011: Environ-mental change and traditional use of the Old Crow Flats in northern Canada: An IPY opportunity to meet the challenges of the new northern research paradigm. *Arctic*, 64: 127-135.

Pisaric, M, & **Porter, T**, 2011: Silent Sentinels, Talking Trees of the Old Crow Flats. *Yukon North of Ordinary (spring issue). Harper Street Publishing, Whitehorse: 15.*

Porter, T, Pisaric, M, Kokelj, S, & Edwards, T, 2009: Climate signals in $\delta^{13}C$ and $\delta^{18}O$ of tree-rings from white spruce in the Mackenzie Delta region, northern Canada. *Arctic, Antarctic, and Alpine Research*, 41: 497-505.

Project reports:

Dick, M., **Porter, T.J.**, and Pisaric, M.F.J., 2012: A dendro-archaeological study of the Anderson Farmstead, 5039 Russell Road, Carlsbad Springs, Ontario, Canada. A report submitted to The National Capital Commission, Heritage Program, 8 pp.

Dick, M., **Porter, T.J.**, and Pisaric, M.F.J., 2012: A dendro-archaeological study of the Brigham-Chamberlin Barn near the intersection of Meech Lake Rd. and Kingsmere Rd., Chelsea, Quebec, Canada. A report submitted to The National Capital Commission, Heritage Program and Gatineau Park, 8 pp.

Dick, M., **Porter, T.J.**, and Pisaric, M.F.J., 2012: A dendro-archaeological study of the Herridge and Healy Lodges in Gatineau Park, Quebec, Canada. A report submitted to The National Capital Commission, Heritage Program & Gatineau Park, 11 pp.

Dick, M., **Porter, T.J.**, and Pisaric, M.F.J., 2012: A dendro-archaeological study of the Lac Philippe and Schnob Barns near Saint-Cécile-de-Masham, Quebec, Canada. A report submitted to The National Capital Commission, Heritage Program and Gatineau Park, 11 pp.

Dick, M., **Porter, T.J.**, and Pisaric, M.F.J., 2012: A dendro-archaeological study of the NCC Site Office and Visitor's Centre at Rideau Hall, 1 Sussex Dr., Ottawa, Ontario, Canada. A report submitted to The National Capital Commission, Heritage Program, 10 pp.

Porter, T, deMontigny, P, & Pisaric, M, 2011: White spruce tree-ring chronologies of the Mackenzie Delta region: Indicators of past climate and environmental change. *A report submitted to Indian and Northern Affairs Canada, Renewable Resources and Environment,* 108 pp.

Porter, T, Pisaric, M, & deMontigny, P, 2010: The influence of climate on white spruce tree-ring growth in the Old Crow Flats region. *A report submitted to Natural Resources Department of Old Crow, Yukon Territory*, 11 pp.

Porter, T, & Pisaric, M, 2006: Mackenzie Delta Stable Isotope Dendroclimatology. *A report submitted to Indian Affairs and Northern Affairs Canada, Water Resources Division*, 32 pp.

Invited presentations:

Porter, T, 2011: Boreal northwestern North America & recent climatic stressors. *Lecture GEOG2020: Physical Environments of Canada, Carleton University, Ottawa, Canada.*

Porter, T, 2008: Stable isotopes and spatiotemporal growth patterns of white spruce in the Old Crow Flats and Mackenzie Delta. *Department of Geography Founder's Seminar Series, Carleton University, Ottawa, Canada.*

Porter, T, Pisaric, M, Kokelj, S, & Edwards, T, 2007: The use of $\delta^{13}C$ and $\delta^{18}O$ from white spruce tree-rings as paleoclimate indicators in the Mackenzie Delta region, Canada. *Biology and Paleo Environment Spring Seminar Series, Lamont-Doherty Earth Observatory, Columbia University, Palisades, USA.*

Conference presentations:

Porter, T, & Pisaric, M, 2012: 'Divergence' and implications for reconstructing warm season temperatures from white spruce tree-rings in Old Crow Flats, Yukon Territory, and neighboring N.W. North America. *International Polar Year: From Knowledge to Action, Montréal, Canada.*

Pisaric, M, **Porter, T**, deMontigny, P, Dick, M, Perrault, J, Robillard, K-L, & Wertheimer, È, 2012: Development of a multicentennial eastern white pine tree ring chronology from salvaged river logs and its utility for Dendroarchaeology dating in Easter Ontario, Canada. *Association of American Geographers Annual Meeting, New York, USA.*

Wilmking, M, Hallinger, M, Jansen, F, **Porter, T**, & Pisaric, M, 2011: Non-linear ecosystem shifts in NW North America: early warning signs in tree-ring series? *Eurodendro 2011, Engelberg, Switzerland.*

Porter, T, Pisaric, M, Kokelj, S, & Edwards, T, 2011: Reconstructed June-July temperatures from $\delta^{13}C$ in white spruce (*Picea glauca* [Moench] Voss) tree-rings, Mackenzie Delta, NW Canada. *Association of American Geographers Annual Meeting, Seattle, USA.*

Porter, T, Pisaric, M, Kokelj, S, & Edwards, T, 2011: June-July temperatures reconstructed from $\delta^{13}C$ in white spruce tree-rings, Mackenzie Delta, northwestern Canada. *Ottawa-Carleton Student Northern Research Symposium, Carleton University, Ottawa, Canada.*

Porter, T, Pisaric, M, & Kokelj, S, 2010: Summer temperatures reconstructed from tree-ring $\delta^{13}C$ at boreal treeline, Mackenzie Delta, northwestern Canada. *American Geophysical Union Fall Meeting, San Francisco, USA.*

Pisaric, M, **Porter, T**, & deMontigny, P, 2010: Are temperature reconstructions from northern treeline (in NW Canada) still possible? *WorldDendro 2010, Rovaniemi, Finland.*

Wilmking, M, Juday, G, Yongxiang, X, Alix, C, Anchukaitis, K, Barber, V, Edward, B, Buckley, B, Bunn, A, Danby, R, D'Arrigo, R, Hogg, T, King, G, Laxton, S, Lloyd, A, Luckman, B, Pisaric, M, **Porter, T**, Roland, C, & Sherriff, R, 2010: A tale of 10,000 trees – The northwestern North American tree ring

synthesis. *WorldDendro 2010, Rovaniemi, Finland.*

Porter, T, Pisaric, M, deMontigny, P, & St. George, S, 2010: Insights on divergence from a regional study of tree growth in Old Crow Flats, NW Canada. *Association of American Geographers Annual Meeting, Washington DC, USA.*

Porter, T, & Pisaric, M, 2009: Climate signals in tree-rings in Old Crow Flats, northern Yukon. *Canadian Association of Geographers Annual Meeting, Carleton University, Ottawa, Canada.*

Lantz, T, **Porter, T**, Tizya-Tramm, E, Froese, D, Pisaric, M, Cooley, D, & Humphries, M, 2009: Environmental Change in Old Crow Flats: A multidisciplinary perspective. *Canadian Society for Ecology and Evolution, Halifax, Canada.*

Porter, T, & Pisaric, M, 2009: Climate-tree growth relations in Old Crow Flats, northern Yukon, Canada. *Association of American Geographers Annual Meeting, Las Vegas, USA.*

Pisaric, M, King, G, and **Porter, T**, 2008: Diverging understanding: do we really understand the linkages between tree growth and climate at latitudinal treeline in northwest Canada? *AmeriDendro 2008, University of British Columbia, Vancouver, Canada.*

Porter, T, Pisaric, M, & Edwards, T, 2008: Coupling $\delta^{13}C$ and $\delta^{18}O$ from tree ring cellulose to resolve moisture and temperature signals in the Mackenzie Delta, NWT. *Geological Association of Canada 2008 Annual Meeting, Quebec City, Canada.*

Porter, T, Pisaric, M, Kokelj, S, & Edwards, T, 2008: The use of stable oxygen isotope ratios in tree-rings for reconstructing flood events in the Mackenzie Delta, Northern Canada. *Association of American Geographers Annual Meeting, Boston, USA.*

Porter, T, Pisaric, M, Kokelj, S, & Edwards, T, 2007: Growth trend divergence and statistical characterization of climate-isotope relations of white spruce in the Mackenzie Delta, N. Canada. *American Geophysical Union Fall Meeting, San Francisco, USA.*

Porter, T, Pisaric, M, Kokelj, S, & Edwards, T, 2007: Past

climatic variability from $\delta^{13}C$ and $\delta^{18}O$ tree ring records, Mackenzie Delta, NWT. *8th International Association of Canadian Universities for Northern Studies, University of Saskatchewan, Saskatoon, Canada.*

Porter, T, Pisaric, M, Kokelj, S, & Edwards, T, 2007: $\delta^{13}C$ and $\delta^{18}O$ in white spruce tree-rings as indicators of past climate, Mackenzie Delta, NWT, Canada. *First Asian Dendrochronology Conference, Mahidol University, Bangkok, Thailand.*

Porter, T, Pisaric, M, Kokelj, S, & Edwards, T, 2007: Paleoclimate potential of $\delta^{13}C$ in white spruce tree-rings, Mackenzie Delta, NWT, Canada. *Association of American Geographers Annual Meeting, San Francisco, USA.*

Porter, T, Pisaric, M, Kokelj, S, & Edwards, T, 2007: Climatic response of stable isotope ratios in white spruce tree-rings, Mackenzie Delta, NWT. *Ottawa-Carleton IPY Launch and Student Northern Research Symposium, Carleton University, Ottawa, Canada.*

Porter, T, Pisaric, M, Kokelj, S, & Edwards, T, 2007: Stable carbon and oxygen isotope ratios in white spruce tree-rings as indicators of past environmental conditions in the Mackenzie Delta. *Canadian Quaternary Association Conference, Carleton University, Ottawa, Canada.*

Porter, T, Pisaric, M, & Kokelj, S, 2006: On the climatic dependence of $\delta^{13}C$ and $\delta^{18}O$ in tree-rings of white spruce in the Mackenzie Delta, NWT. *Canadian Geophysical Union, Hydrology Section, Eastern Student Conference, Carleton University, Ottawa, Canada.*

Porter, T, & Pisaric, M, 2006: Mackenzie Delta Stable Isotope Dendroclimatology. *Ottawa-Carleton Student Northern Research Symposium, University of Ottawa, Ottawa, Canada.*

Public presentations:

Dick, M, **Porter, T**, Wertheimer, E, and Pisaric, M, 2011: Dendroarchaeology of log structures in the Outaouais region. *An invited presentation to the National Capital Commission, Ottawa, Ontario.*

Porter, T, and Pisaric, M, 2010: White spruce tree-rings in Old Crow Flats: records of climatic change. *Annual Meeting of the International Polar Year project Yeendoo Nanh Nakhweenjit K'atr'ahanahtyaa, Old Crow, Yukon Territory.*

Porter, T, 2009: Dendroclimatology in Old Crow Flats, northern Yukon. *An invited presentation given to 9th Grade geography students, Ridgemont High School, Ottawa, Ontario.*

Porter, T, & Pisaric, M., 2009: What can spruce trees in Old Crow Flats tell us about past climate? *Annual Meeting of the International Polar Year project Yeendoo Nanh Nakhweenjit K'atr'ahanahtyaa, Old Crow, Yukon Territory.*